UNIVERSIDADE ESTADUAL PAULISTA

ISTITUTO DE BIOCIÊNCIAS DE BOTUCATU

PROGRAMA DE PÓS-GRADUAÇÃO EM CIENCIAS BIOLÓGICAS (GENÉTICA)

BIOGEOGRAFIA HISTÓRICA E FILOGENÔMICA DE ERYTHRINOIDEA E TAXONOMIA INTEGRATIVA PARA O ESTUDO DO GÊNERO NEOTROPICAL HOPLERYTHRINUS (CHARACIFORMES: ERYTHRINIDAE)

CRISTHIAN CAMILO CONDE SALDAÑA

BOTUCATU-SP

2022

UNIVERSIDADE ESTADUAL PAULISTA

ISTITUTO DE BIOCIÊNCIAS DE BOTUCATU

PROGRAMA DE PÓS-GRADUAÇÃO EM CIENCIAS BIOLÓGICAS (GENÉTICA)

BIOGEOGRAFIA HISTÓRICA E FILOGENÔMICA DE ERYTHRINOIDEA E TAXONOMIA INTEGRATIVA PARA O ESTUDO DO GÊNERO NEOTROPICAL HOPLERYTHRINUS (CHARACIFORMES: ERYTHRINIDAE)

Discente: Cristhian Camilo Conde Saldaña

Orientador: Prof. Dr. Claudio Oliveira

Co-orientadora: Dr(a). Mônica de Toledo-Piza Ragazzo

Tese apresentada ao Programa de Pós-Graduação em Ciências Biológicas (Genética) do Instituto de Biociências de Botucatu, Universidade Estadual Paulista "Júlio de Mesquita Filho", como parte dos requisitos para a obtenção do título de Doutor.

BOTUCATU-SP

2022

FICHA CATALOGRÁFICA ELABORADA PELA SEÇÃO TÉC. AQUIS. TRATAMENTO DA INFORM.
DIVISÃO TÉCNICA DE BIBLIOTECA E DOCUMENTAÇÃO - CÂMPUS DE BOTUCATU - UNESP
BIBLIOTECÁRIA RESPONSÁVEL: ROSEMEIRE APARECIDA VICENTE-CRB 8/5651

Conde, Cristhian Camilo.
Biogeografia histórica e filogenômica de Erythrinoidea e taxonomia integrativa para o estudo do gênero neotropical *Hoplerythrinus* (Characiformes: Erythrinidae) / Cristhian Camilo Conde. - Botucatu, 2022

Tese (doutorado) - Universidade Estadual Paulista "Júlio de Mesquita Filho", Instituto de Biociências de Botucatu
Orientador: Claudio Oliveira
Coorientador: Mônica de Toledo-Piza Ragazzo
Capes: 20000006

1. Peixes de água doce - Filogenia. 2. Biogeografia. 3. Amazonas, Rio. 4. Código de barras de DNA taxonômico.

Palavras-chave: Biogeografia histórica; DNA *barcode*; Filogenômica; Peixes neotropicais de água doce; Rio Amazonas.

Esta pesquisa foi financiada com recursos da

Coordenação de Aperfeiçoamento de Pessoal de Nível Superior (CAPES) e

Fundação de Amparo à Pesquisa do Estado de São Paulo

FAPESP - Processo Número: 2018/09767-6 e 2019/16999-3

A mi familia

AGRADECIMIENTOS

Agradezco a todas las personas e instituciones que de alguna forma contribuyeron para el desarrollo de este trabajo y mi formación a lo largo de este proceso.

A la Fundação de Amparo à Pesquisa do Estado de São Paulo (FAPESP) por la financiación para la consecución de este proyecto a través de los procesos nº 2018/09767-6 y 2019/16999-3.

A la Coordenação de Aperfeiçoamento de Pessoal de Nível Superior (CAPES).

Al Dr. Claudio de Oliveira por la confianza, el apoyo y orientación en las distintas etapas de este proyecto. Gracias por la oportunidad.

Al Dr. James Albert por la amistad, sus enseñanzas y haberme acogido durante mi estadía en la University of Louisiana at Lafayette – USA y el desarrollo del proyecto BEPE.

A la Dr. Mônica Toledo Piza por sus enseñanzas y acompañamiento a lo largo de este proceso.

Al Dr. Bruno Melo por la amistad y acompañamiento incondicional durante todas las etapas de este proyecto.

Al Dr. Fabio Roxo por la amistad y colaboración durante el desarrollo de este proyecto.

Al Dr. Francisco Villa por la mistad, colaboración y enseñanzas desde mis inicios en la ictiología.

A Mark Sabaj y Mariangeles Arce por la gran acogida y disposición en mi visita a la ANSP en Philadelphia, USA.

A Carlos DoNascimiento, Juan Gabriel Albornoz y Alejandro Méndez por la disposición y ayuda durante mi visita al IAvH en Villa de Leyva, Colombia.

Agradezco a todos los integrantes y exintegrantes del Laboratório de Biologia e Genética de Peixes por la amistad, compañerismo y enseñanzas, en especial a Luz Ochoa, Gabriel Costa e Silva, Lais Regia, Bruno Morales, Rafaela Ota, Silvana Melo, Camila Souza, Angélica Dias, Acacio Nogueira, Giovana Ribeiro, Nadayca Mateussi, Aisni Mayumi, Lucas Peres, Ricardo da Silva, Renato Devidé, Fabilene Gomes, Najila Cerqueira, Gabriela Omura, Beatriz Boza, Beatriz Dorini, Andressa Galasso, Lucas Lasmar, André Nobile, Vanessa Paes e Duílio Zerbinato.

A Juan Gabriel Albornoz, Diana Montoya, Margarita Roa, Daniela Bedoya, Jose Poveda por la amistad y aprendizaje en este mundo de los peces.

A los integrantes y exintegrantes del Albert’s Lab en Lafayette por la amistad y enseñanzas, en especial a Jesse Figueiredo, Kevin Torgersen, Shannon Kuznar, Aaron Fronk e Jon Allen.

A mis amigos y compañeros de casa en Botucatu, por el apoyo y amistad, en especial a Bruno Melo, André Nobile, Fabio Cardoso, Felipe Lima, Lucas Lasmar, Ricardo da Silva e Cristian Araya.

Finalmente, agradezco a mi familia, mis padres Gustavo, Lyda y a mi hermanita Vivi por el amor incondicional e incentivo para recorrer estos caminos de aprendizaje.

RESUMO

Erythrinoidea é um clado de Characiformes composto pela enigmática família Tarumaniidae, representada por uma única espécie altamente especializada, *Tarumania walkerae*, que habita poças isoladas da floresta amazônica central, e pela família de ampla distribuição geográfica Erythrinidae, que habita em ambientes lênticos e lóticos na maioria das drenagens da América Central e do Sul. Erythrinidae é composta por três gêneros com representantes viventes (*Erythrinus*, *Hoplias* e *Hoplerythrinus*), onde complexos de espécies têm sido hipotetizados com base na notável variação cariotípica e uniformidade nos dados merísticos e morfométricos. A diversidade e os padrões de distribuição geográfica, bem como os aspectos ecológicos de Erythrinoidea, levantam questões interessantes com relação à diversificação evolutiva de suas linhagens. A maioria dos estudos taxonômicos e filogeográficos têm sido focados em *Hoplias*, no entanto, *Erythrinus* e *Hoplerythrinus* aguardam revisões detalhadas abrangendo toda a sua distribuição geográfica. O presente trabalho tem como objetivo principal investigar padrões biogeográficos e cronológicos de diversificação da superfamília Erythrinoidea e implementar uma abordagem integrativa para investigar a diversidade e a história evolutiva de um grupo particular dentro deste clado, o gênero *Hoplerythrinus*. Combinando dados filogenômicos com elementos ultraconservados (UCEs), paleontológicos (calibrações fósseis), biogeográficos e fontes geológicas, encontramos que a origem de Erythrinoidea é estimada para o Cretáceo Superior ca. 80 Ma, com divergência de clados principais durante o Paleogeno ca. 51-31 Ma, e Erythrinidae se diversificou rapidamente após a formação do rio Amazonas transcontinental ca. 10 Ma, de oito linhagens para pelo menos 28 espécies atuais. Padrões de diversificação em Erythrinoidea também são discutidos à luz da evolução da paisagem. Por outro lado, a integração de DNA *barcode*, filogenômica com UCEs e informações morfológicas forneceram evidências para investigar a história evolutiva de *Hoplerythrinu*s e definir este táxon como um gênero monotípico geograficamente difundido na região Neotropical. Aqui também discutimos detalhes sobre a variação fenotípica e níveis de diferenciação genômica considerando o tempo de divergência e suas afinidades ecológicas.

Palavras chave: Rio Amazonas, DNA *barcode*, biogeografia histórica, peixes neotropicais de água doce, filogenômica, América do Sul, elementos ultraconservados.

ABSTRACT

Erythrinoidea is a characiform clade composed of the enigmatic family Tarumaniidae, represented by a single highly-specialized species, *Tarumania walkerae*, that inhabits isolated pools in the forest floor of central Amazon rainforests, and the geographically widespread family Erythrinidae, which occurs in lentic and lotic habitats in most drainages of Central and South America. Erythrinidae is composed of three extant genera (*Erythrinus*, *Hoplias*, and *Hoplerythrinus*), where species complex had been hypothesized based on remarkable karyotypic variation and uniformity in meristic and morphometric data. Diversity and geographic distribution patterns, as well as ecological aspects of Erythrinoidea, arouse interesting questions concerning to evolutionary diversification of its lineages. Most taxonomic and phylogeographic studies have been focused on *Hoplias*, however, *Erythrinus* and *Hoplerythrinus* are waiting for detailed revisions encompassing their entire distribution. The present work has as the main goal, to investigate biogeographic and chronological patterns of diversification in the superfamily Erythrinoidea and to implement an integrative approach to investigate the diversity and evolutionary history of a particular group within this clade, the genus *Hoplerythrinus*. Combining data from phylogenomics of ultraconserved elements (UCEs), paleontological (fossil calibrations), biogeographic, and geological sources, we found that Erythrinoidea is estimated to have originated in the Late Cretaceous ca. 80 Ma, with divergence of major clades during the Paleogene ca. 51-31 Ma, and Erythrinidae diversified rapidly after the formation of the transcontinental Amazon River ca. 10 Ma, from eight lineages to at least 28 species today. Diversification patterns in Erythrinoidea are also discussed in light of landscape evolution. On the other hand, integrating DNA barcode, phylogenomics of UCEs, and morphological information provided evidence to investigate the evolutionary history of *Hoplerythrinus*, and to define this taxon as a geographically widespread monotypic genus in the Neotropical region. Here, we also discussed details about the phenotypic variation and levels of genomic differentiation considering the divergence time and its ecological affinities.

Keywords: Amazon River, DNA barcode, historical biogeography, Neotropical freshwater fishes, phylogenomics, South America, ultraconserved elements.

SUMÁRIO

INTRODUÇÃO GERAL

Os peixes neotropicais de água doce (NFF) são conhecidos por sua notável diversidade, com mais de 6.350 espécies representando ~ 18% de todas as espécies de peixes na Terra, exibindo a maior disparidade fenotípica e diversidade de características funcionais de qualquer fauna de peixes continentais (Reis et al. 2016; Su et al. 2019; Fricke et al. 2022). A maioria das espécies de NFF pertencem a um único clado, Ostariophysi, distribuídas em três ordens: Siluriformes (bagres e cascudos), Characiformes (lambarias., piabas, curimbas, piranhas, traíras, entre outros) e Gymnotiformes (peixes elétricos neotropicais) (Albert et al. 2020). Particularmente, Characiformes constitui um grupo extremamente diverso com aproximadamente 2.200 espécies e 22 famílias, com representantes habitando ecossistemas tropicais de África e o Neotropico (Nelson et al. 2016; Fricke et al. 2022). A superfamília Erythrinoidea representa um clado enigmático dentro de Characiformes, recentes filogenias moleculares a tem definido como um clado composto por as família Tarumaniidae, representada por uma única espécie altamente especializada, *Tarumania walkerae*, que habita poças isoladas na floresta central amazônica (de Pinna et al. 2017), e Erythrinidae, uma família com ampla distribuição geográfica, ocorrendo em habitats lênticos e lóticos na maioria das drenagens da América Central e do Sul, da Costa Rica ao norte da Argentina (Oyakawa and Mattox 2018).

Representantes da família Erythrinidae, conhecidos popularmente como jejus, aimarás e traíras, são importantes predadores de insetos, crustáceos e outros peixes (Marrero et al. 1997; Lasso and Meri 2001; Oliveira and Garavello 2003; Lasso et al. 2011; Sánchez-Duarte et al. 2011), e em muitas regiões representam componentes importantes dentro da pesca comercial ou de consumo local (Lasso et al. 2011; Oyakawa et al. 2013). Também são bem conhecidos por suas adaptações fisiológicas que lhes permitem tolerar ambientes tóxicos e hipóxicos (Liem 1988; Moraes et al. 2004; Moron et al. 2009; Pelster 2021), e sua capacidade de residir em diversos habitats (Oyakawa et al. 2013; Oyakawa and Mattox 2018). A família é composta por três gêneros com representantes viventes: *Erythrinus*, *Hoplerythrinus* e *Hoplias* (Oyakawa 2003), que englobam complexos de espécies e representam um interessante modelo para estudos evolutivos, permitindo relacionar os padrões de dispersão, diversificação e distribuição com a história geográfica da região Neotropical (Bertollo et al. 2000; Santos et al. 2009; Pereira et al. 2013b; Martinez et al. 2016; Sassi et al.

2021). Erythrinidae também contém o gênero extinto *Paleohoplias*, com uma única espécie †*Paleohoplias assisbrasiliensis* Bocquentin & Negri 2003, descrita com base em restos fosseis da Formação Solimões (final do Mioceno-Plioceno) no Brasil (Gayet et al. 2003).

Os representantes da família Erythrinidae caracterizam-se por corpos cilíndricos, nadadeira caudal arredondada, nadadeira dorsal com 12-16 raios, origem da nadadeira dorsal situada anteriormente à vertical que passa pela origem da nadadeira anal, nadadeira anal curta (10-11 raios), 34-48 escamas na linha lateral e ausência de nadadeira adiposa (Oyakawa et al. 2013; Oyakawa and Mattox 2018). Possuem outras características como a presença de cinco raios branquiostégios, suprapreoperculo lamelar, extremidade anterior do primeiro infra-orbital bifurcada e ausência do antorbital que são úteis para diagnosticar o grupo (Oyakawa 2003). Os três gêneros podem ser distinguidos entre eles por algumas características como a divisão transversal do sexto infraorbital, padrões de coloração e comprimento da maxila (Oyakawa and Mattox 2018), no entanto, a morfologia externa dentro de cada gênero é altamente conservada, revelando uma grande uniformidade em dados merísticos e morfométricos ao longo da distribuição das espécies (Oyakawa et al. 2013). O gênero *Hoplias* está distribuído na maioria das bacias hidrográficas da região trans e cisandina, e atualmente consiste em 15 espécies válidas (Fricke et al. 2022). Alternativamente, *Erythrinus* e *Hoplerythrinus* têm uma ampla distribuição cisandina, apresentando uma aparente menor diversidade (Oyakawa 2003; Fricke et al. 2022).

Para o gênero *Erythrinus* são consideradas duas espécies válidas (Fricke et al. 2022), *E. kessleri* Steindachner, 1876 descrita para Salvador (Brazil), e *E. erythrinus* (Bloch e Schneider, 1801) descrita para Suriname, sendo esta reconhecida como uma espécie de ampla distribuição geográfica, ocorrendo nas bacias do rio Orinoco, Amazonas, Paraná-Paraguay e rios costeiros das Guianas (Oyakawa 2003). O gênero *Hoplerythrinus* também possui uma espécie reconhecida de ampla distribuição, *H. unitaeniatus* (Agassiz, em Spix e Agassiz, 1829), descrita para o rio São Francisco (Brasil), e ocorrendo na maioria das drenagens cisandinas da América do sul (Oyakawa 2003; Oyakawa et al. 2013). Adicionalmente, são listadas outras duas espécies válidas: *H. cinereus* (Gill, 1858) da ilha de Trinidad e *H. gronovii* (Valenciennes, em Cuvier e Valenciennes, 1847) descrita para Cayenne (Guiana Francesa) (Oyakawa 2003; Fricke et al. 2022); porém estas duas espécies são conhecidas apenas do material tipo e apresentam diagnoses incipientes, resultando na

necessidade de uma avaliação detalhada do status taxonômico das espécies do gênero (Oyakawa et al. 2013).

Hipóteses filogenéticas realizadas com dados moleculares para Characiformes, indicaram que os gêneros *Erythrinus* e *Hoplerythrinus* formam um grupo monofiletico que é o grupo irmão do gênero *Hoplias* (Oliveira et al. 2011; Melo et al. 2021). No entanto, os estudos taxonômicos e evolutivos recentes em nível de gênero dentro de Erythrinidae tem se concentrado principalmente no gênero *Hoplias*, avaliando o status taxonômico, descrição de novas espécies (Mattox et al. 2006, 2014; Oyakawa and Mattox 2009; Azpelicueta et al. 2015; Rosso et al. 2016, 2018; Guimarães et al. 2021) e alguns trabalhos tem estudado as relações evolutivas e filogeográficas do complexo *H. malabaricus*, incluindo dados cariotípicos de populações ao longo da sua ampla distribuição geográfica (Dergam et al. 2002; Santos et al. 2009).

Ainda não existem estudos que utilizem marcadores moleculares ou revisões detalhadas para o gênero *Hoplerythrinus*, embora tenham sido publicados estudos citogenéticos que têm revelado uma grande diversidade cariotípica, propondo *H. unitaeniatus* como um complexo de espécies (Giuliano-Caetano et al. 2001; Martinez et al. 2016). As variações numéricas e estruturais têm revelado um número cariotípico 2n = 48 até 2n=52 cromossomos e número fundamental (NF) de 92 a 102, marcações simples e múltiplos de Ag-NOR (Martinez et al. 2016) e polimorfismos com o mapeamento dos rDNA 18S e 5S (Diniz and Bertollo 2003; Martinez et al. 2016). A variabilidade cariotípica dentro do gênero revela a necessidade de ampliar estudos genéticos no grupo, que permitam identificar as linhagens e suas relações com a história geográfica em sua área de distribuição. Uma avaliação detalhada do status taxonômico das espécies que compõem o gênero *Hoplerythrinus* é necessária, além de estudos usando marcadores moleculares para reconstruir a história evolutiva do grupo, incluindo o maior número de populações ao longo da sua distribuição.

O avanço da tecnologia tem desenvolvido mecanismos eficientes em escala genômica, permitindo uma profundidade sem precedentes nas análises de relações entre organismos (McCormack et al. 2013; Zarza et al. 2018). Assim mesmo, o estudo da diversidade e formulação de hipóteses de separação de linhagens em grupos taxonomicamente complexos, tem sido favorecido pela implementação de enfoques integrativos, avaliando níveis de diferenciação genômica, variação fenotípica e tempos de divergência (Struck et al. 2018). Dentro do sequenciamento de nova-

geração tem surgido o uso de elementos ultraconservados (UCEs) como marcadores resolutivos de baixo custo em filogenômica, úteis para uma melhor compressão das relações filogenéticas e os mecanismos evolutivos que regem os grupos de peixes neotropicais (Faircloth et al. 2012; Harrington et al. 2016; Chakrabarty et al. 2017; Alda et al. 2019; Melo et al. 2021). Igualmente, recentes esforços tem integrado diferentes métodos para explorar a diversidade e caracterizar linhagens evolutivas de NFF, como sequencias de *DNA barcode*, tomografia computadorizada e morfometria geométrica e/ou tradicional (Loureiro et al. 2018; Agudelo-Zamora et al. 2020; Anjos et al. 2020; Henschel et al. 2020; Ochoa et al. 2020b; Armbruster et al. 2021; Garavello et al. 2021).

DNA barcode

A metodologia do *DNA barcode* foi proposta como um método de identificação de espécies, na qual utiliza-se fragmentos (~650 bp) do gene mitocondrial citocromo c oxidase subunidade I (COI) (Hebert et al. 2003). Este gene caracteriza-se por apresentar um forte sinal filogenético, possui primers universais robustos e sua evolução é rápida o suficiente para permitir a discriminação não só de espécies próximas, mas também de grupos filogeográficos dentro de uma única espécie (Hebert et al. 2003; Ward et al. 2005; Ivanova et al. 2007), portanto, utilizado amplamente junto com outros marcadores para estimar filogenias moleculares (Patwardhan et al. 2014). Com o desenvolvimento de diferentes modelos para o delineamento de espécies, baseados no marco teórico da coalescência e a teoria filogenética (Puillandre et al. 2012; Ratnasingham and Hebert 2013; Zhang et al. 2013; Hubert and Hanner 2015), o *DNA barcode* tem se tornado uma importante ferramenta para revelar diversidade críptica ou identificar novos táxons em grupos problemáticos com taxonomia incipiente (Hubert et al. 2008; Pereira et al. 2013a; Rossini et al. 2016; Ochoa et al. 2020b).

A metodologia é baseada na diferença entre a divergência genética intraespecífica e interespecífica, conhecido como *barcoding gap* (Meier et al. 2008), permitindo identificar diversificações crípticas (Valdez-Moreno et al. 2009; Pereira et al. 2011; Melo et al. 2016). Estudos em comunidades de peixes de água doce têm confirmado a eficácia da metodologia do DNA *barcode* para identificar espécies, descriminando acima de 95% das espécies estudadas (De Carvalho et al., 2011; Lara et al., 2010; Pereira et al., 2013). No entanto, o uso do gene mitocondrial

COI nem sempre avalia de forma abrangente o fluxo gênico ou o isolamento reprodutivo (Struck et al. 2018), e tem sido menos útil em alguns casos de diversificação rápida ou recente divergência em clados NFF (Rossini et al. 2016; de Queiroz et al. 2020; Ramirez et al. 2020). Porém, a integração do *DNA barcode* como uma rotina na taxonomia atual pode ser considerado um ponto de partida para revisões sistemáticas (DeSalle 2006; Hubert and Hanner 2015). Adicionalmente, as sequências do *barcode* podem ser disponibilizadas através do projeto *International Barcoding of life* (BOLD), gerando um repositório de dados que permite o acesso à informação primária para o uso em outras aplicações (Ratnasingham and Hebert 2007).

Elementos ultraconservados (UCEs)

Os elementos ultraconservados (*ultraconserved elements* - UCEs) são regiões do genoma altamente conservadas e compartilhadas entre organismos de diferentes táxons. Os UCEs foram primeiramente descritos por Bejerano et al. (2004) no genoma humano, no qual encontraram 481 segmentos maiores que 200 pares de bases exclusivos de regiões de RNA ribossômico (rRNA), e amplamente distribuídas no genoma, exceto nos cromossomos 21 e Y. Estudos posteriores mostraram que os UCEs estão presentes em diversos outros organismos, como outros vertebrados, insetos, vermes e fungos (Siepel et al. 2005; Faircloth et al. 2012). O papel dos UCEs no genoma ainda não está bem esclarecido (Dermitzakis et al. 2005), tendo sido associados com a regulação gênica (Pennacchio et al. 2006) ou no desenvolvimento (Sandelin et al. 2004; Woolfe et al. 2005), e normalmente se tem assumido que os UCEs são importantes pela sua natureza extremamente conservada entre grupos muito distantes filogeneticamente.

Os UCEs caracterizam-se por ser encontrados em grande quantidade ao longo de um genoma (Stephen et al. 2008), têm poucas inserções de retroelementos (Simons et al. 2006), e a premissa de contínua variabilidade nas sequências que flanqueam cada UCE sugere que eles podem ser um tipo de “fóssil molecular”, retendo um sinal de história evolutiva em diversas escalas de tempo, dependendo da distância da região central dos UCEs (Faircloth et al. 2012; Gilbert et al. 2015). Para que possam ser utilizados como marcadores genéticos, é comum que aqueles UCEs que aparecem duplicados sejam removidos para evitar paralogia. Dessa maneira, os locus resultantes são altamente conservados e ortólogos, sendo facilmente usados como marcadores moleculares. Os UCEs foram introduzidos como uma nova classe de marcadores moleculares em estudos

filogenéticos através do enriquecimento de bibliotecas genômicas contendo centenas ou milhares de loci nucleares, utilizando sequenciamento de nova-geração (Faircloth et al. 2012). Como o *core* ou região central das sequências de UCEs são altamente conservadas elas são utilizadas para o anelamento de sondas (*probes*), a partir das quais as regiões flanqueadoras são lidas.

Atualmente, estudos vêm sendo conduzidos com Ostariophysi e novas *probe sets* foram desenhadas para capturar cerca de 1500-2000 loci de UCEs (Faircloth et al. 2020). Estes marcadores tem sido utilizados eficientemente para estudar radiações antigas em Gymnotiformes (Alda et al. 2019), entender padrões notáveis de diversidade e diversificação em Characiformes (Melo et al. 2021), e inferir relacionamentos filogenéticos em outros grupos particulares como Serrasalmidae (Mateussi et al. 2020), Trichomycteridae (Ochoa et al. 2020a), Loricariidae (Roxo et al. 2019), Pseudopimelodidae (Silva et al. 2021a) e Heptapteridae (Silva et al. 2021b). Assim, o uso de estes marcadores tem aumentado nos últimos anos, sendo altamente resolutivo no estudo de peixes de água doce neotropicais, sendo favorecido pelas suas características, como a obtenção de informação para estudar eventos de divergência recente e antiga (Faircloth et al. 2013; McGee et al. 2016; Alda et al. 2019) e o baixo custo relativo, dada a grande quantidade de dados gerados.

JUSTIFICATIVA

Erythrinoidea, composta por duas famílias (Erythrinidae e Tarumaniidae) e quatro gêneros (*Erythrinus*, *Hoplias*, *Hoplerythrinus* e *Tarumania*) é conhecida por suas adaptações fisiológicas que lhes permitem tolerar ambientes tóxicos e hipóxicos (Liem 1988; Moraes et al. 2004; Moron et al. 2009; Pelster 2021) e sua capacidade de residir em diversos habitats ao longo da sua distribuição geográfica, desde Costa Rica ao norte da Argentina (Oyakawa et al. 2013; de Pinna et al. 2017; Oyakawa and Mattox 2018). Devido a suas características, este clado amplamente distribuído pode representar um alvo interessante para estudos biogeográficos, fornecendo informações para investigar os efeitos da evolução da paisagem na formação da biodiversidade (Machado et al. 2018; Capobianco and Friedman 2019; Albert et al. 2020; Fontenelle et al. 2021). Além disso, os representantes de Erythrinoidea são reconhecidos por uma taxonomia desafiadora, onde complexos de espécies têm sido propostos baseados em sua variação cariotipica e uniformidade em dados merísticos e morfométricos ao longo da distribuição das espécies (Bertollo et al. 2000; Cioffi et al. 2012; Oyakawa et al. 2013; Martinez et al. 2016). No entanto, estudos taxonômicos e evolutivos tem se concentrado principalmente no gênero *Hoplias* (Mattox et al. 2006, 2014; Oyakawa and Mattox 2009; Azpelicueta et al. 2015; Rosso et al. 2016, 2018; Guimarães et al. 2021), enquanto os gêneros *Erythrinus* e *Hoplerythrinus* aguardam estudos integrativos com o intuito de avaliar detalhadamente o status taxonômico de suas espécies e investigar sua história evolutiva.

OBJETIVOS

Objetivo Geral:

O principal objetivo deste trabalho foi investigar padrões biogeográficos e cronológicos de diversificação para a superfamília Erythrinoidea e implementar um enfoque integrativo para investigar a diversidade e a história evolutiva de um grupo particular dentro de este clado, o gênero *Hoplerythrinus.*

Objetivos específicos

- Investigar e estimar datas de diversificação e reconstruir distribuições geográficas ancestrais em Erythrinoidea.
- Correlacionar padrões de diversificação de Erythrinoidea com eventos geomorfológicos e evolução da paisagem na região Neotropical.
- Avaliar o status taxonômico das espécies do gênero *Hoplerythrinus* integrando sequências de código de barras de DNA, um conjunto de dados filogenômicos de elementos ultraconservados (UCEs), informações morfológicas e uma ampla cobertura da sua distribuição geográfica
- Relacionar os padrões de diversidade dentro de *Hoplerythrinus* com sua história de diversificação.

BIBLIOGRAFIA

Agudelo-Zamora H.D., Tavera J., Murillo Y.D., Ortega-Lara A. 2020. The unknown diversity of the genus *Characidium* (Characiformes: Crenuchidae) in the Chocó biogeographic region, Colombian Andes: Two new species supported by morphological and molecular data. J. Fish Biol. 97:1662–1675.

Albert J.S., Tagliacollo V.A., Dagosta F. 2020. Diversification of Neotropical Freshwater Fishes. Annu. Rev. Ecol. Evol. Syst. 51:27–53.

Alda F., Tagliacollo V.A., Bernt M.J., Waltz B.T., Ludt W.B., Faircloth B.C., Alfaro M.E., Albert J.S., Chakrabarty P. 2019. Resolving Deep Nodes in an Ancient Radiation of Neotropical Fishes in the Presence of Conflicting Signals from Incomplete Lineage Sorting. Syst. Biol. 68:573–593.

Anjos M.S., Bitencourt J.A., Nunes L.A., Sarmento-Soares L.M., Carvalho D.C., Armbruster J.W., Affonso P.R.A.M. 2020. Species delimitation based on integrative approach suggests reallocation of genus in Hypostomini catfish (Siluriformes, Loricariidae). Hydrobiologia. 847:563–578.

Armbruster J.W., Lujan N.K., Bloom D.D. 2021. Redescription of the Guiana Shield Darter Species *Characidium crandellii* and *C. declivirostre* (Crenuchidae) with Descriptions of Two New Species. Ichthyol. Herpetol. 109:102–122.

Azpelicueta M. de las M., Benítez M., Aichino D., Mendez D. 2015. A new species of the genus *Hoplias* (Characiformes , Erythrinidae), a tararira from the lower Paraná River , in Misiones , Argentina. Acta Zool. Lilloana. 59:71–82.

Bejerano G., Pheasant M., Makunin I., Stephen S., Kent W.J., Mattick J.S., Haussler D. 2004. Ultraconserved elements in the human genome. Science (80-.). 304:1321–1325.

Bertollo L.A.C., Born G.G., Dergam J.A., Fenocchio A.S., Moreira-Filho O. 2000. A biodiversity approach in the neotropical Erythrinidae fish, *Hoplias malabaricus*. Karyotypic survey, geographic distribution of cytotypes and cytotaxonomic considerations. Chromosom. Res. 8:603–613.

Capobianco A., Friedman M. 2019. Vicariance and dispersal in southern hemisphere freshwater fish clades: a palaeontological perspective. Biol. Rev. 94:662–699.

De Carvalho D.C., Oliveira D.A.A., Pompeu P.S., Leal C.G., Oliveira C., Hanner R. 2011. Deep

barcode divergence in Brazilian freshwater fishes: The case of the São Francisco River basin. Mitochondrial DNA. 22:80–86.

Chakrabarty P., Faircloth B.C., Alda F., Ludt W.B., McMahan C.D., Near T.J., Dornburg A., Albert J.S., Arroyave J., Stiassny M.L.J., Sorenson L., Alfaro M.E. 2017. Phylogenomic Systematics of Ostariophysan Fishes: Ultraconserved Elements Support the Surprising Non-Monophyly of Characiformes. Syst. Biol. 66:881–895.

Cioffi M. de B., Molina W.F., Artoni R.F., Bertollo L.A.C. 2012. Chromosomes as Tools for Discovering Biodiversity – The Case of Erythrinidae Fish Family. In: Tirunilai P., editor. Recent Trends in Cytogenetic Studies - Methodologies and Applications. Rijeka, Croatia: InTech. p. 125–146.

Dergam J.A., Paiva S.R., Schaeffer C.E., Godinho A.L., Vieira F. 2002. Phylogeography and RAPD-PCR variation in *Hoplias malabaricus* (Bloch, 1794) (Pisces, Teleostei) in southeastern Brazil. Biologia (Bratisl). 387:379–387.

Dermitzakis E.T., Reymond A., Antonarakis S.E. 2005. Conserved non-genic sequences — an unexpected feature of mammalian genomes. Nat. Rev. Genet. 6:151–157.

DeSalle R. 2006. Species discovery versus species identification in DNA barcoding efforts: Response to Rubinoff. Conserv. Biol. 20:1545–1547.

Diniz D., Bertollo L.A.C. 2003. Karyotypic studies on *Hoplerythrinus unitaeniatus* (Pisces, Erythrinidae) populations. A biodiversity analysis. Caryologia. 56:303–313.

Faircloth B.C., Alda F., Hoekzema K., Burns M.D., Oliveira C., Albert J.S., Melo B.F., Ochoa L.E., Roxo F.F., Chakrabarty P., Sidlauskas B.L., Alfaro M.E. 2020. A Target Enrichment Bait Set for Studying Relationships among Ostariophysan Fishes. Copeia. 108:47–60.

Faircloth B.C., McCormack J.E., Crawford N.G., Harvey M.G., Brumfield R.T., Glenn T.C. 2012. Ultraconserved elements anchor thousands of genetic markers spanning multiple evolutionary timescales. Syst. Biol. 61:717–26.

Faircloth B.C., Sorenson L., Santini F., Alfaro M.E. 2013. A Phylogenomic Perspective on the Radiation of Ray-Finned Fishes Based upon Targeted Sequencing of Ultraconserved Elements (UCEs). PLoS One. 8.

Fontenelle J.P., Portella Luna Marques F., Kolmann M.A., Lovejoy N.R. 2021. Biogeography of the neotropical freshwater stingrays (Myliobatiformes: Potamotrygoninae) reveals effects of continent-scale paleogeographic change and drainage evolution. J. Biogeogr. 48:1406–

1419.
Fricke R., Eschmeyer W.N., Van der Laan R. 2022. ESCHMEYER'S CATALOG OF FISHES: GENERA, SPECIES, REFERENCES. Available from http://researcharchive.calacademy.org/research/ichthyology/catalog/fishcatmain.asp.
Garavello J.C., Ramirez J.L., Oliveira A.K. de, Britski H.A., Birindelli J.L.O., Galetti Jr P.M. 2021. Integrative taxonomy reveals a new species of Neotropical headstanding fish in genus *Schizodon* (Characiformes: Anostomidae). Neotrop. Ichthyol. 19:1–32.
Gayet M., Jégu M., Bocquentin J., Negri F.R. 2003. New Characoids from the Upper Cretaceous and Paleocene of Bolivia and the Mio-Pliocene of Brazil : Phylogenetic Position and Paleobiogeographic Implications. J. Vertebr. Paleontol. 23:28–46.
Gilbert P.S., Chang J., Pan C., Sobel E., Sinsheimer J.S., Faircloth B.C., Alfaro M.E. 2015. Genome-wide ultraconserved elements exhibit higher phylogenetic informativeness than traditional gene markers in percomorph fishes. Mol. Phylogenet. Evol. 92:140–146.
Giuliano-Caetano L., Jorge L.C., Moreira-Filho O., Bertollo L.A.C. 2001. Comparative Cytogenetic Studies on *Hoplerythrinus unitaeniatus* Populations (Pisces, Erythrindae). Cytologia (Tokyo). 66:39–43.
Guimarães K.L.A., Rosso J.J., González-Castro M., Souza M.F.B., Díaz de Astarloa J.M., Rodrigues L.R.R. 2021. A new species of *Hoplias malabaricus* species complex (Characiformes: Erythrinidae) from the Crepori River, Amazon basin, Brazil. .
Harrington R.C., Faircloth B.C., Eytan R.I., Smith W.L., Near T.J., Alfaro M.E., Friedman M. 2016. Phylogenomic analysis of carangimorph fishes reveals flatfish asymmetry arose in a blink of the evolutionary eye. BMC Evol. Biol. 16:1–14.
Hebert P.D.N., Cywinska A., Ball S.L., DeWaard J.R. 2003. Biological identifications through DNA barcodes. Proc. R. Soc. B Biol. Sci. 270:313–321.
Henschel E., Lujan N.K., Baskin J.N. 2020. *Ammoglanis natgeorum*, a new miniature pencil catfish (Siluriformes: Trichomycteridae) from the lower Atabapo River, Amazonas, Venezuela. J. Fish Biol. 97:1481–1490.
Hubert N., Hanner R. 2015. DNA Barcoding, species delineation and taxonomy: a historical perspective. DNA Barcodes. 3:44–58.
Hubert N., Hanner R., Holm E., Mandrak N.E., Taylor E., Burridge M., Watkinson D., Dumont P., Curry A., Bentzen P., Zhang J., April J., Bernatchez L. 2008. Identifying Canadian

freshwater fishes through DNA barcodes. PLoS One. 3.

Ivanova N. V., Zemlak T.S., Hanner R.H., Hebert P.D.N. 2007. Universal primer cocktails for fish DNA barcoding. Mol. Ecol. Notes. 7:544–548.

Lara A., Ponce de León J.L., Rodríguez R., Casane D., Côté G., Bernatchez L., García-Machado E. 2010. DNA barcoding of Cuban freshwater fishes: Evidence for cryptic species and taxonomic conflicts. Mol. Ecol. Resour. 10:421–430.

Lasso C., Meri J. 2001. Estructura comunitaria de la ictiofauna en herbazales y bosques inundables del bajo río Guanipa, cuenca del Golfo de Paria, Venezuela. Mem. Fund. La Salle Cienc. Nat. 155:73–90.

Lasso C.A., Morales-Betancourt M., Rivas-Lara T.S., Rincón C.E., González-Cañon G., Galvis-Galindo I. 2011. *Hoplias malabaricus* (Characiformes, Erythrinidae). Capitulo 7. In: Lasso C.A., Agudelo E., Jiménez-Segura L.F., Ramírez-Gil H., Morales-Betancourt M., Ajiaco-Martínez R.E., de Paula-Gutiérrez F., Usma J.S., Muñoz Torres S.E., Sanabria-Ochoa A.I., editors. I. Catálogo de los Recursos Pesqueros Continentales de Colombia. Serie Editorial Recursos Hidrobiológicos y Pesqueros Continentales de Colombia. Bogotá, Colombia: Instituto de Investigación de Recursos Biológicos Alexander von Humboldt (IAvH). p. 294–300.

Liem K.F. 1988. Form and function of lungs: The evolution of air breathing mechanisms. Integr. Comp. Biol. 28:739–759.

Loureiro M., de Sá R., Serra S.W., Alonso F., Lanés L.E.K., Volcan M.V., Calviño P., Nielsen D., Duarte A., Garcia G. 2018. Review of the family Rivulidae (Cyprinodontiformes, Aplocheiloidei) and a molecular and morphological phylogeny of the annual fish genus *Austrolebias* Costa 1998. Neotrop. Ichthyol. 16:1–20.

Machado C.B., Galetti P.M., Carnaval A.C. 2018. Bayesian analyses detect a history of both vicariance and geodispersal in Neotropical freshwater fishes. J. Biogeogr. 45:1313–1325.

Marrero C., Machado-allison A., González V., Velázquez J., Rodríguez-Olarte D. 1997. Los Morichales del Oriente de Venezuela: su importancia en la distribución y ecología de los componentes de la Ictiofauna dulceacuícola regional. Acta Biol. Venez. 17:65–79.

Martinez J.F., Lui R.L., Traldi J.B., Blanco D.R., Moreira-Filho O. 2016. Comparative Cytogenetics of *Hoplerythrinus unitaeniatus* (Agassiz, 1829) (Characiformes, Erythrinidae) Species Complex from Different Brazilian Hydrographic Basins. Cytogenet. Genome Res.

149:191–200.

Mateussi N.T.B., Melo B.F., Ota R.P., Roxo F.F., Ochoa L.E., Foresti F., Oliveira C. 2020. Phylogenomics of the Neotropical fish family Serrasalmidae with a novel intrafamilial classification (Teleostei: Characiformes). Mol. Phylogenet. Evol. 153:106945.

Mattox G.M.T., Bifi A.G., Oyakawa O.T. 2014. Taxonomic study of *Hoplias microlepis* (Günther, 1864), a trans-Andean species of trahiras (Ostariophysi: Characiformes: Erythrinidae). Neotrop. Ichthyol. 12:343–352.

Mattox G.M.T., Toledo-Piza M., Oyakawa O.T. 2006. Taxonomic Study of *Hoplias Aimara* (Valenciennes, 1846) and *Hoplias macrophthalmus* (Pellegrin, 1907) (Ostariophysi, Characiformes, Erythrinidae). Copeia. 2006:516–528.

McCormack J.E., Harvey M.G., Faircloth B.C., Crawford N.G., Glenn T.C., Brumfield R.T. 2013. A Phylogeny of Birds Based on Over 1,500 Loci Collected by Target Enrichment and High-Throughput Sequencing. PLoS One. 8.

McGee M.D., Faircloth B.C., Borstein S.R., Zheng J., Hulsey C.D., Wainwright P.C., Alfaro M.E. 2016. Replicated divergence in cichlid radiations mirrors a major vertebrate innovation. Proc. R. Soc. B Biol. Sci. 283:1–6.

Meier R., Zhang G., Ali F. 2008. The use of mean instead of smallest interspecific distances exaggerates the size of the “barcoding gap” and leads to misidentification. Syst. Biol. 57:809–813.

Melo B.F., Ochoa L.E., Vari R.P., Oliveira C. 2016. Cryptic species in the Neotropical fish genus *Curimatopsis* (Teleostei, Characiformes). Zool. Scr. 45:650–658.

Melo B.F., Sidlauskas B.L., Near T.J., Roxo F.F., Ghezelayagh A., Ochoa L.E., Stiassny M.L.J., Arroyave J., Chang J., Faircloth B.C., MacGuigan D.J., Harrington R.C., Benine R.C., Burns M.D., Hoekzema K., Sanches N.C., Maldonado-Ocampo J.A., Castro R.M.C., Foresti F., Alfaro M.E., Oliveira C. 2021. Accelerated Diversification Explains the Exceptional Species Richness of Tropical Characoid Fishes. Syst. Biol. 0:1–15.

Moraes G., Polez V.L., Iwama G.K. 2004. Biochemical responses of two erythrinidae fish to environmental ammonia. Braz. J. Biol. 64:95–102.

Moron S.E., de Andrade C.A., Fernandes M.N. 2009. Response of mucous cells of the gills of traíra (*Hoplias malabaricus*) and jeju (*Hoplerythrinus unitaeniatus*) (Teleostei: Erythrinidae) to hypo- and hyper-osmotic ion stress. Neotrop. Ichthyol. 7:491–498.

Nelson J.S., Grande T.C., Wilson M.V.H. 2016. Fishes of the World. Hoboken, New Jersey: John Wiley & Sons.

Ochoa L.E., Datovo A., DoNascimiento C., Roxo F.F., Sabaj M.H., Chang J., Melo B.F., Silva G.S.C., Foresti F., Alfaro M., Oliveira C. 2020a. Phylogenomic analysis of trichomycterid catfishes (Teleostei: Siluriformes) inferred from ultraconserved elements. Sci. Rep. 10:1–15.

Ochoa L.E., Melo B.F., García-Melo J.E., Maldonado-Ocampo J.A., Souza C.S., Albornoz-Garzón J.G., Conde-Saldaña C.C., Villa-Navarro F., Ortega-Lara A., Oliveira C. 2020b. Species delimitation reveals an underestimated diversity of Andean catfishes of the family Astroblepidae (Teleostei: Siluriformes). Neotrop. Ichthyol. 18:1–19.

Oliveira A.K. de, Garavello J.C. 2003. Fish assemblage composition in a tributary of the Mogi Guaçu river basin, southeastern Brazil. Iheringia. Série Zool. 93:127–138.

Oliveira C., Avelino G.S., Abe K.T., Mariguela T.C., Benine R.C., Ortí G., Vari R.P., Corrêa E Castro R.M. 2011. Phylogenetic relationships within the speciose family Characidae (Teleostei: Ostariophysi: Characiformes) based on multilocus analysis and extensive ingroup sampling. BMC Evol. Biol. 11:275.

Oyakawa O.T. 2003. Family Erythrinidae. In: Reis R.E., Kullander S.O., Ferraris C.J., editors. Check list of the freshwater fishes of South and Central America. Porto Alegre, Brazil: Edipucrs. p. 238–240.

Oyakawa O.T., Mattox G.. M.T. 2018. Family Erythrinidae - Wolf-fishes and Yarrows. In: van der Sleen P., Albert J.S., editors. Field Guide to the Fishes of the Amazon, Orinoco, and Guianas. Princeton University Press. p. 156–158.

Oyakawa O.T., Mattox G.M.T. 2009. Revision of the Neotropical trahiras of the *Hoplias lacerdae* species-group (Ostariophysi: Characiformes: Erythrinidae) with descriptions of two new species. Neotrop. Ichthyol. 7:117–140.

Oyakawa O.T., Toledo-Piza M., Mattox G.M.T. 2013. Erythrinidae. In: Queiroz L.J., Torrente-Vilara G., Ohara W.N., Silva-Pires T.H., Zuanon J., Doria C.R.C., editors. Peixes do rio Madeira, volume 2. São Paulo, Brazil: Dialeto. p. 351.

Patwardhan A., Ray S., Roy A. 2014. Molecular Markers in Phylogenetic Studies-A Review. J. Phylogenetics Evol. Biol. 02.

Pelster B. 2021. Using the swimbladder as a respiratory organ and/or a buoyancy structure—

Benefits and consequences. J. Exp. Zool. Part A Ecol. Integr. Physiol.:1–12.

Pennacchio L.A., Ahituv N., Moses A.M., Prabhakar S., Nobrega M.A., Shoukry M., Minovitsky S., Dubchak I., Holt A., Lewis K.D., Plajzer-Frick I., Akiyama J., De Val S., Afzal V., Black B.L., Couronne O., Eisen M.B., Visel A., Rubin E.M. 2006. In vivo enhancer analysis of human conserved non-coding sequences. Nature. 444:499–502.

Pereira L., Hanner R., Foresti F., Oliveira C. 2013a. Can DNA barcoding accurately discriminate megadiverse Neotropical freshwater fish fauna? BMC Genet. 14:1–14.

Pereira L.H.G., Pazian M.F., Hanner R., Foresti F., Oliveira C. 2011. DNA barcoding reveals hidden diversity in the Neotropical freshwater fish *Piabina argentea* (Characiformes: Characidae) from the Upper Paran Basin of Brazil. Mitochondrial DNA. 22:87–96.

Pereira T.L., Santos U., Schaefer C.E., Souza G.O., Paiva S.R., Malabarba L.R., Schmidt E.E., Dergam J.A. 2013b. Dispersal and vicariance of *Hoplias malabaricus* (Bloch, 1794) (Teleostei, Erythrinidae) populations of the Brazilian continental margin. J. Biogeogr. 40:905–914.

de Pinna M., Zuanon J., Rapp Py-Daniel L., Petry P. 2017. A new family of neotropical freshwater fishes from deep fossorial amazonian habitat, with a reappraisal of morphological characiform phylogeny (Teleostei: Ostariophysi). Zool. J. Linn. Soc. XX:1–13.

Puillandre N., Lambert A., Brouillet S., Achaz G. 2012. ABGD, Automatic Barcode Gap Discovery for primary species delimitation. Mol. Ecol. 21:1864–1877.

de Queiroz L.J., Cardoso Y., Jacot-des-Combes C., Bahechar I.A., Lucena C.A., Rapp Py-Daniel L., Sarmento Soares L.M., Nylinder S., Oliveira C., Parente T.E., Torrente-Vilara G., Covain R., Buckup P., Montoya-Burgos J.I. 2020. Evolutionary units delimitation and continental multilocus phylogeny of the hyperdiverse catfish genus *Hypostomus*. Mol. Phylogenet. Evol. 145:106711.

Ramirez J.L., Santos C.A., Machado C.B., Oliveira A.K., Garavello J.C., Britski H.A., Galetti P.M. 2020. Molecular phylogeny and species delimitation of the genus *Schizodon* (Characiformes, Anostomidae). Mol. Phylogenet. Evol. 153:106959.

Ratnasingham S., Hebert P.D.N. 2007. BOLD: The Barcode of Life Data System: Barcoding. Mol. Ecol. Notes. 7:355–364.

Ratnasingham S., Hebert P.D.N. 2013. A DNA-Based Registry for All Animal Species: The

Barcode Index Number (BIN) System. PLoS One. 8.

Reis R.E., Albert J.S., Di Dario F., Mincarone M.M., Petry P., Rocha L.A. 2016. Fish biodiversity and conservation in South America. J. Fish Biol. 89:12–47.

Rossini B.C., Oliveira C.A.M., Gonçalves De Melo F.A., De Araú Jo Bertaco V., Díaz De Astarloa J.M., Rosso J.J., Foresti F., Oliveira C. 2016. Highlighting *Astyanax* species diversity through DNA barcoding. PLoS One. 11:1–20.

Rosso J.J., González-Castro M., Bogan S., Cardoso Y.P., Mabragaña E., Delpiani M., Díaz J. de A. 2018. Integrative taxonomy reveals a new species of *Hoplias malabaricus* species complex (Teleostei: Erythrinidae). Ichthyol. Explor. Freshwaters.:1–18.

Rosso J.J., Mabragaña E., González-Castro M., Delpiani M., Avigliano E., Schenone, Díaz de Astarloa J.M. 2016. A new species of the *Hoplias malabaricus* species complex (Characiformes: Erythrinidae) from the La Plata River basin. Cybium. 40:199–208.

Roxo F.F., Ochoa L.E., Sabaj M.H., Lujan N.K., Covain R., Silva G.S.C., Melo B.F., Albert J.S., Chang J., Foresti F., Alfaro M.E., Oliveira C. 2019. Phylogenomic reappraisal of the Neotropical catfish family Loricariidae (Teleostei: Siluriformes) using ultraconserved elements. Mol. Phylogenet. Evol. 135:148–165.

Sánchez-Duarte P., Lasso C.A., González-Cañon G., Nieto-Torres S. 2011. *Hoplerythrinus unitaeniatus* (Characiformes, Erythrinidae). Capitulo 7. In: Lasso C.A., Agudelo E., Jiménez-Segura L.F., Ramírez-Gil H., Morales-Betancourt M., Ajiaco-Martínez R.E., de Paula-Gutiérrez F., Usma J.S., Muñoz Torres S.E., Sanabria-Ochoa A.I., editors. I. Catálogo de los Recursos Pesqueros Continentales de Colombia. Serie Editorial Recursos Hidrobiológicos y Pesqueros Continentales de Colombia. Bogotá, Colombia: Instituto de Investigación de los Recursos Biológicos Alexander von Humboldt (IAvH). p. 291–293.

Sandelin A., Bailey P., Bruce S., Engström P.G., Klos J.M., Wasserman W.W., Ericson J., Lenhard B. 2004. Arrays of ultraconserved non-coding regions span the loci of key developmental genes in vertebrate genomes. BMC Genomics. 5:1–9.

Santos U., Völcker C.M., Belei F.A., Cioffi M.B., Bertollo L.A.C., Paiva S.R., Dergam J.A. 2009. Molecular and karyotypic phylogeography in the Neotropical *Hoplias malabaricus* (Erythrinidae) fish in eastern Brazil. J. Fish Biol. 75:2326–2343.

Sassi F. de M.C., Perez M.F., Oliveira V.C.S., Deon G.A., de Souza F.H.S., Ferreira P.H.N., de Oliveira E.A., Hatanaka T., Liehr T., Bertollo L.A.C., Cioffi M. de B. 2021. High genetic

diversity despite conserved karyotype organization in the giant trahiras from genus *Hoplias* (Characiformes, Erythrinidae). Genes (Basel). 12:1–13.

Siepel A., Bejerano G., Pedersen J.S., Hinrichs A.S., Hou M., Rosenbloom K., Clawson H., Spieth J., Hillier L.D.W., Richards S., Weinstock G.M., Wilson R.K., Gibbs R.A., Kent W.J., Miller W., Haussler D. 2005. Evolutionarily conserved elements in vertebrate, insect, worm, and yeast genomes. Genome Res. 15:1034–1050.

Silva G.S.C., Melo B.F., Roxo F.F., Ochoa L.E., Shibatta O.A., Sabaj M.H., Oliveira C. 2021a. Phylogenomics of the bumblebee catfishes (Siluriformes: Pseudopimelodidae) using ultraconserved elements. J. Zool. Syst. Evol. Res.:1–11.

Silva G.S.C., Roxo F.F., Melo B.F., Ochoa L.E., Bockmann F.A., Sabaj M.H., Jerep F.C., Foresti F., Benine R.C., Oliveira C. 2021b. Evolutionary history of Heptapteridae catfishes using ultraconserved elements (Teleostei, Siluriformes). Zool. Scr. 50:543–554.

Simons C., Pheasant M., Makunin I. V., Mattick J.S. 2006. Transposon-free regions in mammalian genomes. Genome Res. 16:164–172.

Stephen S., Pheasant M., Makunin I. V., Mattick J.S. 2008. Large-scale appearance of ultraconserved elements in tetrapod genomes and slowdown of the molecular clock. Mol. Biol. Evol. 25:402–408.

Struck T.H., Feder J.L., Bendiksby M., Birkeland S., Cerca J., Gusarov V.I., Kistenich S., Larsson K.H., Liow L.H., Nowak M.D., Stedje B., Bachmann L., Dimitrov D. 2018. Finding Evolutionary Processes Hidden in Cryptic Species. Trends Ecol. Evol. 33:153–163.

Su G., Villéger S., Brosse S. 2019. Morphological diversity of freshwater fishes differs between realms, but morphologically extreme species are widespread. Glob. Ecol. Biogeogr. 28:211–221.

Valdez-Moreno M., Ivanova N. V., Elías-Gutiérrez M., Contreras-Balderas S., Hebert P.D.N. 2009. Probing diversity in freshwater fishes from Mexico and Guatemala with DNA barcodes. J. Fish Biol. 74:377–402.

Ward R.D., Zemlak T.S., Innes B.H., Last P.R., Hebert P.D.N. 2005. DNA barcoding Australia's fish species. Philos. Trans. R. Soc. Lond. B. Biol. Sci. 360:1847–1857.

Woolfe A., Goodson M., Goode D.K., Snell P., McEwen G.K., Vavouri T., Smith S.F., North P., Callaway H., Kelly K., Walter K., Abnizova I., Gilks W., Edwards Y.J.K., Cooke J.E., Elgar G. 2005. Highly conserved non-coding sequences are associated with vertebrate

development. PLoS Biol. 3.

Zarza E., Connors E.M., Maley J.M., Tsai W.L.E., Heimes P., Kaplan M., McCormack J.E. 2018. Combining ultraconserved elements and mtDNA data to uncover lineage diversity in a Mexican highland frog (Sarcohyla; Hylidae). PeerJ. 2018:1–25.

Zhang J., Kapli P., Pavlidis P., Stamatakis A. 2013. A general species delimitation method with applications to phylogenetic placements. Bioinformatics. 29:2869–2876.

CHAPTER 1

Landscape evolution drives continental diversification in Neotropical erythrinoid fishes (Teleostei, Characiformes)

Landscape evolution drives continental diversification in Neotropical erythrinoid fishes (Teleostei, Characiformes)

Abstract

Evolutionary diversification and prominent patterns of diversity in Neotropical freshwater fishes may be predicted by the effects of geomorphological settings on landscape evolution. Clades of aquatic taxa have been exposed to different geodynamics on the tectonically active Western margin and the passive Eastern margin of South America, associated with pulsed orogenic uplifts and continuous watershed migrations, respectively. Late Neogene uplifts of the Northern Andean cordilleras profoundly structured freshwater diversity gradients of northern South America by fragmenting the aquatic faunas of cis- and trans-Andean basins as well as portions of the sub-Andean Foreland basin, and merging faunas of the Western and Eastern Amazonia with the onset of the modern transcontinental Amazon River. Using phylogenomic and parametric biogeographic approaches we investigated biogeographical and chronological patterns of diversification for the geographically widespread characiform superfamily Erythrinoidea. Our initial edge-trimmed aligned matrix included 891,068 bp for 2,519 UCE loci and 29 ingroup erythrinoid lineages. The tree was time-calibrated using four fossils and BioGeoBEARS was used to conduct ancestral area estimation. Erythrinoidea is estimated to have originated in the Late Cretaceous *ca.* 80 Ma, with divergence of major clades during the Paleogene *ca.* 51-31 Ma. Erythrinidae diversified rapidly after the formation of the transcontinental Amazon River *ca.* 10 Ma, from eight lineages to at least 28 species today. A majority (22/28 or 78%) of erythrinid species are members of just three relatively young (<13 Ma) clades: *Erythrinus*, *Hoplerythrinus*, and *Hoplias malabaricus* group. Results indicate contrasting patterns of diversification on the two continental margins: a pulsed age-distribution of biogeographic events on the active Western Margin as predicted by discrete tectonic uplifts of the northern Andean cordilleras, and a continuous age-distribution on the passive Eastern Margin as predicted by a westward-propagating watershed migration. We conclude that historical changes in landscape connectivity have influenced diversification on the continentally distributed erythrinoid fish clade, and discuss alternative diversification scenarios consistent with available paleontological, paleogeographic and paleoenvironmental data.

Keywords: Amazon River, Erythrinidae, historical biogeography, phylogenomics, South America, ultraconserved elements.

Introduction

Neotropical freshwater fishes (NFF) includes more than 6,350 species representing ~18% of all fish species on Earth, and exhibiting the greatest phenotypic disparity and functional-trait diversity of any continental fish fauna (Reis et al. 2016; Su et al. 2019; Fricke et al. 2022). Understanding the drivers underlying the formation of such an immense biota requires interdisciplinary data from multiple sciences, including biological, paleontological, geological and paleoclimatic layers (Sanmartín 2012; Antonelli et al. 2018; Bicudo et al. 2019). The extent to which dynamic geological and climatic processes have shaped diversification and diversity gradients of freshwater fishes remains an active area of biodiversity research (Dias et al. 2014; Abreu et al. 2020; Albert et al. 2020; Fontenelle et al. 2021; Pio and Carvalho 2021). The ecophysiological restriction of obligate freshwater fishes to aquatic habitats has made them a useful target for biogeographic studies on the associations between organismal diversification and the evolution of river drainage networks (Smith et al. 2000; Fagan 2002; Burridge et al. 2006; Lovejoy et al. 2010; Dagosta and de Pinna 2017; Albert et al. 2018a; Oberdorff et al. 2019).

At a continental scale, NFF clades have been exposed to tectonic and erosional dynamics affecting river capture for tens of millions of years (Lundberg et al. 1998; Albert et al. 2011). Geological studies have demonstrated that the tempo and mode of river capture differ markedly in river basins draining the tectonically active Western margin (Struth et al. 2015; Mora et al. 2020; Siravo et al. 2021), and tectonically passive Eastern margin (Douglas 2016; Stokes et al. 2018; Calegari et al. 2021; Goldberg et al. 2021) of South America. The Western margin is characterized by high tectonic activity and mountain building as result of the interaction between the South American and Nazca plates, generating the uplifts of the Andean cordilleras, and the formation of present-day boundaries of major river drainage basins in South America (Hoorn et al. 2010; Albert et al. 2018b). The Andes, the longest continental mountain range on Earth, started its mountain building in the Late Cretaceous through a highly diachronous process, with differences in the timing of shortening, exhumation, and surface uplift between the northern, central, and southern portions

(Horton 2018; Boschman 2021). The Andes range constitutes a substantial driver of the diversification and distribution of freshwater fish taxa, pulsed uplifts of the Central Andes during the Oligocene (*ca.* 34-23 Ma) and the Northern Andes during the Neogene (*ca*. 22 - 2.6 Ma) (e.g. Leier et al. 2013; Garzione et al. 2017), drove vicariance and geodispersal among the major sedimentary basins of the sub-Andean foreland (Tagliacollo et al. 2015), cis- and trans-Andean regions (Albert et al. 2006; Montes et al. 2021), and contributed to the onset of the modern transcontinental Amazon River, assembled during the Late Miocene and Pliocene (Albert et al. 2018b).

The Late Neogene (*ca*. 10 – 4.5 Ma) formation of the transcontinental Amazon River is one of the most emblematic landscape reconfigurations in South America, with a pivotal role on diversification and shaping the biodiversity across the entire continent (Albert et al. 2018b, 2021; Defler 2019; Oberdorff et al. 2019). During the Paleogene, the sub-Andean foreland basin was the principal drainage axis of the continental interior, draining lands west to the Purus Arch and river systems draining the emerging Andes from the west, which configured a paleo proto-Orinoco-Amazonas basin that flowed northward to the Caribbean (López-Fernández and Albert 2011; Wesselingh and Hoorn 2011). This system was exposed to episodic marine transgressions and regressions that dramatically affected aquatic habitats over extensive areas (Hoorn et al. 2010; Jaramillo et al. 2017). Subsequently, the Andean back arc basin became flooded, forming the epicontinental Pebas mega wetland system, which expanded into the pericratonic Acre Basin and the intracratonic Solimões Basin during most of the Early and Middle Miocene (23-10 Ma) (Wesselingh and Hoorn 2011). The Pebas system covered an area of more than one million km^2, dominated by shallow lakes, estuaries, and bordered by lowland rainforest (Wesselingh et al. 2002). Finally, during the Late Miocene (~10 Ma), the uplift of the Vaupes Arch which separated the western Amazonian basins from the Orinoco basin (Mora et al. 2010), the rise of the Fitzcarrald Arch, and sediments produced by the erosive process of the uplifting Andes which covered the Purus Arch, contributed to the onset of the modern Amazon River draining towards east (Wesselingh and Hoorn 2011), in a series of river capture events that occurred over a time period of about 5.6–4.9 million years (Albert et al. 2018b).

The passive Eastern margin is the more stable portion of the South American platform, characterized by fault reactivation occurring during the Neogene and Quaternary (Saadi et al. 2002; Ribeiro 2006; Wendt et al. 2019; de Oliveira Andrades–Filho et al. 2021). Erosional forces, resulting in escarpment retreat and gradual migrations of watershed divides (i.e. watershed migrations) across tectonically stable landforms, have influenced the distribution of freshwater fishes along this margin (Ribeiro 2006; Albert and Carvalho 2011; Lima et al. 2017; Santos et al. 2021). Fish faunas have been exposed to historical and perennial landscape evolution on the passive margin, where the consequence of watershed migrations and stream captures on individual taxa can be highly varied. Stream captures may accelerate genetic divergence and speciation (i.e. geographic range fragmentation) in some taxa, sometimes leading to local extinction, while simultaneously facilitating organismal dispersal (geographic range expansion) in other taxa, reducing extinction risk, and exposing these taxa to new ecological opportunities for subsequent diversification (Burridge et al. 2006; Albert et al. 2018a, 2018b). In addition to stream captures, sea-level fluctuations have also had important effects on NFF diversification, especially in low-gradient river basins of the passive margin, promoting paleodrainage connections and isolations at different time scales (Ribeiro 2006; Dias et al. 2014; Albert et al. 2020). In particular, Pleistocene global climate oscillations have been demonstrated empirically to affect several NFF taxa, structuring genetic divergence patterns by altering shorelines and the connections among adjacent river basins (Thomaz et al. 2015, 2019; Wendt et al. 2019; Thomaz and Knowles 2020; Pio and Carvalho 2021).

Many prominent diversity patterns observed in NFF clades may be predicted by the effects of landscape evolution processes operating under different tectonic settings. Clades of aquatic taxa exposed to vicariance on a tectonically more active margin are expected to exhibit multiple and rapid bouts of speciation and extinction associated with pulsed orogenic uplifts. By contrast, clades inhabiting rivers of a passive continental margin with less tectonic activity are expected to undergo a more gradual accumulation of species under the influence of continuous watershed migration (e.g. de Sordi et al. 2018). These watershed rearrangements result from the escarpments slip or erosion-based fragmentation of headwater branches that allow freshwater taxa to expand the distribution to an adjacent river basin (Sacek et al. 2012; Salgado et al. 2014; Lima et al. 2021; Santos et al. 2021).

In this study, we test this landscape-evolution theory using biogeographical and chronological patterns of diversification in the characiform fish clade Erythrinoidea, employing phylogenomics with ultraconserved elements (UCEs: Faircloth et al. 2012, 2020) and parametric biogeographic approaches (Albert and Antonelli 2017). Erythrinoidea, as defined by previous molecular phylogenies (Arcila et al. 2018; Betancur-R. et al. 2019), is a clade composed of the enigmatic family Tarumaniidae, represented by a single highly-specialized species, *Tarumania walkerae*, that inhabits isolated pools in the forest floor of central Amazon rainforests (de Pinna et al. 2017), and the geographically widespread family Erythrinidae, which occurs in lentic and lotic habitats in most drainages of Central and South America, from Costa Rica to northern Argentina (Oyakawa and Mattox 2018). Three extant genera are currently recognized in Erythrinidae: *Erythrinus* Scopoli, 1777, *Hoplerythrinus* Gill, 1896 and *Hoplias* Gill, 1903. *Hoplias* is distributed across most hydrological basins in both trans- and cis-Andean regions and currently includes 14 valid species (Mattox et al. 2006; Oyakawa and Mattox 2009; Rosso et al. 2018; Fricke et al. 2022). *Erythrinus* and *Hoplerythrinus* are restricted to cis-Andean basins of the tropical South America, presenting an apparent lower diversity, with two and three valid species respectively (Fricke et al. 2022), however, to date no study has examined the taxonomic status of species in these two genera.

Widespread clades of obligate freshwater fishes represent a key target for biogeographical studies, providing materials for the study of the effects of landscape evolution on the formation of biodiversity (Machado et al. 2018; Capobianco and Friedman 2019; Albert et al. 2020; Fontenelle et al. 2021). Using a phylogenomic dataset, we investigate three major topics: (i) How does landscape evolution promote (or restrict) diversification in obligate freshwater fishes? (ii) How did the formation of the modern transcontinental Amazon River affect erythrinoid diversification? and (iii) Does the erythrinoid diversification have different patterns on active and passive continental margins? This biogeographic study of Erythrinoidea has a broad taxonomic and geographic coverage, including 11 of the 15 valid *Hoplias* species, plus several undescribed lineages distributed in both trans- and cis-Andean regions, and covering most of the geographic range of *Erythrinus* and *Hoplerythrinus*.

Material and Methods

Taxon sampling.— We chose representatives of each species/lineages to sequencing ultraconserved elements of the genome (UCEs; Faircloth et al. 2012, 2020) based on a previous and extensive DNA barcoding analysis plus morphological examination of 379 samples: 60 *Erythrinus*, 103 *Hoplerythrinus*, and 241 *Hoplias* (our unpublished data). Ingroup sampling comprised 74 samples distributed in the genera *Erythrinus* (15), *Hoplerythrinus* (24), *Hoplias* (34; including 11 out of the 14 current valid species), and *Tarumania* (1), with extensive geographic coverage of the clade distribution. Outgroup taxa were chosen based on previous characiform phylogenies (Betancur-R. et al. 2019; Melo et al. 2021b) and included 23 samples distributed in the characiform families Ctenoluciidae (1), Hepsetidae (1), Alestidae (2), Curimatidae (3), Anostomidae (4), Cynodontidae (3) and Serrasalmidae (9), Supplementary Table S1 summarizes voucher information with institutional acronyms following Sabaj (2020). Information about reads for each species appears in Supplementary Table S2.

DNA extraction, library preparation, target enrichment and sequencing.— Whole genomic DNA was extracted using the DNeasy Tissue kit (Qiagen) following the manufacturer's protocols and 2 µl of each sample were quantified using fluorometry (Qubit, Life Technologies) to verify an ideal concentration (>10 ng/µl). To enrich the libraries, we used the probeset developed for ostariophysan fishes to generate sequence data for about 2,700 UCE loci (Faircloth et al. 2020). Library preparation, sequencing and raw data processing were performed by Arbor Biosciences staff (Ann Arbor, MI, USA), using the following protocol: DNA library preparation by modifying the Nextera (Epicentre Biotechnologies) library preparation protocol for solution-based target enrichment (Faircloth et al. 2012) and increasing the number of PCR cycles following the tagmentation reaction to 20 (Faircloth et al. 2013). The Nextera library preparation protocol of in vitro transposition was used followed by PCR to prune the DNA and attach sequencing adapters, and the Epicentre Nextera kit was used to prepare transposase-mediated libraries with insert sizes averaging 100 bp (95% CI: 45 bp) (Adey et al. 2010).

To prepare libraries, whole genomic DNA (40 ng/ µl) was first sheared with a QSonica Q800R instrument and selected to modal lengths of approximately 500 nt using a dual-step SPRI bead

cleanup. Illumina sequencing libraries were prepared with a slightly modified version of the NEBNext(R) Ultra(TM) DNA Library Prep Kit for Illumina(R). After ligation of sequencing primers, libraries were amplified using KAPA HiFi HotStart ReadyMix (Kapa Biosystems) for six cycles using the manufacturer's recommended thermal profile and dual P5 and P7 indexed primers (Kircher et al. 2012). After purification with SPRI beads, libraries were quantified with the Quant-iT(TM) Picogreen(R) dsDNA Assay kit (ThermoFisher). Pools were enriched comprising 100 ng each of eight libraries (800 ng total) using the MYbaits(R) Target Enrichment system (MYcroarray) following manual version 3.0. After capture cleanup, the bead-bound library was resuspended in the recommended solution and amplified for 10 cycles using a universal P5/P7 primer pair and KAPA HiFi reagents. After purification, each captured library pool was quantified with PicoGreen, and combined with all other pools in projected equimolar ratios prior to sequencing. Sequencing was performed across two Illumina HiSeq paired-end 100 bp lanes using v4 chemistry.

Raw data analysis.— The PHYLUCE pipeline was used for processing target-enriched UCE data (Faircloth, 2016). Adapter contamination and low-quality bases were trimmed using the Illumiprocessor software pipeline developed by Faircloth (2013; https://github.com/faircloth-lab/illumiprocessor/). We assembled reads and generated consensus contigs for each sample using Velvet (Zerbino and Birney 2008) on VelvetOptimiser (https://github.com/tseemann/VelvetOptimiser). We then used the "match_contigs_to_probes" program implemented in PHYLUCE to align species-specific contigs to the ostariophysan probe-UCE set (Faircloth et al. 2020). We created a fasta file containing all data for all taxa. A custom Python program (seqcap_align_2.py) was used to align contigs using the MAFFT algorithm (Katoh et al. 2002) and to perform edge trimming. The trimmed alignment was used to generate two subsets, each including all taxa examined: 75% and 95% completeness matrices. All sequences are available at NCBI Sequence Read Archive submission under the code PRJNA000000 (SAMN0000000 – SAMN00000000).

Phylogenetic analyses.— We analyzed the 75% and 95% concatenated datasets using maximum likelihood (ML) in RAxML v8.1.3 (Stamatakis 2014), Bayesian inference (BI) in ExaBayes v1.4 (Aberer et al. 2014) and coalescent-based analyses in ASTRAL-III v.5.6.2 (Zhang et al. 2018). For

the ML analysis, we used a data-partitioning scheme for each UCE using the program PFinderUCE-SWSC-EN (Tagliacollo and Lanfear 2018) and, posteriorly, the data blocks were analyzed using PartitionFinder v2.1.1 (Lanfear et al. 2016) to performed substitution model selection. We performed ML inferences using five alternative runs on distinct parsimony starting trees to find the best ML tree, adopting the best-fit partitioning schemes and the GTRCAT substitution model. Pseudoreplicates of the ML analysis were obtained using the autoMRE function (Pattengale et al. 2010; number of bootstrap pseudoreplicates automatically determined) to assess bootstrap support for individual nodes.

The BI of the unpartitioned concatenated alignments was performed using two independent runs with two chains each (one cold and one hot) of 10 million generations each using the GTR+G model. The tree space was sampled every 1,000 generations to yield a total of 10,001 trees. The convergence of the posterior distribution was assessed examining the ESS>200 (effective sample size), and evaluating posterior trace distribution in Tracer v 1.6 (Rambaut et al. 2014). We generated the 50% most credible set of trees with 25% burn-in from the posterior distribution of possible topologies using the consensus algorithm of ExaBayes.

To account for gene-tree incongruence due to incomplete lineage sorting (ILS; Alda et al. 2019), a coalescent analysis of species tree was inferred from individual gene trees using a two-step process. First, we used PHYLUCE to resample the 75% and 95% complete matrices by loci and generated a best tree using RAxML for each of those matrices. Then, we used ASTRAL-III v5.6.2 (Zhang et al. 2018) to infer species trees from each of the best tree subsets of loci and generated a majority-rule consensus.

Divergence time estimates.— We used BEAST v2.6.3 (Bouckaert et al. 2014) to estimate divergence times employing the 95% complete edge-trimmed matrix under an uncorrelated log-normal relaxed molecular clock (Drummond et al. 2006). We used a total of five calibration priors that includes a secondary root constraint and four fossil priors. i) A maximum age was assigned to the root of the tree (i.e., including all the taxa), representing the most recent common ancestor (MRCA) of Characoidea and the clade composed by Alestoidea, Erythrinoidea and Curimatoidea (Betancur-R. et al. 2019; Melo et al. 2021b). This calibration point was implemented as a normally

distributed prior with age offset of 116.5 Ma (sigma = 10.5) following the estimation of the phylogeny of Characiformes (Melo et al. 2021b) that is also consistent with the time-calibrated molecular phylogeny of Serrasalmidae and relatives (Kolmann et al. 2021). ii) Isolated teeth from the Cuisian or upper Ypresian Stage of the early Eocene Epoch, approximately 54.8–49.0 Ma (de la Peña 1996; Zanata and Vari 2005). These fragments share similarities with *Alestes*, *Brycinus* and *Bryconaethiops* (Zanata and Vari 2005) and were used to calibrate the node uniting *Alestes* + *Bryconaethiops* (see details in Melo et al. 2021). We set this prior using a lognormal distribution, mean (in real space) = 5.0, logSD = 1.0, and offset = 49.0. iii) We used †*Leporinus scalabrinii* from the Ituzaingó Formation (Late Miocene 9-6 Ma), Paraná, Entre Ríos Providence, Argentina, which has an overall morphology consistent with living species of *Megaleporinus* (Ramirez et al. 2017) but also has been place in clade with *Leporinus striatus*+*Abramites* (Bogan et al. 2012). We therefore assigned this calibration fossil to the MRCA of *Leporinus striatus*, *Megaleporinus* and *Abramites*, setting a lognormal distribution, mean (in real space) = 5.0, logSD = 1.0, and offset = 6.0. iv) We used †*Cyphocharax mosesi* from Tremembé Formation (Oligocene-Miocene boundary at approximately 23.8 Ma), Taubaté basin, São Paulo, Brazil (Travassos and Santos 1955) and possibly related to *C. gilbert*, *C. modestus* and/or *C. santacatarinae* (Malabarba 1996; Melo et al. 2021a). We used this fossil to calibrate the node uniting *Curimatella* and *Cyphocharax*, setting a log-normal distribution, mean (in real space) = 5.0, logSD = 1.0, and offset = 23.8. v) Partial left premaxilla preserving four teeth in the outer teeth row of the extant species *Colossoma macropomum* from the La Venta Formation, upper Magdalena valley dated to the Middle Miocene Honda group of Colombia (Lundberg 1997). Dating and magnetostratigraphic correlations indicates that the Honda group ranges from 13.5 to 11.6 Ma (Flynn et al. 1997). Here we used this fossil evidence to calibrate the crown age of *Colossoma*, setting a log-normal distribution, mean (in real space) = 2.0, logSD = 1.0, and offset = 11.6. We applied an extra constraint to the *Hoplerythrinus* clade, defining *Hoplerythrinus unitaeniatus* as monophyletic, following the topology obtained from the 75% complete matrix.

The BEAST analysis was conducted using a birth-death model prior for diversification likelihood values under the GTR model of molecular evolution with gamma-distributed rate of heterogeneity for the entire matrix. BEAST ran 200 million generations with tree space sampled every 20,000 generations. We used Tracer v1.6 (Rambaut et al. 2014) to evaluate convergence and to verify if

effective sample size (ESS) was at least 200 for all parameters. A consensus tree was built using TreeAnnotator v2.6.3 (Bouckaert et al. 2014). We discarded 10% of the initial sample as burn-in. All clade-age estimates are presented as the mean plus 95% highest posterior density (HPD) values.

Parametric biogeography and diversification.— To infer the biogeographic history of Erythrinoidea, we carried out ancestral area reconstruction analysis using the R package "BioGeoBEARS" (Matzke 2013, 2018), comparing the likelihoods (lnL) and the corrected Akaike Information Criterion (AICc) to choose the best fitting of three models with a two-time slices configuration. These three models are the dispersal–extinction–cladogenesis (DEC) model (Ree and Smith 2008), as well as likelihood interpretations of the DIVA model (Ronquist 1997) and the BayArea model (Landis et al. 2013). We decided not to evaluate the biogeographic models including the funder-event speciation or jump-dispersal (J) parameter. Besides concerns about this parameter (Ree and Sanmartín 2018), obligate freshwater fishes usually are constrained by river connectivity and they are unlikely to undergo a jump speciation process as is favored with this parameter.

We defined 10 biogeographic areas, by merging freshwater ecoregions of the world (Abell et al. 2008): Northern Pacific drainages and Central America (C); Magdalena-Cauca-Sinú (Y); Maracaibo-Caribbean drainages (M); Orinoco (O); Western Amazon (W); Eastern Amazon (E); Amazon Brazilian Shield (B); São Francisco and Northeastern drainages (F); Southeastern Atlantic drainages (A); La Plata basin (L). The western and eastern Amazon lowlands were separated by the Purus Arch, restricting the Western Amazon (W) to the area west of the Purus Arch, and expanding the Eastern Amazon (E) to include the Amazonian lowland area east of the Purus Arch. Considering that *Hoplias malabaricus* inhabits seven of the 10 biogeographic areas proposed, a maximum of seven combined areas was allowed at each node of the time-calibrated tree.

We pruned our time-calibrated tree by selecting a single individual for each hypothesized species, except the widespread *Hoplerythrinus unitaeniatus*, which was represented by four terminals, given the presence of multiple genetic units (data not shown). Data on the geographic distributions of erythrinoids were taken from the original species descriptions, voucher localities and related

taxonomy literature (Mattox et al. 2006; Oyakawa and Mattox 2009; Mattox et al. 2014; Rosso et al. 2018; Guimarães et al. 2021). We incorporated the two time slices in accordance with major geomorphological changes in the continent with potential relevance to dispersal of Neotropical freshwater fishes: (i) a first time slice >10 Ma and (ii) a second time slice 10 Ma to present. Connections between areas were modified in each time slice, establishing the link between Western and Eastern Amazon after 10 Ma according with the formation of the transcontinental Amazon River (Albert et al. 2018b, 2021) and disconnecting trans-Andean areas from cis-Andean areas according with the uplift of the northern Andes cordilleras in the Middle Miocene (Albert et al. 2006; Montes et al. 2021). Additionally, we constructed a semi-logarithmic lineage-through time (LTT) plot by using the function *ltt* in the R package "phytools" (Revell 2012), to visualize temporal variations in diversification rates.

Results

Phylogenomic analyses.— Sequencing and data filtering yielded an initial edge-trimmed aligned matrix comprising 891,068 base pairs (bp) in 2,519 UCE loci for 97 specimens (74 Erythrinoidea and 23 outgroup taxa). Mean locus length after alignment and trimming was 353.7 nucleotides (range: 101–1,276). From the initial edge-trimmed alignment we assembled and analyzed two UCE matrices that differed in their inclusion of loci with varying amounts of missing data: the 75% complete matrix (1,133 loci; 459,670 bp) and the 95% complete matrix (91 loci; 17,715 bp).

All three genera, *Erythrinus*, *Hoplerythrinus*, and *Hoplias* were resolved as monophyletic in all estimated trees (Fig. 1). Reconstructions based on the 75% complete matrix yielded nearly identical topologies with high node support values for the three methods: ML with 83% of nodes > 85% and BI with 9.6.8% of nodes = 1 (Fig. 1; Supplementary Fig. S1), ASTRAL-III with 86.5% of nodes > 0.75 (Supplementary Fig. S2). Similar topologies were obtained with the 95% complete matrix, except for the placement of specimens within *Hoplerythrinus*, which revealed differences between ML and BI reconstructions (Supplementary Fig. S3). The placement of specimens within *Hoplerythrinus* in the analyses with 95% complete matrix also presented differences regarding the results obtained with the 75% complete matrix. Relationships inside *Hoplerythrinus* obtained with Astral-III using the 95% matrix were nearly identical with trees estimated using the 75% matrix,

although some small differences inside the *Hoplias malabaricus* group were observed (Supplementary Fig S4), as for example the placement of *Hoplias teres*, *Hoplias microlepis* and *Hoplias* sp. Xingu. Overall, all inferred trees using both matrices recovered similar topologies with primary differences inside *Hoplerythrinus*.

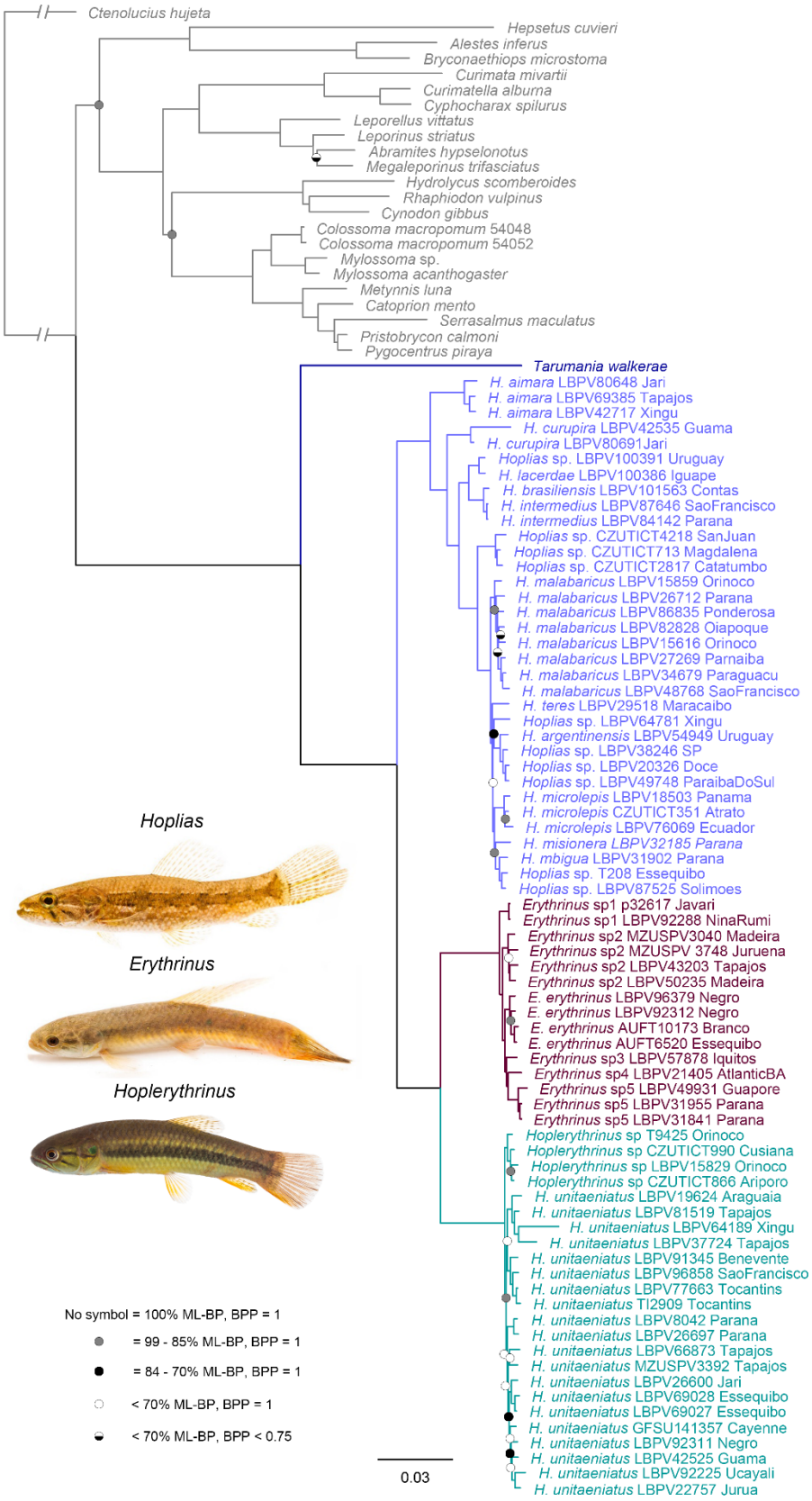
Ctenolucius hujeta
Hepsetus cuvieri
Alestes inferus
Bryconaethiops microstoma
Curimata mivartii
Curimatella alburna
Cyphocharax spilurus
Leporellus vittatus
Leporinus striatus
Abramites hypselonotus
Megaleporinus trifasciatus
Hydrolycus scomberoides
Rhaphiodon vulpinus
Cynodon gibbus
Colossoma macropomum 54048
Colossoma macropomum 54052
Mylossoma sp.
Mylossoma acanthogaster
Metynnis luna
Catoprion mento
Serrasalmus maculatus
Pristobrycon calmoni
Pygocentrus piraya
Tarumania walkerae
H. aimara LBPV80648 Jari
H. aimara LBPV69385 Tapajos
H. aimara LBPV42717 Xingu
H. curupira LBPV42535 Guama
H. curupira LBPV80691Jari
Hoplias sp. LBPV100391 Uruguay
H. lacerdae LBPV100386 Iguape
H. brasiliensis LBPV101563 Contas
H. intermedius LBPV87646 SaoFrancisco
H. intermedius LBPV84142 Parana
Hoplias sp. CZUTICT4218 SanJuan
Hoplias sp. CZUTICT713 Magdalena
Hoplias sp. CZUTICT2817 Catatumbo
H. malabaricus LBPV15859 Orinoco
H. malabaricus LBPV26712 Parana
H. malabaricus LBPV86835 Ponderosa
H. malabaricus LBPV82828 Oiapoque
H. malabaricus LBPV15616 Orinoco
H. malabaricus LBPV27269 Parnaiba
H. malabaricus LBPV34679 Paraguacu
H. malabaricus LBPV48768 SaoFrancisco
H. teres LBPV29518 Maracaibo
Hoplias sp. LBPV64781 Xingu
H. argentinensis LBPV54949 Uruguay
Hoplias sp. LBPV38246 SP
Hoplias sp. LBPV20326 Doce
Hoplias sp. LBPV49748 ParaibaDoSul
H. microlepis LBPV18503 Panama
H. microlepis CZUTICT351 Atrato
H. microlepis LBPV76069 Ecuador
H. misionera LBPV32185 Parana
H. mbigua LBPV31902 Parana
Hoplias sp. T208 Essequibo
Hoplias sp. LBPV87525 Solimoes
Erythrinus sp1 p32617 Javari
Erythrinus sp1 LBPV92288 NinaRumi
Erythrinus sp2 MZUSPV3040 Madeira
Erythrinus sp2 MZUSPV 3748 Juruena
Erythrinus sp2 LBPV43203 Tapajos
Erythrinus sp2 LBPV50235 Madeira
E. erythrinus LBPV96379 Negro
E. erythrinus LBPV92312 Negro
E. erythrinus AUFT10173 Branco
E. erythrinus AUFT6520 Essequibo
Erythrinus sp3 LBPV57878 Iquitos
Erythrinus sp4 LBPV21405 AtlanticBA
Erythrinus sp5 LBPV49931 Guapore
Erythrinus sp5 LBPV31955 Parana
Erythrinus sp5 LBPV31841 Parana
Hoplerythrinus sp T9425 Orinoco
Hoplerythrinus sp CZUTICT990 Cusiana
Hoplerythrinus sp LBPV15829 Orinoco
Hoplerythrinus sp CZUTICT866 Ariporo
H. unitaeniatus LBPV19624 Araguaia
H. unitaeniatus LBPV81519 Tapajos
H. unitaeniatus LBPV64189 Xingu
H. unitaeniatus LBPV37724 Tapajos
H. unitaeniatus LBPV91345 Benevente
H. unitaeniatus LBPV96858 SaoFrancisco
H. unitaeniatus LBPV77663 Tocantins
H. unitaeniatus TI2909 Tocantins
H. unitaeniatus LBPV8042 Parana
H. unitaeniatus LBPV26697 Parana
H. unitaeniatus LBPV66873 Tapajos
H. unitaeniatus MZUSPV3392 Tapajos
H. unitaeniatus LBPV26600 Jari
H. unitaeniatus LBPV69028 Essequibo
H. unitaeniatus LBPV69027 Essequibo
H. unitaeniatus GFSU141357 Cayenne
H. unitaeniatus LBPV92311 Negro
H. unitaeniatus LBPV42525 Guama
H. unitaeniatus LBPV92225 Ucayali
H. unitaeniatus LBPV22757 Jurua
Hoplias
Erythrinus
Hoplerythrinus
No symbol = 100% ML-BP, BPP = 1
= 99 - 85% ML-BP, BPP = 1
= 84 - 70% ML-BP, BPP = 1
< 70% ML-BP, BPP = 1
< 70% ML-BP, BPP < 0.75
0.03

866

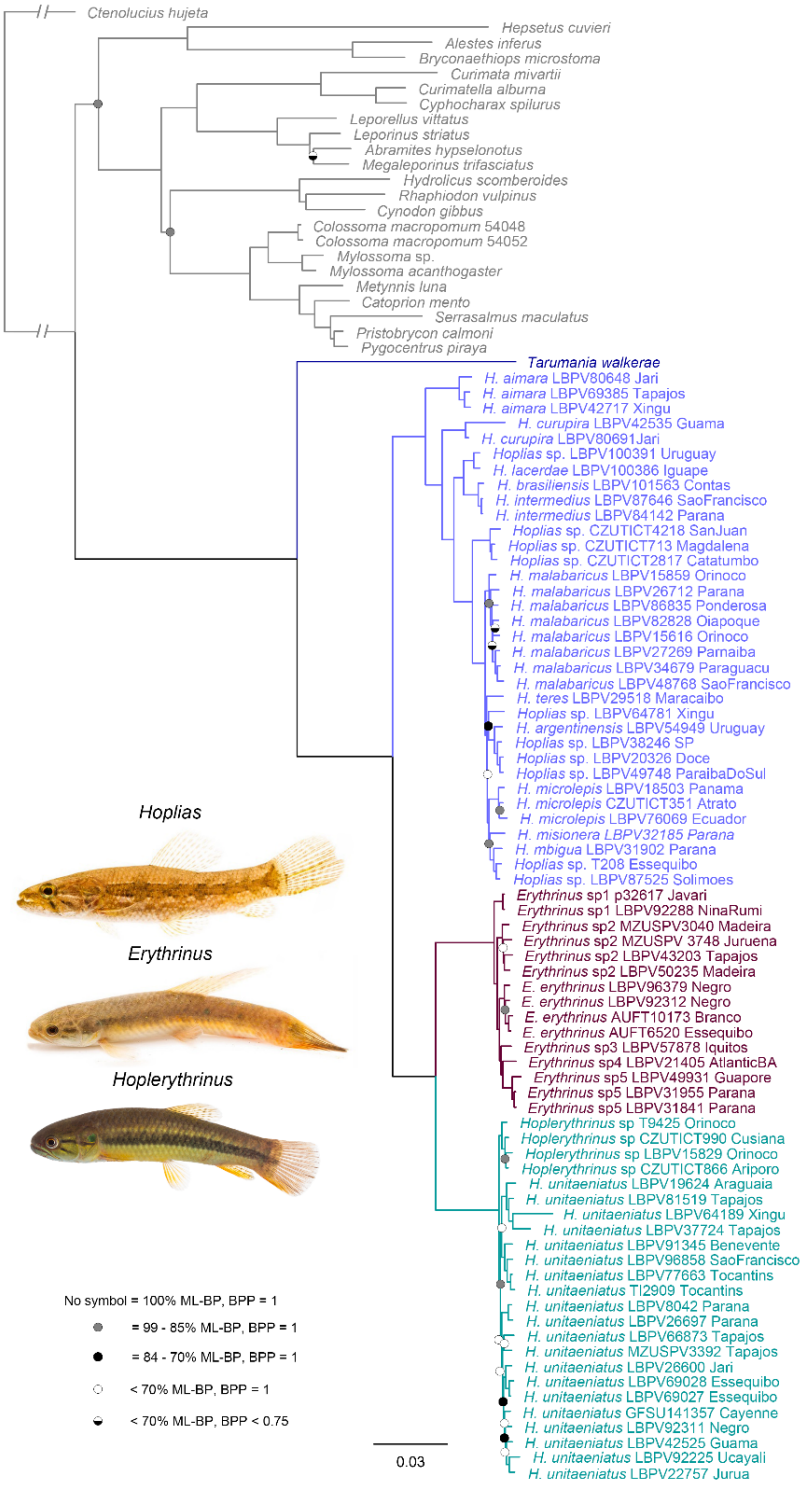

Figure 1. Phylogenetic relationships of Erythrinoidea based on a maximum likelihood analysis of the partitioned 75% complete matrix of ultraconserved elements (1,133 loci with 459,670 bp). Bayesian analysis of the same matrix (75%, edge-trimmed, unpartitioned; data S1) recovered the

same topology. ML-BP = ML bootstrap support values; BPP = Bayesian posterior probabilities. Photographs: *Hoplias* and *Erythrinus* (Martin Taylor), *Hoplerythrinus* (Jorge García-Melo).

Divergence time and ancestral area estimates. — According to our time-tree estimation based on the concatenated 95% complete matrix and five calibration points (Fig. 2), the crown age of Erythrinoidea is estimated in the Late Cretaceous *ca*. 80 Ma (123.1–40.8 Ma, 95% HPD) and the crown age of Erythrinidae is dated to the Eocene *ca*. 50 Ma (96.7–26.2, 95% HPD). The crown age estimated for *Hoplias* is dated to the Late Paleogene *ca*. 34 Ma (66.8–18.3 Ma, 95% HPD), with most internal splits occurring during Middle–Late Miocene and Pliocene. On the other hand, younger crown ages in the Late Neogene were estimated for *Erythrinus* (*ca*. 9.5 Ma, 22.3–4.4 Ma, 95% HPD) and *Hoplerythrinus* (*ca*. 7.1, 15.3–4.1 Ma, 95% HPD).

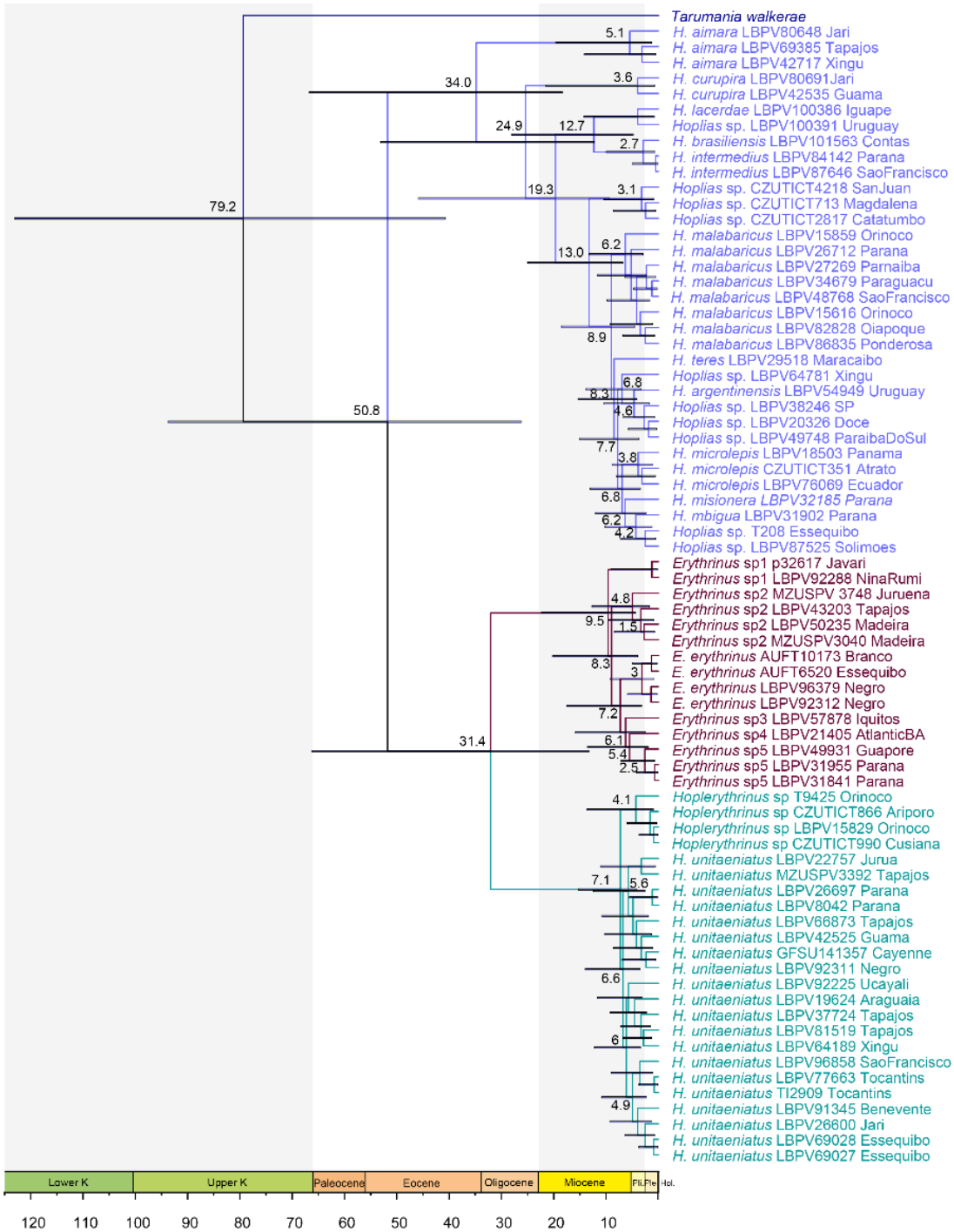

Figure 2. Fossil-calibrated phylogeny of Erythrinoidea inferred from the concatenated 95%-complete matrix of ultraconserved elements (91 loci; 17,715 bp). Numbers at nodes represent mean divergence time estimates and error bars represent 95% highest posterior densities (HPD). Timescale in millions of years ago. K = Cretaceous; Pli. = Pliocene; Ple. = Pleistocene; Hol. = Holocene.

Likelihood scores and ancestral area estimation under each of the models did not vary much (Table 1). The AICc model selection supported BayAreaLike as best-fit model for our data (Table 1), with less than five AICc units lower than the second-best model (DIVALIKE). Probably the slightly best fit to the BayArea model is related with the presence of geographically widespread species in our datasets. The presence of *Hoplias malabaricus* in seven of the 10 biogeographic areas and the set of a maximum of seven combined ancestral areas at nodes could favor higher likelihood values for this model.

Table 1. Two-time slice models implemented in BioGeoBEARS for ancestral range estimation of Erythrinoidea. Log-likelihood (lnL), dispersal (d) and extinction (e) parameters, Corrected Akaike Information criterion (AIC), and difference in AICc values compared to the best-fit model (ΔAIC) are reported.

Model	**lnL**	**d**	**e**	**AICc**	**ΔAIC**
BayAreaLike	-153.6	0.0475	0.1001	311.6	0
DIVALike	-156.03	0.0675	0.0659	316.46	4.9
DEC	-156.64	0.0439	0.0255	317.68	6.1

The reconstruction of ancestral ranges indicates an initial divergence of major clades (*Hoplias* (*Erythrinus*, *Hoplerythrinus*)) under a paleolandscape during the Paleogene *ca*. 51–31 Ma (Fig. 3A). Initial divergence events in *Hoplias* occurred during Late Eocene and Oligocene (35–23 Ma; clades 1 and 3). We detected subsequent dispersal to the La Plata basin and adjacent regions during the Miocene after *ca*. 20 Ma (Clade 4), and divergence of the earliest trans-Andean clade during Middle Miocene *ca*. 13 Ma (Clade 5). We also detected rapid diversification on the modern landscape after the onset of the transcontinental Amazon River (Fig. 3A) *ca*. 10 Ma forming most (26/28 or 93%) extant erythrinid species. These events resulted in the formation of polyphyletic faunas in peripheral Trans-Andean (C, Y, M), La Plata and Southern Atlantic (L, A), and São Francisco and Northeastern drainages (F) areas (Fig 3A), each with multiple independent origins in the Late Neogene (*ca*. 10–2.6 Ma). The LTT plot (Fig 3B) indicates that extant Erythrinidae diversified rapidly in the Late Neogene and Quaternary (from 8 lineages at 10 Ma to 29 hypothesized species today), with a majority (22/28 or 78%) of species being members of just three clades younger than 13 Ma: the *Hoplias malabaricus* group (Clade 6), *Erythrinus* (Clade 7) and *Hoplerythrinus* (Clade 8).

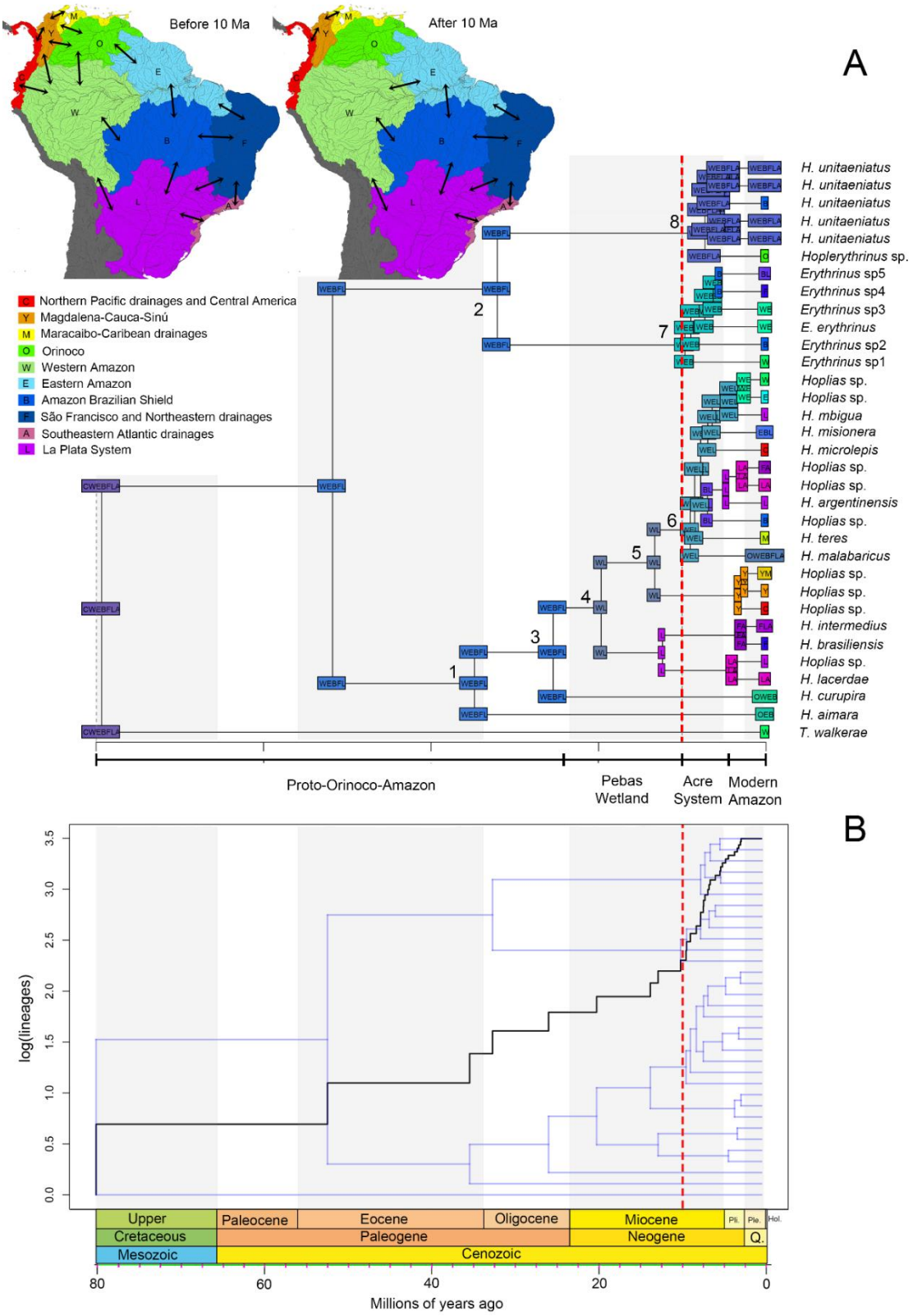

Figure 3. Diversification of Erythrinoidea in time and space. A. Ancestral area estimation of Erythrinoidea from BayAreaLike model implemented in BioGeoBEARS, with maps showing

biogeographic areas considered in this study under a two time-slice configuration. Colored boxes at tips indicate distributions of extant species; pie charts at internal tree nodes indicate relative probabilities of alternative ancestral areas. Vertical dashed red lines indicate initial time of formation of modern transcontinental Amazon River (*ca*. 10 Ma). Numbers in nodes indicate clades 1–8. **B**. Semi-logarithmic lineage-through time (LTT) plot (black) and time-calibrated phylogeny (blue) of Erythrinoidea showing the cumulative number of lineages over time.

Western and Eastern continental margins.— Patterns of erythrinoid diversification differ substantially under the influence of landscape evolution along the tectonically active Western margin and tectonically passive Eastern margin of South America. Results indicate changes in riverine connections among basins of the Western margin tending to be concerted through time (Fig. 4), associated with semi-discrete episodes of mountain uplift in the Andean Cordilleras (Restrepo-Moreno et al. 2019; Noriega-Londoño et al. 2020), and the episodic formation of semi-permeable filter corridors among sedimentary basins of the sub-Andean Foreland basin (Albert and Reis 2011; Tagliacollo et al. 2015). By contrast, changes in riverine connections on escarpments of the passive Eastern margin are distributed more continuously through time, largely due to the gradual migrations of watershed divides and river knickpoints across tectonically stable landforms (Fig. 4).

Biogeographic events in erythrinoid evolution on the Western margin appear to be grouped into three distinct age clusters (horizontal rose bands; Fig. 4B) during the Early Miocene (*ca*. 19.3–12.7 Ma), Middle-Late Miocene (*ca*. 13.0–3.8 Ma), and Quaternary (*ca*. 3.1–1.2 Ma), corresponding closely with major orogenic uplifts of the Northern Andean cordilleras (Mora et al. 2020; Boschman 2021). Events on the Eastern margin exhibit a more continuous age distribution from the Eocene-Oligocene boundary *ca*. 34 Ma to the Pliocene *ca*. 3.6 (Fig. 4B).

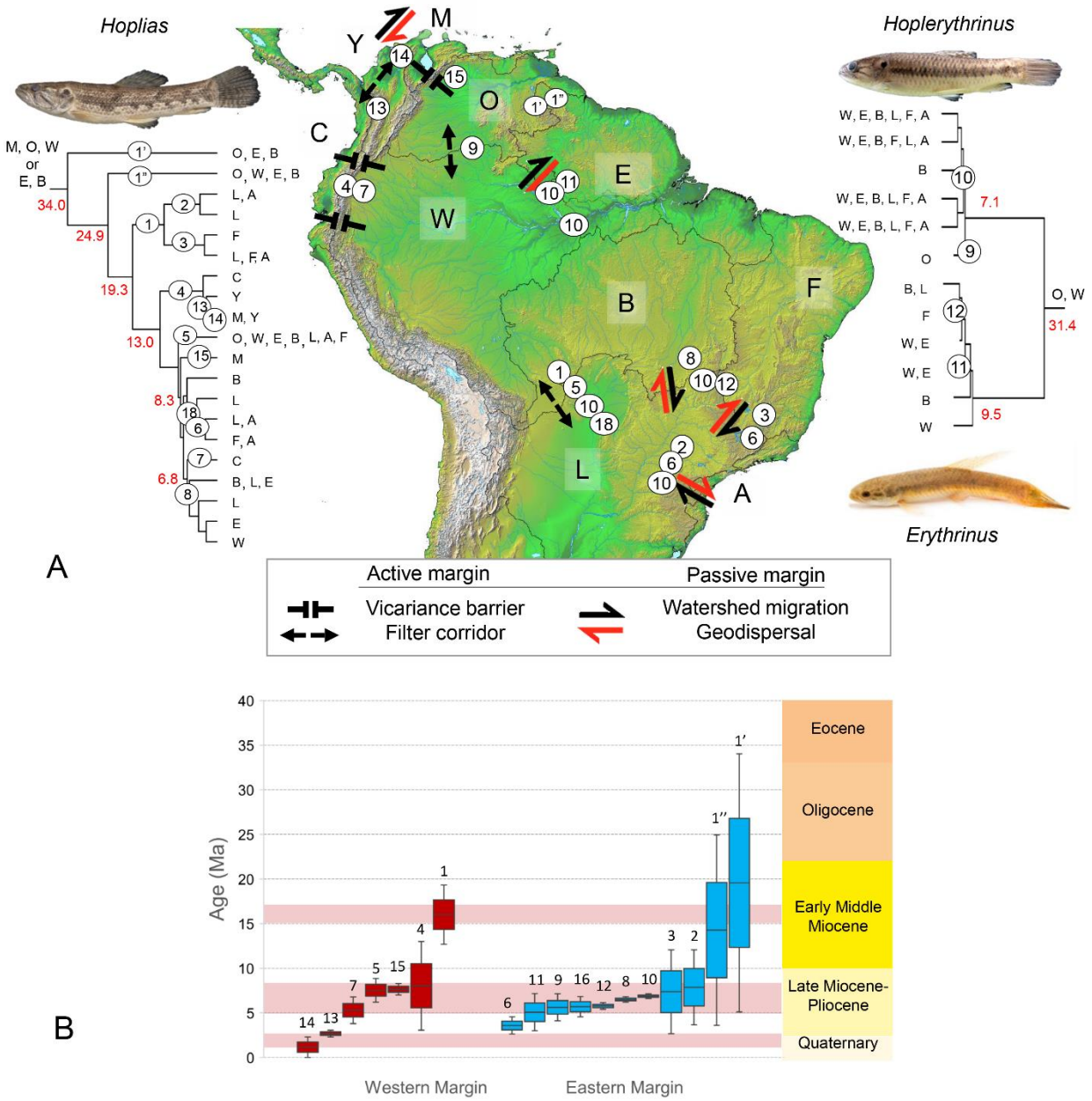

Figure 4. Estimated mean dates for biogeographic events in erythrinid diversification on tectonically active (Western) and passive (Eastern) continental margins. A. Phylogenies of species in erythrinid genera from Fig. 3A. Numbered circles represent biogeographic (dispersal and vicariance) events dated using estimates of landscape events in the geological literature (see Supplementary Table 3). Lettered labels at tree tips (species) represent biogeographic areas on the map. Red numbers at tree nodes represent mean divergence time estimates in millions of years. B. Lineage-age distribution of biogeographic events for clades in panel A. Estimates are reported for minimum, median, and maximum (mean dates from Fig. 2) event age (See Supplementary Table

S3). Ages of tectonic uplifts indicated by horizontal rose bars. Note pulsed age-distribution of biogeographic events in clades on the active Western margin, and the more continuous age-distribution of events on the passive Eastern margin. Age-range estimates of box plots in panel B correspond to numbered nodes and biogeographic events in panel A. Note opposite directions of watershed migration and geodispersal routes.

Discussion

We investigated the diversification history of erythrinoid fishes combining data from genomic (UCEs), paleontological (fossil calibrations), biogeographic, and geological sources. Our estimates place the origin of Erythrinoidea in the Late Cretaceous *ca*. 80 Ma (123.1–40.8 Ma, 95% HPD) and indicate divergence of major clades during the Paleogene *ca*. 51-31 Ma on a paleolandscape quite different from the modern. Erythrinids underwent rapid diversification after *ca*. 10 Ma (Fig. 3), corresponding to the major geological changes responsible for the onset of the modern transcontinental Amazon River and the configuration of the modern landscapes of tropical South America (Hoorn et al. 2010; Albert et al. 2018b). We also recovered two distinct patterns of diversification under the influence of landscape evolution along the different continental margins: a pulsed distribution of biogeographic events through time on the tectonically active Western margin, and a more continuous distribution of events through time on the tectonically passive Eastern margin (Fig. 4). Below we discuss what our findings imply about the divergence history of this geographically widespread clade of freshwater fishes in light of landscape evolution dynamics. We also discuss different scenarios for diversification according to a timeline implied by the known fossil record considering paleogeographic and paleoenvironmental data.

Origins and Early Diversification.— A recently-published time-calibrated phylogeny of Characoidei (including Erythrinoidea) indicates ancient Paleogene origins of the major family-level clades, and identified shifts to higher net diversification rates during the Oligocene at *ca*. 30 Ma (Melo et al. 2021b). However, the areas of origin and diversification history for the major characoid subclades remain poorly understood. Our analysis reveals that Erythrinoidea evolution traces back to the Late Cretaceous at *ca*. 80 Ma (123–41 Ma), and the origin of Erythrinidae to the Eocene at *ca*. 50 Ma (96–26 Ma) (Fig. 2). Our estimates for the age of origin of Erythrinidae is

older than the median estimated age of 31.8 Ma (64.5–16.3 Ma) proposed by Melo et al. (2021), although within the lower bound of their highest posterior density (HPD) interval of 64.5 Ma. Our estimate is also consistent with the age of a †*Tiumpampichthys*, a characoid fossil from the Late Cretaceous-early Paleocene El Molino Formation, which exhibits character states intermediate between Erythrinidae, Hepsetidae, Cynodontidae, and Acestrorhynchidae (Gayet et al. 2003). Despite the associated uncertainty concerning these erythrinid-like fossils and the differences among divergence date estimates, these findings reinforce the hypothesis of Paleogene origins for most generic and family-level NFF taxa (Lundberg et al. 1998; López-Fernández and Albert 2011; Melo et al. 2021b). Our estimate for the origin of Erythrinidae coincides with the early Paleocene-Eocene Thermal Maximum (PETM) and the Early Eocene Thermal Maximum (EETM), times of rapid and high-amplitude shoreline fluctuations (Sluijs et al. 2008; Woodburne et al. 2014; Shcherbinina et al. 2016) that transiently drowned and exposed large lowland areas of interior South America (Westerhold et al. 2020; Scotese et al. 2021), providing multiple opportunities to fragment and merge the biogeographic ranges of freshwater fishes (López-Fernández and Albert 2011; Dias et al. 2014).

Multiple alternative ancestral areas may be estimated for the root and early branches of Erythrinoidea (see Fig. 3), and it was not possible to identify a single region within South America for the origin of these clades. Here we consider two plausible geographic models for early erythrinid diversification based on these results and the literature of NFF taxa more generally. First is the "Eastern Highlands" hypothesis that posits early diversification on upland shields during the early Paleogene, with subsequent dispersal to and diversification within Amazonian lowlands (Eigenmann and Allen 1942; Albert et al. 2011). This model is supported by many NFF clades, which have multiple early-branching, species-poor clades (*sensu* Albert et al. 2017; 2020) occurring in river basins of the upland cratonic shields and adjacent coastal areas; e.g. Lithogeninae and Delturinae in Loricariidae (Lujan et al. 2015; Roxo et al. 2019), *Gladioglanis* and *Myoglanis* in Brachyglaniini (Faustino-Fuster et al. 2021; Silva et al. 2021), and Copionodontinae in Trichomycteridae (Ochoa et al. 2020a). Here, we observed a similar pattern with the divergence of the lineage *Hoplias aimara* (Valenciennes 1847) at about 34 Ma (Fig. 2), a species mostly distributed in coastal rivers of Guiana Shield, tributaries of Lower Orinoco Basin draining from

the Guiana Shield, and tributaries of middle and lower Amazon draining from both, the Brazilian and Guiana shields (Mattox et al. 2006).

A second hypothesis on the geographic origins of NFF clades posits early diversification within the lowland Proto-Orinoco-Amazonas paleobasin of the Sub-Andean foreland, with subsequent dispersal to and along the continental periphery during the Oligocene-Miocene c. 34–10 Ma (Lundberg et al. 1998; López-Fernández and Albert 2011; Oberdorff et al. 2019; Fontenelle et al. 2021; Melo et al. 2021a). This "lowlands-origins" hypothesis implicates rapid global cooling and eustatic sea-level fall at the end of the Eocene (c. 34 Ma; Zachos et al. 2001; Westerhold et al., 2020) that greatly expanded both the total area and connectivity of lowland and coastal freshwater habitats, as a mechanism driving rapid diversification in freshwater taxa (López-Fernández and Albert 2011). Under this hypothesis, the Late Miocene (10 Ma) onset of the transcontinental Amazon River would have allowed expansion and diversification of taxa into the Eastern Amazon and the large tributaries of the cratonic shields (Albert et al. 2018b; 2021). Within Erythrinidae, the first dispersal event to the La Plata basin occurred during the Early Miocene at c. 20 Ma (Clade 4, Fig. 3), presumably associated with tectonic formation of the Bolivian Orocline and associated mega river captures (Albert and Carvalho 2011; Tagliacollo et al. 2015). Similarly, the earliest trans-Andean clade (Clade 5, Fig. 3) is dated to the Middle Miocene c. 13 Ma, possibly a vicariant event resulting from rise of the Northern Andes and uplift of the Eastern Cordillera of Colombia (Albert et al. 2006; Mora et al. 2020).

Overall, we estimate a relatively ancient timeline for the evolution of *Hoplias*, showing initial diversification in the Late Paleogene c. 34 Ma (range 66.8–18.3 Ma), at about the time of the Eocene-Oligocene global cooling event. However, most lineage divergences occurred during the Late Miocene and Pliocene (c. 10.0 – 3.6 Ma), after the formation of the modern transcontinental Amazon River but before the start of the Pleistocene global climate oscillations (i.e. Ice Ages). Erythrinid fossils attributed to *Hoplias* have been found in the Middle Miocene (c. 12 Ma) La Venta Formation in the Upper Magdalena valley of Colombia (Lundberg 1997), and from the Early to Late Miocene Solimões/Pebas Formation in northwestern Amazon (Monsch 1998), suggesting that *Hoplias* was already widely-distributed by the early Neogene. On the other hand, younger timeframes were estimated for *Erythrinus* (c. 9.5 Ma; 22.3–4.4 Ma) and *Hoplerythrinus* (c. 7.1;

15.3–4.1 Ma), with first diversifications in the Late Miocene after the formation of the modern transcontinental Amazon River. Therefore, the absence of these two genera in the trans-Andean regions may be a result from their origination after topographic uplift of the Eastern Cordillera of Colombia at c. 11 Ma (Albert et al. 2006; Mora et al. 2020).

Rapid diversification after c. 10 Ma.— A consistent pattern of positive diversification rates beginning in the Late Miocene has been found in many NFF clades (Cooke et al. 2012; Albert et al. 2021; Fontenelle et al. 2021) and other aquatic taxa (Santos et al. 2009; Roberto et al. 2020). In Erythrinoidea, we detected rapid diversifications starting at c. 10 Ma (Fig. 3), resulting in the formation of most (26/28 or 93%) of the extant species. These diversifications and subsequent dispersal events also resulted in a pattern of polyphyletic modern faunas in peripheral basins (i.e. trans-Andean, São Francisco, Northern Atlantic and Southern Atlantic drainages), each with multiple independent origins in the late Neogene (c. 10–2.6 Ma). This time period is characterized by major geomorphological changes responsible for the configuration of the modern landscapes. The combination of the emerging Northern Andes ranges, and the subdivision of the Sub-Andean Foreland by the rise of the Vaupes and Fitzcarrald Arches, contributed to the formation of the modern transcontinental Amazon river (Hoorn et al. 2010; Albert et al. 2018b). This Late-Miocene-Quaternary configuration generated by the merging of western and eastern Amazon dramatically expanded lowland riverine habitats, allowing dispersal and adaptation of many taxa to previously unavailable habitats (Albert et al. 2018b; Oberdorff et al. 2019). Species-area relationships and environmental stability are expected to have positive effects on the extent of diversification (Kisel et al. 2011; Oberdorff et al. 2019), with larger areas having a greater variety of habitats and larger population sizes, which are therefore less likely to experience stochastic local extinction (Fagan 2002; Ma et al. 2020). This new continental drainage configuration also facilitated geographic range expansions with subsequent geographic isolation (Albert et al. 2021). Our results show that erythrinid species diversified rapidly in the Late Neogene and Quaternary, from eight lineages at 10 Ma to 29 species today, with a majority (22/28 or 78%) of species being members of just three clades younger than 13 Ma: the *Hoplias malabaricus* group, *Erythrinus* and *Hoplerythrinus* (Figs. 2–4).

Major patterns of diversification within Erythrinidae strongly resemble those of most other NFF taxa, supporting a model of continental radiation, in which speciation events occur mainly in allopatry, and in which the processes of speciation and adaptation are largely decoupled (Albert et al. 2020). Species-specific ecological differences could also act as a sieve determining the divergence histories, despite being under strong dispersal constraints (Thomaz and Knowles 2020). Functional traits associated with dispersal capacity, habitat utilization and trophic specialization are widely thought to influence speciation rates in freshwater fishes (Seehausen and Wagner 2014; Miller and Román-Palacios 2021), acting under the perennial influences of landscape and climatic factors that affect the size, conditions, and connections of drainage basins (Lovejoy et al. 2010; Lyons et al. 2020). Under this view, diversification could be influenced by a combination of trophic specializations (Guisande et al. 2012; Kolmann et al. 2021; Melo et al. 2021b), habitat preference (Cooke et al. 2012; Silva et al. 2016; Pires et al. 2018; Albert et al. 2020), genomic potential (McGee et al. 2020), sexual selection (Kraaijeveld et al. 2011; Thomaz et al. 2019) or other derived traits like adult body size and more specialized habitat tolerance (Albert et al. 2020; Melo et al. 2021b). Erythrinids have high vagility, and many species are widely distributed across the Neotropical region (Oyakawa and Mattox 2018), with an apparent generalist pattern of habitat and trophic preferences, and representing important predators of insects, crustaceans and other fishes (Marrero et al. 1997; Lasso and Meri 2001; Oliveira and Garavello 2003; Lasso et al. 2011; Sánchez-Duarte et al. 2011). This group is also characterized by adaptative traits, such as generalist energy-efficient fusiform body (Conde-Saldaña et al. 2017; Larouche et al. 2020), and facultative air-breathing and high tolerance to hypoxia (Wood et al. 2016; Pelster 2021). Therefore, we infer that landscape constrains affecting dispersal over geological time are the major factors of erythrinid diversification, more so than ecological constrains of habitat, diet, or other life-history variables.

Under a constant birth-death model (*sensu* Crisp and Cook 2009), the abrupt increase in lineage diversification rate observed after 10 Ma (Fig. 3B) could also be explained as resulting from a mass extinction event, which has been shown to produce a similar phylogenetic pattern as a rapid diversification or adaptative radiation (Crisp and Cook 2009; Arcila and Tyler 2017; Alfaro et al. 2018). However, this interpretation is not supported by the fossil record, which shows a relatively continuous accumulation of phenotypes and species among extant forms, without any large

phenotypic or biogeographic gaps (Lundberg et al. 2010; Ballen et al. 2021). Indeed, Neotropical freshwater fish diversity has been proposed as the result of both low rates of extinction and high rates of speciation during the Neogene (Lundberg et al. 1998; Albert et al. 2011; 2020; Melo et al. 2021).

Lineage diversification on active vs. passive margins.— Two distinct patterns of diversification were identified in erythrinid fishes under the influence of landscape evolution along the continental margins; a pulsed-age distribution of biogeographic events through time on the tectonically active Western margin, and more continuous distribution of biogeographic events on the tectonically passive Eastern margin (Fig. 4). The active margin in South America represents the boundary between the converging Nazca and South American plates (Hayes 1974), characterized by semi-discrete episodes of mountain uplift in the Andean Cordilleras (Restrepo-Moreno et al. 2019; Noriega-Londoño et al. 2020). The orogenic history of the Andean ranges is based on multiple episodes of tectonism affecting different continental areas at different times, with pronounced impacts on the diversification and distribution of NFF taxa (Albert et al. 2006; Schaefer 2011). Here, we recovered a biogeographic signature in the Sub-Andean Foreland in the area of the Central Andes during the Early Miocene (c. 20 Ma), suggesting that Erythrinidae was exposed to megacapture geodispersal (event 1; Fig.4) during the formation of the Bolivian Orocline, at the headwater region of the Upper Madeira and La Plata basins (Albert and Carvalho 2011). This large-scale biogeographic event may also have affected other NFF clades that evolved within the Proto-Orinoco-Amazonas paleobasin (Tagliacollo et al. 2012, 2015; Silva et al. 2016; Craig et al. 2019; Ottoni et al. 2019; Cardoso et al. 2021).

We also detected a compelling correspondence between the diversification process in Erythrinidae and the orogeny of Northern Andes, which is characterized by three relatively distinct and parallel cordilleras, each resulting of different geological processes at different times (Schaefer 2011; Mora et al. 2020). Here, we found a polyphyletic pattern of *Hoplias* species distributed along the trans-Andean region, resulting from at least three independent events at different times. We recovered the split of earliest trans-Andean clade (event 4, Fig. 4) during the Middle Miocene at c. 13 Ma, likely associated with the initial uplift of the Eastern Cordillera of Colombia (Albert et al. 2006; Mora et al. 2020). The split of the ancestor of *Hoplias teres* (Valenciennes 1847) (event 15; Fig.

4), species today distributed in the Maracaibo Basin, was estimated at c. 8.3 Ma, and is hypothesized to result from the initial rise of the Mérida Andes in Venezuela (~ 8.0 Ma) that isolated the modern Maracaibo and Orinoco basins (Albert et al. 2006; Sánchez-Villagra et al. 2010). Although the Eastern Cordillera of Colombia has been hypothesized as an impermeable barrier to fish dispersal since the Middle Miocene (~ 11 Ma) isolating freshwater fishes from cis- and trans-Andean regions (Albert et al. 2006; Lovejoy et al. 2010; Albert and Carvalho 2011), we estimate the divergence of ancestral of *Hoplias microlepis* (Günther 1864) (event 7; Fig. 4), today distributed along the Chocó biogeographic region, during the Late Miocene (c. 6.3 Ma). This result suggests the possibility that the Eastern Cordillera has in fact been a semipermeable barrier during a long time period of the Late Neogene, with possible passages occurring across the lower mountain passes of the continental divide (e.g. at the Marañon or Tatacoa Portals; e.g. events 4 and 7 in Fig. 4; Lundberg et al. 1998; Ochoa et al. 2020b; Montes et al. 2021).

Lower elevation passes may have occurred intermittently among headwaters along low-shortening segments of the southern and northern Andes (Horton 2018; Mora et al. 2020). Recent geochronological studies suggest the presence of a cis-trans-Andean portal connecting the Pebas system in the Western Amazon with the volcanically active Cauca-Patía Basin during the Middle Miocene to the Pliocene (Montes et al. 2021). This portal may have persisted for several million years, even up to ~ 4 Ma, among the intermontane valleys between the Eastern and Central Cordilleras of Colombia (Montes et al. 2021). The Eastern Cordillera of the Colombian Andes has been proposed as an impermeable barrier to fish dispersal, and its rapid surface uplift starting at ~ 11 Ma has been suggested as a minimum age for the divergence of lineages that inhabit cis- and trans-Andean basins (Albert et al. 2006; Lovejoy et al. 2010). This assumption has been used to estimate clade ages through calibrated trees (Cooke et al. 2012; Machado et al. 2018; Fontenelle et al. 2021). However, the notion that the separation of cis- and trans-Andean fish faunas were shaped by a single tectonic uplift at a single point in time is perhaps an oversimplification of a complex geological history involving events ranging across 2,000 km (from the Merida Andes to the Marañón Portal) and over several millions of years. Time-calibrations using priors with cis- and trans-Andean biogeographic distributions should be viewed with caution according the abovementioned evidence.

The passive Eastern margin is the more stable portion of the South American platform, where escarpment retreat and gradual migrations of watershed divides and river knickpoints across relatively tectonically stable landforms exert a strong influence on the distributions of freshwater fishes (Ribeiro 2006; Albert and Carvalho 2011; Santos et al. 2021). The largest watershed divides on the Eastern margin are between three major river basins: the Amazon (including the Tocantins, Xingu, and Tapajós basins), Paraná-Paraguay, and São Francisco river basins (Ribeiro et al. 2018), with a pivotal role for geodispersal due to watershed migration and river capture across these watersheds (De Podestà Uchôa de Aquino and Rinaldi Colli 2017; Albert et al. 2018a; Dagosta and de Pinna 2019; Bagley et al. 2021). We detected the signature of a gradual accumulation of geodispersal events in Erythrinidae across these watershed divides, with most events occurring during the Middle and Late Miocene and Pliocene, and a pattern of polyphyletic fauna on the periphery following common dispersal routes at different times (Thomaz and Knowles 2020). We also detected a geodispersal signal between Southeastern coastal basins expanding at expense of interior-draining tributaries (events 3, 6; Fig. 4), following a pattern of faunal interchange between the upland crystalline shield and coastal Atlantic rivers throughout the Neogene (Ribeiro 2006; Albert and Carvalho, 2011). Among these events we highlight divergence estimated in the Pliocene c. 2.8 Ma, between the stem of *Hoplias brasiliensis* (Spix & Agassiz 1829) distributed in Atlantic coastal drainages of Bahia, and of *Hoplias intermedius* (Günther 1864) distributed in the São Francisco and Paraná river basins. This observation is consistent with other Plio-Pleistocene ichthyofauna exchanges reported between coastal Brazilian drainages, São Francisco and Paraná basins (Machado et al. 2018; Cardoso et al. 2021; de Queiroz et al. 2021; Santos et al. 2021).

Other results from biogeographic events in erythrinid diversification (Fig. 4) allow additional insights into geological events of the Amazon-Orinoco-Guiana (AOG) core (*sensu* Albert et al. 2011). In *Erythrinus erythrinus* we found Early Pleistocene divergence between lineages in the Branco and Essequibo drainages, and Late Pliocene divergence of these two lineages with a lineage in the Negro basin (Fig. 2). These results support the hypothesis that one or more river capture events transferred freshwater clades from the Negro (Amazon) basin to the Essequibo (Atlantic) basins of the Guianas Shield (Lujan and Armbruster 2011). We estimated the first divergence in *Hoplerythrinus* at c. 7.1 Ma, splitting the stems of the geographically widespread species *H. unitaeniatus* (Spix & Agassiz 1829) and a lineage with a relatively long branch restricted to the

Orinoco Basin. This cladogenetic event could be related with the Late Miocene uplift of the Vaupes Arch and separation of the Amazon and Orinoco basins (Albert et al. 2018b), although the Pleistocene or Holocene formation of the Casiquiare Canal represents a modern dispersal corridor for fish species between these two major basins (Lujan and Armbruster 2011).

Perspectives. — The distinct phylogenetic and biogeographic patterns of erythrinids documented here on active and passive continental margins demonstrate the pivotal role that landscape evolution processes can play in driving evolutionary diversification in widely-distributed NFF clades. Future studies can test these interpretations by comparing results of co-distributed fish taxa that exhibit different functional traits thought to influence dispersal and divergence under the influence of river capture. The river capture model makes distinct predictions regarding the temp and mode of evolution in fish taxa that inhabit certain habitats (large river channels vs. small headwater streams) under different tectonic settings.

For example, members of the geographically wide-spread erythrinid clades (i.e. *H. malabaricus* group, *Erythrinus*, *Hoplerythrinus*) possess adaptations (e.g. smaller body size, facultative air-breathing) that allows them to survive in small, seasonally-variable headwater streams near watershed divides, including hypoxic wetlands at low-elevation watershed divides (e.g. Rupununi and Izozog swamps). Similar traits are also present in other species-rich NFF clades with broad geographic distributions in which multiple sister-species pairs inhabit waterways either side of low-elevation watershed divides; e.g. the electric fishes *Brachyhypopomus* (Crampton et al. 2016) and *Gymnotus* (Craig et al. 2019); the catfishes Heptapteridae (Faustino-Fuster et al. 2021; Silva et al. 2021) and *Hypostomus* (Cardoso et al. 2021); and the cyprinodontiforms *Phalloceros* (Thomaz et al. 2019) and Rivulidae (Loureiro et al. 2018). These patterns contrast with those of NFF taxa with larger body sizes that are ecophysiologically restricted to inhabit deep (10-100 m) river channels of larger rivers (i.e. Strahler stream orders 6-10), which have been shown to be constrained by the action of rare but large-scale megariver events (>10,000 sq. km); e.g. pimelodid catfishes (Tagliacollo et al. 2015), freshwater potamotrygonid stingrays (Fontenelle et al. 2021), ghost electric fishes (Apteronotidae; Albert et al. 2021), and detritivorous curimatid (Melo et al. 2021a) and prochilodontid fishes (Santos et al. 2021). Comparative studies among fish taxa with distinct ecological attributes and life-history profiles, and which have all diversified across the

South American platform, will afford the community multiple tests of the role of landscape evolution mechanisms in contributing to the formation of megadiverse Neotropical aquatic faunas.

Acknowledgments

We are grateful to Mariangeles Arce and Mark H. Sabaj (ANSP), Francisco Villa-Navarro and Diana Montoya (CZUT-IC), Mary Burridge (ROM), María Fernanda Castillo (STRI), Raphael Covain (MHNG), Hernán Ortega (MUSM) for the loan of tissues. We thank the following colleagues for stimulating discussions, Jonathan Armbruster, Maxwell Bernt, Tiago Carvalho, Jack Craig, William Crampton, Aaron Fronk, Flávio Lima, Nathan Lujan, John Lundberg, Hernán López-Fernández, Nathan Lovejoy, Nathan Lyons, Luiz Malabarba, Thierry Oberdorff, Javier Maldonado-Ocampo, Paulo Petry, Mário de Pinna, Ying Reinfelder, Roberto Reis, Alexandre Ribeiro, Gabriel Silva, Bruno Morales, Rafaela Ota, Gerald Smith, Victor Tagliacollo, Pablo Tedesco, Andrea Thomaz, Hanna Tuomisto, Peter Van der Sleen, Brandon Waltz, and Jane Willenbring. Analyses were performed on Zungaro and Brycon servers at LBP/UNESP funded by FAPESP proc. 2014/26508-3 (CO), and in the Center for Scientific Computing (NCC/GridUNESP) of the São Paulo State University. C.C.C-S. is funded by FAPESP (grant nos. 2018/09767-6 and 2019/16999-3).

References

Abell R., Thieme M.L., Revenga C., Bryer M., Kottelat M., Bogutskaya N., Coad B., Mandrak N., Balderas S.C., Bussing W., Stiassny M.L.J., Skeleton P., Allen G.R., Unmack P., Naseka A., NG R., Sindorf N., Robertson J., Armijo E., Higgins J. V., Heibel T.J., Wikramanayake E., Olson D., López H.L., Reis R.E., Lundberg J.G., Sabaj M.H., Petry P. 2008. Freshwater Ecoregions of the World: A New Map of Biogeographic Units for Freshwater Biodiversity Conservation. Bioscience. 58:403–414.

Aberer A.J., Kobert K., Stamatakis A. 2014. Exabayes: Massively parallel bayesian tree inference for the whole-genome era. Mol. Biol. Evol. 31:2553–2556.

Abreu J.M.S., Saraiva A.C.S., Albert J.S., Piorski N.M. 2020. Paleogeographic influences on freshwater fish distributions in northeastern Brazil. J. South Am. Earth Sci. 102.

Adey A., Morrison H.G., Asan, Xun X., Kitzman J.O., Turner E.H., Stackhouse B., MacKenzie A.P., Caruccio N.C., Zhang X., Shendure J. 2010. Rapid, low-input, low-bias construction

of shotgun fragment libraries by high-density in vitro transposition. Genome Biol. 11:R119.

Albert J.S., Antonelli A. 2017. Society for the study of systematic biology symposium: Frontiers in parametric biogeography. Syst. Biol. 66:125–127.

Albert J.S., Bernt M.J., Fronk A.H., Fontenelle J.P., Kuznar S.L., Lovejoy N.R. 2021. Late Neogene megariver captures and the Great Amazonian Biotic Interchange. Glob. Planet. Change. 205:103554.

Albert J.S., Carvalho T.P. 2011. Neogene assembly of modern faunas. In: Albert J.S., Reis R.E., editors. Historical Biogeography of Neotropical Freshwater Fishes. University of California Press. p. 119–136.

Albert J.S., Craig J.M., Tagliacollo V.A., Petry P. 2018a. Upland and Lowland Fishes: A Test of the River Capture Hypothesis. In: Hoorn C., Perrigo A., Antonelli A., editors. Mountains, Climate and Biodiversity. John Wiley & Sons. p. 273–294.

Albert J.S., Lovejoy N.R., Crampton W.G.R. 2006. Miocene tectonism and the separation of cis- and trans-Andean river basins: Evidence from Neotropical fishes. J. South Am. Earth Sci. 21:14–27.

Albert J.S., Petry P., Reis R.E. 2011. Major biogeographic and phylogenetic patterns. In: Albert J.S., Reis R.E., editors. Historical Biogeography of Neotropical Freshwater Fishes. University of California Press. p. 21–58.

Albert J.S., Reis R.E. 2011. Introduction to Neotropical Freshwaters. In: Albert J.S., Reis R.E., editors. Historical Biogeography of Neotropical Freshwater Fishes. University of California Press. p. 1–20.

Albert J.S., Schoolmaster D.R., Tagliacollo V., Duke-Sylvester S.M. 2017. Barrier displacement on a neutral landscape: Toward a theory of continental biogeography. Syst. Biol. 66:167–182.

Albert J.S., Tagliacollo V.A., Dagosta F. 2020. Diversification of Neotropical Freshwater Fishes. Annu. Rev. Ecol. Evol. Syst. 51:27–53.

Albert J.S., Val P., Hoorn C. 2018b. The changing course of the Amazon River in the Neogene: center stage for Neotropical diversification. Neotrop. Ichthyol. 16:1–24.

Alda F., Tagliacollo V.A., Bernt M.J., Waltz B.T., Ludt W.B., Faircloth B.C., Alfaro M.E., Albert J.S., Chakrabarty P. 2019. Resolving Deep Nodes in an Ancient Radiation of Neotropical Fishes in the Presence of Conflicting Signals from Incomplete Lineage Sorting.

Syst. Biol. 68:573–593.
Alfaro M.E., Faircloth B.C., Harrington R.C., Sorenson L., Friedman M., Thacker C.E., Oliveros C.H., Černý D., Near T.J. 2018. Explosive diversification of marine fishes at the Cretaceous-Palaeogene boundary. Nat. Ecol. Evol. 2:688–696.
Antonelli A., Ariza M., Albert J., Andermann T., Azevedo J., Bacon C., Faurby S., Guedes T., Hoorn C., Lohmann L.G., Matos-Maraví P., Ritter C.D., Sanmartín I., Silvestro D., Tejedor M., Ter Steege H., Tuomisto H., Werneck F.P., Zizka A., Edwards S. V. 2018. Conceptual and empirical advances in Neotropical biodiversity research. PeerJ. 2018:1–53.
Arcila D., Petry P., Ortí G. 2018. Phylogenetic relationships of the family Tarumaniidae (Characiformes) based on nuclear and mitochondrial data. Neotrop. Ichthyol. 16:16–19.
Arcila D., Tyler J.C. 2017. Mass extinction in tetraodontiform fishes linked to the Palaeocene-Eocene thermal maximum. Proc. R. Soc. B Biol. Sci. 284.
Bagley J.C., de Aquino P.D.P.U., Hrbek T., Hernandez-Rangel S., Langeani F., Colli G.R. 2021. Using ddRAD-seq phylogeography to test for genetic effects of headwater river capture in suckermouth armored catfish (Loricariidae: *Hypostomus*) from the central Brazilian Shield. bioRxiv.:2021.04.18.440224.
Ballen G.A., Jaramillo C., Dagosta F.C.P., De Pinna M.C.C. 2021. A fossil fish assemblage from the middle Miocene of the Cocinetas Basin, northern Colombia. bioRxiv.:2021.04.19.440491.
Betancur-R. R., Arcila D., Vari R.P., Hughes L.C., Oliveira C., Sabaj M.H., Ortí G. 2019. Phylogenomic incongruence, hypothesis testing, and taxonomic sampling: The monophyly of characiform fishes. Evolution (N. Y). 73:329–345.
Bicudo T.C., Sacek V., de Almeida R.P., Bates J.M., Ribas C.C. 2019. Andean Tectonics and Mantle Dynamics as a Pervasive Influence on Amazonian Ecosystem. Sci. Rep. 9:1–11.
Bogan S., Sidlauskas B., Vari R.P., Agnolin F. 2012. *Arrhinolemur scalabrinii* Ameghino, 1898, of the late Miocene - A taxonomic journey from the Mammalia to the Anostomidae (Ostariophysi: Characiformes). Neotrop. Ichthyol. 10:555–560.
Boschman L.M. 2021. Andean mountain building since the Late Cretaceous: A paleoelevation reconstruction. Earth-Science Rev. 220:103640.
Bouckaert R., Heled J., Kühnert D., Vaughan T., Wu C.H., Xie D., Suchard M.A., Rambaut A., Drummond A.J. 2014. BEAST 2: A Software Platform for Bayesian Evolutionary Analysis.

PLoS Comput. Biol. 10:1–6.
Burridge C.P., Craw D., Waters J.M. 2006. River Capture, Range Expansion, and Cladogenesis: the Genetic Signature of Freshwater Vicariance. Evolution (N. Y). 60:1038.
Calegari S.S., Peifer D., Neves M.A., Caxito F. de A. 2021. Post-Miocene topographic rejuvenation in an elevated passive continental margin not characterized by a sharp escarpment (northern end of the Mantiqueira Range, Brazil). Geomorphology. 393:107946.
Capobianco A., Friedman M. 2019. Vicariance and dispersal in southern hemisphere freshwater fish clades: a palaeontological perspective. Biol. Rev. 94:662–699.
Cardoso Y.P., Jardim de Queiroz L., Bahechar I.A., Posadas P.E., Montoya-Burgos J.I. 2021. Multilocus phylogeny and historical biogeography of *Hypostomus* shed light on the processes of fish diversification in La Plata Basin. Sci. Rep. 11:1–14.
Conde-Saldaña C.C., Albornoz-Garzón J.G., López-Delgado E.O., Villa-Navarro F.A. 2017. Ecomorphological relationships of fish assemblages in a trans-Andean drainage, Upper Magdalena River Basin, Colombia. Neotrop. Ichthyol. 15:1–12.
Cooke G.M., Chao N.L., Beheregaray L.B. 2012. Marine incursions, cryptic species and ecological diversification in Amazonia: The biogeographic history of the croaker genus *Plagioscion* (Sciaenidae). J. Biogeogr. 39:724–738.
Craig J.M., Kim L.Y., Tagliacollo V.A., Albert J.S. 2019. Phylogenetic revision of Gymnotidae (Teleostei: Gymnotiformes), with descriptions of six subgenera. .
Crampton W.G.R., De Santana C.D., Waddell J.C., Lovejoy N.R. 2016. Phylogenetic systematics, biogeography, and ecology of the electric fish genus *Brachyhypopomus* (Ostariophysi: Gymnotiformes). PLoS One. 11.
Crisp M.D., Cook L.G. 2009. Explosive radiation or cryptic mass extinction? interpreting signatures in molecular phylogenies. Evolution (N. Y). 63:2257–2265.
Dagosta F.C.P., de Pinna M. 2017. Biogeography of Amazonian fishes: Deconstructing river basins as biogeographic units. Neotrop. Ichthyol. 15:1–24.
Dagosta F.C.P., de Pinna M. 2019. The Fishes of the Amazon: Distribution and Biogeographical Patterns, with a Comprehensive List of Species. Bull. Am. Museum Nat. Hist. 431:1–163.
Defler T. 2019. The genesis of the modern Amazon River Basin and Andean uplift and their roles in mammalian diversification. In: Defler T., editor. History of terrestrial mammals in South America. Bogotá, Colombia: p. 235–257.

Dias M.S., Oberdorff T., Hugueny B., Leprieur F., Jézéquel C., Cornu J.F., Brosse S., Grenouillet G., Tedesco P.A. 2014. Global imprint of historical connectivity on freshwater fish biodiversity. Ecol. Lett. 17:1130–1140.

Douglas M.M. 2016. Constraints on Passive Margin Escarpment Evolution from River Basin Reorganization in Brazil. Massachusetts Institute of Technology. p. 1-40. .

Drummond A.J., Ho S.Y.W., Phillips M.J., Rambaut A. 2006. Relaxed phylogenetics and dating with confidence. PLoS Biol. 4:699–710.

Eigenmann C.H., Allen W.R. 1942. Fishes of Western South America. Lexington, Kentucky: The University of Kentucky.

Fagan W.F. 2002. Connectivity, fragmentation, and extinction risk in dendritic metapopulations. Ecology. 83:3243–3249.

Faircloth B.C. 2013. illumiprocessor: a trimmomatic wrapper for parallel adapter and quality trimming. http://dx.doi.org/10.6079/J9ILL. .

Faircloth B.C. 2016. PHYLUCE is a software package for the analysis of conserved genomic loci. Bioinformatics. 32:786–788.

Faircloth B.C., Alda F., Hoekzema K., Burns M.D., Oliveira C., Albert J.S., Melo B.F., Ochoa L.E., Roxo F.F., Chakrabarty P., Sidlauskas B.L., Alfaro M.E. 2020. A Target Enrichment Bait Set for Studying Relationships among Ostariophysan Fishes. Copeia. 108:47–60.

Faircloth B.C., McCormack J.E., Crawford N.G., Harvey M.G., Brumfield R.T., Glenn T.C. 2012. Ultraconserved elements anchor thousands of genetic markers spanning multiple evolutionary timescales. Syst. Biol. 61:717–26.

Faircloth B.C., Sorenson L., Santini F., Alfaro M.E. 2013. A Phylogenomic Perspective on the Radiation of Ray-Finned Fishes Based upon Targeted Sequencing of Ultraconserved Elements (UCEs). PLoS One. 8.

Faustino-Fuster D.R., Meza-Vargas V., Lovejoy N.R., Lujan N.K. 2021. Multi-locus phylogeny with dense Guiana Shield sampling supports new suprageneric classification of the neotropical three-barbeled catfishes (Siluriformes: Heptapteridae). Mol. Phylogenet. Evol. 162.

Flynn J.J., Guerrero J., Swisher III C.C. 1997. Geochronology of the Honda Group. In: Kay R.F., Madden R.H., Cifelli R.L., Flynn J.J., editors. Vertebrate Paleontology in the Neotropics: the Miocene Fauna of La Venta, Colombia. Smithsonian Institution Press. p. 44–60.

Fontenelle J.P., Portella Luna Marques F., Kolmann M.A., Lovejoy N.R. 2021. Biogeography of the neotropical freshwater stingrays (Myliobatiformes: Potamotrygoninae) reveals effects of continent-scale paleogeographic change and drainage evolution. J. Biogeogr. 48:1406–1419.

Fricke R., Eschmeyer W.N., Van der Laan R. 2022. ESCHMEYER'S CATALOG OF FISHES: GENERA, SPECIES, REFERENCES. Available from http://researcharchive.calacademy.org/research/ichthyology/catalog/fishcatmain.asp.

Garzione C.N., McQuarrie N., Perez N.D., Ehlers T.A., Beck S.L., Kar N., Eichelberger N., Chapman A.D., Ward K.M., Ducea M.N., Lease R.O., Poulsen C.J., Wagner L.S., Saylor J.E., Zandt G., Horton B.K. 2017. Tectonic Evolution of the Central Andean Plateau and Implications for the Growth of Plateaus. Annu. Rev. Earth Planet. Sci. 45:529–559.

Gayet M., Jégu M., Bocquentin J., Negri F.R. 2003. New Characoids from the Upper Cretaceous and Paleocene of Bolivia and the Mio-Pliocene of Brazil : Phylogenetic Position and Paleobiogeographic Implications. J. Vertebr. Paleontol. 23:28–46.

Goldberg S.L., Schmidt M.J., Perron J.T. 2021. Fast response of Amazon rivers to Quaternary climate cycles. JGR Earth Surf.

Guimarães K.L.A., Rosso J.J., Souza M.F.B., Díaz de Astarloa J.M., Rodrigues L.R.R. 2021. Integrative taxonomy reveals disjunct distribution and first record of Hoplias misionera (Characiformes: Erythrinidae) in the Amazon River basin: morphological, DNA barcoding and cytogenetic considerations. Neotrop. Ichthyol. 19:1–20.

Guisande C., Pelayo-Villamil P., Vera M., Manjarrés-Hernández A., Carvalho M.R., Vari R.P., Jiménez L.F., Fernández C., Martínez P., Prieto-Piraquive E., Granado-Lorencio C., Duque S.R. 2012. Ecological factors and diversification among Neotropical characiforms. Int. J. Ecol. 2012.

Hayes D.E. 1974. Continental Margin of Western South America. In: Burk C.A., Drake C.L., editors. The Geology of Continental Margins. Springer Science+Business Media New York. p. 581–590.

Hoorn C., Wesselingh F.P., ter Steege H., Bermudez M.A., Mora A., Sevink J., Sanmartín I., Sanchez-Meseguer A., Anderson C.L., Figueiredo J.P., Jaramillo C., Riff D., Negri F.R., Hooghiemstra H., Lundberg J., Stadler T., Särkinen T., Antonelli A. 2010. Amazonia Through Time: Andean. Science. 330:927–931.

Horton B.K. 2018. Sedimentary record of Andean mountain building. Earth-Science Rev. 178:279–309.

Jaramillo C., Romero I., D'Apolito C., Bayona G., Duarte E., Louwye S., Escobar J., Luque J., Carrillo-Briceño J.D., Zapata V., Mora A., Schouten S., Zavada M., Harrington G., Ortiz J., Wesselingh F.P. 2017. Miocene flooding events of western Amazonia. Sci. Adv. 3:1–11.

Katoh K., Misawa K., Kuma K.I., Miyata T. 2002. MAFFT: A novel method for rapid multiple sequence alignment based on fast Fourier transform. Nucleic Acids Res. 30:3059–3066.

Kircher M., Sawyer S., Meyer M. 2012. Double indexing overcomes inaccuracies in multiplex sequencing on the Illumina platform. Nucleic Acids Res. 40:1–8.

Kisel Y., Mcinnes L., Toomey N.H., Orme C.D.L. 2011. How diversification rates and diversity limits combine to create large-scale species-area relationships. Philos. Trans. R. Soc. B Biol. Sci. 366:2514–2525.

Kolmann M.A., Hughes L.C., Hernandez L.P., Arcila D., Betancur-R R., Sabaj M.H., López-Fernández H., Ortí G. 2021. Phylogenomics of Piranhas and Pacus (Serrasalmidae) Uncovers How Dietary Convergence and Parallelism Obfuscate Traditional Morphological Taxonomy. Syst. Biol. 70:576–592.

Kraaijeveld K., Kraaijeveld-Smit F.J.L., Maan M.E. 2011. Sexual selection and speciation: The comparative evidence revisited. Biol. Rev. 86:367–377.

de la Peña A. 1996. Characid Teeth from the Lower Eocene of the Ager Basin (Lérida, Spain): Paleobiogeographical Comments. Copeia.:746–750.

Landis M.J., Matzke N.J., Moore B.R., Huelsenbeck J.P. 2013. Bayesian analysis of biogeography when the number of areas is large. Syst. Biol. 62:789–804.

Lanfear R., Frandsen P.B., Wright A.M., Senfeld T., Calcott B. 2016. Partitionfinder 2: New methods for selecting partitioned models of evolution for molecular and morphological phylogenetic analyses. Mol. Biol. Evol. 34:772–773.

Larouche O., Benton B., Corn K.A., Friedman S.T., Gross D., Iwan M., Kessler B., Martinez C.M., Rodriguez S., Whelpley H., Wainwright P.C., Price S.A. 2020. Reef-associated fishes have more maneuverable body shapes at a macroevolutionary scale. Coral Reefs. 39:1427–1439.

Lasso C., Meri J. 2001. Estructura comunitaria de la ictiofauna en herbazales y bosques inundables del bajo río Guanipa, cuenca del Golfo de Paria, Venezuela. Mem. Fund. La

Salle Cienc. Nat. 155:73–90.

Lasso C.A., Morales-Betancourt M., Rivas-Lara T.S., Rincón C.E., González-Cañon G., Galvis-Galindo I. 2011. *Hoplias malabaricus* (Characiformes, Erythrinidae). Capitulo 7. In: Lasso C.A., Agudelo E., Jiménez-Segura L.F., Ramírez-Gil H., Morales-Betancourt M., Ajiaco-Martínez R.E., de Paula-Gutiérrez F., Usma J.S., Muñoz Torres S.E., Sanabria-Ochoa A.I., editors. I. Catálogo de los Recursos Pesqueros Continentales de Colombia. Serie Editorial Recursos Hidrobiológicos y Pesqueros Continentales de Colombia. Bogotá, Colombia: Instituto de Investigación de Recursos Biológicos Alexander von Humboldt (IAvH). p. 294–300.

Leier A., McQuarrie N., Garzione C., Eiler J. 2013. Stable isotope evidence for multiple pulses of rapid surface uplift in the central andes, bolivia. Earth Planet. Sci. Lett. 371–372:49–58.

Lima S.M.Q., Berbel-Filho W.M., Araújo T.F.P., Lazzarotto H., Tatarenkov A., Avise J.C. 2017. Headwater capture evidenced by paleo-rivers reconstruction and population genetic structure of the armored catfish (*Pareiorhaphis garbei*) in the Serra do Mar mountains of southeastern Brazil. Front. Genet. 8.

Lima S.M.Q., Berbel-Filho W.M., Vilasboa A., Lazoski C., de Assis Volpi T., Lazzarotto H., Russo C.A.M., Tatarenkov A., Avise J.C., Solé-Cava A.M. 2021. Rio de Janeiro and other palaeodrainages evidenced by the genetic structure of an Atlantic Forest catfish. J. Biogeogr. 48:1475–1488.

López-Fernández H., Albert J.S. 2011. Paleogene radiations. In: Albert J.S., Reis R.E., editors. Historical Biogeography of Neotropical Freshwater Fishes. University of California Press. p. 105–118.

Loureiro M., de Sá R., Serra S.W., Alonso F., Lanés L.E.K., Volcan M.V., Calviño P., Nielsen D., Duarte A., Garcia G. 2018. Review of the family Rivulidae (Cyprinodontiformes, Aplocheiloidei) and a molecular and morphological phylogeny of the annual fish genus *Austrolebias* Costa 1998. Neotrop. Ichthyol. 16:1–20.

Lovejoy N.R., Willis S.C., Albert J.S. 2010. Molecular Signatures of Neogene Biogeographical Events in the Amazon Fish Fauna. Amaz. Landsc. Species Evol. A Look into Past.:405–417.

Lujan N.K., Armbruster J.W. 2011. The Guiana Shield. In: Albert J.S., Reis R.E., editors. Historical Biogeography of Neotropical Freshwater Fishes. University of California Press.

p. 211–224.

Lujan N.K., Armbruster J.W., Lovejoy N.R., López-Fernández H. 2015. Multilocus molecular phylogeny of the suckermouth armored catfishes (Siluriformes: Loricariidae) with a focus on subfamily Hypostominae. Mol. Phylogenet. Evol. 82:269–288.

Lundberg J.G. 1997. Freshwater fishes and their paleobiotic implications. In: Kay R.F., Madden R.H., Cifelli R.L., Flynn J.J., editors. Vertebrate Paleontology in the Neotropics: The Miocene Fauna of La Venta, Colombia. Smithsonian Institution Press. p. 67–91.

Lundberg J.G., Marshall L.G., Guerrero J., Horton B., Malabarba M.C.S.L., Wesselingh F. 1998. The stage for neotropical fish diversification a history of tropical south american rivers. Phylogeny Classif. Neotrop. Fishes.:603.

Lundberg J.G., Pérez M.H.S., Dahdul W.M., Aguilera O.A. 2010. The Amazonian Neogene Fish Fauna. Amaz. Landsc. Species Evol. A Look into Past.:281–301.

Lyons N., Val P., Albert J., Willenbring J., Gasparini N. 2020. Topographic controls on divide migration, stream capture, and diversification in riverine life. Earth Surf. Dyn. Discuss.:1–29.

Ma C., Shen Y., Bearup D., Fagan W.F., Liao J. 2020. Spatial variation in branch size promotes metapopulation persistence in dendritic river networks. Freshw. Biol. 65:426–434.

Machado C.B., Galetti P.M., Carnaval A.C. 2018. Bayesian analyses detect a history of both vicariance and geodispersal in Neotropical freshwater fishes. J. Biogeogr. 45:1313–1325.

Malabarba M.C. 1996. Reassessment and relationships of *Curimata mosesi* Travassos & Santos, a fossil fish (Teleostei: Characiformes: Curimatidae) from the tertiary of São Paulo, Brazil. Comun. do Mus. Ciências e Tecnol. da PUCRS.:55–63.

Marrero C., Machado-allison A., González V., Velázquez J., Rodríguez-Olarte D. 1997. Los Morichales del Oriente de Venezuela: su importancia en la distribución y ecología de los componentes de la Ictiofauna dulceacuícola regional. Acta Biol. Venez. 17:65–79.

Mattox G.M.T., Bifi A.G., Oyakawa O.T. 2014. Taxonomic study of *Hoplias microlepis* (Günther, 1864), a trans-Andean species of trahiras (Ostariophysi: Characiformes: Erythrinidae). Neotrop. Ichthyol. 12:343–352.

Mattox G.M.T., Toledo-Piza M., Oyakawa O.T. 2006. Taxonomic Study of *Hoplias Aimara* (Valenciennes, 1846) and *Hoplias macrophthalmus* (Pellegrin, 1907) (Ostariophysi, Characiformes, Erythrinidae). Copeia. 2006:516–528.

Matzke N.J. 2013. BioGeoBEARS: Biogeography with Bayesian (and likelihood) evolutionary analysis in R scripts. University of California, Berkeley. .

Matzke N.J. 2018. BioGeoBEARS: Biogeography with Bayesian (and likelihood) Evolutionary Analysis with R Scripts. version 1.1.1, published on GitHub on November 6, 2018. DOI: http://dx.doi.org/10.5281/zenodo.1478250. .

McGee M.D., Borstein S.R., Meier J.I., Marques D.A., Mwaiko S., Taabu A., Kishe M.A., O'Meara B., Bruggmann R., Excoffier L., Seehausen O. 2020. The ecological and genomic basis of explosive adaptive radiation. Nature. 586:75–79.

Melo B.F., Albert J.S., Dagosta F.C.P., Tagliacollo V.A. 2021a. Biogeography of curimatid fishes reveals multiple lowland-upland river transitions and differential diversification in the Neotropics (Teleostei, Curimatidae). Ecol. Evol.:1–18.

Melo B.F., Sidlauskas B.L., Near T.J., Roxo F.F., Ghezelayagh A., Ochoa L.E., Stiassny M.L.J., Arroyave J., Chang J., Faircloth B.C., MacGuigan D.J., Harrington R.C., Benine R.C., Burns M.D., Hoekzema K., Sanches N.C., Maldonado-Ocampo J.A., Castro R.M.C., Foresti F., Alfaro M.E., Oliveira C. 2021b. Accelerated Diversification Explains the Exceptional Species Richness of Tropical Characoid Fishes. Syst. Biol. 0:1–15.

Miller E.C., Román-Palacios C. 2021. Evolutionary time best explains the latitudinal diversity gradient of living freshwater fish diversity. Glob. Ecol. Biogeogr. 30:749–763.

Monsch K.A. 1998. Miocene fish faunas from the northwestern Amazonia basin (Colombia, Peru, Brazil) with evidence of marine incursions. Palaeogeogr. Palaeoclimatol. Palaeoecol. 143:31–50.

Montes C., Silva C.A., Bayona G.A., Villamil R., Stiles E., Rodriguez-Corcho A.F., Beltran-Triviño A., Lamus F., Muñoz-Granados M.D., Pérez-Angel L.C., Hoyos N., Gomez S., Galeano J.J., Romero E., Baquero M., Cardenas-Rozo A.L., von Quadt A. 2021. A Middle to Late Miocene Trans-Andean Portal: Geologic Record in the Tatacoa Desert. Front. Earth Sci. 8:587022.

Mora A., Baby P., Roddaz M., Parra M., Brusset S., Hermoza W., Espurt N. 2010. Tectonic History of the Andes and Sub-Andean Zones: Implications for the Development of the Amazon Drainage Basin. In: Hoorn C., Wesselingh F.P., editors. Amazonia, Landscape and Species Evolution: A Look into the Past. Blackwell Publishing. p. 38–60.

Mora A., Villagómez D., Parra M., Caballero V.M., Spikings R., Horton B.K., Mora-Bohórquez

J.A., Ketcham R.A., Arias-Martínez J.P. 2020. Late Cretaceous to Cenozoic uplift of the northern Andes: Paleogeographic implications. Paleogene-Neogene. Serv. Geológico Colomb. Publi-caciones Geológicas Espec. 3:89–121.

Noriega-Londoño S., Restrepo-Moreno S.A., Vinasco C., Bermúdez M.A., Min K. 2020. Thermochronologic and geomorphometric constraints on the Cenozoic landscape evolution of the Northern Andes: Northwestern Central Cordillera, Colombia. Geomorphology. 351:106890.

Oberdorff T., Dias M.S., Jézéquel C., Albert J.S., Arantes C.C., Bigorne R., Carvajal-Valleros F.M., De Wever A., Frederico R.G., Hidalgo M., Hugueny B., Leprieur F., Maldonado M., Maldonado-Ocampo J., Martens K., Ortega H., Sarmiento J., Tedesco P.A., Torrente-Vilara G., Winemiller K.O., Zuanon J. 2019. Unexpected fish diversity gradients in the Amazon basin. Sci. Adv. 5:1–9.

Ochoa L.E., Datovo A., DoNascimiento C., Roxo F.F., Sabaj M.H., Chang J., Melo B.F., Silva G.S.C., Foresti F., Alfaro M., Oliveira C. 2020a. Phylogenomic analysis of trichomycterid catfishes (Teleostei: Siluriformes) inferred from ultraconserved elements. Sci. Rep. 10:1–15.

Ochoa L.E., Melo B.F., García-Melo J.E., Maldonado-Ocampo J.A., Souza C.S., Albornoz-Garzón J.G., Conde-Saldaña C.C., Villa-Navarro F., Ortega-Lara A., Oliveira C. 2020b. Species delimitation reveals an underestimated diversity of Andean catfishes of the family Astroblepidae (Teleostei: Siluriformes). Neotrop. Ichthyol. 18:1–19.

Oliveira A.K. de, Garavello J.C. 2003. Fish assemblage composition in a tributary of the Mogi Guaçu river basin, southeastern Brazil. Iheringia. Série Zool. 93:127–138.

de Oliveira Andrades–Filho C., Rossetti D. de F., Rego Bezerra F.H. 2021. The unsteady post-rift stage of the South American passive margin based on the tectono-sedimentary evolution of the onshore Paraíba Basin, NE Brazil. Quat. Int. 580:100–119.

Ottoni F.P., Mattos J.L.O., Katz A.M., Bragança P.H.N. 2019. Phylogeny and species delimitation based on molecular approaches on the species of the *Australoheros autrani* group (Teleostei, Cichlidae), with biogeographic comments. Zoosystematics Evol. 95:49–64.

Oyakawa O.T., Mattox G.M.T. 2009. Revision of the Neotropical trahiras of the *Hoplias lacerdae* species-group (Ostariophysi: Characiformes: Erythrinidae) with descriptions of

two new species. Neotrop. Ichthyol. 7:117–140.

Oyakawa O.T., Mattox G.M.T. 2018. Family Erythrinidae - Wolf-fishes and Yarrows. In: van der Sleen P., Albert J.S., editors. Field Guide to the Fishes of the Amazon, Orinoco, and Guianas. Princeton University Press. p. 156–158.

Pattengale N.D., Alipour M., Bininda-Emonds O.R.P., Moret B.M.E., Stamatakis A. 2010. How Many Bootstrap Replicates Are Necessary? J. Comput. Biol. 17:337–354.

Pelster B. 2021. Using the swimbladder as a respiratory organ and/or a buoyancy structure—Benefits and consequences. J. Exp. Zool. Part A Ecol. Integr. Physiol.:1–12.

de Pinna M., Zuanon J., Rapp Py-Daniel L., Petry P. 2017. A new family of neotropical freshwater fishes from deep fossorial amazonian habitat, with a reappraisal of morphological characiform phylogeny (Teleostei: Ostariophysi). Zool. J. Linn. Soc. XX:1–13.

Pio N.L., Carvalho T.P. 2021. Evidence on the paleodrainage connectivity during Pleistocene: Phylogeography of a hypoptopomatine endemic to southeastern Brazilian coastal drainages. Neotrop. Ichthyol. 19:1–15.

Pires T.H.S., Borghezan E.A., Machado V.N., Powell D.L., Röpke C.P., Oliveira C., Zuanon J., Farias I.P. 2018. Testing Wallace's intuition: water type, reproductive isolation and divergence in an Amazonian fish. J. Evol. Biol. 31:882–892.

De Podestà Uchôa de Aquino P., Rinaldi Colli G. 2017. Headwater captures and the phylogenetic structure of freshwater fish assemblages: a case study in central Brazil. J. Biogeogr. 44:207–216.

de Queiroz L.J., Meyer X., Cardoso Y.P., Bahechar I.A., Covain R., Parente T.E., Torrente-Vilara G., Buckup P.A., Montoya-Burgos J.I. 2021. Western Amazon was a center of Neotropical fish dispersal, as evidenced by the continental-wide time-stratified biogeographic analysis of the hyper-diverse *Hypostomus* catfish. bioRxiv.:2021.06.03.446980.

Rambaut A., Suchard M.A., Xie D., Drummond A.J. 2014. Tracer v1.6. Available from http://beast.bio.ed.ac.uk/Tracer. .

Ramirez J.L., Birindelli J.L., Carvalho D.C., Affonso P.R.A.M., Venere P.C., Ortega H., Carrillo-Avila M., Rodríguez-Pulido J.A., Galetti P.M. 2017. Revealing hidden diversity of the underestimated neotropical ichthyofauna: DNA barcoding in the recently described

genus *Megaleporinus* (Characiformes: Anostomidae). Front. Genet. 8:149.

Ree R.H., Sanmartín I. 2018. Conceptual and statistical problems with the DEC+J model of founder-event speciation and its comparison with DEC via model selection. J. Biogeogr. 45:741–749.

Ree R.H., Smith S.A. 2008. Maximum likelihood inference of geographic range evolution by dispersal, local extinction, and cladogenesis. Syst. Biol. 57:4–14.

Reis R.E., Albert J.S., Di Dario F., Mincarone M.M., Petry P., Rocha L.A. 2016. Fish biodiversity and conservation in South America. J. Fish Biol. 89:12–47.

Restrepo-Moreno S.A., Foster D.A., Bernet M., Min K., Noriega S. 2019. Morphotectonic and orogenic development of the Northern Andes of Colombia: A low-temperature thermochronology perspective. In: Cediel F., Shaw R.P., editors. Geology and Tectonics of Northwestern South America. Springer. p. 749–832.

Revell L.J. 2012. phytools: An R package for phylogenetic comparative biology (and other things). Methods Ecol. Evol. 3:217–223.

Ribeiro A.C. 2006. Tectonic history and the biogeography of the freshwater fishes from the coastal drainages of eastern Brazil: An example of faunal evolution associated with a divergent continental margin. Neotrop. Ichthyol. 4:225–246.

Ribeiro A.C., Riccomini C., Leite J.A.D. 2018. Origin of the largest South American transcontinental water divide. Sci. Rep. 8:1–8.

Roberto I.J., Bittencourt P.S., Muniz F.L., Hernández-Rangel S.M., Nóbrega Y.C., Ávila R.W., Souza B.C., Alvarez G., Miranda-Chumacero G., Campos Z., Farias I.P., Hrbek T. 2020. Unexpected but unsurprising lineage diversity within the most widespread Neotropical crocodilian genus *Caiman* (Crocodylia, Alligatoridae). Syst. Biodivers. 18:377–395.

Ronquist F. 1997. Dispersal-Vicariance Analysis : A New Approach to the Quantification of Historical Biogeography. Syst. Biol. 46:195–203.

Rosso J.J., González-Castro M., Bogan S., Cardoso Y.P., Mabragaña E., Delpiani M., Díaz J. de A. 2018. Integrative taxonomy reveals a new species of *Hoplias malabaricus* species complex (Teleostei: Erythrinidae). Ichthyol. Explor. Freshwaters.:1–18.

Roxo F.F., Ochoa L.E., Sabaj M.H., Lujan N.K., Covain R., Silva G.S.C., Melo B.F., Albert J.S., Chang J., Foresti F., Alfaro M.E., Oliveira C. 2019. Phylogenomic reappraisal of the Neotropical catfish family Loricariidae (Teleostei: Siluriformes) using ultraconserved

elements. Mol. Phylogenet. Evol. 135:148–165.

Saadi A., Machette M.N., Haller K.M., Dart R.L., Bradley L., Souza A.M.P.D. 2002. Map and database of Quaternary faults and lineaments in Brazil. USGS Open-File Rep. 02–230:59.

Sabaj M.H. 2020. Codes for natural history collections in ichthyology and herpetology. Copeia. 108:593–669.

Sacek V., Braun J., Van Der Beek P. 2012. The influence of rifting on escarpment migration on high elevation passive continental margins. J. Geophys. Res. Solid Earth. 117.

Salgado A.A.R., Marent B.R., Cherem L.F.S., Bourlès D., Santos L.J.C., Braucher R., Barreto H.N. 2014. Denudation and retreat of the Serra do Mar escarpment in southern Brazil derived from in situ-produced 10Be concentration in river sediment. Earth Surf. Process. Landforms. 39:311–319.

Sánchez-Duarte P., Lasso C.A., González-Cañon G., Nieto-Torres S. 2011. *Hoplerythrinus unitaeniatus* (Characiformes, Erythrinidae). Capitulo 7. In: Lasso C.A., Agudelo E., Jiménez-Segura L.F., Ramírez-Gil H., Morales-Betancourt M., Ajiaco-Martínez R.E., de Paula-Gutiérrez F., Usma J.S., Muñoz Torres S.E., Sanabria-Ochoa A.I., editors. I. Catálogo de los Recursos Pesqueros Continentales de Colombia. Serie Editorial Recursos Hidrobiológicos y Pesqueros Continentales de Colombia. Bogotá, Colombia: Instituto de Investigación de los Recursos Biológicos Alexander von Humboldt (IAvH). p. 291–293.

Sánchez-Villagra M.R., Aguilera O.A., Carlini A.A. 2010. Urumaco and Venezuelan paleontology: the fossil record of the Northern Neotropics. Indiana University Press.

Sanmartín I. 2012. Historical Biogeography: Evolution in Time and Space. Evol. Educ. Outreach. 5:555–568.

Santos J.C., Coloma L.A., Summers K., Caldwell J.P., Ree R., Cannatella D.C. 2009. Amazonian amphibian diversity is primarily derived from late Miocene Andean lineages. PLoS Biol. 7:0448–0461.

Santos R.P., Melo B.F., Yazbeck G.M., Oliveira R.S., Hilário H.O., Prosdocimi F., Carvalho D.C. 2021. Diversification of *Prochilodus* in the eastern Brazilian Shield: Evidence from complete mitochondrial genomes (Teleostei, Prochilodontidae). J. Zool. Syst. Evol. Res. 59:1053–1063.

Schaefer S. 2011. The Andes: Riding the Tectonic Uplift. In: Albert J.S., Reis R., editors. Historical Biogeography of Neotropical Freshwater Fishes. University of California Press.

p. 259–278.
Scotese C.R., Song H., Mills B.J.W., van der Meer D.G. 2021. Phanerozoic paleotemperatures: The earth's changing climate during the last 540 million years. Earth-Science Rev. 215:103503.
Seehausen O., Wagner C.E. 2014. Speciation in freshwater fishes. Annu. Rev. Ecol. Evol. Syst. 45:621–651.
Shcherbinina E., Gavrilov Y., Iakovleva A., Pokrovsky B., Golovanova O., Aleksandrova G. 2016. Environmental dynamics during the Paleocene-Eocene thermal maximum (PETM) in the northeastern Peri-Tethys revealed by high-resolution micropalaeontological and geochemical studies of a Caucasian key section. Palaeogeogr. Palaeoclimatol. Palaeoecol. 456:60–81.
Silva G.S.C., Roxo F.F., Lujan N.K., Tagliacollo V.A., Zawadzki C.H., Oliveira C. 2016. Transcontinental dispersal, ecological opportunity and origins of an adaptive radiation in the Neotropical catfish genus *Hypostomus* (Siluriformes: Loricariidae). Mol. Ecol. 25:1511–1529.
Silva G.S.C., Roxo F.F., Melo B.F., Ochoa L.E., Bockmann F.A., Sabaj M.H., Jerep F.C., Foresti F., Benine R.C., Oliveira C. 2021. Evolutionary history of Heptapteridae catfishes using ultraconserved elements (Teleostei, Siluriformes). Zool. Scr. 50:543–554.
Siravo G., Molin P., Sembroni A., Fellin M.G., Faccenna C. 2021. Tectonically driven drainage reorganization in the Eastern Cordillera, Colombia. Geomorphology. 389:107847.
Sluijs A., Brinkhuis H., Crouch E.M., John C.M., Handley L., Munsterman D., Bohaty S.M., Zachos J.C., Reichart G.J., Schouten S., Pancost R.D., Damsté J.S.S., Welters N.L.D., Lotter A.F., Dickens G.R. 2008. Eustatic variations during the Paleocene-Eocene greenhouse world. Paleoceanography. 23:1–18.
Smith G.R., Morgan N., Gustafson E. 2000. Fishes of the Mio-Pliocene Ringold Formation, Washington: Pliocene capture of the Snake River by the Columbia River. .
de Sordi M.V., Salgado A.A.R., Siame L., Bourlès D., Paisani J.C., Léanni L., Braucher R., do Couto E.V. 2018. Implications of drainage rearrangement for passive margin escarpment evolution in southern Brazil. Geomorphology. 306:155–169.
Stamatakis A. 2014. RAxML version 8: A tool for phylogenetic analysis and post-analysis of large phylogenies. Bioinformatics. 30:1312–1313.

Stokes M.F., Goldberg S.L., Perron J.T. 2018. Ongoing River Capture in the Amazon. Geophys. Res. Lett. 45:5545–5552.

Struth L., Babault J., Teixell A. 2015. Drainage reorganization during mountain building in the river system of the Eastern Cordillera of the Colombian Andes. Geomorphology. 250:370–383.

Su G., Villéger S., Brosse S. 2019. Morphological diversity of freshwater fishes differs between realms, but morphologically extreme species are widespread. Glob. Ecol. Biogeogr. 28:211–221.

Tagliacollo V.A., Lanfear R. 2018. Estimating improved partitioning schemes for ultraconserved elements. Mol. Biol. Evol. 35:1798–1811.

Tagliacollo V.A., Roxo F.F., Duke-Sylvester S.M., Oliveira C., Albert J.S. 2015. Biogeographical signature of river capture events in Amazonian lowlands. J. Biogeogr. 42:2349–2362.

Tagliacollo V.A., Souza-Lima R., Benine R.C., Oliveira C. 2012. Molecular phylogeny of Aphyocharacinae (Characiformes, Characidae) with morphological diagnoses for the subfamily and recognized genera. Mol. Phylogenet. Evol. 64:297–307.

Thomaz A.T., Carvalho T.P., Malabarba L.R., Knowles L.L. 2019. Geographic distributions, phenotypes, and phylogenetic relationships of *Phalloceros* (Cyprinodontiformes: Poeciliidae): Insights about diversification among sympatric species pools. Mol. Phylogenet. Evol. 132:265–274.

Thomaz A.T., Knowles L.L. 2020. Common barriers, but temporal dissonance: Genomic tests suggest ecological and paleo-landscape sieves structure a coastal riverine fish community. Mol. Ecol. 29:783–796.

Thomaz A.T., Malabarba L.R., Bonatto S.L., Knowles L.L. 2015. Testing the effect of palaeodrainages versus habitat stability on genetic divergence in riverine systems: Study of a Neotropical fish of the Brazilian coastal Atlantic Forest. J. Biogeogr. 42:2389–2401.

Travassos H., Santos R.S. 1955. Caracídeos fósseis da bacia do Paraíba. An. Acad. Bras. Ciências. 27:313–321.

Wendt E.W., Silva P.C., Malabarba L.R., Carvalho T.P. 2019. Phylogenetic relationships and historical biogeography of *Oligosarcus* (Teleostei: Characidae): Examining riverine landscape evolution in southeastern South America. Mol. Phylogenet. Evol. 140:106604.

Wesselingh F.P., Hoorn C. 2011. Geological development of Amazon and Orinoco basins. Hist. Biogeogr. Neotrop. Freshw. Fishes.:59–68.

Wesselingh F.P., Rasanen M.E., Irion G., Vonhof H.B., Kaandorp R., Renema W., Romero-Pittman L., Gingras M. 2002. Lake Pebas: a paleoecological reconstruction of a Miocene, long-lived lake complex in western Amazonia. Cainozoic Res. 1:35–81.

Westerhold T., Marwan N., Drury A.J., Liebrand D., Agnini C., Anagnostou E., Barnet J.S.K., Bohaty S.M., De Vleeschouwer D., Florindo F., Frederichs T., Hodell D.A., Holbourn A.E., Kroon D., Lauretano V., Littler K., Lourens L.J., Lyle M., Pälike H., Röhl U., Tian J., Wilkens R.H., Wilson P.A., Zachos J.C. 2020. An astronomically dated record of Earth's climate and its predictability over the last 66 million years. Science (80-.). 369:1383–1388.

Wood C.M., Pelster B., Giacomin M., Sadauskas-Henrique H., Almeida-Val V.M.F., Val A.L. 2016. The transition from water-breathing to air-breathing is associated with a shift in ion uptake from gills to gut: a study of two closely related erythrinid teleosts, *Hoplerythrinus unitaeniatus* and *Hoplias malabaricus*. J. Comp. Physiol. B Biochem. Syst. Environ. Physiol. 186:431–445.

Woodburne M.O., Goin F.J., Bond M., Carlini A.A., Gelfo J.N., López G.M., Iglesias A., Zimicz A.N. 2014. Paleogene Land Mammal Faunas of South America; a Response to Global Climatic Changes and Indigenous Floral Diversity. .

Zachos J., Pagani H., Sloan L., Thomas E., Billups K. 2001. Trends, rhythms, and aberrations in global climate 65 Ma to present. Science (80-.). 292:686–693.

Zanata A.M., Vari R.P. 2005. The family Alestidae (Ostariophysi, Characiformes): A phylogenetic analysis of a trans-Atlantic clade. Zool. J. Linn. Soc. 145:1–144.

Zerbino D.R., Birney E. 2008. Velvet: Algorithms for de novo short read assembly using de Bruijn graphs. Genome Res. 18:821–829.

Zhang C., Rabiee M., Sayyari E., Mirarab S. 2018. ASTRAL-III: Polynomial time species tree reconstruction from partially resolved gene trees. BMC Bioinformatics. 19.

Supplementary material

Table S1. Collection numbers and localities for all specimens analyzed in this study.

Catalog number	Tissue	Taxon	Locality	Basin	City/State	Country
ANSP 178126	1712	*Abramites hypselonotus*	Rio Napo	Amazonas	Maynas/Loreto	Peru
AMNH 242137	333238	*Alestes inferus*	Congo River	Congo	Bas Congo Province	Democratic Republic of Congo
OS 19665	BLS14-013	*Bryconaethiops microstoma*	Ogooeé river	Ogooeé	Doumé Village/Province del'Ogooué-Lolo	Gabon
LBP 7556	35626	*Catoprion mento*	Rio Cuiabá	Paraguay	Barão de Melgaço/MT	Brazil
LBP 12838	54048	*Colossoma macropomum*	Rio Tapajos	Amazonas	Itaituba/PA	Brazil
LBP 12838	54052	*Colossoma macropomum*	Rio Tapajos	Amazonas	Itaituba/PA	Brazil
LBP 6136	29524	*Ctenolucius hujeta*	Rio Santa Rosa	Maracaibo	Machiques de Perijá/Zulia	Venezuela
LBP 24318	91518	*Curimata mivartii*	Río Nare	Middle Magdalena	Puerto Nare/Antioquia	Colombia
LBP 5431	27171	*Curimatella alburna*	Rio Jari	Amazonas	Almeirim/PA	Brazil
LBP 10227	43105	*Cynodon gibbus*	Rio Apure	Orinoco	Cabruta/Guárico	Venezuela
LBP 15139	62363	*Cyphocharax spilurus*	Rio Branco	Negro/Amazonas	Boa Vista/RR	Brazil
LBP 25856	LBPV96379	*Erythrinus erythrinus*	Igarapé no Ramal 2	Negro/Amazonas	São Gabriel da Cachoeira/AM	Brazil
LBP 23561	LBPV92312	*Erythrinus erythrinus*	Igarapé Tarumã-Mirim	Negro/Amazonas	Manaus/AM	Brazil
AUM 62923	AUFT 6520	*Erythrinus erythrinus*	Potaro River	Essequibo	Potaro/Siparuni	Guyana
AUM 67125	AUFT 10173	*Erythrinus erythrinus*	Ireng River	Branco/Negro/Amazonas	Potaro/Siparuni	Guyana
INPA-ICT 056178	P32617	*Erythrinus* sp. 1	Rio Itaquaí	Javari/Amazonas	Atalaia do Norte/AM	Brazil
LBP 23551	LBPV92288	*Erythrinus* sp. 1	Igarapé Nina Rumi	Amazonas	Mayanas/Loreto	Peru
LBP 8518	LBPV43203	*Erythrinus* sp. 2	Rio Sucuruina	Rio Tapajós/Amazonas	Diamantino/MT	Brazil
MZUSP 117564	MZUSPV 3040	*Erythrinus* sp. 2	Afluente Rio Juma	Madeira/Amazonas	Apuí/AM	Brazil
LBP 10907	LBPV50235	*Erythrinus* sp. 2	Rio Jaci-Paraná	Madeira/Amazonas	Porto Velho/RO	Brazil
MZUSP 118308	MZUSPV 3748	*Erythrinus* sp. 2	Igarapé afluente 12 de Outubro	Juruena/Amazonas	Vilhena/RO	Brazil
LBP 14851	LBPV57878	*Erythrinus* sp. 3	Aquario	Amazonas	Iquitos/Loreto	Peru
LBP 2137	LBPV21405	*Erythrinus* sp. 4	Riacho Rosario	Atlantic drainage	Canavieiras/BA	Brazil
LBP 6583	LBPV31841	*Erythrinus* sp. 5	Lagoa Marginal Rio Paraná	Paraná	Marilena/PR	Brazil

Catalog number	Tissue	Taxon	Locality	Basin	City/State	Country
LBP 6625	LBPV31955	*Erythrinus* sp. 5	Lagoa Marginal Rio Paraná	Paraná	Marilena/PR	Brazil
LBP 10802	LBPV49931	*Erythrinus* sp. 5	Afluente Rio Guaporé	Madeira/Amazonas	Vila Bela da Santíssima Trindade/MT	Brazil
AMNH 242489	353404	*Hepsetus cuvieri*	Lac Nkolentulu	Lac Nkolentulu	Mai Ndombe/Bandudu	Democratic Republic of Congo
LBP 2298	LBPV15829	*Hoplerythrinus* sp.	Lagoa marginal, Rio Orinoco	Orinoco	Caicara del Orinoco /Bolivar	Venezuela
CZUT-IC 12980	CZUT-IC-TE 866	*Hoplerythrinus* sp.	Cañada Guafila	Ariporo/Meta/Orinoco	Hato Corozal/Casanare	Colombia
CZUT-IC 11490	CZUT-IC-TE 990	*Hoplerythrinus* sp.	Caño Cusiba	Cusiana/Meta/Orinoco	Maní/Casanare	Colombia
ROM 92359	T09425	*Hoplerythrinus* sp.	Caño Tigre	Orinoco	Yacapana/Amazonas	Venezuela
LBP 4237	LBPV22757	*Hoplerythrinus unitaeniatus*	Rio Juruá	Amazonas	Cruzeiro do Sul/AC	Brazil
LBP 9152	LBPV42525	*Hoplerythrinus unitaeniatus*	Igarapé das Pedras	Guamá/Amazonas	Ourém/PA	Brazil
LBP 23527	LBPV92225	*Hoplerythrinus unitaeniatus*	Lagoa Avispa	Ucayali/Amazonas	Requena/Loreto	Peru
LBP 2980	LBPV19624	*Hoplerythrinus unitaeniatus*	Lagoa da Égua	Araguaia/Tocantins	Cocalinho/MT	Brazil
LBP 25545	LBPV91345	*Hoplerythrinus unitaeniatus*	Riacho Pongal	Benevente/Atlantic drainage	Anchieta/ES	Brazil
LBP 17450	LBPV69028	*Hoplerythrinus unitaeniatus*	Amaila River	Potaro/Essequibo	Potaro-Siparuni	Guyana
LBP 5507	LBPV26600	*Hoplerythrinus unitaeniatus*	Rio Jari	Amazonas	Laranjal do Jari/AP	Brazil
LBP 23560	LBPV92311	*Hoplerythrinus unitaeniatus*	Igarapé Tarumã-Mirim	Negro/Amazonas	Manaus/AM	Brazil
LBP 5180	LBPV26697	*Hoplerythrinus unitaeniatus*	Rio Paraná	Paraná	Porto Rico/PR	Brazil
LBP 651	LBPV8042	*Hoplerythrinus unitaeniatus*	Afluente Rio Pirai	Cuiabá/Paraguay	Poconé/MT	Brazil
LBP 8025	LBPV37724	*Hoplerythrinus unitaeniatus*	Riacho sem nome	Arinos/Tapajos/Amazonas	Nova Mutum/MT	Brazil
LBP 16143	LBPV66873	*Hoplerythrinus unitaeniatus*	Igarapé Nambuaí	Tapajos/Amazonas	Itaituba/PA	Brazil
LBP 19217	LBPV77663	*Hoplerythrinus unitaeniatus*	Ribeirão Brejão	Tocantins	Mateiros/TO	Brazil
LBP 17450	LBPV69027	*Hoplerythrinus unitaeniatus*	Amaila River	Potaro/Essequibo	Potaro-Siparuni	Guyana
LBP 15875	LBPV64189	*Hoplerythrinus unitaeniatus*	Tributário Rio Coluene	Xingu	Canarana/MT	Brazil
LBP 28291	LBPV96858	*Hoplerythrinus unitaeniatus*	Lagoas Rio da Prata	Paracatú/São Francisco	João Pinheiro/MG	Brazil
MHNG 2755.083	GFSU14-1357	*Hoplerythrinus unitaeniatus*	Kaw River	Atlantic drainage	Régina/Cayenne	French Guiana
LBP 20882	LBPV81519	*Hoplerythrinus unitaeniatus*	Afluente Rio Lagoa Rosa	Arinos/Tapajós/Amazonas	Diamantino/MT	Brazil
MZUSP 96825	MZUSP3392	*Hoplerythrinus unitaeniatus*	Tributário Rio Braço Norte	Teles Pires/Tapajos	Novo Progresso/PA	Brazil

Catalog number	Tissue	Taxon	Locality	Basin	City/State	Country
TIUFRN2909	TI2909	*Hoplerythrinus unitaeniatus*	Riacho dos Porcos	Tocantins	São Félix do Tocantins/TO	Brazil
LBP 13248	LBPV69385	*Hoplias aimara*	Riacho Alegre	Tapajós/Amazonas	Diamantino/MT	Brazil
LBP 9101	LBPV42717	*Hoplias aimara*	Rio Sete de Setembro	Xingu/Amazonas	Canarana/MT	Brazil
LBP 20520	LBPV80648	*Hoplias aimara*	Rio Jari	Amazonas	Laranjal do Jari/AP	Brazil
LBP 13122	LBPV54949	*Hoplias argentinensis*	Ricaho sem nome	Uruguay	Ijuí/RS	Brazil
LBP 29138	LBPV101563	*Hoplias brasiliensis*	Rio Santo Antônio	Río das Contas/Atlantic drainage	Itagi/BA	Brazil
LBP 20412	LBPV80691	*Hoplias curupira*	Igarape Pacanari	Jari/Amazonas	Almeirim/Pará	Brazil
LBP 9302	LBPV42535	*Hoplias curupira*	Igarapé Vermelho	Guamá/Amazonas	Ourém/PA	Brazil
LBP 22828	LBPV87646	*Hoplias intermedius*	Riacho Vargem do Lobo	São Francisco	Lagoa Santa/MG	Brazil
LBP 21874	LBPV84142	*Hoplias intermedius*	Rio Grande	Paraná	Miguelópolis/SP	Brazil
LBP 28564	LBPV100386	*Hoplias lacerdae*	Rio Ribeira de Iguape	Atlantic drainage	Registro/SP	Brazil
LBP 7174	LBPV34679	*Hoplias malabaricus*	Rio Coité	Paraguaçu/Atlantic drainage	Lençóis/BA	Brazil
LBP 2211	LBPV15616	*Hoplias malabaricus*	Laguna de Castilleros	Orinoco	Caicara del Orinoco /Bolivar	Venezuela
LBP 22429	LBPV86835	*Hoplias malabaricus*	Quebrada La Ponderosa	Amazonas	Leticia/Amazonas	Colombia
LBP 5200	LBPV26712	*Hoplias malabaricus*	Rio Paraná	Paraná	Porto Rico/PR	Brazil
LBP 2315	LBPV15859	*Hoplias malabaricus*	Rio Parguaza	Orinoco	Cedeño /Bolívar	Venezuela
LBP 5564	LBPV27269	*Hoplias malabaricus*	Rio Tapuiu	Parnaíba	Santa Filomena/PI	Brazil
LBP 11283	LBPV48768	*Hoplias malabaricus*	Lagoa Temporária	São Francisco	Gararu/SE	Brazil
LBP 21115	LBPV82828	*Hoplias malabaricus*	Igarapé do Quatorze	Oiapoque/Amazonas	Oiapoque/AP	Brazil
LBP 6595	LBPV31902	*Hoplias mbigua*	Rio Paraná	Paraná	Marilena/PR	Brazil
LBP 2763	LBPV18503	*Hoplias microlepis*	Río Llano Sucio	Atlantic drainage	Santa Rita Arriba/Colón	Panamá
CZUT-IC 12752	CZUT-IC-TE 351	*Hoplias microlepis*	Ciénaga de Marriaga	Atrato	Ungía/Chocó	Colombia
LBP 19353	LBPV76069	*Hoplias microlepis*	Santa Ines	Pacific drainage	Machala/El Oro	Ecuador
LBP 6697	LBPV32185	*Hoplias misionera*	Lagoa Marginal	Paraná	Marilena/PR	Brazil
CZUT-IC-TE 2817	CZUT-IC-TE 2817	*Hoplias* sp.	Río Peralonso	Catatumbo/Maracaibo	El Zulia/Norte de Santander	Colombia
CZUT-IC 11923	CZUT-IC-TE 713	*Hoplias* sp.	Quebrada Bacalla	Upper Magdalena	Suárez/Tolima	Colombia
LBP10740	LBPV49748	*Hoplias* sp.	Rio Macabu	Paraíba do Sul	Conceição do Macabu/RJ	Brazil
LBP 3446	LBPV20326	*Hoplias* sp.	Córrego Chumbado	Doce	Sooretama/ES	Brazil

Catalog number	Tissue	Taxon	Locality	Basin	City/State	Country
LBP 8231	LBPV38246	*Hoplias* sp.	Rio Preto	Atlantic drainage	Mongaguá/SP	Brazil
LBP 15788	LBPV64781	*Hoplias* sp.	Afluente Rio Feio	Xingu/Amazonas	Querência/MT	Brazil
LBP 22500	LBPV87525	*Hoplias* sp.	Lago Yahuarcaca	Amazonas	Letícia/Amazonas	Colombia
ANSP 179202	T208	*Hoplias* sp.	Two Puddle Creek	Rupununi/Essequibo	Upper Takutu-Upper Essequibo	Guyana
CZUT-IC 21422	CZUT-IC-TE4218	*Hoplias* sp.	Río San Juan	Pacific drainage	Tadó/Chocó	Colombia
LBP 28727	LBPV100391	*Hoplias* sp.	Quebrada Grande	Uruguay	Paysandú	Uruguay
LBP 6138	LBPV29518	*Hoplias teres*	Rio Santa Rosa	Maracaibo	Machiques de Perijá/Zulia	Venezuela
LBP 9789	53212	*Hydrolycus scomberoides*	Rio Itaya	Amazonas	Iquitos/Loreto	Peru
ANSP 182609	P6322	*Leporellus vittatus*	Nanay	Amazonas	Maynas/Loreto	Peru
LBP 3180	16871	*Leporinus striatus*	Reservatório de Jurumirim	Paranapanema	Itatinga/SP	Brazil
OS 18311	PE10108	*Megaleporinus trifasciatus*	Nanay	Amazonas	Maynas/Loreto	Peru
LBP 18398	42589	*Metynnis luna*	Rio Guamá	Amazonas	Ourém/PA	Brazil
LBP 24311	91508	*Mylossoma acanthogaster*	Rio Sardinata	Catatumbo/Maracaibo	Tibu/Santander	Colombia
LBP 2190	15518	*Mylossoma* sp.	Laguna de Castilleros	Orinoco	Caicara del Orinoco /Bolivar	Venezuela
LBP 2191	15554	*Pristobrycon calmoni*	Laguna de Castilleros	Orinoco	Caicara del Orinoco /Bolivar	Venezuela
LBP 11336	45523	*Pygocentrus piraya*	Lagoa da Tiririca	São Francisco	Pirapora/MG	Brazil
LBP 12660	43557	*Rhaphiodon vulpinus*	Rio Araguaia	Amazonas	Cocalinho/MT	Brazil
LBP21610	61612	*Serrasalmus maculatus*	Brejo a beira da BR 230	Tapajós/Amazonas	Itaituba/PA	Brazil
LBP 22727	86548	*Tarumania walkerae*	Rio Tarumã-Mirim	Rio Negro	Manaus/AM	Brazil

Table S2. Summary of descriptive statistics, sequencing and UCE loci for each specimen used in present study.

Catalog number	Tissue	Taxon	Number of reads	Total trimmed reads bp	Mean length	95 CI length	Min length	Max length	Median length
ANSP 178126	1712	*Abramites hypselonotus*	2,283,524	216,021,253	94.60	0.009	40	101	101
AMNH 242137	333238	*Alestes inferus*	1,847,106	219,360,249	118.76	0.012	40	125	125
OS 19665	BLS14-013	*Bryconaethiops microstoma*	2,209,167	261,327,383	118.29	0.011	40	125	125
LBP 7556	35626	*Catoprion mento*	2,966,961	354,179,635	119.37	0.009	40	125	125
LBP 12838	54048	*Colossoma macropomum*	3,854,360	464,026,488	120.39	0.007	40	125	125
LBP 12838	54052	*Colossoma macropomum*	2,066,137	247,191,696	119.64	0.010	40	125	125
LBP 6136	29524	*Ctenolucius hujeta*	3,758,899	450,475,073	119.84	0.008	40	125	125
LBP 24318	91518	*Curimata mivartii*	2,580,568	297,492,588	115.28	0.013	40	125	125
LBP 5431	27171	*Curimatella alburna*	5,439,333	515,320,036	94.74	0.006	40	101	101
LBP 10227	43105	*Cynodon gibbus*	1,365,513	160,488,638	117.53	0.015	40	125	125
LBP 15139	62363	*Cyphocharax spilurus*	6,353,243	602,681,597	94.86	0.006	40	101	101
AUM 67125	AUFT 10173	*Erythrinus erythrinus*	4,086,117	598,768,909	146.54	0.009	40	151	151
AUM 62923	AUFT 6520	*Erythrinus erythrinus*	4,212,083	616,543,613	146.37	0.009	40	151	151
LBP 25856	LBPV 96379	*Erythrinus erythrinus*	2,950,479	430,870,030	146.03	0.011	40	151	151
LBP 23561	LBPV 92312	*Erythrinus erythrinus*	3,035,309	444,575,823	146.47	0.010	40	151	151
INPA-ICT 056178	P32617	*Erythrinus* sp. 1	6,450,764	944,990,904	146.49	0.007	40	151	151
LBP 23551	LBPV 92288	*Erythrinus* sp. 1	2,947,188	430,049,312	145.92	0.011	40	151	151
LBP 10907	LBPV 50235	*Erythrinus* sp. 2	3,151,410	460,069,608	145.99	0.010	40	151	151
MZUSP 118308	MZUSPV 3748	*Erythrinus* sp. 2	3,215,766	470,854,816	146.42	0.010	40	151	151
MZUSP 117564	MZUSPV 3040	*Erythrinus* sp. 2	2,550,623	372,910,701	146.20	0.011	40	151	151
LBP 8518	LBPV 43203	*Erythrinus* sp. 2	2,862,753	418,031,256	146.02	0.011	40	151	151
LBP 14851	LBPV 57878	*Erythrinus* sp. 3	2,681,729	391,962,761	146.16	0.011	40	151	151
LBP 2137	LBPV 21405	*Erythrinus* sp. 4	4,108,852	601,178,140	146.31	0.009	40	151	151
LBP 6625	LBPV 31955	*Erythrinus* sp. 5	3,639,480	432,231,750	118.76	0.008	40	125	125
LBP 10802	LBPV49931	*Erythrinus* sp. 5	14,907,021	2,184,214,050	146.52	0.004	40	151	151
LBP 6583	LBPV 31841	*Erythrinus* sp. 5	2,967,690	433,450,448	146.06	0.011	40	151	151
AMNH 242489	353404	*Hepsetus cuvieri*	6,075,880	735,331,117	121.02	0.005	40	125	125
LBP 2298	LBPV 15829	*Hoplerythrinus* sp.	4,963,170	728,841,092	146.85	0.008	40	151	151

Catalog number	Tissue	Taxon	Number of reads	Total trimmed reads bp	Mean length	95 CI length	Min length	Max length	Median length
CZUT-IC 12980	CZUT-IC-TE 866	*Hoplerythrinus* sp.	2,993,807	439,650,068	146.85	0.010	40	151	151
CZUT-IC 11490	CZUT-IC-TE 990	*Hoplerythrinus* sp.	6,231,258	910,996,123	146.20	0.007	40	151	151
ROM 92359	T09425	*Hoplerythrinus* sp.	10,161,699	1,483,467,132	145.99	0.006	40	151	151
LBP 4237	LBPV 22757	*Hoplerythrinus unitaeniatus*	7,978,079	1,171,316,858	146.82	0.006	40	151	151
LBP 9152	LBPV 42525	*Hoplerythrinus unitaeniatus*	6,776,036	991,677,716	146.35	0.007	40	151	151
LBP 23527	LBPV 92225	*Hoplerythrinus unitaeniatus*	7,549,190	1,108,276,759	146.81	0.006	40	151	151
LBP 2980	LBPV 19624	*Hoplerythrinus unitaeniatus*	8,886,680	1,301,538,188	146.46	0.006	40	151	151
LBP 25545	LBPV 91345	*Hoplerythrinus unitaeniatus*	8,617,078	1,262,370,474	146.50	0.006	40	151	151
LBP 17450	LBPV 69028	*Hoplerythrinus unitaeniatus*	6,701,133	982,572,827	146.63	0.007	40	151	151
LBP 5507	LBPV 26600	*Hoplerythrinus unitaeniatus*	6,639,113	975,725,191	146.97	0.006	40	151	151
MHNG 2755.083	GFSU14-1357	*Hoplerythrinus unitaeniatus*	4,175,434	609,161,268	145.89	0.009	40	151	151
LBP 23560	LBPV 92311	*Hoplerythrinus unitaeniatus*	2,501,242	366,513,597	146.53	0.011	40	151	151
LBP 28291	LBPV 96858	*Hoplerythrinus unitaeniatus*	3,200,574	467,484,134	146.06	0.010	40	151	151
LBP 5180	LBPV 26697	*Hoplerythrinus unitaeniatus*	6,296,134	920,286,976	146.17	0.007	40	151	151
LBP 651	LBPV 8042	*Hoplerythrinus unitaeniatus*	4,869,252	710,784,728	145.97	0.008	40	151	151
LBP 8025	LBPV 37724	*Hoplerythrinus unitaeniatus*	8,216,696	1,207,360,438	146.94	0.006	40	151	151
LBP 16143	LBPV 66873	*Hoplerythrinus unitaeniatus*	7,621,070	1,121,031,434	147.10	0.006	40	151	151
LBP 20882	LBPV 81519	*Hoplerythrinus unitaeniatus*	2,971,285	431,598,743	145.26	0.011	40	151	151
MZUSP 96825	MZUSP3392	*Hoplerythrinus unitaeniatus*	5,316,906	772,300,932	145.25	0.008	40	151	151
LBP 19217	LBPV 77663	*Hoplerythrinus unitaeniatus*	5,325,817	779,993,109	146.46	0.008	40	151	151
TIUFRN2909	TI2909	*Hoplerythrinus unitaeniatus*	12,293,948	1,764,189,712	143.50	0.006	40	151	151
LBP 17450	LBPV 69027	*Hoplerythrinus unitaeniatus*	2,156,813	255,234,898	118.34	0.011	40	125	125
LBP 15875	LBPV 64189	*Hoplerythrinus unitaeniatus*	7,318,442	1,072,821,808	146.59	0.006	40	151	151
LBP 20520	LBPV80648	*Hoplias aimara*	4,012,378	586,877,733	146.27	0.009	40	151	151
LBP 13248	LBPV69385	*Hoplias aimara*	3,944,887	576,152,506	146.05	0.009	40	151	151
LBP 9101	LBPV42717	*Hoplias aimara*	3,127,071	455,358,750	145.62	0.011	40	151	151
LBP 13122	LBPV 54949	*Hoplias argentinensis*	4,327,022	628,486,554	145.25	0.010	40	151	151
LBP 29138	LBPV101563	*Hoplias brasiliensis*	8,084,569	1,146,999,768	141.88	0.009	40	151	151
LBP 20412	LBPV80691	*Hoplias curupira*	1,853,591	218,156,654	117.69	0.013	40	125	125
LBP 9302	LBPV42535	*Hoplias curupira*	7,792,719	1,139,364,950	146.21	0.006	40	151	151

Catalog number	Tissue	Taxon	Number of reads	Total trimmed reads bp	Mean length	95 CI length	Min length	Max length	Median length
LBP 21874	LBPV 84142	*Hoplias intermedius*	4,142,852	486,200,993	117.36	0.008	40	125	125
LBP 22828	LBPV 87646	*Hoplias intermedius*	4,802,847	658,679,151	137.14	0.013	40	151	151
LBP 28564	LBPV100386	*Hoplias lacerdae*	2,443,420	356,908,430	146.07	0.012	40	151	151
LBP 7174	LBPV 34679	*Hoplias malabaricus*	3,634,610	530,750,271	146.03	0.010	40	151	151
LBP 21115	LBPV 82828	*Hoplias malabaricus*	4,029,168	586,826,092	145.64	0.010	40	151	151
LBP 2315	LBPV 15859	*Hoplias malabaricus*	2,851,692	417,225,803	146.31	0.011	40	151	151
LBP 5200	LBPV 26712	*Hoplias malabaricus*	3,552,975	517,400,368	145.62	0.010	40	151	151
LBP 5564	LBPV 27269	*Hoplias malabaricus*	2,400,740	349,713,369	145.67	0.012	40	151	151
LBP 11283	LBPV 48768	*Hoplias malabaricus*	4,083,175	597,461,611	146.32	0.009	40	151	151
LBP 2211	LBPV 15616	*Hoplias malabaricus*	3,195,624	464,997,410	145.51	0.011	40	151	151
LBP 22429	LBPV 86835	*Hoplias malabaricus*	3,181,192	463,646,790	145.75	0.011	40	151	151
LBP 6595	LBPV 31902	*Hoplias mbigua*	2,083,677	304,339,863	146.06	0.013	40	151	151
CZUT-IC 12752	CZUT-IC-TE 351	*Hoplias microlepis*	3,182,650	466,067,289	146.44	0.010	40	151	151
LBP 19353	LBPV 76069	*Hoplias microlepis*	991,285	116,503,006	117.53	0.017	40	125	125
LBP 2763	LBPV 18503	*Hoplias microlepis*	2,201,180	321,911,314	146.24	0.012	40	151	151
LBP 6697	LBPV 32185	*Hoplias misionera*	3,382,955	493,980,206	146.02	0.010	40	151	151
CZUT-IC 11923	CZUT-IC-TE 713	*Hoplias* sp.	3,275,405	478,554,534	146.11	0.010	40	151	151
CZUT-IC-TE 2817	CZUT-IC-TE 2817	*Hoplias* sp.	2,572,528	375,912,330	146.13	0.011	40	151	151
LBP 8231	LBPV 38246	*Hoplias* sp.	3,064,063	446,121,967	145.60	0.011	40	151	151
LBP 3446	LBPV 20326	*Hoplias* sp.	3,947,269	574,432,557	145.53	0.010	40	151	151
ANSP 179202	T208	*Hoplias* sp.	8,927,165	1,306,689,154	146.37	0.006	40	151	151
LBP 22500	LBPV 87525	*Hoplias* sp.	2,655,010	387,685,835	146.02	0.011	40	151	151
LBP10740	LBPV 49748	*Hoplias* sp.	4,085,021	596,081,663	145.92	0.009	40	151	151
CZUT-IC 21422	CZUT-IC-TE4218	*Hoplias* sp.	9,833,657	1,442,854,956	146.73	0.005	40	151	151
LBP 28727	LBPV100391	*Hoplias* sp.	5,787,247	842,522,769	145.58	0.008	40	151	151
LBP 15788	LBPV 64781	*Hoplias* sp.	3,801,549	555,254,174	146.06	0.009	40	151	151
LBP 6138	LBPV 29518	*Hoplias teres*	3,320,915	484,296,293	145.83	0.010	40	151	151
LBP 9789	53212	*Hydrolycus scomberoides*	4,947,174	580,719,580	117.38	0.008	40	125	125
ANSP 182609	P6322	*Leporellus vittatus*	3,928,683	373,831,133	95.15	0.007	40	101	101
LBP 3180	16871	*Leporinus striatus*	3,742,443	355,408,855	94.97	0.007	40	101	101

Catalog number	Tissue	Taxon	Number of reads	Total trimmed reads bp	Mean length	95 CI length	Min length	Max length	Median length
OS 18311	PE10108	*Megaleporinus trifasciatus*	6,704,325	639,267,872	95.35	0.005	40	101	101
LBP 18398	42589	*Metynnis luna*	2,101,237	251,487,319	119.69	0.010	40	125	125
LBP 24311	91508	*Mylossoma acanthogaster*	1,606,554	192,937,936	120.09	0.012	40	125	125
LBP 2190	15518	*Mylossoma* sp.	1,597,330	190,446,081	119.23	0.012	40	125	125
LBP 2191	15554	*Pristobrycon calmoni*	1,792,409	213,813,471	119.29	0.011	40	125	125
LBP 11336	45523	*Pygocentrus piraya*	938,112	111,074,054	118.40	0.017	40	125	125
LBP 12660	43557	*Rhaphiodon vulpinus*	2,299,180	268,969,641	116.99	0.012	40	125	125
LBP21610	61612	*Serrasalmus maculatus*	2,720,253	321,831,707	118.31	0.010	40	125	125
LBP 22727	86548	*Tarumania walkerae*	2,842,215	340,092,503	119.66	0.009	40	125	125

Table S3. Biogeographic (dispersal and vicariance) events dates using literature and other estimates of paleogeographic events. Event timings are based on, and ordered by, maximum age estimate. POA = Proto-Orinoco-Amazon basins. GS = Guiana Shield. GAzBI = Great Amazonian Biotic Interchange. Other acronyms as in Fig. 4.

Clade	Margin	Age (Ma): Mean estimates			Epoch from max estimates	Event	Event Reference
		min	max	median			
14	Western	0	2.3	1.2	Pleistocene	Separation among NW trans-Andean basins	This study
13	Western	2.3	3.1	2.7	Pliocene	Separation among NW trans-Andean basins	This study
6	Eastern	2.6	4.6	3.6	Pliocene	Watershed migration Serra do Mar	Salgado et al., 2014
12	Eastern	5.4	6.1	5.8	Late Miocene	River capture across Central Brazilian Shield	Bagley et al., 2021
7	Western	3.8	6.8	5.3	Late Miocene	River capture across Tatacoa Portal	Montes et al., 2021
16	Eastern	4.6	6.8	5.7	Late Miocene	River capture across Izozog Portal	Carvalho & Albert, 2011
8	Eastern	6.2	6.8	6.5	Late Miocene	River capture across Central Brazilian Shield	Bagley et al., 2021
9	Eastern	4.1	7.1	5.6	Late Miocene	Uplift Vaupes Arch	Albert et al., 2018
10	Eastern	6.6	7.1	6.9	Late Miocene	GAzBI: Dispersal filter: W←→ E	Albert et al., 2021
15	Western	8.0	8.3	8.2	Late Miocene	Uplift Merida Andes	Albert et al., 2006
11	Eastern	7.2	8.3	7.7	Late Miocene	GAzBI: Dispersal filter: W←→ E	Albert et al., 2021
5	Western	6.2	8.9	7.5	Late Miocene	River capture across Izozog Portal	Carvalho & Albert, 2011
3	Eastern	2.7	12.1	7.4	Middle Miocene	Watershed migration Serra do Mar	Salgado et al., 2014
2	Eastern	3.7	12.1	7.9	Middle Miocene	Watershed migration Serra do Mar	Salgado et al., 2014
4	Western	4.0	13.0	8.5	Middle Miocene	Watershed migration Eastern Cordillera Colombia	Montes et al., 2021
1	Western	12.7	19.3	16.0	Early Miocene	River capture across Izozog Portal	Tagliacollo et al., 2015
1"	Eastern	3.6	25.0	14.3	Oligocene	Dispersal filter: POA ←→ GS	This study
1'	Eastern	10.0	34.0	22.0	Late Eocene	Dispersal filter: POA ←→ GS + B	This study

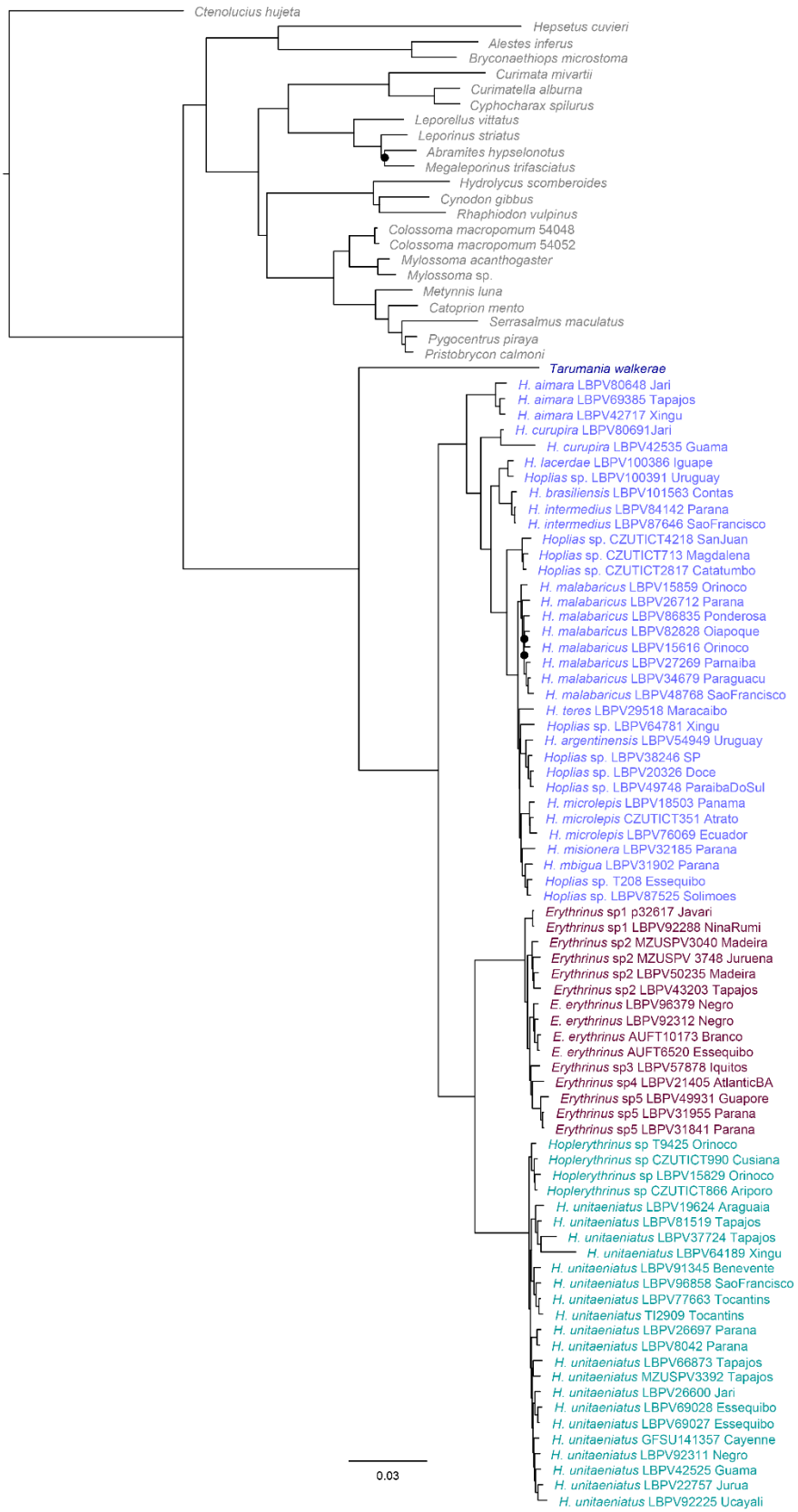

Fig S1. Bayesian inference (BI) using 75% complete matrix (edge-trimmed, unpartitioned). No symbols at nodes indicate Bayesian posterior probabilities of 1, and black circles denoted nodal support inferior to 0.75.

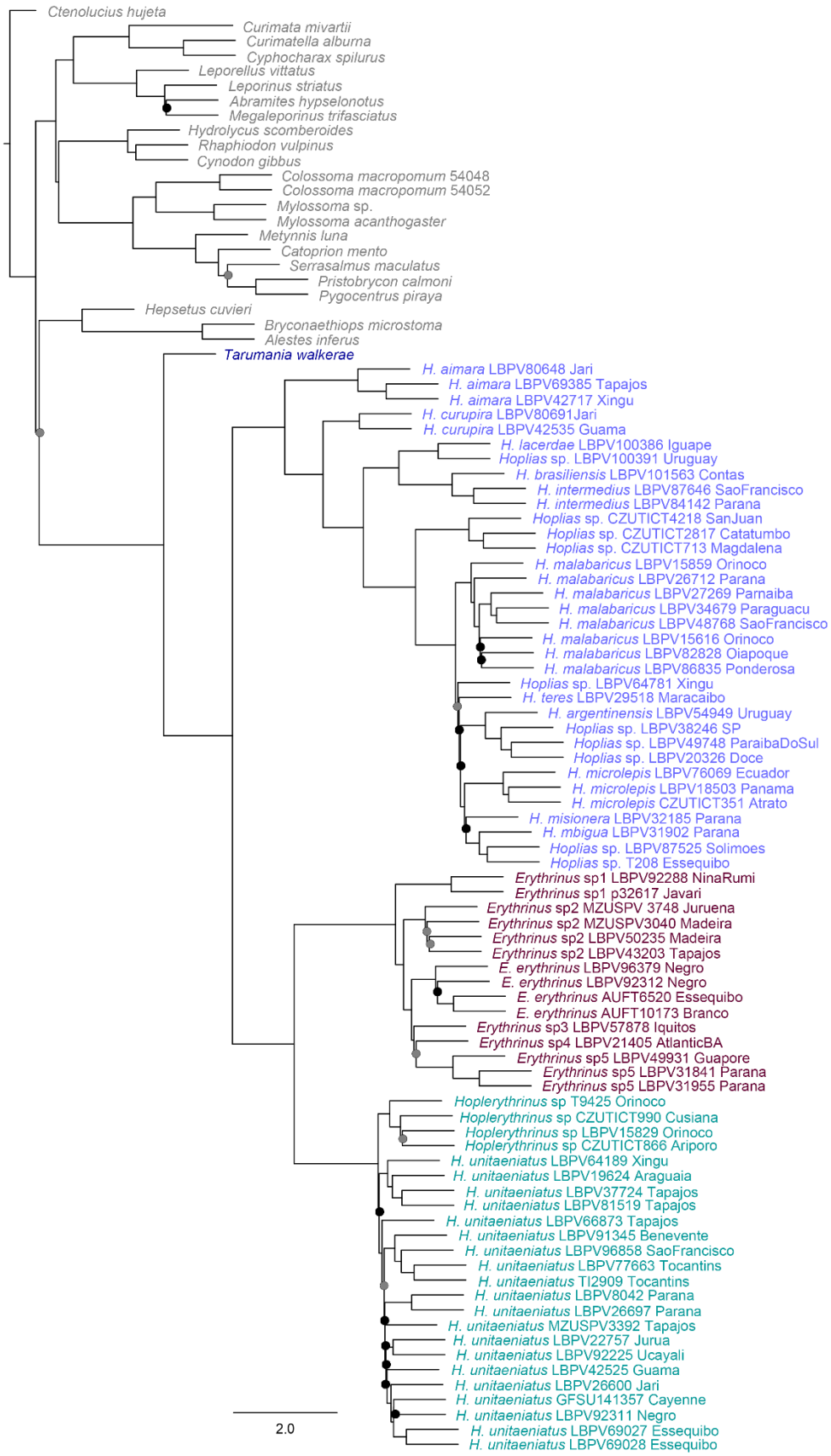

Fig S2. Species tree inference from Astral-III, based on the 75% complete matrix. No symbols at nodes indicate support values between 1-0.90, gray circle denoted nodal support between 0.89-0.75, and black circles denoted nodal support inferior to 0.75.

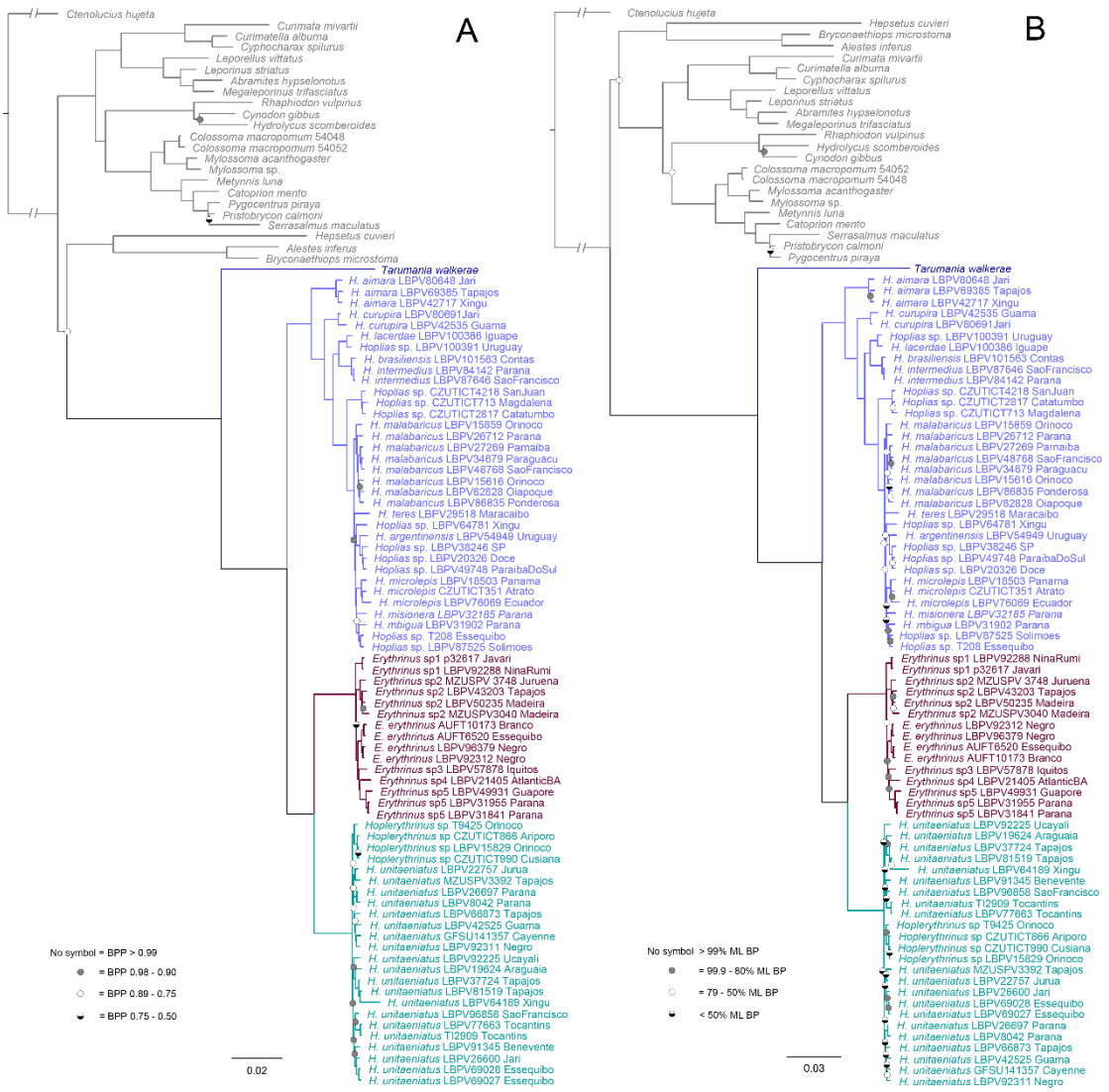

Fig S3. Phylogenetic relationships of Erythrinoidea based using the 95% complete matrix of ultraconserved elements. Data for 91 loci and 17715 bp. **A.** Bayesian analysis (edge-trimmed, unpartitioned) and, **B.** maximum likelihood (ML) analysis (edge-trimmed, partitioned). ML BP = ML bootstrap support values; BPP = Bayesian posterior probabilities.

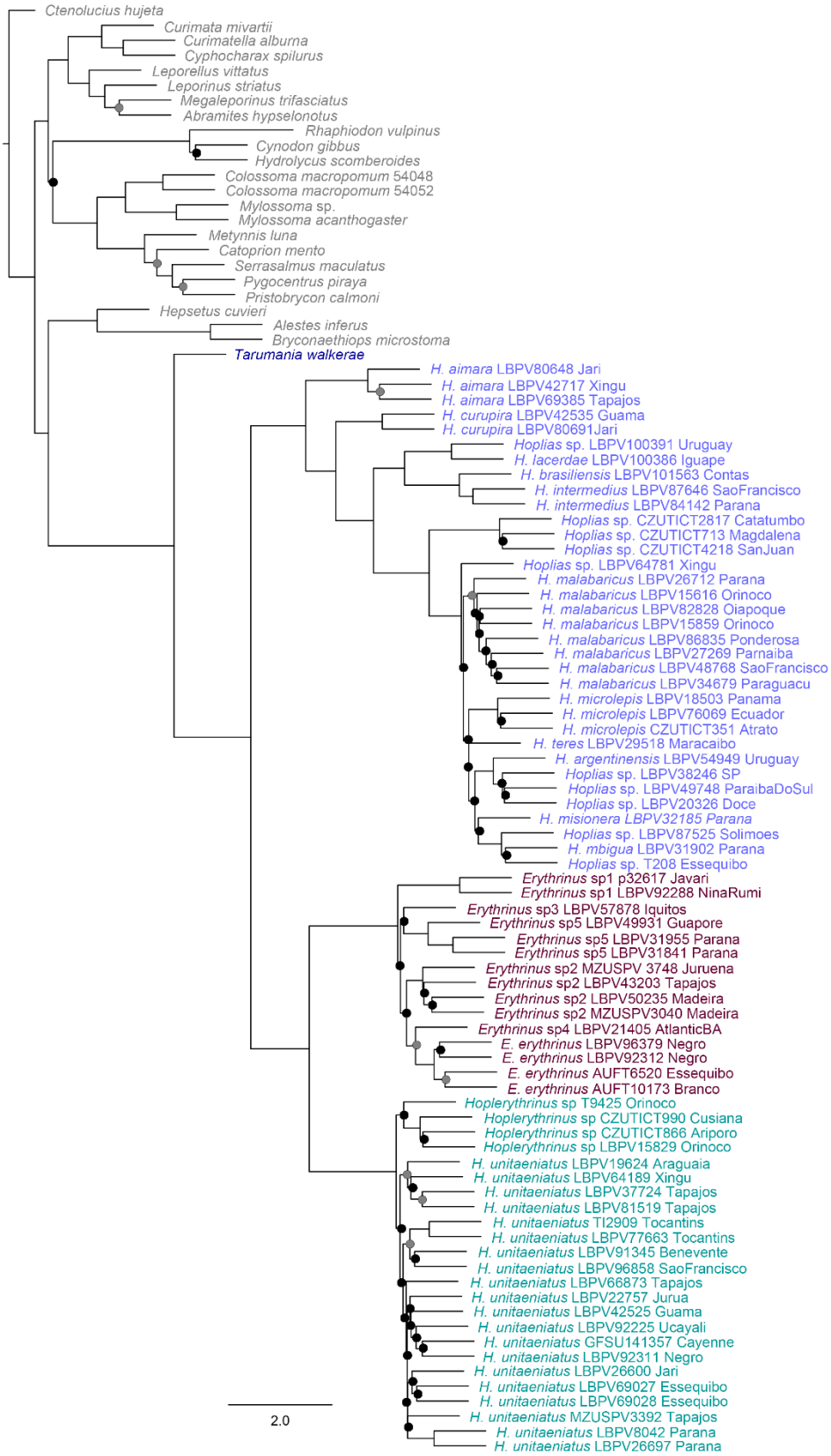

Fig S4. Species tree inference from Astral, based on the 95% complete matrix. No symbols at nodes indicate support values between 1-0.90, gray circle denoted nodal support between 0.89-0.75, and black circles denoted nodal support inferior to 0.75.

CHAPTER 2

Is *Hoplerythrinus* (Characiformes, Erythrinidae) a geographically widespread monotypic fish genus? An integrative approach using phylogenomic, DNA barcode, and morphological data

Is *Hoplerythrinus* (Characiformes, Erythrinidae) a geographically widespread monotypic fish genus? An integrative approach using phylogenomic, DNA barcode, and morphological data

Abstract

Delimiting species boundaries is difficult when taxa do not exhibit clear divergence across their geographic range. Discovering and documenting species often requires an integrative approach assessing genomic differentiation, phenotypic variation, and divergence times. The Neotropical freshwater fish (NFF) *Hoplerythrinus* is widely distributed throughout cis-Andean tropical South America, with the type species *H. unitaeniatus* described from the Rio São Francisco, and two other species only known from the type material although listed as valid in literature: *H. gronovii* from Cayenne in French Guiana and *H. cinereus* from Trinidad Island. No studies have yet been conducted to assess the taxonomic status of these nominal species, and diversity in this group remains poorly understood. Here, we integrate DNA barcode sequences, a phylogenomic dataset of ultraconserved elements (UCEs), morphological information, and extensive coverage of geographic distribution to investigate the diversity and evolutionary history of *Hoplerythrinus*. Three mtDNA lineages were identified: one widely-distributed cluster present in all major cis-Andean basins, a second cluster from upper portions of Amazonian versants draining the Brazilian Shield, and a third cluster from the Río Orinoco Basin. Reciprocal monophyly of these clusters was not always recovered in phylogenomic analyses using UCEs data. Discordant assignments of representatives from the Orinoco basin comparing mitochondrial and nuclear datasets suggest gene flow between these regions. Additionally, no morphological characters were found to distinguish the three lineages. Based on these multiple lines of evidence, we propose *Hoplerythrinus* as a monotypic genus distributed throughout the cis-Andean drainages of tropical South America. *Hoplerythrinus* reveals low species accumulation rates considering its divergence time (*c.* 7.1 Ma), similar to patterns exhibited by some NFF genera. Results indicate that the time of divergence has not been enough to establish full divergence among the lineages, and therefore they cannot be unambiguously diagnosed as discrete species.

Keywords: DNA barcode, Neotropical freshwater fishes, phylogenomics, species richness, Teleostei, ultraconserved elements

1. Introduction

One of the major objectives of evolutionary biology is to explain organismal diversity, which exists at many levels (Butlin et al. 2012; Seehausen and Wagner 2014). In this sense, recognizing and delimiting biological units are pivotal steps to understanding the underlying evolutionary processes (Willis 2017; Fišer et al. 2018; Struck and Cerca 2019). Speciation is the process by which new species are formed, in which different properties such as, reproductive isolation, ecological differentiation, and/or reciprocal monophyly are acquired over evolutionary time (De Queiroz 2005, 2007; Fišer et al. 2018; Galtier 2019). However, these properties can emerge at different rates or never even appear during the existence of lineages (De Queiroz 2007). Rates of genetic and phenotypic divergence depend on highly dynamic processes involving landscape evolution and genetic, ecological, and behavioral mechanisms (Norris and Hull 2012; Albert et al. 2020; McGee et al. 2020). In some cases, these dynamics can generate subtle differences that obscure clear delineation of species boundaries (Korshunova et al. 2019; Struck and Cerca 2019; Carneiro et al. 2021).

A robust hypothesis of lineage separation often requires data from multiple lines of investigation (De Queiroz 2007). Studies of taxa that exhibit intermediate levels of divergence benefit from a framework that assesses genomic differentiation, phenotypic variation, and divergence times (Struck et al. 2018). Newly developed procedures for acquiring and integrating different data types to establish a robust consensus of lineage separation have been proposed (Padial et al. 2010; Schlick-Steiner et al. 2010). Recent efforts are integrating different technologies and methods to explore diversity and characterize evolutionary lineages of Neotropical freshwater fishes (NFF), such as high-throughput DNA sequencing (Aguilar et al. 2019; Rincon-Sandoval et al. 2019; Mateussi et al. 2020; Kolmann et al. 2021; Melo et al. 2021), DNA barcode sequences (Agudelo-Zamora et al. 2020; Anjos et al. 2020; Ochoa et al. 2020; Garavello et al. 2021), computer tomography (Henschel et al. 2022), geometric and traditional morphometrics (Loureiro et al. 2018; Armbruster et al. 2021). However, even integrating multiple evidences, disentangling some groups represents a challenge due to their evolutionary complexity (Carneiro et al., 2021; Melo et al., 2016b).

Representatives of the NFF family Erythrinidae are widely distributed in most drainages of Central and South America, from Costa Rica to Argentina (Oyakawa and Mattox 2018), and possess a complex taxonomy, where cataloging its diversity has represented a multidisciplinary challenge (Bertollo et al. 2004; da Rosa et al. 2012; Rosso et al. 2018; Guimarães et al. 2021a; Sassi et al. 2021). Erythrinids live in lentic and lotic habitats where they prey on insects, crustaceans and other fishes (Marrero et al. 1997; Lasso and Meri 2001; Oliveira and Garavello 2003; Lasso et al. 2011) and have relevant importance within commercial fisheries or local consumption in many regions (Lasso et al. 2011; Oyakawa et al. 2013). Three extant genera are currently recognized in the family: *Erythrinus* Scopoli, 1777, *Hoplerythrinus* Gill, 1896 and *Hoplias* Gill, 1903 (Oyakawa 2003), each of them including species with wide distributions that represent interesting groups for evolutionary studies (Born and Bertollo 2000; Dergam et al. 2002; Cioffi et al. 2009; Pereira et al. 2013b; Martinez et al. 2016). *Hoplias* is distributed across most hydrological basins in both trans- and cis-Andean region and currently consists of 15 valid species. Alternatively, *Erythrinus* and *Hoplerythrinus* have a wide cis-Andean distribution, presenting a lower diversity (Oyakawa 2003; Fricke et al. 2022).

In *Hoplerythrinus*, three species are considered as valid (Oyakawa 2003; Fricke et al. 2022), however, no study has yet examined the taxonomic status of these taxa. *Hoplerythrinus unitaeniatus* (Agassiz, in Spix and Agassiz, 1829) originally described from the Rio São Francisco has been the only species of the genus identified in current literature, presenting a wide geographic distribution throughout most cis-Andean drainages of South America (Oyakawa and Mattox 2018), and being considered as a species complex (Giuliano-Caetano et al. 2001; Martinez et al. 2016). The other two species considered valid (Oyakawa 2003) are only known from the type material with poor diagnoses and descriptions: *H. gronovii* (Valenciennes, in Cuvier and Valenciennes, 1847) described from Cayenne in French Guiana and *H. cinereus* (Gill 1858) from the Trinidad Island. Cytogenetic studies have revealed a discrete karyotypic variation within *Hoplerythrinus*, with diploid numbers 2n = 48 to 2n = 52 chromosomes and fundamental numbers 92 to 102, single and multiples Ag-NORs (Giuliano-Caetano et al. 2001; Martinez et al. 2016) and polymorphisms related to 5S and 18S rDNA (Diniz and Bertollo 2003; Martinez et al. 2016). However, representatives of this genus have revealed an apparent uniformity of meristic and morphometric data throughout their distribution area

(Oyakawa et al. 2013), and a study focusing on the taxonomic status and examination of diversity is yet to be conducted.

Under this context we integrate DNA barcode sequences, a phylogenomic dataset of ultraconserved elements (UCEs), morphological information (color patterns, standard morphometrics and meristic) and an extensive taxon coverage in its geographic distribution area to investigated the evolutionary history and to assess the species diversity throughout the wide distribution of *Hoplerythrinus*. Based on our results, novel taxonomic decisions are made and their implications are discussed according to divergence time, ecological affinities and karyotypic variation of this erythinid fish genus.

2. Material and Methods

2.1 Taxon sampling for molecular approaches

This study includes 107 samples of *Hoplerythrinus* with an extensive geographic coverage and additional 30 samples were included as outgroup taxa (Fig. 1, Table S1). Molecular delimitation analyses were implemented based on 105 samples, of which 100 were new generated COI sequences and five were obtained from GenBank. Based on this extensive DNA barcoding analysis, we chose 24 samples including representatives of relevant lineages for phylogenomic analysis through sequencing of ultraconserved elements of the genome (UCEs; Faircloth et al., 2020, 2012). Samples were obtained from field expeditions or donations from scientific collections (Table S1). Institutional acronyms follow Sabaj (2020).

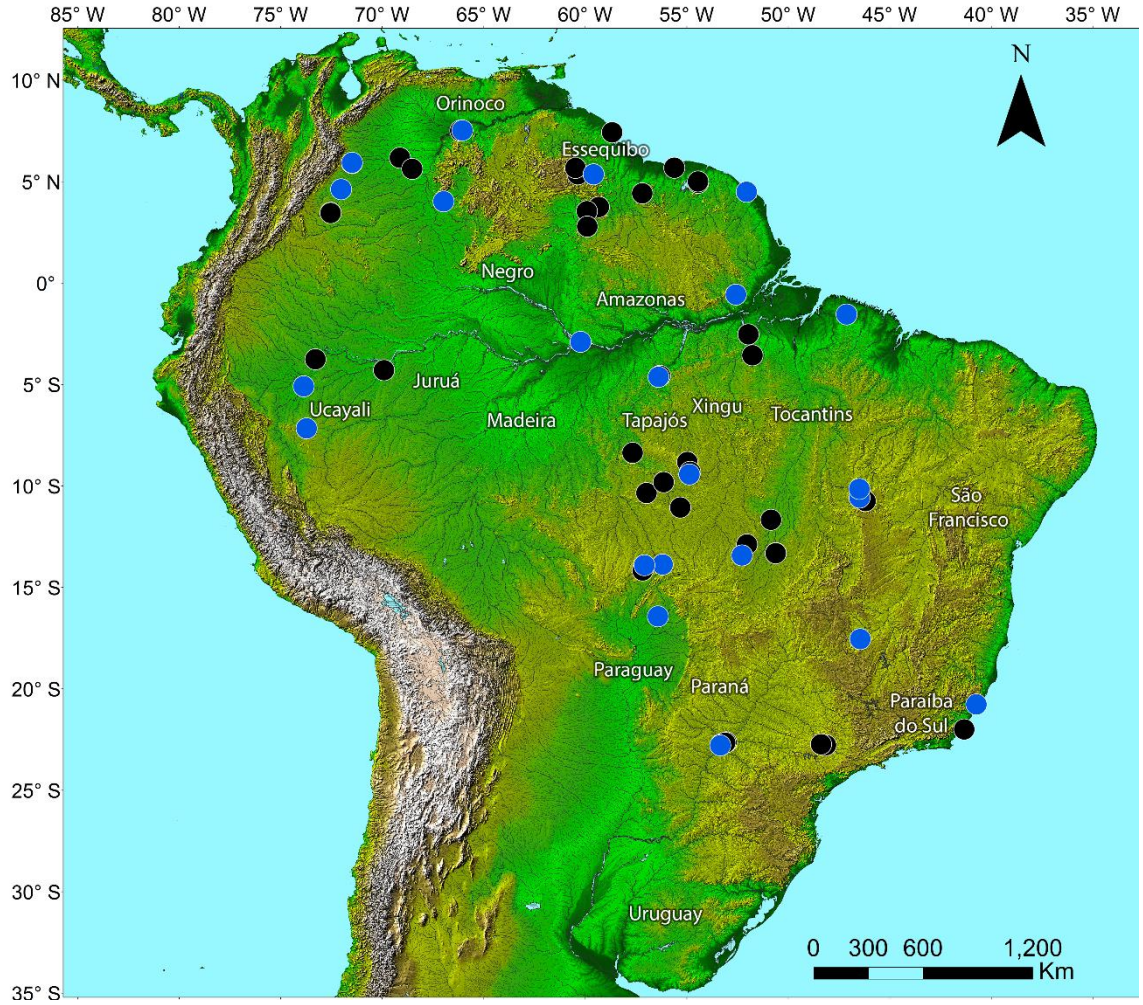

Figure 1. Geographic distribution of *Hoplerythrinus* samples. Black circles show localities of specimens included in the barcode analysis; blue circles show localities of specimens included in either the phylogenomic analysis or both analyses.

2.2 Molecular species delimitation

2.2.1 DNA extraction, amplification and sequencing

Genomic DNA was extracted from gill filaments, muscle or fin tissues preserved in 95% ethanol with a DNeasy Blood & Tissue kit (Qiagen Inc.; http://www.qiagen.com) according to manufacturer's instructions. Partial sequences of the mitochondrial gene cytochrome oxidase c subunit I (COI) were amplified using one round of polymerase chain reaction (PCR) using different combinations of primers Fish F1 and Fish R1 (Ward et al. 2005), L5698-Asn and H7271-COXI (Melo et al. 2011). The PCR reactions were carried out in a reaction volume of 12.5 µl containing: 8.15 µl of H_20, 1.25 µl of 10× Taq buffer (500 mM KCl; 200 mM Tris-HCl), 0.4 µl of $MgCl_2$ (50 mM), 0.5 µl of dNTPs (8

mM), 0.25 µl of each primer (10µM), 0.2 µl (5U/µl) of Taq polymerase (Phoneutria®), and 1.5 µl of template DNA (50 ng/µl). The PCR conditions consisted of 3 min at 95°C (initial denaturation) followed by 35 cycles of 45s at 94°C (denaturation), 30s at 50–54°C (primer annealing), and 60s at 68°C (nucleotide extension). After the cycles, we performed a final extension of 10 minutes at 68ºC. Amplified products were checked on 1% agarose gel. Amplicons were then purified with ExoSAP-IT (USB Corporation) following the manufacturer's protocol. The purified products were used as template to sequence both DNA strands using the BigDye Terminator v3.1 Cycle Sequencing Ready Reaction kit (Applied Biosystems) and sequenced on an ABI3130 Genetic Analyzer (Applied Biosystems).

2.2.2 Alignment and species delimitation analyses

Consensus sequences were assembled and edited in Geneious v. 7.1.3 (Kearse et al. 2012), and aligned using MUSCE algorithm (Edgar 2004) in Geneious 7.1.3. The aligned matrix was tested for occurrence of substitution saturation through the index of substitution saturation in asymmetrical (Iss.cAsym) and symmetrical (Iss.cSym) topologies in DAMBE v7.0.28 (Xia 2018).

Species delimitation approaches involved four methods: the first (a) general mixed Yule coalescent (GMYC; Fujisawa and Barraclough, 2013; Pons et al., 2006) using the single threshold parameter at the webserver (https://species.h-its.org/gmyc/), and an ultrametric gene tree as input (removing some samples with repeated haplotypes). BEAST v1.8 package (Drummond et al. 2012) was utilized to estimate the ultrametric gene tree under the constant size coalescent model (Kingman 1982) and the lognormal relaxed clock model (Drummond et al. 2006). The nucleotide evolutionary model used to estimate the ultrametric tree was the GTR+I+G model, as estimated by PartitionFinder v1.1.0 (Lanfear et al. 2012). Markov chains of Monte Carlo included a total of 300.000.000 generations, sampling trees every 30,000 generations. The convergence of the values was checked in Tracer v1.6 (Rambaut et al. 2014), and only runs with effective sample size (ESS) > 200 were accepted. The first 10% generations were discarded as burn-in and the remaining trees were used to build a majority consensus tree in TreeAnnotator v1.8. Second method (b) the Bayesian Poisson Tree Processes (PTP; Zhang et al., 2013) was performed at the PTP webserver (http://species.h-its.org/ server), using 300,000 generations (thinning = 300) and the maximum likelihood (ML) tree as input, obtained through a ML analysis.

The ML analysis was performed with RaxML v8.2 (Stamatakis 2014) under the GTR-GAMMA model, a maximum parsimony starting tree, and a posteriori analysis of bootstrap with the autoMRE function (Pattengale et al. 2010). Third method (c) the Multi-Rate Poisson Tree Process (mPTP) was performed at the mPTP webserver (https://mptp.h-its.org/#/tree) with parameters at default, using the ML tree as input. Fourth method (d) the Automatic Barcode Gap Discovery (ABGD; Puillandre et al., 2012) was performed at the ABGD webserver (wwwabi.snv.jussieu.fr/public/abgd/abgdweb.html), with the Kimura-2-Parameter (K2P) model (Kimura 1980), default number of steps, relative gap width (X) of 0.75, and initial partition with prior maximal distance P= 0.0077.

A final delimitation criterion was established based on a 75% consensus among methods (i.e., congruence in at least three methods). When a 50% congruence among methods was obtained, the most conservative hypothesis was chosen. Sequences were binned into groups according to the results of species delimitation methods, aimed to assess the 2% cutoff value based on genetic distances approach (Pereira et al., 2013; Pugedo et al., 2016). Genetic distances were calculated using the Tamura-Nei (TN93) model (Tamura and Nei 1993) and 1.000 bootstrap replicates in MEGA X (Kumar et al. 2018).

2.3 Phylogenomic analysis

2.3.1 DNA extraction, library preparation, target enrichment and sequencing

Whole genomic DNA was extracted using the DNeasy Tissue kit (Qiagen) following the manufacturer's protocols and 2 µl of each sample were quantified using fluorometry (Qubit, Life Technologies) to verify an ideal concentration (>10 ng/µl). To enrich the libraries, we used the probeset developed for ostariophysan fishes to generate sequence data for 2,708 UCE loci (Faircloth et al. 2020). Library preparation, sequencing and raw data processing were performed by Arbor Biosciences staff (Ann Arbor, MI, USA), using the following protocol: DNA library preparation by modifying the Nextera (Epicentre Biotechnologies) library preparation protocol for solution-based target enrichment (Faircloth et al. 2012) and increasing the number of PCR cycles following the tagmentation reaction to 20 (Faircloth et al. 2013). The Nextera library preparation protocol of in vitro transposition was used followed by PCR to prune the DNA and attach sequencing adapters, and the Epicentre Nextera kit was used to prepare transposase-mediated libraries with insert sizes averaging 100 bp (95% CI: 45 bp) (Adey et al. 2010).

To prepare libraries, whole genomic DNA (40 ng/µl) was first sheared with a QSonica Q800R instrument and selected to modal lengths of approximately 500 nt using a dual-step SPRI bead cleanup. Illumina sequencing libraries were prepared with a slightly modified version of the NEBNext(R) Ultra(TM) DNA Library Prep Kit for Illumina(R). After ligation of sequencing primers, libraries were amplified using KAPA HiFi HotStart ReadyMix (Kapa Biosystems) for six cycles using the manufacturer's recommended thermal profile and dual P5 and P7 indexed primers (Kircher et al. 2012). After purification with SPRI beads, libraries were quantified with the Quant-iT(TM) Picogreen(R) dsDNA Assay kit (ThermoFisher). Pools were enriched comprising 100 ng each of eight libraries (800 ng total) using the MYbaits(R) Target Enrichment system (MYcroarray) following manual version 3.0. After capture cleanup, the bead-bound library was resuspended in the recommended solution and amplified for 10 cycles using a universal P5/P7 primer pair and KAPA HiFi reagents. After purification, each captured library pool was quantified with PicoGreen, and combined with all other pools in projected equimolar ratios prior to sequencing. Sequencing was performed across two Illumina HiSeq paired-end 100 bp lanes using v4 chemistry.

2.3.2 Raw data analysis

The PHYLUCE pipeline was used for processing target-enriched UCE data (Faircloth, 2016). Adapter contamination and low-quality bases were trimmed using the Illumiprocessor software pipeline (Faircloth 2013). We assembled reads and generated consensus contigs for each sample using Velvet (Zerbino and Birney 2008) on VelvetOptimiser (https://github.com/tseemann/VelvetOptimiser). We then used the "match_contigs_to_probes" code implemented on PHYLUCE to align species-specific contigs to the ostariophysan probe-UCE set (Faircloth et al. 2020). We created a fasta file containing all data for all taxa. A custom Python program (seqcap_align_2.py) was used to align contigs using the MAFFT algorithm (Katoh et al. 2002) and to perform edge trimmings. The trimmed alignment was used to generate two subsets, each including all taxa examined: 75% and 90% complete matrices. All sequences are deposited at NCBI Sequence Read Archive submission under the code PRJNA000000 (SAMN0000000 – SAMN00000000).

2.3.3 Phylogenetic analyses

The 75% and 90% concatenated datasets were used in using maximum likelihood (ML) in RAxML v8.1.3 (Stamatakis 2014), Bayesian inference (BI) in ExaBayes v1.4 (Aberer et al. 2014) and coalescent-based analysis in ASTRAL-III v.5.6.2 (Zhang et al. 2018). For the ML analysis, we used a data partitioning scheme of each UCE with PFinderUCE-SWSC-EN (Tagliacollo and Lanfear 2018), and estimated the models using data blocks in PartitionFinder v2.1.1 (Lanfear et al. 2016). We performed ML inferences using five alternative runs on distinct parsimony starting trees to find the best ML tree, adopting the best-fit partitioning schemes and the GTRCAT substitution model. Pseudoreplicates of the ML analysis were obtained using the autoMRE function (Pattengale et al. 2010; number of bootstrap replicates automatically determined) to assess bootstrap support for individual nodes.

The BI of the unpartitioned concatenated alignments was performed using two independent runs with two chains each (one cold and one hot) of 5 million generations each using the GTR+G model. The tree space was sampled at every 500 generations yielding a total of 10,001 trees. The convergence of the posterior distribution was assessed examining the ESS>200, and evaluating posterior trace distribution in Tracer v 1.6 (Rambaut et al. 2014). The 50% most credible set of trees with 25% burn-in from the posterior distribution of possible topologies were generated using the consensus algorithm of ExaBayes.

To account for gene-tree incongruence due to incomplete lineage sorting (ILS; Alda et al. 2019), a coalescent analysis of species tree was inferred from individual gene trees using a two-step process. First, the program Phyluce was used to resample the 75% and 90% complete matrices by loci and generated ML trees for each loci and each of those matrices using RAxML. Then the ASTRAL-III v5.6.2 (Zhang et al. 2018) was used to infer species trees from each of the best tree subsets of loci and generated a majority-rule consensus tree.

2.4 Morphology

A total of 93 lots (183 specimens) with an extensive geographic coverage were examined. Type specimens of all nominal species of *Hoplerythrinus* with known type material were examined from photographs and radiographs, and only meristic counts were taken (scale,

vertebral, and fin ray counts). The material examined is listed in Table S2. Morphological standard measurements and counts of specimens were done following pertinent taxonomic literature of erythrinids (Mattox et al. 2006, 2014a). Measurements were taken point-to-point with a digital caliper, with 0.1 mm accuracy, on left side of specimens whenever possible. Measurements were expressed as percentages of standard length (SL) or head length (HL). Number of pre-dorsal scales did not include the modified scale just before the insertion of the dorsal fin nor first two scales on head. Number of scales of lateral line system did not include first one or two unperforated scales beneath the opercle membrane nor last unperforated scales on caudal fin. Counts of scales above and below lateral line did not include scales in the middorsal and pelvic-fin insertion series, respectively. Osteological nomenclature follows Mattox et al. (2014b). Vertebral counts include the anterior four vertebrae of the Weberian apparatus and were made on radiographed specimens or on cleared and stained specimens (C&S) prepared following Taylor and Van Dyke (1985).

A principal component analysis (PCA) on the morphometric measurements (excluding standard length) was performed to examine morphological differences. Specimens in the PCA were separated and compared according to localities and corresponding with probable groups defined by molecular approaches. The PCA was performed in RStudio (RStudio-Team, 2020, Inc., Version 1.4.1106) using the FactoMineR package (Lê et al. 2008). Additionally, one specimen of each genus within Erythrinidae was scanned through computed tomography (CT) at Rice University using a Bruker SkyScan1273, with the aim of illustrating some of the diagnostic characters of the genus *Hoplerythrinus*. CT data were visualized in the open-source visualization software 3D slicer (Kikinis et al. 2014).

3. Results

3.1 Molecular species delimitation

Barcode sequences for 105 specimens of *Hoplerythrinus* from major cis-Andean river drainages were analyzed. Stop codons, deletions or insertions were absent in all sequences. After alignment and editing, the final matrix had 642 pb with a total of 489 sites excluding missing data, of which 361 were conserved and 128 were variable. Base composition was 23.8% adenine, 28.4% cytosine, 18.3% guanine and 29.5% thymine.

The substitution saturation test revealed Iss values lower than Iss.cSym and Iss.cAsym values, which mean the lack of a saturation signal in the matrix.

All the delimitation methods yielded different numbers of splits ranging from three (GMYC), four (ABGD), six (PTP) or nine (mPTP) clusters (Fig. 2). The GMYC and ABGD defined a widely distributed cluster (dark blue cluster 1; Fig. 2), occurring throughout most of principal cis-Andean drainages: western and eastern Amazon, Orinoco, Paraná, São Francisco, Essequibo, Atlantic coastal drainages of Guianas and Southeastern Brazil. However, PTP and mPTP over-split this cluster, separating populations from the Rio São Francisco, Rio Tocantins, and lower Rio Tapajos basins, as a different group. Additionally, populations from the Rio Paraná basin were divided into two groups and samples from Atlantic coastal drainages of Southeastern Brazil were delimited as another group. The GMYC also recovered a group from the Rio Orinoco basin, which matched with mPTP and ABGD results (orange cluster 2; Fig. 2).

The GMYC and PTP delimited one group including samples from the Rio Tapajos, upper Rio Xingu and upper Rio Araguaia basins. However, this group was divided in three groups according mPTP and in two groups according to ABGD. The mPTP delimited a first group including specimens from the upper Rio Xingu (Culuene, Curuá, Suiá-Missú) and Rio Tapajós (Arinos, Teles Pires, Braço do Norte), a second group exclusively with specimens from the upper Rio Arinos, and a fourth group including specimens from the upper Rio Araguaia. The ABGD only separated the group from the upper Rio Araguaia (Fig. 2). Finally, considering a congruence in at least three delimitation methods, we defined three clusters as a final consensus: the widely distributed group from all major cis-Andean river drainages, the group from the Orinoco basin and the last group from the upper portions of Xingu, Tapajos and Araguaia river basins (Fig. 2).

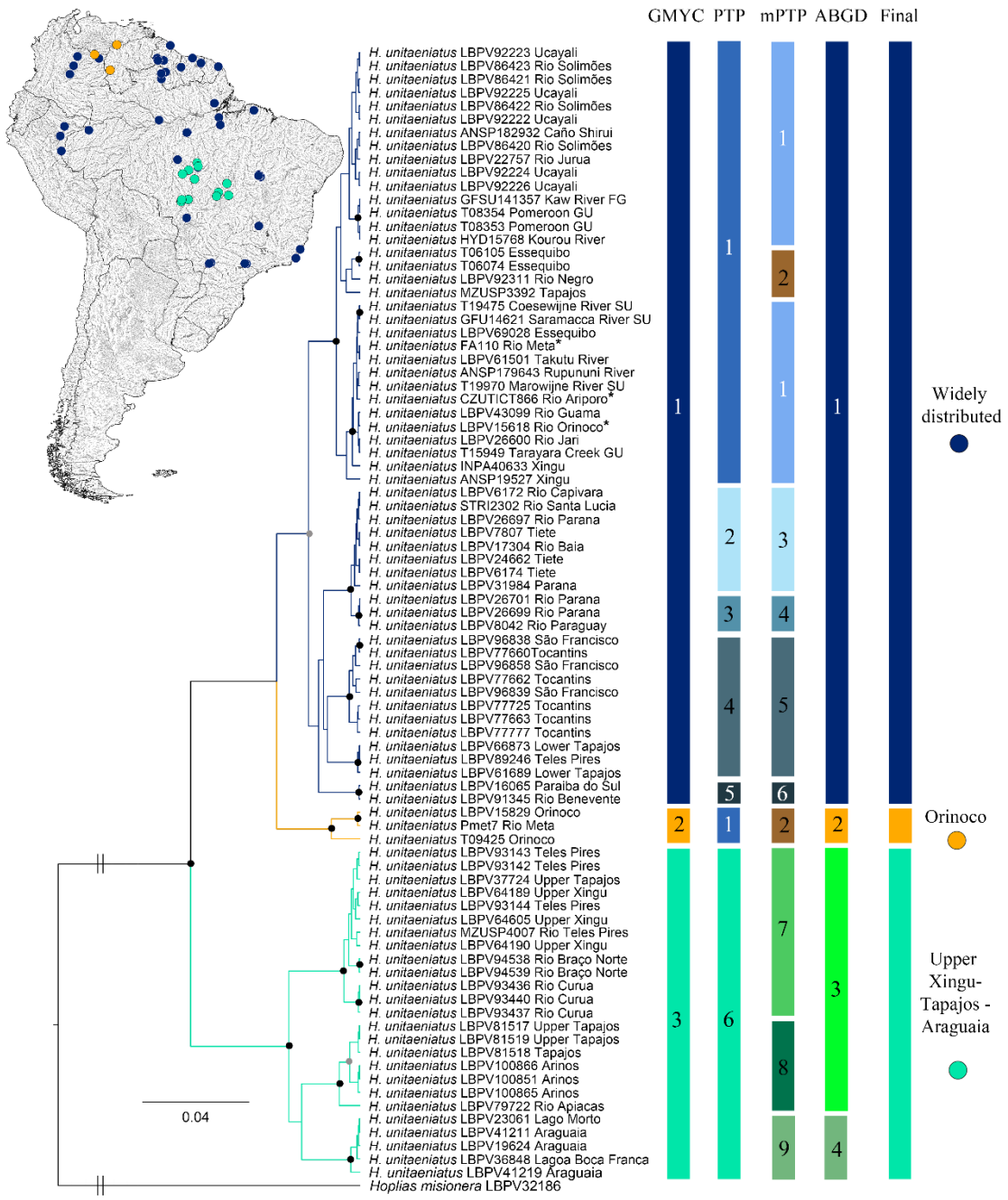

Figure 2. Bayesian phylogenetic tree representing species delimitation analysis of *Hoplerythrinus*. Vertical colored bars represents results of the four species delimitation analyses; for each method, the same color and number in bars represents the same cluster. Bayesian posterior probability (pp) support values are indicated on tree nodes as: black circles (0.95-1) and grey circles (0.80-0.94). Asterisks in some names indicate representatives from the Río Orinoco basin nested into the widely distributed cluster, together with specimens FA051, CZUTICT990, CZUTICT869, CZUTICT868, CZUTICT867 and BI1 which were removed from the Bayesian inference because they presented the same haplotype as samples FA110 and LBPV15618. Map inset shows the

geographic distribution of samples from analyzed specimens with dots colored according to the final consensus of delimitation analysis.

The analysis of pairwise genetic distances revealed relatively low intraspecific genetic variation (< 2.2±0.4%) for each of the three clusters, and interspecific distances higher than 2%, ranging from 3.8±0.8% to 6.9±1.0% (Table 1).

Table 1. Pairwise analyses using TN93 genetic distance, among clusters of *Hoplerythrinus*, defined by species delimitation methods. The mean and standard error values given in percent (%). Bold numbers represent intraspecific genetic variation.

Clusters	1	2	3
1. Widely distributed group	**1.30±0.30**		
2. Orinoco Basin group	3.80±0.80	**1.30±0.40**	
3. Upper Tapajos-Xingu-Araguaia group	6.60±1.00	6.90±1.00	**2.20±0.40**

3.3 Phylogenomic analysis

Sequencing and data filtering yielded a phylogenomic data set comprising 54 specimens (24 *Hoplerythrinus* and 30 outgroup taxa). Outgroups showed in figures correspond to three *Erythrinus* and six *Hoplias* for family Erythrinidae, and one *Tarumania* for family Tarumaniidae; other no erythrynoid outgroup taxa were pruned to facilitate presentation of figures. We assembled and analyzed two UCE matrices that differed in their inclusion of loci with varying amounts of missing data: the 75% complete matrix (925 loci; 297,653 bp) and the 90% completeness matrix (110 loci; 57,514 bp).

Reconstructions of ML and BI methods based on the 75% complete matrix yielded nearly identical topologies with high node support values: ML with 60.9% of ingroup nodes with > 85% of bootstrap (Fig. 3) and BI with 95.7% of ingroup nodes = 1 (Supplementary Fig. S1), showing *Hoplerythrinus unitaeniatus* from the Río Orinoco Basin as sister group of the remaining samples from other cis-Andean drainages. Within these remaining samples, two clades were found: 1) upper portions of the Xingu, Tapajós, Araguaia, São Francisco, Tocantins river basins and coastal drainages of southeastern Brazil; 2) Paraná-Paraguay, Amazon river basins (Lower Tapajos, Negro, Guamá, Ucayali, Juruá, Jari drainages) and Atlantic coastal drainages of Guianas (Fig. 3; and Supplementary Fig. S1). Using the coalescent-based method (ASTRAL-III) in which a species tree history is estimated from

independent gene histories, we recovered a topology partially concordant with the concatenated analysis (Supplementary Fig. S2). In this analysis we recovered the clade from upper portions of the Xingu, Tapajós and Araguaia River basins as sister group of the remaining samples of *H. unitaeniatus* and 65.2% of ingroup node support values > 0.85.

Reconstructions based on the 95% complete matrix yielded similar topologies between ML and BI methods, and also compared with results obtained with the 75% matrix, showing *Hoplerythrinus unitaeniatus* from the Río Orinoco Basin as sister group of the remaining samples, although recovering reciprocal monophyly for the clade of upper portions of the Xingu, Tapajós and Araguaia river basins and relatively high node support values: ML with 43.5% of ingroup nodes > 85% (Supplementary Fig. S3) and BI with 73.9% of nodes = 1 (Supplementary Fig. S4). ASTRAL-III analysis with the 90% matrix as showed using the 75% matrix, recovered samples from upper portions of the Xingu, Tapajós and Araguaia river basins as sister group of the remaining samples of *H. unitaeniatus* with just 39.1% of ingroup node support values > 0.85 (Supplementary Fig. S5). Worth mentioning also is the fact that the samples from the Río Orinoco Basin, which were split into different clusters in the single-locus barcode analysis (Fig. 2), were grouped in the same clade in the phylogenomic approach, recovering as reciprocally monophyletic in all reconstructions (Fig. 3; Supplementary Figs. S1–S5).

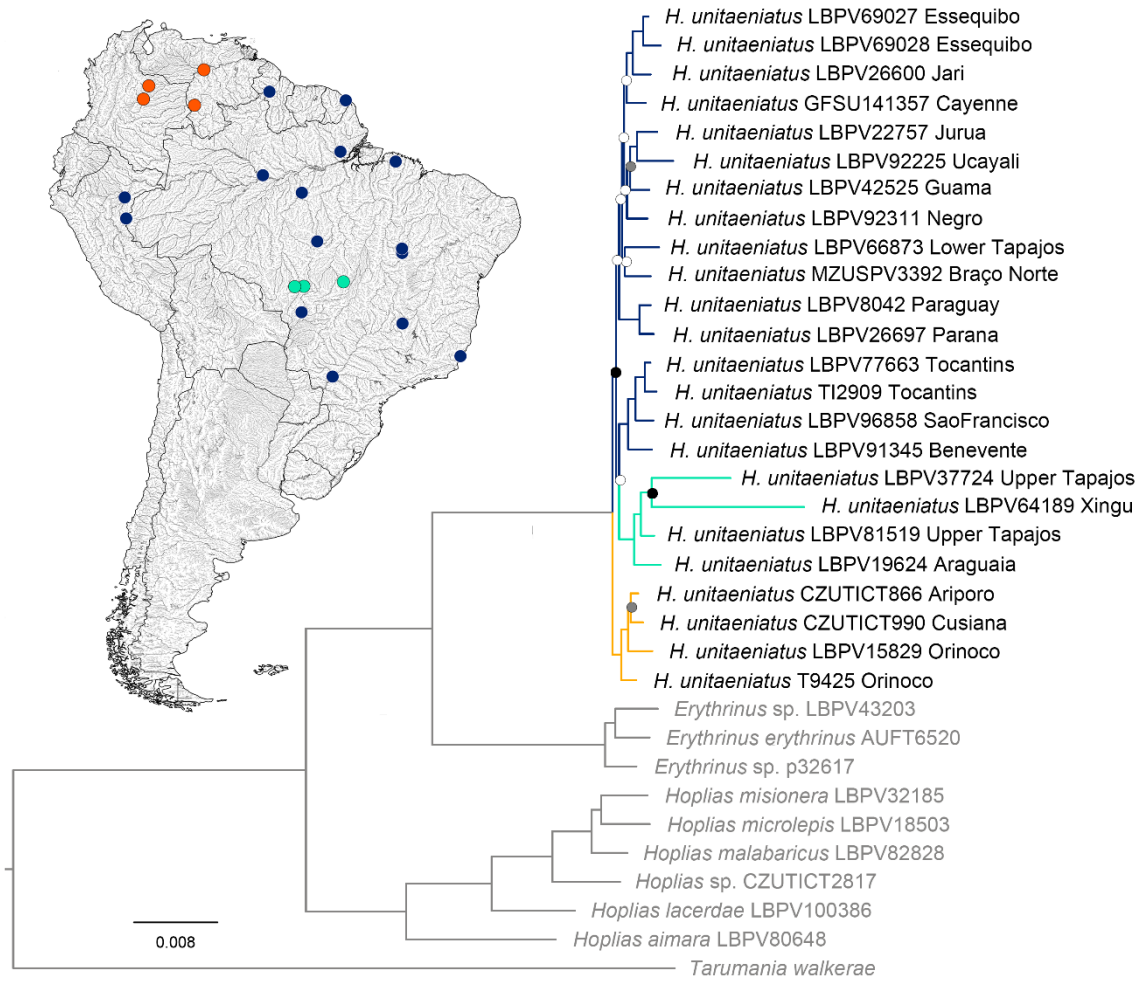

Figure 3. Phylogenetic relationships of *Hoplerythrinus* based on a maximum likelihood analysis of the edge-trimmed and partitioned 75% complete matrix of ultraconserved elements (925 loci; 297,653 bp). No symbols at nodes indicated bootstrap support values (ML-BP) of 100%, black circles denoted values between 85-99, gray circles denoted values between 60-85, and white circles denoted values less than 60.

3.4 Morphological comparison

We initially examined the specimens according to hydrographic basins and using the combination of color pattern, meristics, and morphometric data but no apparent patterns were found. In addition, separating groups by location in agreement with molecular results did not reveal any differences in the traditional morphometric PCA (Fig. 5). The PCA showed extensive overlap between the three groups recognized in molecular analyses. The PC1 explained 31.9% of variation mainly focused on differences in orbital diameter, pre-pectoral length and interorbital width. The PC2 explained 25% of the

variation focused on differences in the anal-fin base length, anal-fin length, and caudal peduncle length (Table S3). Ranges of all morphometric measurements overlap among the three groups partially recognized by molecular analyses (Table 2). Similarly, meristic data did not show any character useful to distinguish these groups, however, some slightly differences in the modal number were found for maxillary teeth and vertebral counts (Table 3). However, despite these subtle differences, the data did not allow the recognition of more than one distinct species, and *Hoplerythrinus* is supported as a monotypic genus, as revealed by genetic analyses.

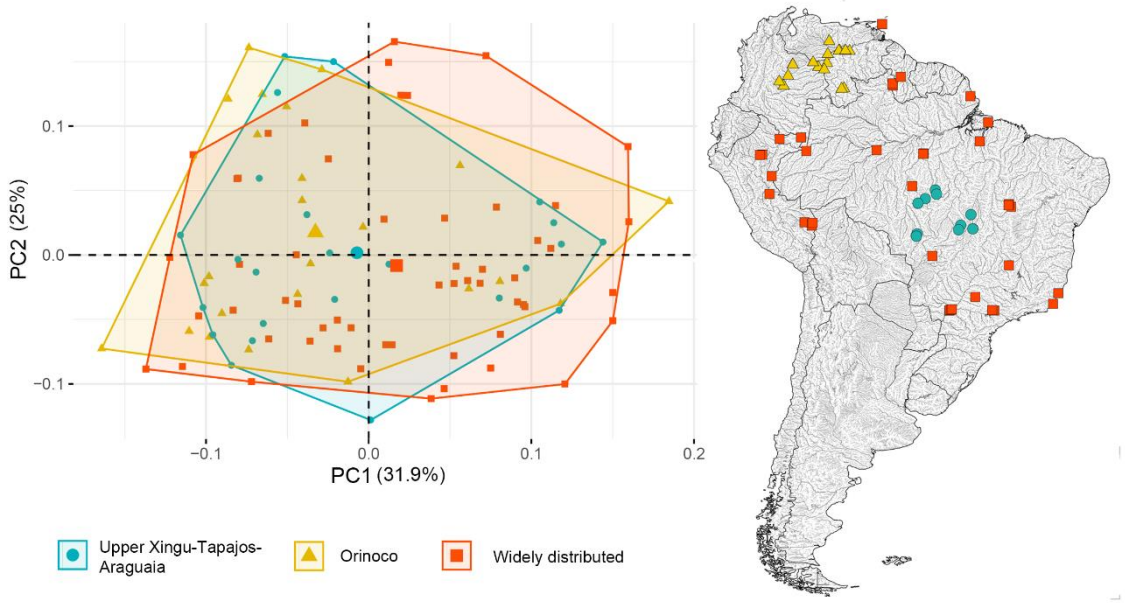

Figure 4. Results of PCA based on morphometric measurements of *Hoplerythrinus unitaeniatus*; specimens grouped by location following molecular results. Map showing geographic distribution of lots examined with morphometric measurements.

Table 2. Morphometric data for *Hoplerythrinus unitaeniatus*, showing unified and separated values for each molecular delimited group. n = number of examined specimens, Avg. = average, S.D = standard deviation.

	***H. unitaeniatus* Total**				*H. unitaeniatus* "Widespread"				*H. unitaeniatus* "Orinoco"				*H. unitaeniatus* "Xingu-Tapajós-Araguaia"			
	n=111				n=59				n=25				n=27			
	min	max	Avg.	S.D	min	max	Avg.	S.D	min	max	Avg.	S.D	min	max	Avg.	S.D
Standard length (mm)	30.0	229.5	130.2		50.1	229.5	130.5		30.0	213.7	134.9		58.4	201.1	124.7	
Percents of standard length																
Body depth	18.5	30.9	24.5	2.0	19.8	27.7	24.3	1.7	20.6	30.9	24.9	2.6	22.0	27.7	24.7	1.6
Head length	27.3	34.6	30.8	1.5	28.8	34.6	31.1	1.3	27.3	33.2	30.1	1.5	27.8	34.2	30.8	1.8
Pectoral-fin length	15.1	27.1	18.9	1.3	17.1	22.0	19.2	0.9	16.6	20.8	18.5	1.0	15.1	27.1	18.8	2.1
Pelvic-fin length	15.4	20.5	18.3	0.9	16.3	20.4	18.4	0.9	16.5	20.5	18.0	0.8	15.4	20.1	18.2	1.1
Anal-fin length	17.9	26.0	21.3	1.8	18.0	26.0	21.3	1.8	17.9	24.2	21.2	1.9	18.2	24.6	21.4	1.7
Dorsal-fin length	23.9	30.5	26.8	1.4	24.1	30.5	27.0	1.3	23.9	30.3	26.1	1.4	24.3	29.5	27.1	1.4
Dorsal-fin base length	12.1	26.5	13.9	1.5	12.6	15.7	13.9	0.8	12.2	26.5	14.0	2.7	12.1	15.4	13.9	0.9
Anal-fin base length	8.1	15.0	10.7	1.8	8.1	14.7	10.5	1.7	8.4	15.0	11.1	1.9	8.1	14.9	10.8	1.7
Pre-pectoral length	24.7	32.9	28.0	1.7	24.7	32.6	28.0	1.6	25.3	32.1	27.4	1.5	24.7	32.9	28.2	2.2
Pre-pelvic length	52.2	59.6	56.1	1.7	52.2	59.0	56.2	1.5	52.3	59.6	56.3	1.8	52.9	59.0	55.8	1.9
Pre-dorsal length	51.7	58.6	54.7	1.5	51.7	58.6	54.9	1.6	52.4	57.2	54.7	1.3	51.9	58.1	54.6	1.7
Pre-anal length	73.9	83.1	78.5	2.0	74.2	82.5	78.5	1.9	74.0	83.1	79.2	2.0	73.9	81.8	77.9	2.0
Caudal-peduncle depth	13.3	17.7	15.6	0.9	13.3	17.5	15.3	1.0	14.1	17.7	15.9	0.9	14.4	17.3	15.9	0.7
Caudal-peduncle length	12.7	18.0	15.4	1.2	12.7	17.7	15.5	12.7	12.8	18.0	15.2	1.4	13.6	17.9	15.5	1.2
Percents of head length																
Head depth at quadrate	52.6	67.6	60.3	3.1	52.6	67.6	60.0	3.3	57.1	65.6	61.1	2.5	55.3	66.1	60.3	3.3
Head depth at eye	40.2	55.4	45.5	2.3	41.5	55.4	45.2	2.2	42.5	50.1	46.7	2.4	40.2	48.2	45.0	2.0
Snout length	21.8	29.0	25.2	1.2	21.8	29.0	25.3	1.3	23.9	27.8	25.7	1.1	22.8	26.4	24.7	0.8
Snout width	21.7	30.9	25.8	1.6	21.7	28.3	25.5	1.5	24.6	30.9	27.0	1.6	22.8	27.8	25.3	1.2
Pre-nasal distance	13.0	18.4	15.6	1.0	13.0	18.4	15.6	1.0	14.5	18.1	15.8	0.8	13.5	18.4	15.7	1.0
Orbital diameter	13.4	25.9	18.3	3.3	13.4	25.9	19.0	3.4	14.0	25.7	17.2	3.1	13.5	23.7	17.7	3.0
Interorbital bony width	29.3	40.8	36.1	2.2	32.2	40.8	36.3	2.1	31.8	39.7	36.9	1.8	29.3	39.5	35.2	2.7
Upper jaw length	45.6	53.4	50.3	1.7	46.7	53.4	50.3	1.9	45.6	53.3	50.4	1.8	47.3	52.5	50.0	1.3

Table 3. Meristic data for examined *Hoplerythrinus unitaeniatus* with separated values for each molecular delimited group.

	***H. unitaeniatus* Total**				*H. unitaeniatus* "Widespread"				*H. unitaeniatus* "Orinoco"				*H. unitaeniatus* "Xingu-Tapajós-Araguaia"			
	min	max	mode	n	min	max	mode	n	min	max	mode	n	min	max	mode	n
Maxillary teeth	21	34	25	77	21	34	25	36	24	32	27	19	25	40	28	22
Scales above lateral line	3	3	3	109	3	3	3	56	3	3	3	26	3	3	3	27
Scales between lateral line and anal-fin origin	3	3	3	109	3	3	3	56	3	3	3	26	3	3	3	27
Scales between lateral line and pelvic-fin origin	3	3	3	109	3	3	3	56	3	3	3	26	3	3	3	27
Scales around caudal peduncle	16	16	16	109	16	16	16	56	16	16	16	26	16	16	16	27
Predorsal scales	9	12	10	109	10	12	11	59	11	12	11	23	10	11	10	27
Posdorsal scales	12	17	15	110	12	16	15	59	13	17	15	24	14	16	14	27
Lateral-line scales	31(3), 32(6), 33(23), 34(37), 35(31), 36(9), 37(1)				31(2), 32(3), 33(13), 34(21), 35(15), 36(4)				33(1), 34(3), 35(15), 36(5), 37(1)				31(1), 32(3), 33(9), 34(13), 35(1)			
Vertebral counts	33(4), 34(17), 35(322), 36(24)				33(1), 34(10), 35(19), 36(7)				34(1), 35(9), 36(17)				33(3), 34(6), 35(4)			
Precaudal vertebrae	20(1), 21(24), 22(36), 23(16)				20(1), 21(10), 22(19), 23(7)				21(1), 22(17), 23(9)				21 (13)			
Dorsal-fin rays	ii,8(7), 9(77) or iii,7(1), 8(20), 9(3)				ii,8(2), 9(49) or iii,8(6)				ii,8(3), 9(11) or iii,8(10), 9(1)				ii,8(2), 9(17) or iii,7(1), 8(4), 9(2)			
Anal-fin rays	iii,8(42), 9(66)				iii,8(15), 9(43)				iii,8(15), 9(11)				iii,8(12), 9(12)			
Pectoral-fin rays	i,10(2), 11(14), 12(37), 13(39), 14(16), 15(2)				i,11(3), 12(14), 13(24), 14(15), 15(2)				i,11(2), 12(10), 13(12), 14(1)				i,10(2), 11(9), 12(13), 13(3)			
Pelvic-fin rays	i,7(110), 8(1)				i,7(58), 8(1)				i,7(25)				i,7(27)			
Caudal-fin rays	i,13(1) or 15(54) or 16(1),i				i,13(1) or 15(54) or 16(1),i				i,15(23),i				i,14(1), 15(26),i			

3.5 Taxonomic considerations

Hoplerythrinus unitaeniatus (Agassiz, in Spix & Agassiz, 1829) originally described from the Rio São Francisco basin has been the only species of this genus identified in recent literature (at least in the last 60 years). However, prior to the present study, two other species only known from the type material, have been listed as valid (Oyakawa 2003; Fricke et al. 2022): *H. gronovii* (Valenciennes, in Cuvier and Valenciennes, 1847) described from Cayenne in French Guiana and *H. cinereus* (Gill 1858) from Trinidad Island. In the present study, we analyzed both genetic and morphological data of specimens from the Rio São Francisco basin as well as many other localities along the geographic range of *Hoplerythrinus*, including samples from type localities for most of the nominal species (Cayenne, Suriname, Trinidad Island) (Tables S1 and S2).

In his description of *H. gronovii*, Valenciennes (1847: 500) highlighted the presence of long papillae on the tongue, a black spot on the opercle, and a color pattern with four or five poorly defined vertical lines towards the posterior region of body. Although differentiation in the shape of papillae in the tongue may be related to ontogenetic variation (Elgendy et al., 2016), here we found no apparent variation in this character in the material examined. Likewise, a coloration pattern with irregular blotches on scales forming transversal and sinusoidal stripes along the posterior portion of body was also found in some specimens throughout the geographic distribution of the examined material. In the genetic analyses we included two specimens collected in French Guiana, one of them specifically from the Kaw River in Cayenne, however, these samples were nested with the widespread lineage, including western and eastern Amazon, Orinoco, Paraná, São Francisco, Essequibo, Atlantic coastal drainages of Guianas and Southeastern Brazil. The examination of meristic characters and coloration pattern from photograph of syntypes of *H. gronovii* (MNHN-IC 0099; Supplementary Fig. S6) also did not show any additional information supporting the validity of this nominal species. The number of perforated scales in the lateral line (32), scales above the lateral line (3) and between the lateral line and pelvic-fin and anal-fin origins (3), and caudal-fin rays (i,15,i) fall within ranges presented by the lineages of *H. unitaeniatus*.

In a short description, Gill (1858) does not highlight any character to distinguish *H. cinereus* from its previously described congeners, although some features are mentioned: the presence of 35 perforated scales on the lateral line, dorsal fin with 10 rays, anal fin

with 11, caudal fin with 16, pectoral fin with 15, ventral fin with 8, and an ash coloration pattern with a lighter abdominal region, hyaline fins except for dorsal fin that has about four rows of dusky spots between the rays. These features, together with what was observed from the photograph of holotype of *H. cinereus* (USNM 5882; Supplementary Fig, S7), and three examined specimens from Trinidad Island (FMNH 50088, ROM 61642, USNM 5882), did not provide information to diagnosed this nominal species, which present characteristics common to those observed throughout the distribution of *H. unitaeniatus*.

Additionally, three other nominal species have already been considered as junior synonyms of *H. unitaeniatus* (de Jongh 1991; Oyakawa 2003; Fricke et al. 2022): *Erythrinus salvus* Agassiz, in Spix & Agassiz, 1829 described based on a single specimen found in the stomach of a specimen of *Hoplias malabaricus* (his *Erythrinus macrodon*) collected in the São Francisco river; *Erythrinus vittatus* Valenciennes, in Cuvier & Valenciennes, 1847, described based on specimens from Brazil (according to MNHN information from Rio de Janeiro), Cayenne and Suriname; *Pseuderythrinus rosapinnis* Hoedeman, 1950 described based upon one specimen from Suriname ("a ditch near Paramaribo"). *Erythrinus salvus* was described by Agassiz in Spix & Agassiz, 1829 based on a specimen in poor condition, no types are known for this nominal species and its description (based mainly on dentition) does not differ substantially from the original description of *H. unitaeniatus*. The names *E. salvus* and *E. unitaeniatus* were published together by Spix & Agassiz, 1829. Eigenmann (1912) seems to be the first author to consider *E. salvus* as a synonym of *H. unitaeniatus*, thus acting as First Reviser (ICZN 1999, Art. 24.2) giving precedence to *H. unitaeniatus*, thus the valid name. Our results presented above, the inclusion of tissue samples from Suriname, Atlantic coastal drainages of Southeastern Brazil and Cayenne, and examination of photographs of syntypes of *Erythrinus vittatus* (MNHN-IC 9758 to 9767; Supplementary Figs., S8-S11), as well as photographs and x-rays of the holotype of *Pseuderythrinus rosapinnis* (ZMA.PISC 100.310; Supplementary Figs., S12-S13), support the current taxonomic status of these nominal species as junior synonyms of *H. unitaeniatus*.

According to our findings, we define *Hoplerythrinus* as a monotypic genus, with only *H. unitaeniatus* occurring in most cis-Andean drainages. Below, we present a diagnosis of the genus based on a compilation of characters available in the literature (Géry 1977; de

Pinna et al. 2017; Oyakawa and Mattox 2018), with the inclusion of an additional character examined herein that is useful to distinguish *Hoplerythrinus* from *Erythrinus*. This character refers to the relative size of infraorbital-6 elements, however, this character needs to be more exhaustively examined in representatives of *Erythrinus*. A redescription of *H. unitaeniatus* is provided based on the examination of specimens from the Rio São Francisco Basin (two localities: Río Sapão, affluent of Rio Preto and Rio Grande, and the Rio Paracatu), and also including information about variation found in specimens from other localities along the geographic range of the species (Orinoco, Western Amazon, Xingu, Tapajós, Paraná-Paraguay, and Atlantic coastal drainages of Southeastern Brazil). The synonymy lists include only the literature associated with original descriptions of nominal species. Although no types are known for *H. unitaeniatus*, we did not designate a neotype. Following the International Code of Zoological Nomenclature (ICZN, 1999, Art. 75.3), the designation of a neotype is an exceptional need, and here there is not express purpose of clarifying taxonomic status or type locality since we found no genetic or morphological disparity among populations examined.

***Hoplerythrinus* Gill, 1896**

Hoplerythrinus Gill, 1896: 208 [Type species: *Erythrinus unitaeniatus* Agassiz, 1829 by monotypy].

Ophiocephalops Fowler, 1906: 293 [Type species: *Erythrinus unitaeniatus* Agassiz, 1829. Type by original designation].

Pseuderythrinus Hoedeman, 1950: 79 [Type species: *Pseuderythrinus rosapinnis* Hoedeman, 1950 by original designation].

Diagnosis. *Hoplerythrinus* can be distinguished from the genera of Erythrinidae by fusion of postcleithra 2 and 3 (Char. 60, de Pinna et al., 2017) (vs. separate, ossified as autogenous units in *Erythrinus* and *Hoplias*) and by teeth present on the endopterygoid (Char. 23, de Pinna et al., 2017; Gill, 1896) (vs. absent in *Erythrinus* and *Hoplias*). Furthermore, *Hoplerythrinus* is distinguished from *Hoplias* by the sixth infraorbital divided transversally into two elements (Char. 128, de Pinna et al., 2017) (Fig. 5; vs sixth infraorbital as a single element), and by having all infraorbital bones contacting the orbital rim (Fig. 5; infraorbital 3 and/or 4 completely excluded or barely reaching the orbital rim). *Hoplerythrinus* also differs from *Erythrinus* by the presence of a black round spot on posterodorsal region of opercle (vs. absence), presence of a fleshy rounded mark above the base of anal fin in mature males (vs. anal-fin base region without a mark in both

sexes), lack of modifications in dorsal-fin shape of mature males (vs, pointed and elongated dorsal fin in mature males), a dark longitudinal midlateral stripe along the body usually present (vs. rarely present), anterior element of infraorbital 6 usually bigger than posterior element (Fig. 5; vs. usually smaller).

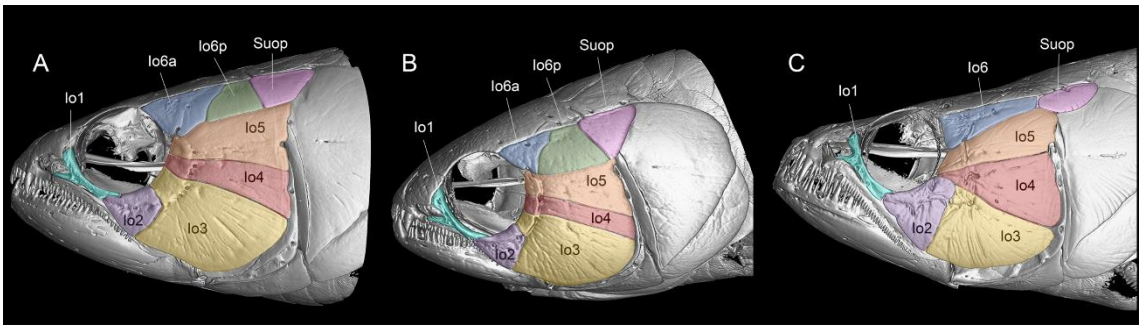

Figure 5. Circumorbital series of (A) *Hoplerythrinus unitaeniatus* (MUSM xxx; 130 mm SL); (B) *Erythrinus erythrinus* (MUSM 0000; 81 mm SL); and (C) *Hoplias malabaricus* (MUSM 0000; 154 mm SL). **Io1-6**, infraorbital 1-6; **Io6a**, anterior element of infraorbital 6; **Io6p**, posterior element of infraorbital 6; **Suop**, supraopercle.

***Hoplerythrinus unitaeniatus* (Agassiz in Spix & Agassiz, 1829)**

(Figs. 6-9; Tab 2-3; Supplementary Figs S6-S13)

Erythrinus salvus Agassiz, in Spix & Agassiz, 1829: 41 [original description based on single specimen found in stomach of *Hoplias malabaricus* (*Erythrinus macrodon*); no types known; type locality: São Francisco].

Erythrinus unitaeniatus Agassiz, in Spix & Agassiz, 1829: 42, pl. 19 [original description based on single specimen; no types known; type locality: São Francisco basin, Brazil].

Erythrinus vittatus Valenciennes, in Cuvier & Valenciennes, 1847: 499, pl. 585 [original description; syntypes: MNHN A-9758 to 9761 (4); type locality: Rio de Janeiro (Brazil), Cayenne (French Guiana), Suriname].

Erythrinus gronovii Valenciennes, in Cuvier & Valenciennes, 1847: 500 [original description; syntypes: MNHN 0099 (3); Type locality: Cayenne, French Guiana].

Erythrinus cinereus Gill, 1858: 413 [original description; holotype: USNM 5882; type locality: western Portion of the Island of Trinidad].

Pseuderythrinus rosapinnis Hoedeman, 1950: 82, figs.1a-e, 2, 3 [original description; holotype: ZMA PISC 100.310; type locality: near Paramaribo, Suriname].

Description. Body subcylindrical, deeper than wide. Snout profile rounded in lateral view. Dorsal head profile varying from straight to slightly convex. Dorsal body profile straight to slightly convex from vertical through first scale to dorsal-fin origin, slightly convex along dorsal-fin base, and straight to slightly concave from insertion of last dorsal-fin ray to origin of dorsal-most procurrent caudal-fin ray. Ventral head profile slightly convex, slanted posteroventrally. Medial margins of contralateral dentaries approximately parallel. Ventral profile of body convex to pelvic-fin origin, varying from slightly concave to slightly convex from latter point to anal-fin origin, straight to slightly convex and posterodorsally inclined along anal-fin base, and slightly concave to straight from base of last anal-fin ray to anterior most ventral procurrent caudal-fin ray.

Figure 6. Dorsal, lateral, and ventral views of *Hoplerythrinus unitaeniatus*, LBP 5180, 165.8 mm SL, Rio Paraná, Brazil. Scale bar = 10 mm.

Figure 7. Dorsal, lateral, and ventral views of *Hoplerythrinus unitaeniatus*, LBP 28484, 200.1 mm SL, Ribeirão Santo Antonio, Rio Tapajós, Brazil. Scale bar = 10 mm.

Upper jaw usually as long as lower jaw, slightly shorter in some specimens, more so in specimens larger than 180 mm SL. Posterior tip of maxilla surpassing posterior margin of eye, slightly surpassing in specimens shorter than 65 mm SL. Posterior portion of maxilla dorsally extended, covered by second and third infraorbitals. Upper and lower lips fleshy with short skin projections covering part of canines externally. Anterior nostril tubular, separated from posterior one. Nostrils situated along horizontal through ventral half of the orbit. Infraorbital bones well developed. Infraorbital bones well developed and horizontally elongated. All infraorbitals reaching orbital rim. Infraorbital 6 divided transversally in two elements; anterior element usually bigger than posterior element (Fig. 5A). Supraopercle somewhat triangular, its anteroventral tip contacting posterodorsal tip of infraorbital 5.

Teeth in both jaws conical or caniniform. Premaxillary teeth in a single row, varying in size. Single premaxillary tooth row with 9 (5), 10 (18), 11 (26), 12 (21),13 (12), 14 (2) or 15 (2) teeth. First premaxillary teeth large and caniniform, then 3 (3), 4 (37), 5 (32), 6

(11) or 7 (5) smaller teeth followed by other large canine, in this series the largest. Then, 3(8), 4 (42), 5 (22), 6 (14) or 7 (2) small teeth almost in contact with small first maxillary tooth. Maxilla with 21-34 teeth (mode: 25, n = 77). Dentary with anterior external row of teeth and posterior internal row. External series with an anterior first tooth small and conical, followed by 2-3 (mode: 3, n = 83) teeth large and caniniform, increasing progressively in size; then 19-31 (7) small conical teeth decreasing progressively in size. Internal series beginning at level to antepenultimate or last conical tooth of external row and composed of 7-12 (6) small teeth. Ectopterygoids with series of small villiform teeth. Accessory ectopterygoid absent.

Distal margins of all fins strongly or slightly rounded. Dorsal-fin rays ii,8(7), 9(77) or iii,7(1), 8(20), 9(3). Dorsal-fin origin placed at mid-body, slightly anterior to vertical through pelvic fin origin. Tip of longest ray of depressed dorsal fin extending beyond vertical through anal-fin origin, without surpassing anal-fin base. Anal fin base short. Anal-fin rays iii,8(42), 9(66). Pectoral-fin origin located at about vertical through median region of opercle. Tip of pectoral fin separated from pelvic-fin origin by three to four scales. Pectoral and pelvic fins of similar size. Pectoral-fin rays i,10(2), 11(14), 12(37), 13(39), 14(16), 15(2). Pelvic-fin origin situated at midbody. Tip of pelvic fin surpassing vertical through dorsal-fin base terminus. Pelvic-fin rays i,7(110), 8(1). Caudal-fin rays i,13(1) or 15(54) or 16(1),i.

Well-developed cycloid scales imbricated along body. Series of dorsal scales overlapping supraoccipital spine. Last vertical series of scales on caudal peduncle forming slightly convex arch on caudal-fin base in lateral view; two or three last rows of scales on caudal-fin rays smaller than those of body. Anterior margin of scales undulated, with small notch at midpoint and posterior margin rounded. Three to eleven *radii* extending from center of scale to anterior margin and five to ten *radii*, extending from center of scale to dorsal, posterior, and ventral margin. Lateral line straight and complete, extending from posteroventral margin of supracleithrum to middle caudal-fin rays. Lateral-line scales with single laterosensory canal. Lateral line with 31-37 (mode: 34, n = 109) perforated scales, plus one or two unperforated scales anteriorly and located beneath opercle membrane or one to three unperforated scales posteriorly and located on the middle caudal-fin rays. Longitudinal series of scales between lateral line and dorsal-fin origin 3 (n = 109); longitudinal series of scales between lateral line and pelvic-fin origin 3 (n =

109); scales in median series between tip of longitudinal series of scales around caudal peduncle, invariable 16 (n = 109).

First epibranchial with 9 to 13 (6) gill rakers, most in form of denticulated plates. One raker on cartilage. First ceratobranchial with five (3) to six (2) more elongated rakers, near cartilage, followed by 8-10 (5) plate-like rakers. Latero-sensory canal along ventral surface of dentary normally with four pores. Six laterosensory pores in preopercle (n = 110, five specimens with seven pores on one side of the head).

Laterosensory canal along infraorbitals with 9 (2), 10 (17) or 11 (2) pores. Infraorbital 1: 2-3, infraorbital 2: 1-3, infraorbital 3: 1-2, infraorbital 4: 1, infraorbital 5 lacking pores and infraorbital 6 with 2-4. Laterosensory system of dorsal surface of head with 9 pores; nasal bone: 2 pores, frontal bone: 4 pores, pterotic bone: 2 pores. One pore between parietal bones, on the posterior end of suture. Total vertebrae 33-36 (mode: 35, n = 77); precaudal vertebrae 20-23 (mode: 22, n = 77).

Coloration in alcohol. Ground coloration of head and body light brown, darker dorsally and paler ventrally (Figs. 6-7). Ventral region homogenously light yellow. Dorsal surface of head dark brown. Posterodorsal region of the opercle with a black and round spot usually followed by a dark longitudinal midlateral strip along the body. Most specimens with two dark diagonal stripes radiating posteriorly from eye; first stripe along the infraorbital 6, extending to opercle where it splits in two portions around the dark spot on opercle; second strip along infraorbital 3. Some specimens with irregular blotches on scales forming transversal and sinusoidal strips along the posterior portion of body. Some specimens, principally populations from upper portions of Xingu, Tapajos, Paraguay river basins, and some specimens from the Rio Paraná basin present small dark spots on dorsal surface of head and/or body (Fig. 7). All fins dark to light brown usually with dark spots on rays and membranes forming pattern of irregular dark stripes; many specimens without these spots on caudal pelvic and pectoral fins.

Coloration in life. Similar to color in alcohol. Dark areas more intense with olive green tonalities and light areas yellow or light brown. Some specimens with red tonalities in ventral region. Fins with intense yellow coloration at base and along first rays (Fig. 8).

Figure 8. *Hoplerythrinus unitaeniatus* in life, IAvH-P 19884, 87.1 mm SL, Jaguey Maracay, Río Meta, Orinoco basin, Meta, Colombia. Photo by Jorge García-Melo.

Sexual dimorphism. Mature males develop a rounded mark above the base of anal fin, this mark resemble a bite mark and is delimited by a series of scales. Anal fin of these males become fleshy (Fig. 9).

Figure 9. Detail of the rounded mark three scales above anal-fin base in mature males of *Hoplerythrinus unitaeniatus*. (A) LBP 22310, 229.5 mm SL, Río Solimões, Tabatinga, Amazonas, Brazil; (B) LBP 14945, 132.7 mm SL, afluente Rio Takutu, Amazonas, Brazil.

Distribution. *Hoplerythrinus unitaeniatus* is widely distributed occurring in most drainages of cis-Andean region of South America.

Ecological notes. Stomach contents of three specimens included high proportion of aquatic insects of the families Leptoceridae, Gerridae, Hydroptilidae, Odonata as well terrestrial insect (Formicidae), and fish scraps.

4. Discussion

Integrating DNA barcode, phylogenomics of ultraconserved elements (UCEs), and morphological information provided evidence to investigate the evolutionary history of *Hoplerythrinus,* and to define this taxon as a geographically widespread monotypic genus in the Neotropical region. Here, we discuss details about the phenotypic variation and levels of genomic differentiation considering the divergence time and ecological affinities.

4.1 Data congruence and recognition of lineages

Understand the diversity of *Hoplerythrinus* represent a challenge even under the light of an integrative approach, using different tools for the investigation of its evolutionary history and diversification. Here, we found different levels of incongruence between our genetic approaches (DNA barcode and high-throughput sequencing of ultraconserved elements). The use of a single mtDNA locus has been used to assess genetic disparity and applied as evidence to resolve taxonomic uncertainties, revealing undescribed diversity (Anjos et al. 2020; Garavello et al. 2021) or expanding range distribution of NFF taxa (Cardoso et al. 2018; Ochoa et al. 2020; Guimarães et al. 2021b). Here, the use of mitochondrial COI barcodes revealed three divergent lineages in *Hoplerythrinus*: a widely distributed cluster from all major cis-Andean river drainages, the cluster from upper portions of Amazonian versants draining the Brazilian Shield (Xingu, Tapajos and Araguaia river basins), and the cluster composed by samples from the Río Orinoco Basin (Fig. 2), however, these entities were only partially supported by the phylogenomic approach (UCEs (Fig. 3; Supplementary Figs. S1–S5).

Different levels of incongruence were also detected among phylogenomic analyses. The analysis with the concatenated 75% and 95% complete matrices of UCEs (ML and BI) agree to support the reciprocal monophyly of the clade from the Río Orinoco Basin, but with discordance in the placement of the clade from upper portions of Amazonian versants draining the Brazilian Shield (Fig. 3; Supplementary Figs. S1, S3, S4). Additionally, the coalescent-based method (ASTRAL-III) yielded topologies discordant with the concatenated analyses, showing the clade from upper portions of the Xingu, Tapajós and Araguaia river basins as sister group of the remaining samples of *Hoplerythrinus* (Supplementary Figs. S2, S5). Coalescent-based methods have showed robust results in the reconstruction of relationships in ancient radiations or higher-level taxa (Shi and Yang 2018; Alda et al. 2019). However, discrepancies between methods can arise due to early isolation of lineages, short internode branch lengths or lack of phylogenetic signal in individual loci (Longo et al. 2017; Mclean et al. 2019; Parada et al. 2021). Topological incongruences between the ASTRAL-III and BI/ML analyses in *Hoplerythrinus* might correspond to short branch lengths and low genetic differentiation among lineages. Despite incongruences among methods, it is evident the complexity to establish the relationships among lineages of *Hoplerythrinus* with accuracy, which is not observed in the species/lineage-level relationships inside other genera of Erythrinidae (*Hoplias* or *Erythrinus*) using ultraconserved elements (Conde et al., in prep).

Another interesting finding is the polyphyletic arrangement of representatives from the Río Orinoco basin using COI barcodes in species delimitation analyses, since some samples were nested inside the widely distributed cluster and others outside (Fig. 2). In contrast, all phylogenomic analyses portrayed the representatives from the Río Orinoco basin to be monophyletic (Fig. 3; Supplementary Figs. S1-S5). These results suggest some degree of genetic differentiation but also gene flow between these lineages of *Hoplerythrinus*. Secondary contacts and mitochondrial introgression had an important role in evolutionary histories of other groups (Barton and Hewitt 1985; Roux et al. 2016). This process can be evidenced with discordant assignments of individuals based on mitochondrial and nuclear datasets and can occur as consequence of geographic range expansion (Mastrantonio et al. 2016; Çoraman et al. 2020).

Analysis of divergence time in Erythrinoidea estimated a crown age for *Hoplerythrinus* at c. 7.1 Ma (15.3–4.1 Ma), when representatives of the Río Orinoco basin diverged from

others (Conde et al., in prep). A plausible hypothesis, supported by information presented above, is that the genetic differentiation between these lineages could have been caused by the Late Miocene uplift of the Vaupes Arch c. 10 Ma and the separation of the Western Amazon and Orinoco basins (Mora et al. 2010; Albert et al. 2018). Secondary contacts may have occurred during the Pleistocene or Holocene formation of the Casiquiare Canal, which represented a more recent dispersal corridor for fish species between these two major basins (Lujan and Armbruster 2011). Such secondary contact can provide opportunities for genetic exchange among previously allopatric but not yet fully reproductively isolated lineages (Mastrantonio et al. 2016; Willis 2017). The Casiquiare portal may have allowed a secondary contact between these lineages of *Hoplerythrinus* allowing mitochondrial introgression or admixture pattern. According with proximity among COI sequences of representatives from the Rio Orinoco and representatives from Atlantic coastal drainages of Guianas and Rio Jari, another possible scenario therefore is secondary contact due to river capture of headwaters across the upper Caroni and Cuyuni/Mazaruni watersheds, which would have facilitate faunal exchanges between the upper Orinoco and Essequibo basins (Lujan and Armbruster 2011). However, there is little empirical evidence to support the presence of this corridor and these basins present a predominant pattern of endemism suggesting long-term isolation (Lujan and Armbruster 2011). We associated this gene sharing to introgression; incomplete lineage sorting could be excluded since both lineages (Río Orinoco basin and widely distributed) were recovered reciprocally monophyletic in all phylogenomic reconstructions, and discordant individuals would be expected to be randomly distributed rather than being geographically structured (Çoraman et al. 2020).

The use of uniparental markers, such as the mtDNA COI as a method of species delimitation in animals, does not always comprehensively assess gene flow or reproductive isolation (Struck et al. 2018), and it has been less useful in some cases of rapid diversification or recent divergence in NFF clades (Rossini et al. 2016; de Queiroz et al. 2020; Ramirez et al. 2020). As we showed in *Hoplerythrinus*, relying on COI barcodes as the only source of genetic divergence in taxa traditionally consider as species complexes should be viewed with caution and integrated with nuclear markers since inferences could reflect population structure rather than species differences (Cong et al. 2017; Willis 2017; Struck et al. 2018).

4.2 Hoplerythrinus as a geographically widespread monotypic fish genus

Under the unified species concept as being separately evolving metapopulation lineages, different equivalent properties can be used as lines of evidence to assessing lineage separation (De Queiroz 2005, 2007). Morphological distinguishability, reproductive isolation and reciprocal monophyly remain as best and commonly examined properties (Hart 2011; Fišer et al. 2018). However, speciation is a process that occurs continuously involving different levels of differentiation over different time frames (Butlin et al. 2012; Seehausen and Wagner 2014). It can therefore be a challenge to delineate species in taxa that are recently or incompletely diverged (Struck and Cerca 2019). The present results showed three lineages with some degree of genetic differentiation in *Hoplerythrinus*, but failed to recover its reciprocal monophyly in phylogenomic analyses, except between the widely distributed and Orinoco basin lineages. However, discordant assignments of representatives from the Orinoco basin comparing mitochondrial and nuclear datasets, suggest the presence of gene flow between these lineages at some point in the relatively recent past. Additionally, no morphological characters were found to distinguish these lineages, revealing substantial uniformity of coloration pattern, meristic and morphometric data throughout their distribution area as reported in previous examinations (Oyakawa et al. 2013).

Erythrinids are well known for their physiological adaptations that allow them to tolerate toxic and hypoxic environments (Liem 1988; Moraes et al. 2004; Moron et al. 2009; Pelster 2021), and capacities to reside in varied habitats (Oyakawa et al. 2013; Oyakawa and Mattox 2018). Particularly, *Hoplerythrinus* uses its well-vascularized swimbladder as an air-breathing organ, being less impacted to variations in water oxygen levels, an ability that allows it to survive in habitats that are inhospitable to many other fishes (Wood et al. 2016; Pelster et al. 2018). This genus is also characterized by other adaptative traits such parental care and a generalist diet, feeding on a wide range of insects, crustaceous, fishes, but also fruits (Taphorn 2003; Sánchez-Duarte et al. 2011; Oyakawa and Mattox 2018). Theory predicts that ecologically generalist lineages with broad or flexible resource utilization should undergo lower net diversification rates than ecological specialists (Vrba 1987; Birand et al. 2012; Rolland and Salamin 2016). From this perspective the eurytopic habitat and trophic requirements of *H. unitaeniatus* could be important drivers in reducing rates of speciation and extinction, or rates of net species

turnover. Probably, ecological specializations were not a trigger during its relatively recent time of diversification (*c.* 7.1 Ma), while landscape constrains affecting dispersal over geological time could be more relevant (Conde et al., in prep).

Compared to many NFF genera, *Hoplerythrinus* exhibits a low number of species per millions of years (0.14 spp/Ma). However, this species accumulation rate is similar to other NFF clades, such as *Pimelodus ornatus* catfish (0.13 spp/Ma), *Lepidosiren* lungfishes (0.14 spp/Ma), *Potamorhina* saguirus (0.14 spp/Ma) or *Plesiotrygon* stingrays (0.16 spp/Ma), some of which also exhibit a broad geographic distribution (Table 4). Additionally, *Hoplerythrinus* appears to have a relatively short diversification time, however, other genera such as *Schizodon* headstanders, *Oligosarcus* tambicus or *Pygocentrus* piranas, with similar or shorter times, reveal higher species accumulation rates (Table 4). Speciation rates vary among lineages, and the number of species at any given time depend of ecological and historical process (Sobel et al. 2010; Norris and Hull 2012), however, the mechanisms and constrains impacting on patterns of species richness among clades remains as an active area of research (Castro-Insua et al. 2018; Diaz et al. 2019; Albert et al. 2020). Considering ecological traits of *Hoplerythrinus*, it is possible that its time of divergence (*c.* 7.1 Ma) has not been enough for the establishment of disparity among lineages, and due to their evolutionary dynamics cannot be unambiguously rendered as discrete units. Probably this taxon is in the gray zone of speciation, where intermediate divergence levels generate an intrinsic difficulty to delineating species (De Queiroz 2007; Roux et al. 2016).

Table 4. Rates of species richness per time of diversification in 24 freshwater Neotropical fish genera. Ma = Millions of years ago; AOG = Amazon, Orinoco and Guianas. Species richness per time were estimated following Melo et al (2021).

Clade	Order	Family	Species richness	Mean crown age (Ma)	Reference	Species per Ma	Distribution	Range
Hypostomus	Siluriformes	Loricariidae	149	12.1	de Queiroz et al., 2021	12.31	cis- & trans-Andean	Widespread
Hypostomus	Siluriformes	Loricariidae	149	20.9	Cardoso et al., 2021	7.13	cis- & trans-Andean	Widespread
Oligosarcus	Characiformes	Characidae	22	4.1	Wendt et al., 2019	5.33	cis-Andean	Paraná-Paraguay, Coastal Brazil
Schizodon	Characiformes	Anostomidae	17	7.6	Ramirez et al., 2020	2.25	cis- & trans-Andean	Maracaibo, AOG, Paraná-Paraguay, Coastal Brazil, São Francisco
Potamotrygon	Myliobatiformes	Potamotrygonidae	32	14.3	Fontenelle et al., 2021	2.25	cis- & trans-Andean	Widespread
Metynnis	Characiformes	Serrasalmidae	15	11.6	Kolmann et al., 2021	1.29	cis-Andean	AOG, Paraná-Paraguay, Coastal Brazil
Prochilodus	Characiformes	Prochilodontidae	13	11.3	Santos et al., 2021	1.15	cis- & trans-Andean	Widespread
Steindachnerina	Characiformes	Curimatidae	24	29.1	Melo et al., 2021	0.82	cis- & trans-Andean	Atrato, AOG, Paraná-Paraguay, Coastal Brazil
Pygocentrus	Characiformes	Serrasalmidae	3	3.7	Kolmann et al., 2021	0.81	cis-Andean	AOG, São Francisco
Tetragonopterus	Characiformes	Characidae	12	15.3	Melo et al., 2016a	0.78	cis-Andean	AOG, Paraná-Paraguay, Coastal Brazil
Triportheus	Characiformes	Triportheidae	16	20.7	Mariguela et al., 2016	0.77	cis- & trans-Andean	Magdalena, AOG, Paraná-Paraguay, São Francisco
Copionodon	Siluriformes	Trichomycteridae	5	10.8	Ochoa et al., 2017	0.46	cis-Andean	Coastal Brazil
Hoplias	Characiformes	Erythrinidae	15	34.0	Conde et al., in prep.	0.44	cis- & trans-Andean	Widespread
Plagioscion	Perciformes	Sciaenidae	7	17.8	Cooke et al., 2012	0.39	cis- & trans-Andean	Magdalena, AOG, Paraná-Paraguay, São Francisco
Pseudoplatystoma	Siluriformes	Pimelodidae	8	21.3	Tagliacollo et al., 2015	0.38	cis- & trans-Andean	Widespread
Megalonema	Siluriformes	Pimelodidae	7	19.1	Tagliacollo et al., 2015	0.37	cis- & trans-Andean	Magdalena, Maracaibo, AOG, Paraná-Paraguay
Psectrogaster	Characiformes	Curimatidae	8	24.3	Melo et al., 2021	0.33	cis-Andean	AOG, Paraguay
Curimata	Characiformes	Curimatidae	13	40.3	Melo et al., 2021	0.32	cis- & trans-Andean	Magdalena, AOG, Parnaíba
Sorubim	Siluriformes	Pimelodidae	5	15.8	Tagliacollo et al., 2015	0.32	cis- & trans-Andean	Magdalena, Sinú, Maracaibo, AOG, Parnaíba, Paraná-Paraguay
Acnodon	Characiformes	Serrasalmidae	3	10.1	Kolmann et al., 2021	0.30	cis-Andean	AG
Curimatopsis	Characiformes	Curimatidae	11	44.1	Melo et al., 2021	0.25	cis-Andean	AOG
Pseudocurimata	Characiformes	Curimatidae	6	24.7	Melo et al., 2021	0.24	trans-Andean	Atrato, Pacific slope rivers from Colombia, Ecuador, Peru
Plesiotrygon	Myliobatiformes	Potamotrygonidae	2	12.8	Fontenelle et al., 2021	0.16	cis-Andean	Amazon

Clade	Order	Family	Species richness	Mean crown age (Ma)	Reference	Species per Ma	Distribution	Range
Potamorhina	Characiformes	Curimatidae	5	34.7	Melo et al., 2021	0.14	cis- & trans-Andean	Maracaibo, AOG, Paraná-Paraguay
Lepidosiren	Ceradontiformes	Lepidosirenidae	1	7.8	Carneiro et al., 2021	0.14	cis-Andean	AOG, Paraná-Paraguay
Hoplerythrinus	Characiformes	Erythrinidae	1	7.1	Conde et al., in prep.	0.14	cis-Andean	AOG, Paraná-Paraguay, Coastal Brazil, São Francisco
Pimelodus ornatus	Siluriformes	Pimelodidae	1	7.8	Tagliacollo et al., 2015	0.13	cis-Andean	AOG, Paraná-Paraguay

Hoplerythrinus also exhibits large karyotypic variation at both the inter-and intra-populational levels, with five different karyomorphs ranging from 2n = 48-52 chromosomes (Diniz and Bertollo 2003; Martinez et al. 2016). Three different karyomorphs with 2n=48 have been reported from coastal drainages of Suriname and the upper Rio Paraná, Rio Paraguay and Amazon basins (Giuliano-Caetano et al. 2001; Diniz and Bertollo 2003; da Rosa et al. 2012; Martinez et al. 2016). In contrast, the analysis of populations from the upper Rio Arinos and upper Rio Araguaia revealed a different karyomorph with 2n=52 (Martinez et al. 2016), which could be associated with the pattern of genetic differentiation of the lineage we recovered from upper portions of Amazonian versants draining the Brazilian Shield. The diploid chromosome number 2n=52 has also been reported from the Rio São Francisco and coastal drainages of southeastern Brazil (Giuliano-Caetano et al. 2001; Diniz and Bertollo 2003; Martinez et al. 2015), even within the Rio Sao Francisco basin, another karyomorph with 2n = 50 has also been reported, as well as the presence of putative hybrids with 2n=51 (Diniz and Bertollo 2003; Martinez et al. 2015). Although several chromosomal rearrangements can contribute to speciation (Butlin et al. 2012), differences in chromosome numbers do not necessarily represent a reproductive barrier, even in distant freshwater fish species, hybridization can produce fertile lineages in cases when the number of maternal chromosomes is larger that of parental chromosomes (Ou et al. 2018; Liu et al. 2020).

Here, based on our lines of evidence and details discussed above, we propose *Hoplerythrinus* as a monotypic genus with *H. unitaeniatus* widely distributed throughout most cis-Andean drainages of tropical South America. A pattern of broad geographic distribution has been identified for several fish species in the cis-Andean region, however, most of them have never been the object of detailed studies or recognized through integrative approaches (Dagosta and de Pinna 2019). Thus, *H. unitaeniatus* exhibits one of the largest geographic ranges of fishes within the Neotropical region. Other NFF species exhibit similar widespread geographic distributions. The South American lungfish *Lepidosiren paradoxa* (Lepidosirenidae) exhibits divergent genetic lineages based on mtDNA markers but no morphological disparity has been reported (Carneiro et al. 2021). The characiform *Rhaphiodon vulpinus* (Cynodontidae) has been assessed only under morphological data (Toledo-Piza 2000). *Hemisorubim platyrhynchos* (Pimelodidae) reveals an apparently conserved karyotype among populations (Swarça et al. 2013). However, no studies attempting to evaluate its taxonomic status and

evolutionary history have been conducted. Some nominal NFF morphospecies exhibit substantial phenotypic differences in coloration and body proportions across an immense geographic range from northern Argentina to Panama, but with varying degrees of karyotypic variation; e.g. the catfish *Rhamdia quelen* (Heptapteridae) (Usso et al. 2019), and the electric fishes *Gymnotus carapo* (Gymnotidae) (Craig et al. 2017) and *Sternopygus macrurus* (Sternopygidae) (Hulen et al. 2005; Silva et al. 2008). In these morphospecies, efforts to identify species boundaries have been hindered by high amounts of local phenotypic variation and spotty geographic sampling (Kim et al. 2020).

Different levels of karyotypic variation have also been described for other wide distributed species such as *Ageneiosus inermis* (Lui et al. 2013), *Callichthys callichthys* (Almeida et al. 2013; Konerat et al. 2014), *Corydoras aeneus* (Oliveira et al. 1988), *Erythrinus erythrinus* (Bertollo et al. 2004), *Gymnotus carapo* (Milhomem et al. 2008; Nagamachi et al. 2010), *Hoplias malabaricus* (Bertollo et al. 2000; Marques et al. 2013), *Hoplosternum littorale* (Konerat et al. 2014), *Leporellus vittatus* (de Aguilar and Galetti 2008), *Pimelodus ornatus* (Swarça et al. 2007), *Plagioscion squamosissimus* (Feldberg et al. 1999), *Sorubim lima* (Martins-Santos et al. 1996; Neto et al. 2011), *Sternopygus macrurus* (Silva et al. 2008; Fernandes et al. 2017), *Synbranchus marmoratus* (Torres et al. 2005), and *Trachelyopterus galeatus* (Lui et al. 2010; Dos Santos et al. 2021), but also are waiting for detailed revisions encompassing their entire distribution. Most of this species have in common with *H. unitaeniatus* a generalist diet (Lasso et al. 2011; van der Sleen and Albert 2018; Neto et al. 2019), and species as *Callichthys callichthys*, *Corydoras aeneus*, *Gymnotus carapo*, *Hoplias malabaricus*, *Lepidosiren paradoxa*, *Synbranchus marmoratus*, and *Trachelyopterus galeatus* share the capacity to survive in hypoxic habitats, in some cases due to their air breathing ability (Eduardo et al. 1979; Liem 1988; Jucá-Chagas 2004; Galvis et al. 2006; Jucá-Chagas and Boccardo 2006; Persaud et al. 2006; Pelster et al. 2018).

Confusing separately evolving lineages as a single nominal species can obscure population structure and our understanding of ongoing diversification (Willis 2017). Considering *H. unitaeniatus* as an evolving set of metapopulation lineages can aid future studies of population-level variation and processes (Hart 2011). For example, according to the geographic correspondences among the three lineages recognized in *Hoplerythrinus*, future studies could examine the genetic consequences and dynamics of

genomic architecture associated with the secondary contact through the Casiquiare Canal (Stokes et al. 2018). Another fruitful path could focus on the genetic differentiation associated with endemism in upper portions of Amazonian versants draining the Brazilian Shield (Lima and Moreira 2003; Netto-Ferreira 2012). Similarly, future studies could evaluate ontogenetic or ecological mechanisms underlying stasis observed in *Hoplerythrinus* by studying the developmental and selective levels of morphological organization (Struck and Cerca 2019), and assessing relationships between morphological differentiation and ecological affinities (e.g. generalist versus specialists).

Acknowledgments

We are grateful to Francisco Villa-Navarro and Diana Montoya (CZUT-IC), Nathan Lujan and Mary Burridge (ROM), María Fernanda Castillo (STRI), Hernán Ortega (MUSM), Raphael Covain (MHNG) for the loan of tissues. Special thanks to Mariangeles Arce and Mark H. Sabaj for loan of tissues samples and also for support and facilitating access to specimen and data at the Academy of Natural Sciences of Drexel University (ANSP). We thank Esther Dondorp (Naturalis Biodiversity Center) for photographs and x-rays of holotype of *Pseuderythrinus rosapinnis*. Analyses were performed on Zungaro and Brycon servers at LBP/UNESP funded by FAPESP proc. 2014/26508-3 (CO), and in the Center for Scientific Computing (NCC/GridUNESP) of the São Paulo State University. C.C.C-S. is funded by FAPESP (grant nos. 2018/09767-6 and 2019/16999-3).

References

Aberer A.J., Kobert K., Stamatakis A. 2014. Exabayes: Massively parallel bayesian tree inference for the whole-genome era. Mol. Biol. Evol. 31:2553–2556.

Adey A., Morrison H.G., Asan, Xun X., Kitzman J.O., Turner E.H., Stackhouse B., MacKenzie A.P., Caruccio N.C., Zhang X., Shendure J. 2010. Rapid, low-input, low-bias construction of shotgun fragment libraries by high-density in vitro transposition. Genome Biol. 11:R119.

Agudelo-Zamora H.D., Tavera J., Murillo Y.D., Ortega-Lara A. 2020. The unknown diversity of the genus *Characidium* (Characiformes: Crenuchidae) in the Chocó

biogeographic region, Colombian Andes: Two new species supported by morphological and molecular data. J. Fish Biol. 97:1662–1675.

Aguilar C., Miller M.J., Loaiza J.R., González R., Krahe R., De León L.F. 2019. Tempo and mode of allopatric divergence in the weakly electric fish *Sternopygus dariensis* in the Isthmus of Panama. Sci. Rep. 9:1–11.

de Aguilar C.T., Galetti P.M. 2008. Chromosome mapping of 5S rRNA genes differentiates Brazilian populations of *Leporellus vittatus* (Anostomidae, Characiformes). Genet. Mol. Biol. 31:188–194.

Albert J.S., Tagliacollo V.A., Dagosta F. 2020. Diversification of Neotropical Freshwater Fishes. Annu. Rev. Ecol. Evol. Syst. 51:27–53.

Albert J.S., Val P., Hoorn C. 2018. The changing course of the Amazon River in the Neogene: center stage for Neotropical diversification. Neotrop. Ichthyol. 16:1–24.

Alda F., Tagliacollo V.A., Bernt M.J., Waltz B.T., Ludt W.B., Faircloth B.C., Alfaro M.E., Albert J.S., Chakrabarty P. 2019. Resolving Deep Nodes in an Ancient Radiation of Neotropical Fishes in the Presence of Conflicting Signals from Incomplete Lineage Sorting. Syst. Biol. 68:573–593.

Almeida J.S., Affonso P.R.A. de M., Diniz D., Carneiro P.L.S., Dias A.L. 2013. Chromosomal Variation in the Tropical Armored Catfish *Callichthys Callichthys* (Siluriformes, Callichthyidae): Implications for Conservation and Taxonomy in a Species Complex from a Brazilian Hotspot. Zebrafish. 10:451–458.

Anjos M.S., Bitencourt J.A., Nunes L.A., Sarmento-Soares L.M., Carvalho D.C., Armbruster J.W., Affonso P.R.A.M. 2020. Species delimitation based on integrative approach suggests reallocation of genus in Hypostomini catfish (Siluriformes, Loricariidae). Hydrobiologia. 847:563–578.

Armbruster J.W., Lujan N.K., Bloom D.D. 2021. Redescription of the Guiana Shield Darter Species *Characidium crandellii* and *C. declivirostre* (Crenuchidae) with Descriptions of Two New Species. Ichthyol. Herpetol. 109:102–122.

Barton N.H., Hewitt G.M. 1985. Analysis of hybrid zones. Annu. Rev. Ecol. Syst. Vol. 16.:113–148.

Bertollo L.A.C., Born G.G., Dergam J.A., Fenocchio A.S., Moreira-Filho O. 2000. A

biodiversity approach in the neotropical Erythrinidae fish, *Hoplias malabaricus*. Karyotypic survey, geographic distribution of cytotypes and cytotaxonomic considerations. Chromosom. Res. 8:603–613.

Bertollo L.A.C., Oliveira C., Molina W.F., Margarido V.P., Fontes M.S., Pastori M.C., Falcão J.D.N., Fenocchio A.S. 2004. Chromosome evolution in the erythrinid fish, *Erythrinus erythrinus* (Teleostei: Characiformes). Heredity (Edinb). 93:228–233.

Birand A., Vose A., Gavrilets S. 2012. Patterns of species ranges, speciation, and extinction. Am. Nat. 179:1–21.

Born G.G., Bertollo L.A.C. 2000. An XX/XY sex chromosome system in a fish species, *Hoplias malabaricus*, with a polymorphic NOR-bearing X chromosome. Chromosom. Res. 8:111–118.

Butlin R., Debelle A., Kerth C., Snook R.R., Beukeboom L.W., Castillo Cajas R.F., Diao W., Maan M.E., Paolucci S., Weissing F.J., van de Zande L., Hoikkala A., Geuverink E., Jennings J., Kankare M., Knott K.E., Tyukmaeva V.I., Zoumadakis C., Ritchie M.G., Barker D., Immonen E., Kirkpatrick M., Noor M., Garcia M.C., Schmitt T., Schilthuizen M. 2012. What do we need to know about speciation? Trends Ecol. Evol. 27:27–39.

Cardoso Y.P., Jardim de Queiroz L., Bahechar I.A., Posadas P.E., Montoya-Burgos J.I. 2021. Multilocus phylogeny and historical biogeography of *Hypostomus* shed light on the processes of fish diversification in La Plata Basin. Sci. Rep. 11:1–14.

Cardoso Y.P., Rosso J.J., Mabragaña E., González-Castro M., Delpiani M., Avigliano E., Bogan S., Covain R., Schenone N.F., Díaz de Astarloa J.M. 2018. A continental-wide molecular approach unraveling mtDNA diversity and geographic distribution of the Neotropical genus *Hoplias*. PLoS One. 13:1–25.

Carneiro J., Dutra G.M., Nobre R.M., Pinheiro L.M. de L., Oliva P.A.C., Sampaio I., Schneider H., Schneider I. 2021. Evidence of cryptic speciation in South American lungfish. J. Zool. Syst. Evol. Res. 59:760–771.

Castro-Insua A., Gómez-Rodríguez C., Wiens J.J., Baselga A. 2018. Climatic niche divergence drives patterns of diversification and richness among mammal families. Sci. Rep. 8:1–12.

Cioffi M.B., Martins C., Centofante L., Jacobina U., Bertollo L.A.C. 2009. Chromosomal variability among allopatric populations of erythrinidae fish *Hoplias malabaricus*: Mapping of three classes of repetitive DNAs. Cytogenet. Genome Res. 125:132–141.

Cong Q., Shen J., Borek D., Robbins R.K., Opler P.A., Otwinowski Z., Grishin N. V. 2017. When coi barcodes deceive: Complete genomes reveal introgression in hairstreaks. Proc. R. Soc. B Biol. Sci. 284.

Cooke G.M., Chao N.L., Beheregaray L.B. 2012. Marine incursions, cryptic species and ecological diversification in Amazonia: The biogeographic history of the croaker genus *Plagioscion* (Sciaenidae). J. Biogeogr. 39:724–738.

Çoraman E., Dundarova H., Dietz C., Mayer F. 2020. Patterns of mtDNA introgression suggest population replacement in Palaearctic whiskered bat species: Population replacement in whiskered bats. R. Soc. Open Sci. 7.

Craig J.M., Crampton W.G.R., Albert J.S. 2017. Revision of the polytypic electric fish Gymnotus carapo (Gymnotiformes, Teleostei), with descriptions of seven subspecies. Zootaxa. 4318:401–438.

Cuvier G., Valenciennes A. 1847. Histoire naturelle des poissons. Tome dix-neuvième. Suite du livre dix-neuvième. Brochets ou Lucioïdes. Livre vingtième. De quelques familles de Malacoptérygiens, intermédiaires entre les Brochets et les Clupes. Ch. Pitois, & V.e Levrault, Paris & Strasbo. .

Dagosta F.C.P., de Pinna M. 2019. The Fishes of the Amazon: Distribution and Biogeographical Patterns, with a Comprehensive List of Species. Bull. Am. Museum Nat. Hist. 431:1–163.

Dergam J.A., Paiva S.R., Schaeffer C.E., Godinho A.L., Vieira F. 2002. Phylogeography and RAPD-PCR variation in *Hoplias malabaricus* (Bloch, 1794) (Pisces, Teleostei) in southeastern Brazil. Biologia (Bratisl). 387:379–387.

Diaz L.F.H., Harmon L.J., Sugawara M.T.C., Miller E.T., Pennell M.W. 2019. Macroevolutionary diversification rates show time dependency. Proc. Natl. Acad. Sci. U. S. A. 116:7403–7408.

Diniz D., Bertollo L.A.C. 2003. Karyotypic studies on *Hoplerythrinus unitaeniatus*

(Pisces, Erythrinidae) populations. A biodiversity analysis. Caryologia. 56:303–313.

Drummond A.J., Ho S.Y.W., Phillips M.J., Rambaut A. 2006. Relaxed phylogenetics and dating with confidence. PLoS Biol. 4:699–710.

Drummond A.J., Suchard M.A., Xie D., Rambaut A. 2012. Bayesian phylogenetics with BEAUti and the BEAST 1.7. Mol. Biol. Evol. 29:1969–1973.

Edgar R.C. 2004. MUSCLE: multiple sequence alignment with high accuracy and high throughput. Nucleic Acids Res. 32:1792–1797.

Eduardo J., Bicudo P.W., Johansen K. 1979. Respiratory gas exchange in the airbreathing fish, *Synbranchus marmoratus*. Environ. Biol. Fishes. 4:55–64.

Eigenmann C.H. 1912. The freshwater fishes of British Guiana, including a study of the ecological grouping of species, and the relation of the fauna of the plateau to that of the lowlands. Mem. Carnegie Museum. 5:819.

Faircloth B.C. 2013. illumiprocessor: a trimmomatic wrapper for parallel adapter and quality trimming. http://dx.doi.org/10.6079/J9ILL. .

Faircloth B.C. 2016. PHYLUCE is a software package for the analysis of conserved genomic loci. Bioinformatics. 32:786–788.

Faircloth B.C., Alda F., Hoekzema K., Burns M.D., Oliveira C., Albert J.S., Melo B.F., Ochoa L.E., Roxo F.F., Chakrabarty P., Sidlauskas B.L., Alfaro M.E. 2020. A Target Enrichment Bait Set for Studying Relationships among Ostariophysan Fishes. Copeia. 108:47–60.

Faircloth B.C., McCormack J.E., Crawford N.G., Harvey M.G., Brumfield R.T., Glenn T.C. 2012. Ultraconserved elements anchor thousands of genetic markers spanning multiple evolutionary timescales. Syst. Biol. 61:717–26.

Faircloth B.C., Sorenson L., Santini F., Alfaro M.E. 2013. A Phylogenomic Perspective on the Radiation of Ray-Finned Fishes Based upon Targeted Sequencing of Ultraconserved Elements (UCEs). PLoS One. 8.

Feldberg E., Porto J.I.R., Dos Santos E.B.P., Valentim F.C.S. 1999. Cytogenetic studies of two freshwater sciaenids of the genus *Plagioscion* (Perciformes, Sciaenidae)

from the Central Amazon. Genet. Mol. Biol. 22:351–356.

Fernandes C.A., Baumgärtner L., Paiz L.M., Margarido V.P., De Brito Portela-Castro A.L. 2017. Chromosomal characteristics of rDNA in a conserved karyotype of two *Sternopygus macrurus* (Gymnotiformes: Sternopygidae) populations from upper Paraná River basin. Biol. 72:680–685.

Fišer C., Robinson C.T., Malard F. 2018. Cryptic species as a window into the paradigm shift of the species concept. Mol. Ecol. 27:613–635.

Fontenelle J.P., Portella Luna Marques F., Kolmann M.A., Lovejoy N.R. 2021. Biogeography of the neotropical freshwater stingrays (Myliobatiformes: Potamotrygoninae) reveals effects of continent-scale paleogeographic change and drainage evolution. J. Biogeogr. 48:1406–1419.

Fricke R., Eschmeyer W.N., Van der Laan R. 2022. ESCHMEYER'S CATALOG OF FISHES: GENERA, SPECIES, REFERENCES. Available from http://researcharchive.calacademy.org/research/ichthyology/catalog/fishcatmain.asp.

Fujisawa T., Barraclough T.G. 2013. Delimiting species using single-locus data and the generalized mixed yule coalescent approach: A revised method and evaluation on simulated data sets. Syst. Biol. 62:707–724.

Galtier N. 2019. Delineating species in the speciation continuum: A proposal. Evol. Appl. 12:657–663.

Galvis G., Mojica J.I., Duque S.R., Castellanos C., Sánchez-duarte P., Arce M., Gutierrez Á., Jiménez L.F., Santos M., Vejarano S., Arbeláez F., Prieto E., Leiva M. 2006. Peces del medio Amazonas. Región de Leticia. Bogotá: Forma e Impresos.

Garavello J.C., Ramirez J.L., Oliveira A.K. de, Britski H.A., Birindelli J.L.O., Galetti Jr P.M. 2021. Integrative taxonomy reveals a new species of Neotropical headstanding fish in genus *Schizodon* (Characiformes: Anostomidae). Neotrop. Ichthyol. 19:1–32.

Géry J. 1977. Characoids of the world. New Jersey: T. F. H. Publications, Inc. Ltd.

Gill T.N. 1858. Synopsis of the fresh water fishes of the western portion of the island of

Trinidad, W. I. Ann. Lyc. Nat. Hist. N. Y., 6 (10-13): 363-430. .

Gill T.N. 1896. The differential characters of characinoid and erythrinoid fishes. Proc. United States Natl. Museum. 18:205–209.

Giuliano-Caetano L., Jorge L.C., Moreira-Filho O., Bertollo L.A.C. 2001. Comparative Cytogenetic Studies on *Hoplerythrinus unitaeniatus* Populations (Pisces, Erythrindae). Cytologia (Tokyo). 66:39–43.

Guimarães K.L.A., Rosso J.J., González-Castro M., Souza M.F.B., Díaz de Astarloa J.M., Rodrigues L.R.R. 2021a. A new species of *Hoplias malabaricus* species complex (Characiformes: Erythrinidae) from the Crepori River, Amazon basin, Brazil. .

Guimarães K.L.A., Rosso J.J., Souza M.F.B., Díaz de Astarloa J.M., Rodrigues L.R.R. 2021b. Integrative taxonomy reveals disjunct distribution and first record of Hoplias misionera (Characiformes: Erythrinidae) in the Amazon River basin: morphological, DNA barcoding and cytogenetic considerations. Neotrop. Ichthyol. 19:1–20.

Hart M.W. 2011. The species concept as an emergent property of population biology. Evolution (N. Y). 65:613–616.

Henschel E., Bernt M.J., Baskin J.N., Schmidt R.E., Lujan N.K. 2022. Osteology-focused redescription and description of the blood-feeding candirus *Paracanthopoma parva* and *Paravandellia alleynei* sp.n. (Trichomycteridae: Vandelliinae). J. Fish Biol. 100:161–174.

Hulen K.G., Crampton W.G.R., Albert J.S. 2005. Phylogenetic systematics and historical biogeography of the Neotropical electric fish *Sternopygus* (Teleostei: Gymnotiformes). Syst. Biodivers. 3:407–432.

ICZN. 1999. International Code of Zoological Nomenclature. London: International Trust for Zoological Nomenclature.

de Jongh B.O. 1991. Reexamination of the Holotype of Pseuderythrinus rosapinnis Hoedeman, 1950, a synonym of Hoplerythrinus unitaeniatus Agassiz, 1829 (Pisces, Characiformes, Erythrinidae). Bull. Zoölogisch Museum. 13:57–62.

Jucá-Chagas R. 2004. Air breathing of the neotropical fishes *Lepidosiren paradoxa*,

Hoplerythrinus unitaeniatus and *Hoplosternum littorale* during aquatic hypoxia. Comp. Biochem. Physiol. - A Mol. Integr. Physiol. 139:49–53.

Jucá-Chagas R., Boccardo L. 2006. The air-breathing cycle of *Hoplosternum littorale* (Hancock, 1828) (Siluriformes: Callichthyidae). Neotrop. Ichthyol. 4:371–373.

Katoh K., Misawa K., Kuma K.I., Miyata T. 2002. MAFFT: A novel method for rapid multiple sequence alignment based on fast Fourier transform. Nucleic Acids Res. 30:3059–3066.

Kearse M., Moir R., Wilson A., Stones-Havas S., Cheung M., Sturrock S., Buxton S., Cooper A., Markowitz S., Duran C., Thierer T., Ashton B., Meintjes P., Drummond A. 2012. Geneious Basic: An integrated and extendable desktop software platform for the organization and analysis of sequence data. Bioinformatics. 28:1647–1649.

Kikinis R., Pieper S.D., Vosburgh K.G. 2014. Intraoperative Imaging and Image-Guided Therapy. In: Jolesz F., editor. Intraoperative Imaging and Image-Guided Therapy. New york: Springer. p. 277–289.

Kim L.Y., Crampton W.G.R., Albert J.S. 2020. Two new species of *Gymnotus* (Gymnotiformes: Gymnotidae) from Brazil and historical biogeography of the subgenus *Lamontianus*. Copeia. 108:468–484.

Kimura M. 1980. Journal of Molecular Evolution A Simple Method for Estimating Evolutionary Rates of Base Substitutions Through Comparative Studies of Nucleotide Sequences. J. Mol. Evol. 16:111–120.

Kingman J.F.C. 1982. The coalescent. Stoch. Process. their Appl. 13:235–248.

Kircher M., Sawyer S., Meyer M. 2012. Double indexing overcomes inaccuracies in multiplex sequencing on the Illumina platform. Nucleic Acids Res. 40:1–8.

Kolmann M.A., Hughes L.C., Hernandez L.P., Arcila D., Betancur-R R., Sabaj M.H., López-Fernández H., Ortí G. 2021. Phylogenomics of Piranhas and Pacus (Serrasalmidae) Uncovers How Dietary Convergence and Parallelism Obfuscate Traditional Morphological Taxonomy. Syst. Biol. 70:576–592.

Konerat J.T., Bueno V., Martins-Santos I.C., Margarido V.P. 2014. Karyotypic diversity and chromosome evolution in the armored catfishes Callichthyinae (Siluriformes,

Callichthyidae). Caryologia. 67:140–148.

Korshunova T., Picton B., Furfaro G., Mariottini P., Pontes M., Prkić J., Fletcher K., Malmberg K., Lundin K., Martynov A. 2019. Multilevel fine-scale diversity challenges the ‘cryptic species’ concept. Sci. Rep. 9:1–23.

Kumar S., Stecher G., Li M., Knyaz C., Tamura K. 2018. MEGA X: Molecular evolutionary genetics analysis across computing platforms. Mol. Biol. Evol. 35:1547–1549.

Lanfear R., Calcott B., Ho S.Y.W., Guindon S. 2012. PartitionFinder: Combined selection of partitioning schemes and substitution models for phylogenetic analyses. Mol. Biol. Evol. 29:1695–1701.

Lanfear R., Frandsen P.B., Wright A.M., Senfeld T., Calcott B. 2016. Partitionfinder 2: New methods for selecting partitioned models of evolution for molecular and morphological phylogenetic analyses. Mol. Biol. Evol. 34:772–773.

Lasso C., Meri J. 2001. Estructura comunitaria de la ictiofauna en herbazales y bosques inundables del bajo río Guanipa, cuenca del Golfo de Paria, Venezuela. Mem. Fund. La Salle Cienc. Nat. 155:73–90.

Lasso C.A., Agudelo E., Jiménez-Segura L.F., Ramírez-Gil H., Morales-Betancourt M., Ajiaco-Martínez R.E., de Paula-Gutiérrez F., Usma J.S., Muñoz Torres S.E., Sanabria-Ochoa A.I. 2011. I. Catálogo de los Recursos Pesqueros Continentales de Colombia. Serie Editorial Recursos Hidrobiológicos y Pesqueros Continentales de Colombia. Bogotá, D. C., Colombia: Instituto de Investigación de Recursos Biológicos Alexander von Humboldt (IAvH).

Lê S., Josse J., Husson F. 2008. FactoMineR: An R Package for Multivariate Analysis. J. Stat. Softw. 25:1–18.

Liem K.F. 1988. Form and function of lungs: The evolution of air breathing mechanisms. Integr. Comp. Biol. 28:739–759.

Lima F.C.T., Moreira C.R. 2003. Three new species of *Hyphessobrycon* (Characiformes: Characidae) from the upper rio Araguaia basin in Brazil. Neotrop. Ichthyol. 1:21–33.

Liu Q., Liu J., Yuan L., Li L., Tao M., Zhang C., Qin Q., Chen B., Ma M., Tang C., Liu

S. 2020. The establishment of the fertile fish lineages derived from distant hybridization by overcoming the reproductive barriers. Reproduction. 159:R237–R249.

Longo S.J., Faircloth B.C., Meyer A., Westneat M.W., Alfaro M.E., Wainwright P.C. 2017. Phylogenomic analysis of a rapid radiation of misfit fishes (Syngnathiformes) using ultraconserved elements. Mol. Phylogenet. Evol. 113:33–48.

Loureiro M., de Sá R., Serra S.W., Alonso F., Lanés L.E.K., Volcan M.V., Calviño P., Nielsen D., Duarte A., Garcia G. 2018. Review of the family Rivulidae (Cyprinodontiformes, Aplocheiloidei) and a molecular and morphological phylogeny of the annual fish genus *Austrolebias* Costa 1998. Neotrop. Ichthyol. 16:1–20.

Lui R.L., Blanco D.R., Margarido V.P., Moreira Filho O. 2010. Chromosome characterization and biogeographic relations among three populations of the driftwood catfish *Parauchenipterus galeatus* (Linnaeus, 1766) (Siluriformes: Auchenipteridae) in Brazil. Biol. J. Linn. Soc. 99:648–656.

Lui R.L., Blanco D.R., Martinez J. de F., Margarido V.P., Venere P.C., Moreira Filho O. 2013. The role of chromosomal fusion in the karyotypic evolution of the genus *Ageneiosus* (Siluriformes: Auchenipteridae). Neotrop. Ichthyol. 11:327–334.

Lujan N.K., Armbruster J.W. 2011. The Guiana Shield. In: Albert J.S., Reis R.E., editors. Historical Biogeography of Neotropical Freshwater Fishes. University of California Press. p. 211–224.

Mariguela T.C., Roxo F.F., Foresti F., Oliveira C. 2016. Phylogeny and biogeography of Triportheidae (Teleostei: Characiformes) based on molecular data. Mol. Phylogenet. Evol. 96:130–139.

Marques D.F., Santos F.A. dos, Silva S.S. da, Sampaio I., Rodrigues L.R.R. 2013. Cytogenetic and DNA barcoding reveals high divergence within the trahira, *Hoplias malabaricus* (Characiformes: Erythrinidae) from the lower Amazon River. Neotrop. Ichthyol. 11:459–466.

Marrero C., Machado-allison A., González V., Velázquez J., Rodríguez-Olarte D. 1997. Los Morichales del Oriente de Venezuela: su importancia en la distribución y

ecología de los componentes de la Ictiofauna dulceacuícola regional. Acta Biol. Venez. 17:65–79.

Martinez J.D.F., Lui R.L., Traldi J.B., Blanco D.R., Moreira-Filho O. 2015. Occurrence of natural hybrids among sympatric karyomorphs in *Hoplerythrinus unitaeniatus* (Characiformes, Erythrinidae). Zebrafish. 12:281–287.

Martinez J.F., Lui R.L., Traldi J.B., Blanco D.R., Moreira-Filho O. 2016. Comparative Cytogenetics of *Hoplerythrinus unitaeniatus* (Agassiz, 1829) (Characiformes, Erythrinidae) Species Complex from Different Brazilian Hydrographic Basins. Cytogenet. Genome Res. 149:191–200.

Martins-Santos I.C., Julio H.F., Burin I. 1996. Karyotypic studies of four species of the Sorubiminae subfamily (Pisces, Siluriformes). Caryologia. 49:73–80.

Mastrantonio V., Porretta D., Urbanelli S., Crasta G., Nascetti G. 2016. Dynamics of mtDNA introgression during species range expansion: Insights from an experimental longitudinal study. Sci. Rep. 6:1–8.

Mateussi N.T.B., Melo B.F., Ota R.P., Roxo F.F., Ochoa L.E., Foresti F., Oliveira C. 2020. Phylogenomics of the Neotropical fish family Serrasalmidae with a novel intrafamilial classification (Teleostei: Characiformes). Mol. Phylogenet. Evol. 153:106945.

Mattox G.M.T., Bifi A.G., Oyakawa O.T. 2014a. Taxonomic study of *Hoplias microlepis* (Günther, 1864), a trans-Andean species of trahiras (Ostariophysi: Characiformes: Erythrinidae). Neotrop. Ichthyol. 12:343–352.

Mattox G.M.T., Britz R., Toledo-Piza M. 2014b. Skeletal development and ossification sequence of the characiform *Salminus brasiliensis* (Ostariophysi: Characidae). Ichthyol. Explor. Freshwaters. 25:103–158.

Mattox G.M.T., Toledo-Piza M., Oyakawa O.T. 2006. Taxonomic Study of *Hoplias Aimara* (Valenciennes, 1846) and *Hoplias macrophthalmus* (Pellegrin, 1907) (Ostariophysi, Characiformes, Erythrinidae). Copeia. 2006:516–528.

McGee M.D., Borstein S.R., Meier J.I., Marques D.A., Mwaiko S., Taabu A., Kishe M.A., O'Meara B., Bruggmann R., Excoffier L., Seehausen O. 2020. The ecological and genomic basis of explosive adaptive radiation. Nature. 586:75–79.

Mclean B.S., Bell K.C., Allen J.M., Helgen K.M., Cook J.A. 2019. Impacts of Inference Method and Data set Filtering on Phylogenomic Resolution in a Rapid Radiation of Ground Squirrels (Xerinae: Marmotini). Syst. Biol. 68:298–316.

Melo B.F., Albert J.S., Dagosta F.C.P., Tagliacollo V.A. 2021. Biogeography of curimatid fishes reveals multiple lowland-upland river transitions and differential diversification in the Neotropics (Teleostei, Curimatidae). Ecol. Evol.:1–18.

Melo B.F., Benine R.C., Mariguela T.C., Oliveira C. 2011. A new species of *Tetragonopterus* cuvier, 1816 (Characiformes: Characidae: Tetragonopterinae) from the rio Jari, Amapá, northern Brazil. Neotrop. Ichthyol. 9:49–56.

Melo B.F., Benine R.C., Silva G.S.C., Avelino G.S., Oliveira C. 2016a. Molecular phylogeny of the Neotropical fish genus *Tetragonopterus* (Teleostei: Characiformes: Characidae). Mol. Phylogenet. Evol. 94:709–717.

Melo B.F., Ochoa L.E., Vari R.P., Oliveira C. 2016b. Cryptic species in the Neotropical fish genus *Curimatopsis* (Teleostei, Characiformes). Zool. Scr. 45:650–658.

Milhomem S.S.R., Pieczarka J.C., Crampton W.G.R., Silva D.S., De Souza A.C.P., Carvalho J.R., Nagamachi C.Y. 2008. Chromosomal evidence for a putative cryptic species in the *Gymnotus carapo* species-complex (Gymnotiformes, Gymnotidae). BMC Genet. 9:1–10.

Mora A., Baby P., Roddaz M., Parra M., Brusset S., Hermoza W., Espurt N. 2010. Tectonic History of the Andes and Sub-Andean Zones: Implications for the Development of the Amazon Drainage Basin. In: Hoorn C., Wesselingh F.P., editors. Amazonia, Landscape and Species Evolution: A Look into the Past. Blackwell Publishing. p. 38–60.

Moraes G., Polez V.L., Iwama G.K. 2004. Biochemical responses of two erythrinidae fish to environmental ammonia. Braz. J. Biol. 64:95–102.

Moron S.E., de Andrade C.A., Fernandes M.N. 2009. Response of mucous cells of the gills of traíra (*Hoplias malabaricus*) and jeju (*Hoplerythrinus unitaeniatus*) (Teleostei: Erythrinidae) to hypo- and hyper-osmotic ion stress. Neotrop. Ichthyol. 7:491–498.

Nagamachi C.Y., Pieczarka J.C., Milhomem S.S.R., O'Brien P.C.M., de Souza A.C.P.,

Ferguson-Smith M.A. 2010. Multiple rearrangements in cryptic species of electric knifefish, *Gymnotus carapo* (Gymnotidae, Gymnotiformes) revealed by chromosome painting. BMC Genet. 11.

Neto A.M., da Silva M., Matoso D.A., Vicari M.R., de Almeida M.C., Collares-Pereira M.J., Artoni R.F. 2011. Karyotype variability in neotropical catfishes of the family Pimelodidae (teleostei: Siluriformes). Neotrop. Ichthyol. 9:97–105.

Neto A.O., Franceschini L., de Oliveira Manoel L., Veríssimo-Silveira R., Delariva R.L., Ramos I.P. 2019. Biology of non-native species (*Rhaphiodon vulpinus* Agassiz, 1829) (Characiformes, Cynodontidae) in a cage fish farm area, Upper Paraná River Basin, Brazil. Acta Limnol. Bras. 31.

Netto-Ferreira A.L. 2012. Three new species of *Lebiasina* (Characiformes: Lebiasinidae) from the Brazilian shield border at Serra do Cachimbo, Pará, Brazil. Neotrop. Ichthyol. 10:487–498.

Norris R.D., Hull P.M. 2012. The temporal dimension of marine speciation. Evol. Ecol. 26:393–415.

Ochoa L.E., Melo B.F., García-Melo J.E., Maldonado-Ocampo J.A., Souza C.S., Albornoz-Garzón J.G., Conde-Saldaña C.C., Villa-Navarro F., Ortega-Lara A., Oliveira C. 2020. Species delimitation reveals an underestimated diversity of Andean catfishes of the family Astroblepidae (Teleostei: Siluriformes). Neotrop. Ichthyol. 18:1–19.

Ochoa L.E., Roxo F.F., DoNascimiento C., Sabaj M.H., Datovo A., Alfaro M., Oliveira C. 2017. Multilocus analysis of the catfish family Trichomycteridae (Teleostei: Ostariophysi: Siluriformes) supporting a monophyletic Trichomycterinae. Mol. Phylogenet. Evol. 115:71–81.

Oliveira A.K. de, Garavello J.C. 2003. Fish assemblage composition in a tributary of the Mogi Guaçu river basin, southeastern Brazil. Iheringia. Série Zool. 93:127–138.

Oliveira C., Toledo L.F.A., Foresti F., Toledo S.A. 1988. Supernumerary chromosomes, Robertsonian rearrangement and multiple NORs in *Corydoras aeneus* (Pisces, Siluriformes, Callichthyidae). Caryologia. 41:227–236.

Ou M., Zhao J., Luo Q., Hong X., Zhu X., Liu H., Chen K. 2018. Characteristics of

hybrids derived from *Channa argus* ♀ × *Channa maculata* ♂. Aquaculture. 492:349–356.

Oyakawa O.T. 2003. Family Erythrinidae. In: Reis R.E., Kullander S.O., Ferraris C.J., editors. Check list of the freshwater fishes of South and Central America. Porto Alegre, Brazil: Edipucrs. p. 238–240.

Oyakawa O.T., Mattox G.M.T. 2018. Family Erythrinidae - Wolf-fishes and Yarrows. In: van der Sleen P., Albert J.S., editors. Field Guide to the Fishes of the Amazon, Orinoco, and Guianas. Princeton University Press. p. 156–158.

Oyakawa O.T., Toledo-Piza M., Mattox G.M.T. 2013. Erythrinidae. In: Queiroz L.J., Torrente-Vilara G., Ohara W.N., Silva-Pires T.H., Zuanon J., Doria C.R.C., editors. Peixes do rio Madeira, volume 2. São Paulo, Brazil: Dialeto. p. 351.

Padial J.M., Miralles A., De la Riva I., Vences M. 2010. The integrative future of taxonomy Review. :1–14.

Parada A., Hanson J., D'Elía G. 2021. Ultraconserved Elements Improve the Resolution of Difficult Nodes within the Rapid Radiation of Neotropical Sigmodontine Rodents (Cricetidae: Sigmodontinae). Syst. Biol. 0:1–11.

Pattengale N.D., Alipour M., Bininda-Emonds O.R.P., Moret B.M.E., Stamatakis A. 2010. How Many Bootstrap Replicates Are Necessary? J. Comput. Biol. 17:337–354.

Pelster B. 2021. Using the swimbladder as a respiratory organ and/or a buoyancy structure—Benefits and consequences. J. Exp. Zool. Part A Ecol. Integr. Physiol.:1–12.

Pelster B., Wood C.M., Jung E., Val A.L. 2018. Air-breathing behavior, oxygen concentrations, and ROS defense in the swimbladders of two erythrinid fish, the facultative air-breathing jeju, and the non-air-breathing traira during normoxia, hypoxia and hyperoxia. J. Comp. Physiol. B Biochem. Syst. Environ. Physiol. 188:437–449.

Pereira L., Hanner R., Foresti F., Oliveira C. 2013a. Can DNA barcoding accurately discriminate megadiverse Neotropical freshwater fish fauna? BMC Genet. 14:1–14.

Pereira T.L., Santos U., Schaefer C.E., Souza G.O., Paiva S.R., Malabarba L.R., Schmidt E.E., Dergam J.A. 2013b. Dispersal and vicariance of *Hoplias malabaricus* (Bloch, 1794) (Teleostei, Erythrinidae) populations of the Brazilian continental margin. J. Biogeogr. 40:905–914.

Persaud D.I., Ramnarine I.W., Agard J.B.R. 2006. Trade-off between digestion and respiration in two air-breathing callichthyid catfishes *Holposternum littorale* (Hancock) and *Corydoras aeneus* (Gill). Environ. Biol. Fishes. 76:159–165.

de Pinna M., Zuanon J., Rapp Py-Daniel L., Petry P. 2017. A new family of neotropical freshwater fishes from deep fossorial amazonian habitat, with a reappraisal of morphological characiform phylogeny (Teleostei: Ostariophysi). Zool. J. Linn. Soc. XX:1–13.

Pons J., Barraclough T.G., Gomez-Zurita J., Cardoso A., Duran D.P., Hazell S., Kamoun S., Sumlin W.D., Vogler A.P. 2006. Sequence-based species delimitation for the DNA taxonomy of undescribed insects. Syst. Biol. 55:595–609.

Pugedo M.L., de Andrade Neto F.R., Pessali T.C., Birindelli J.L.O., Carvalho D.C. 2016. Integrative taxonomy supports new candidate fish species in a poorly studied neotropical region: the Jequitinhonha River Basin. Genetica. 144:341–349.

Puillandre N., Lambert A., Brouillet S., Achaz G. 2012. ABGD, Automatic Barcode Gap Discovery for primary species delimitation. Mol. Ecol. 21:1864–1877.

De Queiroz K. 2005. A Unified Concept of Species and Its Consequences for the Future of Taxonomy. Ecology. 56.

De Queiroz K. 2007. Species concepts and species delimitation. Syst Biol. 56:879–886.

de Queiroz L.J., Cardoso Y., Jacot-des-Combes C., Bahechar I.A., Lucena C.A., Rapp Py-Daniel L., Sarmento Soares L.M., Nylinder S., Oliveira C., Parente T.E., Torrente-Vilara G., Covain R., Buckup P., Montoya-Burgos J.I. 2020. Evolutionary units delimitation and continental multilocus phylogeny of the hyperdiverse catfish genus *Hypostomus*. Mol. Phylogenet. Evol. 145:106711.

de Queiroz L.J., Meyer X., Cardoso Y.P., Bahechar I.A., Covain R., Parente T.E., Torrente-Vilara G., Buckup P.A., Montoya-Burgos J.I. 2021. Western Amazon was a center of Neotropical fish dispersal, as evidenced by the continental-wide

time-stratified biogeographic analysis of the hyper-diverse *Hypostomus* catfish. bioRxiv.:2021.06.03.446980.

Rambaut A., Suchard M.A., Xie D., Drummond A.J. 2014. Tracer v1.6. Available from http://beast.bio.ed.ac.uk/Tracer. .

Ramirez J.L., Santos C.A., Machado C.B., Oliveira A.K., Garavello J.C., Britski H.A., Galetti P.M. 2020. Molecular phylogeny and species delimitation of the genus *Schizodon* (Characiformes, Anostomidae). Mol. Phylogenet. Evol. 153:106959.

Rincon-Sandoval M., Betancur-R R., Maldonado-Ocampo J.A. 2019. Comparative phylogeography of trans-Andean freshwater fishes based on genome-wide nuclear and mitochondrial markers. Mol. Ecol. 28:1096–1115.

Rolland J., Salamin N. 2016. Niche width impacts vertebrate diversification. Glob. Ecol. Biogeogr. 25:1252–1263.

da Rosa R., Rubert M., Martins-Santos I.C., Giuliano-Caetano L. 2012. Evolutionary trends in *Hoplerythrinus unitaeniatus* (Agassiz 1829) (Characiformes, Erythrinidae). Rev. Fish Biol. Fish. 22:467–475.

Rossini B.C., Oliveira C.A.M., Gonçalves De Melo F.A., De Araú Jo Bertaco V., Díaz De Astarloa J.M., Rosso J.J., Foresti F., Oliveira C. 2016. Highlighting *Astyanax* species diversity through DNA barcoding. PLoS One. 11:1–20.

Rosso J.J., González-Castro M., Bogan S., Cardoso Y.P., Mabragaña E., Delpiani M., Díaz J. de A. 2018. Integrative taxonomy reveals a new species of *Hoplias malabaricus* species complex (Teleostei: Erythrinidae). Ichthyol. Explor. Freshwaters.:1–18.

Roux C., Fraïsse C., Romiguier J., Anciaux Y., Galtier N., Bierne N. 2016. Shedding Light on the Grey Zone of Speciation along a Continuum of Genomic Divergence. PLoS Biol. 14:1–22.

RStudio-Team. 2020. RStudio: Integrated Development for R. .

Sabaj M.H. 2020. Codes for natural history collections in ichthyology and herpetology. Copeia. 108:593–669.

Sánchez-Duarte P., Lasso C.A., González-Cañon G., Nieto-Torres S. 2011.

Hoplerythrinus unitaeniatus (Characiformes, Erythrinidae). Capitulo 7. In: Lasso C.A., Agudelo E., Jiménez-Segura L.F., Ramírez-Gil H., Morales-Betancourt M., Ajiaco-Martínez R.E., de Paula-Gutiérrez F., Usma J.S., Muñoz Torres S.E., Sanabria-Ochoa A.I., editors. I. Catálogo de los Recursos Pesqueros Continentales de Colombia. Serie Editorial Recursos Hidrobiológicos y Pesqueros Continentales de Colombia. Bogotá, Colombia: Instituto de Investigación de los Recursos Biológicos Alexander von Humboldt (IAvH). p. 291–293.

Dos Santos D.P., Felicetti D., Baumgärtner L., Margarido V.P., Blanco D.R., Moreira-Filho O., Lui R.L. 2021. Contributions to the taxonomy of *Trachelyopterus* (Siluriformes): Comparative cytogenetic analysis in three species of Auchenipteridae. Neotrop. Ichthyol. 19:1–12.

Santos R.P., Melo B.F., Yazbeck G.M., Oliveira R.S., Hilário H.O., Prosdocimi F., Carvalho D.C. 2021. Diversification of *Prochilodus* in the eastern Brazilian Shield: Evidence from complete mitochondrial genomes (Teleostei, Prochilodontidae). J. Zool. Syst. Evol. Res. 59:1053–1063.

Sassi F. de M.C., Perez M.F., Oliveira V.C.S., Deon G.A., de Souza F.H.S., Ferreira P.H.N., de Oliveira E.A., Hatanaka T., Liehr T., Bertollo L.A.C., Cioffi M. de B. 2021. High genetic diversity despite conserved karyotype organization in the giant trahiras from genus *Hoplias* (Characiformes, Erythrinidae). Genes (Basel). 12:1–13.

Schlick-Steiner B.C., Steiner F.M., Seifert B., Stauffer C., Christian E., Crozier R.H. 2010. Integrative taxonomy: A multisource approach to exploring biodiversity. Annu. Rev. Entomol. 55:421–438.

Seehausen O., Wagner C.E. 2014. Speciation in freshwater fishes. Annu. Rev. Ecol. Evol. Syst. 45:621–651.

Shi C.M., Yang Z. 2018. Coalescent-Based Analyses of Genomic Sequence Data Provide a Robust Resolution of Phylogenetic Relationships among Major Groups of Gibbons. Mol. Biol. Evol. 35:159–179.

Silva D. dos S., Milhomem S.S.R., de Souza A.C.P., Pieczarka J.C., Nagamachi C.Y. 2008. A conserved karyotype of Sternopygus macrurus (Sternopygidae, Gymnotiformes) in the Amazon region: Differences from other hydrographic

basins suggest cryptic speciation. Micron. 39:1251–1254.

van der Sleen P., Albert J.S. 2018. Field Guide to the Fishes of the Amazon, Orinoco & Guianas. Princeton University Press.

Sobel J.M., Chen G.F., Watt L.R., Schemske D.W. 2010. The biology of speciation. Evolution (N. Y). 64:295–315.

Spix J.B., Agassiz F.C. 1829. Selecta Genera et Species Piscium Brasiliensium. .

Stamatakis A. 2014. RAxML version 8: A tool for phylogenetic analysis and post-analysis of large phylogenies. Bioinformatics. 30:1312–1313.

Stokes M.F., Goldberg S.L., Perron J.T. 2018. Ongoing River Capture in the Amazon. Geophys. Res. Lett. 45:5545–5552.

Struck T.H., Cerca J. 2019. Cryptic Species and Their Evolutionary Significance. eLS.:1–9.

Struck T.H., Feder J.L., Bendiksby M., Birkeland S., Cerca J., Gusarov V.I., Kistenich S., Larsson K.H., Liow L.H., Nowak M.D., Stedje B., Bachmann L., Dimitrov D. 2018. Finding Evolutionary Processes Hidden in Cryptic Species. Trends Ecol. Evol. 33:153–163.

Swarça A.C., Fenocchio A.S., Dias A.L. 2007. An update cytogenetic review for species of the families Pseudopimelodidae, Pimelodidae and Heptapteridae (Pisces, Siluriformes). Suggestion of a cytotaxonomical classification. Caryologia. 60:338–348.

Swarça A.C., Sanchez S., Dias A.L., Fenocchio A.S. 2013. Cytogenetics of the Porthole Shovelnose Catfish, *Hemisorubim platyrhynchos* (Valenciennes, 1840) (Siluriformes, Pimelodidae), a widespread species in South American rivers. Comp. Cytogenet. 7:1–8.

Tagliacollo V.A., Lanfear R. 2018. Estimating improved partitioning schemes for ultraconserved elements. Mol. Biol. Evol. 35:1798–1811.

Tagliacollo V.A., Roxo F.F., Duke-Sylvester S.M., Oliveira C., Albert J.S. 2015. Biogeographical signature of river capture events in Amazonian lowlands. J. Biogeogr. 42:2349–2362.

Tamura K., Nei M. 1993. Estimation of the number of nucleotide substitutions in the control region of mitochondrial DNA in humans and chimpanzees. Mol. Biol. Evol. 10:512–526.

Taphorn D.C. 2003. Manual de identificación de los peces Characiformes de la cuencaa del Río Apure en Venezuela. Guanare: Universidad Nacional Experimental De los Llanos Occidentales UNELLEZ.

Taylor W., Van Dyke G. 1985. Revised procedures for staining and clearing small fishes and other vertebrates for bone and cartilage study. Cybium. 9:107–119.

Toledo-Piza M. 2000. The Neotropical Fish Subfamily Cynodontinae (Teleostei: Ostariophysi: Characiformes): A Phylogenetic Study and a Revision of *Cynodon* and *Rhaphiodon*. Am. Museum Nat. Hist.:1–88.

Torres R.A., Roper J.J., Foresti F., Oliveira C. 2005. Surprising genomic diversity in the Neotropical fish *Synbranchus marmoratus* (Teleostei: Synbranchidae): how many species? Neotrop. Ichthyol. 3:277–284.

Usso M.C., Santos A.R. Dos, Gouveia J.G., Frantine-Silva W., Araya-Jaime C., Oliveira M.L.M. De, Foresti F., Giuliano-Caetano L., Dias A.L. 2019. Genetic and chromosomal differentiation of *Rhamdia quelen* (Siluriformes, Heptapteridae) revealed by repetitive molecular markers and DNA barcoding. Zebrafish. 16:87–97.

Vrba E.S. 1987. Ecology in relation to speciation rates: some case histories of Miocene-Recent mammal clades. Evol. Ecol. 1:283–300.

Ward R.D., Zemlak T.S., Innes B.H., Last P.R., Hebert P.D.N. 2005. DNA barcoding Australia's fish species. Philos. Trans. R. Soc. Lond. B. Biol. Sci. 360:1847–1857.

Wendt E.W., Silva P.C., Malabarba L.R., Carvalho T.P. 2019. Phylogenetic relationships and historical biogeography of *Oligosarcus* (Teleostei: Characidae): Examining riverine landscape evolution in southeastern South America. Mol. Phylogenet. Evol. 140:106604.

Willis S.C. 2017. One species or four? Yes!…and, no. Or, arbitrary assignment of lineages to species obscures the diversification processes of Neotropical fishes. PLoS One. 12:1–26.

Wood C.M., Pelster B., Giacomin M., Sadauskas-Henrique H., Almeida-Val V.M.F., Val A.L. 2016. The transition from water-breathing to air-breathing is associated with a shift in ion uptake from gills to gut: a study of two closely related erythrinid teleosts, *Hoplerythrinus unitaeniatus* and *Hoplias malabaricus*. J. Comp. Physiol. B Biochem. Syst. Environ. Physiol. 186:431–445.

Xia X. 2018. DAMBE7: New and improved tools for data analysis in molecular biology and evolution. Mol. Biol. Evol. 35:1550–1552.

Zerbino D.R., Birney E. 2008. Velvet: Algorithms for de novo short read assembly using de Bruijn graphs. Genome Res. 18:821–829.

Zhang C., Rabiee M., Sayyari E., Mirarab S. 2018. ASTRAL-III: Polynomial time species tree reconstruction from partially resolved gene trees. BMC Bioinformatics. 19.

Zhang J., Kapli P., Pavlidis P., Stamatakis A. 2013. A general species delimitation method with applications to phylogenetic placements. Bioinformatics. 29:2869–2876.

Supplementary material

Table S1. Material analyzed in genetic approach, including catalog number, voucher code, locality, and geographic origin giving River basin, city/state, and country.

Taxon	Catalog number	Voucher code	Locality	River basin	City, State	Country	COI	UCEs
Hoplerythrinus unitaeniatus	ANSP T2197	T2197	Two Puddle Creek	Rupununi	Takutu	Guiana	X	
Hoplerythrinus unitaeniatus	ANSP 182932	ANSP182932	Cano Shirui	Amazonas	Iquitos/Loreto	Peru	X	
Hoplerythrinus unitaeniatus	ANSP 195271	ANSP19527	Tributario Rio Xingu	Xingu/Amazonas	Senador José Porfírio/Pará	Brazil	X	
Hoplerythrinus unitaeniatus	ANSP179643	ANSP179643	Two Puddle Creek	Rupununi	Yapukarri	Guiana	X	
Hoplerythrinus unitaeniatus	CZUT-IC 11490	CZUTICT866	Cañada Guafila	Ariporo/Orinoco	Hato Corozal/Casanare	Colombia	X	X
Hoplerythrinus unitaeniatus	CZUT-IC 12996	CZUTICT867	Cañada NN	Ariporo/Orinoco	Hato Corozal/Casanare	Colombia	X	
Hoplerythrinus unitaeniatus	CZUT-IC 12996	CZUTICT869	Cañada NN	Ariporo/Orinoco	Hato Corozal/Casanare	Colombia	X	
Hoplerythrinus unitaeniatus	CZUT-IC 12996	CZUTICT868	Cañada NN	Ariporo/Orinoco	Hato Corozal/Casanare	Colombia	X	
Hoplerythrinus unitaeniatus	CZUT-IC 13027	CZUTICT990	Caño Cusiaba	Cusiana/Orinoco	Maní/Casanare	Colombia	X	X
Hoplerythrinus unitaeniatus	IAvH-P-19171	BI1	Morichal caño NN	Bita, Orinoco	Puerto Carreño/Vichada	Colombia	X	
Hoplerythrinus unitaeniatus	IAvH-P-19206	Pmet7	Bocas del caño Parurito	Meta/Orinoco	La Primavera/Vichada	Colombia	X	
Hoplerythrinus unitaeniatus	IAvH-P-19884	FA051	Jaguey Mararay	Manacacias/Orinoco	Mararay, Meta	Colombia	X	
Hoplerythrinus unitaeniatus	IAvH-P-20191	FA110	Morichal NN	Manacacias/Orinoco	San Martín/Meta	Colombia	X	
Hoplerythrinus unitaeniatus	INPA 40633	INPA40633	Rio Xingu	Xingu/Amazonas	Porto de Moz/Pará	Brazil	X	
Hoplerythrinus unitaeniatus	LBP 12740	LBP41211	Rio Araguaia	Tocantins/Amazonas	Cocalinho/MT	Brazil	X	
Hoplerythrinus unitaeniatus	LBP 12740	LBP41219	Rio Araguaia	Tocantins/Amazonas	Cocalinho/MT	Brazil	X	
Hoplerythrinus unitaeniatus	LBP 14945	LBP61501	Afluente Rio Takutu	Amazonas	Normandia/RR	Brazil	X	
Hoplerythrinus unitaeniatus	LBP 14945	LBP61502	Afluente Rio Takutu	Amazonas	Normandia/RR	Brazil	X	
Hoplerythrinus unitaeniatus	LBP 15042	LBP61689	Brejo a beira da BR 230	Tapajós/Amazonas	Itaituba/PA	Brazil	X	
Hoplerythrinus unitaeniatus	LBP 15723	LBP64605	Tributário rio Suiá-Missu	Xingu/Amazonas	Ribeirão Cascalheira/MT	Brazil	X	
Hoplerythrinus unitaeniatus	LBP 15875	LBP64190	Tributário rio Coluene	Xingu/Amazonas	Canarana/MT	Brazil	X	
Hoplerythrinus unitaeniatus	LBP 15875	LBP64189	Tributário rio Coluene	Xingu/Amazonas	Canarana/MT	Brazil	X	X
Hoplerythrinus unitaeniatus	LBP 16143	LBP66873	Igarapé Nambuaí	Tapajós/Amazonas	Itaituba/PA	Brazil	X	X
Hoplerythrinus unitaeniatus	LBP 17450	LBP69028	Amaila River	Potaro/Essequibo	Potaro-Siparuni	Guiana	X	X
Hoplerythrinus unitaeniatus	LBP 17450	LBPV 69027	Amaila River	Potaro/Essequibo	Potaro-Siparuni	Guiana		X

Taxon	Catalog number	Voucher code	Locality	River basin	City, State	Country	COI	UCEs
Hoplerythrinus unitaeniatus	LBP 19217	LBP77660	Ribeirão Brejão	Tocantins/Amazonas	Mateiros/TO	Brazil	X	
Hoplerythrinus unitaeniatus	LBP 19217	LBP77662	Ribeirão Brejão	Tocantins/Amazonas	Mateiros/TO	Brazil	X	
Hoplerythrinus unitaeniatus	LBP 19217	LBP77663	Ribeirão Brejão	Tocantins/Amazonas	Mateiros/TO	Brazil	X	X
Hoplerythrinus unitaeniatus	LBP 19234	LBP77725	Ribeirão sem nome	Tocantins/Amazonas	Mateiros/TO	Brazil	X	
Hoplerythrinus unitaeniatus	LBP 19252	LBP77777	Ribeirão sem nome	Tocantins/Amazonas	Mateiros/TO	Brazil	X	
Hoplerythrinus unitaeniatus	LBP 20253	LBP79722	Rio Apiacás	Tapajós/Amazonas	Alta Floresta/MT	Brazil	X	
Hoplerythrinus unitaeniatus	LBP 20882	LBP81518	Afluente rio Lagoa Rosa	Arinos/Tapajós/Amazonas	Diamantino/MT	Brazil	X	
Hoplerythrinus unitaeniatus	LBP 20882	LBP81517	Afluente rio Lagoa Rosa	Arinos/Tapajós/Amazonas	Diamantino/MT	Brazil	X	
Hoplerythrinus unitaeniatus	LBP 20882	LBP81519	Afluente rio Lagoa Rosa	Arinos/Tapajós/Amazonas	Diamantino/MT	Brazil	X	X
Hoplerythrinus unitaeniatus	LBP 2212	LBP15618	Laguna de Castilleros	Orinoco	Caicara del Orinoco /Bolivar	Venezuela	X	
Hoplerythrinus unitaeniatus	LBP 22310	LBP86422	Rio Solimões	Amazonas	Tabatinga/AM	Brazil	X	
Hoplerythrinus unitaeniatus	LBP 22310	LBP86421	Rio Solimões	Amazonas	Tabatinga/AM	Brazil	X	
Hoplerythrinus unitaeniatus	LBP 22310	LBP86423	Rio Solimões	Amazonas	Tabatinga/AM	Brazil	X	
Hoplerythrinus unitaeniatus	LBP 22310	LBP86420	Rio Solimões	Amazonas	Tabatinga/AM	Brazil	X	
Hoplerythrinus unitaeniatus	LBP 2298	LBP15829	Lagoa marginal do rio Orinoco	Orinoco	Caicara del Orinoco /Bolivar	Venezuela	X	X
Hoplerythrinus unitaeniatus	LBP 23527	LBP92225	Lagoa Avispa	Ucayali/Amazonas	Requena/Loreto	Peru	X	X
Hoplerythrinus unitaeniatus	LBP 23527	LBP92222	Lagoa Avispa	Ucayali/Amazonas	Requena/Loreto	Peru	X	
Hoplerythrinus unitaeniatus	LBP 23527	LBP92223	Lagoa Avispa	Ucayali/Amazonas	Requena/Loreto	Peru	X	
Hoplerythrinus unitaeniatus	LBP 23527	LBP92226	Lagoa Avispa	Ucayali/Amazonas	Requena/Loreto	Peru	X	
Hoplerythrinus unitaeniatus	LBP 23527	LBP92224	Lagoa Avispa	Ucayali/Amazonas	Requena/Loreto	Peru	X	
Hoplerythrinus unitaeniatus	LBP 23560	LBP92311	Igarapé Tarumã-Mirim	Negro/Amazonas	Manaus/AM	Brazil	X	X
Hoplerythrinus unitaeniatus	LBP 2379	LBP16065	Lagoa Feia	Rio Paraíba do Sul/Leste	Campos dos Goytacazes/RJ	Brazil	X	
Hoplerythrinus unitaeniatus	LBP 24733	LBP89246	Entrada de Igarapé	Teles Pires/Amazonas	Jacareacanga/PA	Brazil	X	
Hoplerythrinus unitaeniatus	LBP 24858	LBP93142	Ribeirão Taxidermista	Teles Pires/Amazonas	Alta Floresta/MT	Brazil	X	
Hoplerythrinus unitaeniatus	LBP 24858	LBP93143	Ribeirão Taxidermista	Teles Pires/Amazonas	Alta Floresta/MT	Brazil	X	
Hoplerythrinus unitaeniatus	LBP 24858	LBP93144	Ribeirão Taxidermista	Teles Pires/Amazonas	Alta Floresta/MT	Brazil	X	
Hoplerythrinus unitaeniatus	LBP 25107	LBP93437	Riacho afluente do rio Curuá	Xingu/Amazonas	Altamira/PA	Brazil	X	
Hoplerythrinus unitaeniatus	LBP 25107	LBP93436	Riacho afluente do rio Curuá	Xingu/Amazonas	Altamira/PA	Brazil	X	
Hoplerythrinus unitaeniatus	LBP 25107	LBP93440	Riacho afluente do rio Curuá	Xingu/Amazonas	Altamira/PA	Brazil	X	
Hoplerythrinus unitaeniatus	LBP 25265	LBP94539	Afluente Rio Braço do Norte	Tapajós/Amazonas	Novo Progresso/PA	Brazil	X	

Taxon	Catalog number	Voucher code	Locality	River basin	City, State	Country	COI	UCEs
Hoplerythrinus unitaeniatus	LBP 25265	LBP94538	Afluente Rio Braço do Norte	Tapajós/Amazonas	Novo Progresso/PA	Brazil	X	
Hoplerythrinus unitaeniatus	LBP 25545	LBP91345	Riacho Pongal	Benevente	Anchieta/ES	Brazil	X	X
Hoplerythrinus unitaeniatus	LBP 2642	LBP17304	Rio Baia	Paraná	Porto Rico/PR	Brazil	X	
Hoplerythrinus unitaeniatus	LBP 28154	LBP96839	Rio Sapão	São Francisco	Formosa do Rio Preto/BA	Brazil	X	
Hoplerythrinus unitaeniatus	LBP 28154	LBP96838	Rio Sapão	São Francisco	Formosa do Rio Preto/BA	Brazil	X	
Hoplerythrinus unitaeniatus	LBP 28291	LBP96858	Lagoas rio da Prata	Paracatu/São Francisco	João Pinheiro/MG	Brazil	X	X
Hoplerythrinus unitaeniatus	LBP 28484	LBP100853	Ribeirao Santo Antonio	Arinos/Amazonas	Diamantino/MT	Brazil	X	
Hoplerythrinus unitaeniatus	LBP 28484	LBP100851	Ribeirao Santo Antonio	Arinos/Amazonas	Diamantino/MT	Brazil	X	
Hoplerythrinus unitaeniatus	LBP 2980	LBP19624	Lagoa da Égua	Araguaia/Amazonas	Cocalinho/MT	Brazil	X	X
Hoplerythrinus unitaeniatus	LBP 4002	LBP23061	Lago Morto	Araguaia/Amazonas	São Félix do Araguaia/MT	Brazil	X	
Hoplerythrinus unitaeniatus	LBP 4237	LBP22757	Rio Juruá	Amazonas	Cruzeiro do Sul/AC	Brazil	X	X
Hoplerythrinus unitaeniatus	LBP 4590	LBP24661	Rio do Peixe	Tietê/Paraná	Anhembi/SP	Brazil	X	
Hoplerythrinus unitaeniatus	LBP 4590	LBP24660	Rio do Peixe	Tietê/Paraná	Anhembi/SP	Brazil	X	
Hoplerythrinus unitaeniatus	LBP 4590	LBP24662	Rio do Peixe	Tietê/Paraná	Anhembi/SP	Brazil	X	
Hoplerythrinus unitaeniatus	LBP 493	LBP6174	Rio Capivara	Tietê/Paraná	Botucatu/SP	Brazil	X	
Hoplerythrinus unitaeniatus	LBP 493	LBP6172	Rio Capivara	Tietê/Paraná	Botucatu/SP	Brazil	X	
Hoplerythrinus unitaeniatus	LBP 5180	LBP26697	Rio Paraná	Paraná	Porto Rico/PR	Brazil	X	X
Hoplerythrinus unitaeniatus	LBP 5180	LBP26701	Rio Paraná	Paraná	Porto Rico/PR	Brazil	X	
Hoplerythrinus unitaeniatus	LBP 5180	LBP26699	Rio Paraná	Paraná	Porto Rico/PR	Brazil	X	
Hoplerythrinus unitaeniatus	LBP 5507	LBP26598	Rio Jari	Amazonas	Laranjal do Jari/AP	Brazil	X	
Hoplerythrinus unitaeniatus	LBP 5507	LBP26600	Rio Jari	Amazonas	Laranjal do Jari/AP	Brazil	X	X
Hoplerythrinus unitaeniatus	LBP 5507	LBP26599	Rio Jari	Amazonas	Laranjal do Jari/AP	Brazil	X	
Hoplerythrinus unitaeniatus	LBP 651	LBP8042	Afluente rio Pirai	Cuiabá/Paraguay	Poconé, MT	Brazil	X	X
Hoplerythrinus unitaeniatus	LBP 6614	LBP31940	Córrego das três lagoas	Paraná	Marilena/PR	Brazil	X	
Hoplerythrinus unitaeniatus	LBP 6639	LBP31984	Lagoa do João	Paraná	Marilena/PR	Brazil	X	
Hoplerythrinus unitaeniatus	LBP 7838	LBP36848	Lagoa da Boca Franca	Araguaia/Amazonas	Cocalinho/MT	Brazil	X	
Hoplerythrinus unitaeniatus	LBP 788	LBP7807	Afluente Rio do Peixe	Tietê/Paraná	Bofete/SP	Brazil	X	
Hoplerythrinus unitaeniatus	LBP 8025	LBP37724	Riacho sem nome	Arinos/Tapajós/Amazonas	Nova Mutum/MT	Brazil	X	X
Hoplerythrinus unitaeniatus	LBP 9152	LBP42525	Igarapé das Pedras	Guamá/Amazonas	Ourém/PA	Brazil	X	X
Hoplerythrinus unitaeniatus	LBP 9152	LBP43098	Igarapé das Pedras	Guamá/Amazonas	Ourém/PA	Brazil	X	

Taxon	Catalog number	Voucher code	Locality	River basin	City, State	Country	COI	UCEs
Hoplerythrinus unitaeniatus	LBP 9152	LBP43099	Igarapé das Pedras	Guamá/Amazonas	Ourém/PA	Brazil	X	
Hoplerythrinus unitaeniatus	LBP28484	LBP100866	Ribeirao Santo Antonio	Arinos/Amazonas	Diamantino/MT	Brazil	X	
Hoplerythrinus unitaeniatus	LBP28484	LBP100865	Ribeirao Santo Antonio	Arinos/Amazonas	Diamantino/MT	Brazil	X	
Hoplerythrinus unitaeniatus	MHNG 2.736.033	GFU12422	Cascade Moi Moi	Kabalebo/Corantijne	Kabalebo/Sipaliwini	Suriname	X	
Hoplerythrinus unitaeniatus	MHNG 2.755.083	GFSU141357	kaw River	Kaw	Cayenne	French Guiana	X	X
Hoplerythrinus unitaeniatus	MHNG GFU14-621	GFU14621	Saramacca River	Saramacca	Unknown	Suriname	X	
Hoplerythrinus unitaeniatus	MHNG HYD15-768	HYD15768	Kourou River	Kourou	Unknown	French Guiana	X	
Hoplerythrinus unitaeniatus	MZUSP 096825	MZUSP3392	Tributário do Rio Braço Norte	Tapajós/Amazonas	Novo Progresso/Pará	Brazil	X	X
Hoplerythrinus unitaeniatus	MZUSP 95898	MZUSP4007	Rio Teles Pires	Tapajós/Amazonas	Itauba/Mato Grosso	Brazil	X	
Hoplerythrinus unitaeniatus	ROM 083694	T06074	Kukui River	Mazaruni/Essequibo	Cuyuni-Mazaruni	Guiana	X	
Hoplerythrinus unitaeniatus	ROM 083743	T06105	Mazaruni River	Essequibo	Cuyuni-Mazaruni	Guiana	X	
Hoplerythrinus unitaeniatus	ROM 092359	T09425	Caño Tigre	Ventuari/Orinoco	Yacapan/Amazonas	Venezuela	X	X
Hoplerythrinus unitaeniatus	ROM 095911	T15949	Tarayara Creek	Amazonas	Dahdaad	Guiana	X	
Hoplerythrinus unitaeniatus	ROM 095911	T15948	Tarayara Creek	Amazonas	Dahdaad	Guiana	X	
Hoplerythrinus unitaeniatus	ROM 098770	T19475	Coesewijne River	Cosewijne	Tijgerkreek	Suriname	X	
Hoplerythrinus unitaeniatus	ROM 100856	T19814	Marowijne River	Marowijne	Sipaliwini	Suriname	X	
Hoplerythrinus unitaeniatus	ROM 87221	T08354	Akawini Creek	Pomeroon	Pomeroon-Supenaam	Guiana	X	
Hoplerythrinus unitaeniatus	ROM 87221	T08353	Akawini Creek	Pomeroon	Pomeroon-Supenaam	Guiana	X	
Hoplerythrinus unitaeniatus	ROM T12679	T12679	Amaila River	Essequibo	Potaro-Siparuni	Guiana	X	
Hoplerythrinus unitaeniatus	ROM T19970	T19970	Marowijne River	Marowijne	Tapanahoni/Sipaliwini	Suriname	X	
Hoplerythrinus unitaeniatus	STRI 2302	STRI2302	Rio Santa Lucia	Paraná	Unknown	Argentina	X	
Hoplerythrinus unitaeniatus	TIUFRN2909	TI2909	Riacho dos Porcos	Tocantins	São Félix do Tocantins/TO	Brazil		X
Erythrinus sp. 2	LBP 8518	LBPV 43203	Rio Sucuruina	Rio Tapajós/Amazonas	Diamantino/MT	Brazil		X
Erythrinus erythrinus	AUM 62923	AUFT 6520	Potaro River	Essequibo	Potaro/Siparuni	Guiana		X
Erythrinus erythrinus	AUM 62923	AUFT 6520	Potaro River	Essequibo	Potaro/Siparuni	Guiana		X
Hoplias misionera	LBP 6697	LBPV 32185	Lagoa Marginal	Paraná	Marilena/PR	Brazil		X
Hoplias misionera	LBP 6697	LBPV32186	Lagoa Marginal	Paraná	Marilena/PR	Brazil	X	
Hoplias microlepis	LBP 2763	LBPV 18503	Río Llano Sucio	Atlantic drainage	Santa Rita Arriba/Colón	Panamá		X
Hoplias malabaricus	LBP 21115	LBPV 82828	Igarapé do Quatorze	Oiapoque/Amazonas	Oiapoque/AP	Brazil		X
Hoplias sp.	CZUT-IC-TE 2817	CZUT-IC-TE 2817	Río Peralonso	Catatumbo/Maracaibo	El Zulia/Norte de Santander	Colombia		X

Taxon	Catalog number	Voucher code	Locality	River basin	City, State	Country	COI	UCEs
Hoplias lacerdae	LBP 28564	LBPV100386	Rio Ribeira de Iguape	Atlantic drainage	Registro/SP	Brazil		X
Hoplias aimara	LBP 20520	LBPV80648	Rio Jari	Amazonas	Laranjal do Jari/AP	Brazil		X
Tarumania walkerae	LBP 22727	86548	Rio Tarumã-Mirim	Rio Negro	Manaus/AM	Brazil		X
Pygocentrus piraya	LBP 11336	45523	Lagoa da Tiririca	São Francisco	Pirapora/MG	Brazil		X
Pristobrycon calmoni	LBP 2191	15554	Laguna de Castilleros	Orinoco	Caicara del Orinoco /Bolivar	Venezuela		X
Serrasalmus maculatus	LBP21610	61612	Brejo a beira da BR 230	Tapajós/Amazonas	Itaituba/PA	Brazil		X
Catoprion mento	LBP 7556	35626	Rio Cuiabá	Paraguay	Barão de Melgaço/MT	Brazil		X
Metynnis luna	LBP 18398	42589	Rio Guamá	Amazonas	Ourém/PA	Brazil		X
Mylossoma sp.	LBP 2190	15518	Laguna de Castilleros	Orinoco	Caicara del Orinoco /Bolivar	Venezuela		X
Mylossoma acanthogaster	LBP 24311	91508	Rio Sardinata	Catatumbo/Maracaibo	Tibu/Santander	Colombia		X
Colossoma macropomum	LBP 12838	54048	Rio Tapajos	Amazonas	Itaituba/PA	Brazil		X
Colossoma macropomum	LBP 12838	54052	Rio Tapajos	Amazonas	Itaituba/PA	Brazil		X
Abramites hypselonotus	ANSP 178126	1712	Rio Napo	Amazonas	Maynas/Loreto	Peru		X
Megaleporinus trifasciatus	OS 18311	PE10108	Nanay	Amazonas	Maynas/Loreto	Peru		X
Leporellus vittatus	ANSP 182609	P6322	Nanay	Amazonas	Maynas/Loreto	Peru		X
Leporinus striatus	LBP 3180	16871	Reservatório de Jurumirim	Paranapanema	Itatinga/SP	Brazil		X
Curimata mivartii	LBP 24318	91518	Río Nare	Middle Magdalena	Puerto Nare/Antioquia	Colombia		X
Curimatella alburna	LBP 5431	27171	Rio Jari	Amazonas	Almeirim/PA	Brazil		X
Cyphocharax spilurus	LBP 15139	62363	Rio Branco	Negro/Amazonas	Boa Vista/RR	Brazil		X
Alestes inferus	AMNH 242137	333238	Congo River	Congo	Bas Congo Province	Democratic Republic of Congo		X
Bryconaethiops microstoma	OS 19665	BLS14-013	Ogooeé river	Ogooeé	Doumé Village/Province del'Ogooué-Lolo	Gabon		X
Hepsetus cuvieri	AMNH 242489	353404	Lac Nkolentulu	Lac Nkolentulu	Mai Ndombe/Bandudu	Democratic Republic of Congo		X
Ctenolucius hujeta	LBP 6136	29524	Rio Santa Rosa	Maracaibo	Machiques de Perijá/Zulia	Venezuela		X

Table S2. Examined material under morphological approach, including catalog number, locality, and geographic origin giving River basin, city/state, country, Latitude (Lat), Longitud (Long), and altitude. The number of specimens examined from photographs, radiographs (X-ray), and cleared and stained (C&S) are indicated. Lin = Lineage assigned (W = Widespread, O = Orinoco, BS = upper Xingu-Tapajós-Araguaia), N = number of specimens in lots. MNHN-IC 0099 correspond to syntypes of *Erythrinus gronovii*, MNHN-IC 9758-9761 to syntypes of *Erythrinus vittatus*, USNM to holotype of *Erythrinus cinereus*, and ZMA.PISC 100.310 to holotype of *Pseuderythrinus rosapinnis*.

Lin.	Catalog number	N	SL range	Locality	Basin	City, State	Country	Photo	X-ray	C&S	Lat	Long	Altitude
W	ANSP 130580	1	87.4	Stream trib. of Rio Conejo	Aguarico-Napo	Santa Cecilia/Misiones	Ecuador		1		0.06277	-77.12641	358
W	ANSP 170274	1	104.8	Marsh by road 3.4 km towards Yabebyry from Santa Rita	Paraná	Misiones	Paraguay		1		-27.13824	-57.03246	76
W	ANSP 175534	1	129.3	Tributary of Burro Burro River	Siparuni River	Potaro-Siparuni	Guyana				4.29817	-58.97756	79
W	ANSP 175534	2	112.4–130.3	Trib. of Burro Burro River	Essequibo	Potaro-Siparuni	Guyana		2		4.29817	-58.97756	79
W	ANSP 178370	5	105.9–138.0	Rio Yanayacu	Amazonas	Loreto	Peru		5		-4.64833	-73.79000	89
W	FMNH 50088	5	110.0–139.3	Mayoro, Plaisance	Coastal drainage	Mayaro	Trinidad and Tobago		4		10.28333	-61.00000	12
W	FMNH 53689	1	153.2	Nickaparoo	Unknown	Unknown	Guyana		1		Unknown	Unknown	
W	FMNH 53690	1	105.40	Pacopoo Pan	Unknown	Unknown	Guyana		1		Unknown	Unknown	
W	FMNH 57596	2	77.0–91.1	Rio Sapão	Rio Preto-São Francisco	Prazeres/Bahia	Brasil		1		-10.78528	-46.08528	614
W	FMNH 76288	3	111.8–133.8	Urucum	Paraguay	Ladário/Mato Grosso	Brazil		3		-19.15000	-57.63333	139
W	LBP 11366	1	124.3	Corrego Goulart	Paraná	Birigui/SP	Brazil				-21.21694	-50.35282	377
W	LBP 14945	3	124.12–153.33	Afluente Rio Takutu	Amazonas	Normandia/RR	Brazil				3.54253	-59.91711	78
W	LBP 14946	2	112.40–126.2	Lagoa proxima rio Takatu	Amazonas	Bonfim/RR	Brazil				3.29017	-59.89667	84
W	LBP 15042	1	137.1	Brejo a beira da BR 230	Tapajós-Amazonas	Itaituba/PA	Brazil				-4.56886	-56.31372	61
W	LBP 16143	1	95.5	Igarapé Nambuaí	Tapajós-Amazonas	Itaituba/PA	Brazil				-4.62444	-56.38833	64
W	LBP 19217	4	44.5–105.6	Ribeirão Brejão	Tocantins-Amazonas	Mateiros/TO	Brazil				-10.57486	-46.48692	477
W	LBP 19234	1	75.8	Ribeirão sem nome	Tocantins-Amazonas	Mateiros/TO	Brazil				-10.44081	-46.45939	501
W	LBP 21209	1	100.48	Igarape Balneario Santa Bárbara	Ampá-Amazonas	Amapá/AP	Brazil				2.06189	-50.90419	19
W	LBP 22310	2	227.7–229.5	Rio Solimões	Amazonas	Tabatinga/AM	Brazil				-4.29244	-69.91542	62

Lin.	Catalog number	N	SL range	Locality	Basin	City, State	Country	Photo	X-ray	C&S	Lat	Long	Altitude
W	LBP 2379	1	218.8	Lagoa Feia	Rio Paraíba do Sul	Campos dos Goytacazes/RJ	Brazil				-22.00000	-41.33333	1
W	LBP 24733	1	128.4	Entrada de Igarapé	Teles Pires-Amazonas	Jacareacanga/PA	Brazil				-8.36553	-57.66515	108
W	LBP 25545	1	166.57	Riacho Pongal	Benevente	Anchieta/ES	Brazil				-20.77156	-40.73441	6
W	LBP 2642	1	114.6	Rio Baia	Paraná	Porto Rico/PR	Brazil				-22.71756	-53.29100	236
W	LBP 27089	1	81.6	Lagoa NN	Paraguai	Santo Antônio do Leverger/MT	Brazil				-16.45072	-55.32017	287
W	LBP 28154	2	78.6–105.8	Rio Sapão	São Francisco	Formosa do Rio Preto/BA	Brazil			1	-10.74558	-46.19600	614
W	LBP 28291	2	50.1–51.2	Lagoas rio da Prata	Paracatu-São Francisco	João Pinheiro/MG	Brazil				-17.54650	-46.45351	526
W	LBP 28430	1	212.7	Igarape sem nome	Baia de Marajó (confluencia Tocantins-Acará-Guamá)	Cachoeira do Arari/PA	Brazil				-0.96819	-48.85914	3
W	LBP 29146	1	111.08	Río Jacundá	Amazonas	Baião/PA	Brazil				-3.16853	-49.82332	33
W	LBP 29330	2	184.2–191.5	Lago Peauzinho	Purus, Amazonas	Beruri/AM	Brazil				-4.19153	-61.76886	10
W	LBP 4590	3	168.8–174.6	Rio do Peixe	Tietê-Paraná	Anhembi/SP	Brazil				-22.77497	-48.14542	452
W	LBP 493	3	92.0–124.7	Rio Capivara	Tietê-Paraná	Botucatu/SP	Brazil				-22.73333	-48.38333	507
W	LBP 5180	5	128.4–190.6	Rio Paraná	Paraná	Porto Rico/PR	Brazil				-22.79139	-53.34944	240
W	LBP 6614	1	66.86	Córrego das três lagoas	Paraná	Marilena/PR	Brazil				-22.63258	-53.05261	244
W	LBP 6639	2	94.4–103.2	Lagoa do João	Paraná	Marilena/PR	Brazil				-22.66256	-53.10472	236
W	LBP 788	1	167.42	Afluente Rio do Peixe	Tietê-Paraná	Bofete/SP	Brazil				Unknown	Unknown	
W	MNHN-IC 0099	3	103.4–116.9	Cayenne	Unknown	Cayenne	French Guiana	3			Unknown	Unknown	
W	MNHN-IC-A 9758	1	123.5	Rio de Janeiro	Unknown	Rio de Janeiro	Brazil	1			Unknown	Unknown	
W	MNHN-IC-A 9759	2	107.7–130.2	Rio de Janeiro	Unknown	Rio de Janeiro	Brazil	2			Unknown	Unknown	
W	MNHN-IC-A 9760	2	110.1–120.8	Cayenne	Unknown	Cayenne	French Guiana	2			Unknown	Unknown	
W	MNHN-IC-A 9761	1	254.8	Unknown	Unknown	Unknown	Suriname	1			Unknown	Unknown	
W	MUSM 21673	1	117.22	Río Los Amigos Aguajal Cicra	Madre de Dios	Madre de Dios	Peru				-12.55853	-70.12316	234
W	MUSM 30478	1	119.11	Río Tambopata	Madre de Dios	Tambotapa/MO	Peru				-12.61648	-69.19082	177
W	MUSM 329	1	170.44	Reserva Natural de Tambopata	Madre de Dios	La Torre	Peru				-12.93200	-69.27279	229
W	MUSM 38048	1	172.8	Qda Lopéz	Marañon	Andoas/Loreto	Peru				Unknown	Unknown	203
W	MUSM 4191	8	107.67–129.2	Qda S/N, km 3 camino a cocococha	Madre de Dios	Tambopata	Peru				-12.78803	-69.26311	208
W	MUSM 52996	2	16.49–168.5	Cocha Paichillo	Ucayali-Amazonas	Loreto	Peru				Unknown	Unknown	

Lin.	Catalog number	N	SL range	Locality	Basin	City, State	Country	Photo	X-ray	C&S	Lat	Long	Altitude
W	MUSM 542546	1	138.29	Qda S/N	Ucayali-Amazonas	Iparía	Peru				-9.26920	-74.17528	163
W	MUSM 58009	2	54.89–66.6	Río Marañon	Marañon	Loreto	Peru				Unknown	Unknown	
W	MUSM 61573	1	107.75	Río Yaguas	Putumayo-Amazonas	Loreto	Peru				-2.72814	-70.52837	84
W	MUSM 62597	1	106.82	Río Tapiche	Ucayali-Amazonas	Loreto	Peru				-7.19953	-73.93331	220
W	MUSM 63819	1	106.56	Subca. Marañon	Marañon	Urarinas/Loreto	Peru				-4.75393	-75.28865	119
W	MUSM 64145	1	92.21	Subca. Algodón	Putumayo-Amazonas	Putumayo/Loreto	Peru				-2.89017	-73.01172	103
W	MUSM 67673	1	119.17	Río Marañon	Amazonas	Urarinas/Loreto	Peru				-4.70765	-75.01274	95
W	ROM 61642	1	123.32	Unknown	Unknown	Mayaro–Rio Claro	Trinidad and Tobago				10.41667	-61.13333	27
W	USNM 167753	1	144.2	Brook Near Rio Itaya	Unknown	Loreto	Peru		1		Unknown	Unknown	
W	USNM 225299	9	67.1–188.1	Kapoeri Creek	Corantijn	Nickerie District	Suriname		5		5.26667	-57.16667	24
W	USNM 232226	1	102.7	Unknown	Unknown	Presidente Hayes	Paraguay		1		Unknown	Unknown	
W	USNM 232227	1	125.5	Teniente Martinez	Unknown	Chaco/Beni	Paraguay		1		Unknown	Unknown	
W	USNM 303111	9	99.2–170.3	Lago Normandia	Madre de Dios	Ballivia/Beni	Bolivia		6		-14.92000	-66.30000	192
W	USNM 5882	1	187.1	Western Portion of Trinidad	Unknown	Unknown	Trinidad and Tobago				Unknown	Unknown	
W	USNM 88284	1	93.2	Maranhão	Unknown		Brazil		1		Unknown	Unknown	
W	ZMA.PISC 100.310	1	104.6	Near Paramaribo	Unknown	Paramaribo	Suriname	1	1		Unknown	Unknown	
O	ANSP 127508	3	72.6–86.9	Rio Guariquito	Orinoco	Guarico	Venezuela				8.63867	-67.26666	69
O	ANSP 127513	3	162.6–181.7	Stream Hacienda Humacita	Meta-Orinoco	Meta	Colombia				3.95799	-73.05453	182
O	ANSP 127513	6	166–180.7	Lake Mozambique complex	Metica-Orinoco	Meta	Colombia		3		3.95799	-73.05453	182
O	ANSP 135693	1	125.6	Morichal Zamorai	Orinoco	Bolivar	Venezuela				7.49119	-64.90035	38
O	ANSP 135693	1	128.4	Morichal Zamorai	Orinoco	Bolivar	Venezuela		1		7.49119	-64.90035	39
O	ANSP 140317	1	115.7	Caño Potosi	Orinoco	Meta	Colombia		1		4.14218	-72.64349	209
O	ANSP 160806	5	76.5–131.7	Small stream crossing Caicara	Orinoco	Bolivar	Venezuela		5		7.03448	-66.49872	71
O	ANSP 160936	4	77.9–149.5	Caño Hacienda Fundo Malama	Orinoco	Bolivar	Venezuela				7.54158	-65.38994	51
O	ANSP 161628	5	176.8–213.7	Río Orinoco	Orinoco	Amazonas	Venezuela				3.16812	-65.54352	115
O	ANSP 161631	3	106.1–164.6	Cano Caripo	Casiquiare	Amazonas	Venezuela				3.10806	-65.83230	121
O	ANSP 165196	1	67.6	Laguna Los Laureles	Apure-Orinoco	Roblito/Guarico	Venezuela		1		8.10664	-67.51599	49
O	ANSP 165285	1	134.5	Caño near El Yagua	Arauca-Orinoco	Apure	Venezuela		1		7.53608	-68.32166	68
O	ANSP 165386	2	75.9–159.2	Río Claro	Orinoco	Apure	Venezuela				7.13533	-67.42422	46

Lin.	Catalog number	N	SL range	Locality	Basin	City, State	Country	Photo	X-ray	C&S	Lat	Long	Altitude
O	ANSP 182233	3	89.6–105.8	Small trib to Rio Manapiare	Ventuari-Orinoco	Guaviarito/Amazonas	Venezuela		3		5.43694	-66.16507	124
O	CZUT-IC 11490	1	212.5	Cañada Guafila	Ariporo-Orinoco	Hato Corozal/Casanare	Colombia				5.93461	-71.48653	167
O	CZUT-IC 12996	7	130–165.9	Cañada NN	Ariporo-Orinoco	Hato Corozal/Casanare	Colombia				5.91325	-71.48492	167
O	CZUT-IC 13027	1	116.8	Caño Cusiaba	Cusiana-Orinoco	Maní/Casanare	Colombia				4.62556	-72.02528	154
O	FMNH 85450	2	80.5–82.7	Borrow pit on E of Road at 14km N Camaguan	Apure-Orinoco	Guárico	Venezuela		2		Unknown	Unknown	
O	FMNH 85525	2	94.4–113.0	Tiny Creek about 33 km from San Mariapo	Orinoco	Amazonas	Venezuela		2		Unknown	Unknown	
O	IAvH-P 13836	38	69.8–127.3	Morichal La Calandria	Meta-Orinoco	Cravo Norte/Arauca	Colombia			1	6.26519	-69.71222	97
O	IAvH-P 16946	5	90.7–126.8	Morichal NN	Tomo-Orinoco	Puerto Carreño/Vichada	Colombia			1	5.54725	-68.46797	80
O	IAvH-P 21228	2	76.8–96.4	Reserva Natural Bojonawi	Bita-Orinoco	Puerto Carreño/Vichada	Colombia				6.09942	-67.52186	55
O	IAvH-P-19171	1	177.5	Morichal caño NN	Bita, Orinoco	Puerto Carreño/Vichada	Colombia				5.62942	-68.52514	105
O	IAvH-P-19206	1	30	Bocas del caño Parurito	Meta-Orinoco	La Primavera/Vichada	Colombia				6.17681	-69.12856	77
O	IAvH-P-19884	1	87.1	Jaguey Mararay	Manacacias-Orinoco	Mararay, Meta	Colombia				3.46833	-72.54315	214
O	IAvH-P-20191	1	38.4	Morichal NN	Manacacias-Orinoco	San Martín/Meta	Colombia				3.45506	-72.54047	209
O	IAvH-P-21851	1	192.4	Río Guaviare	Guaviare-Orinoco	Unknown	Colombia				Unknown	Unknown	
O	IAvH-P-4102	1	112.6	Boca de laguna al río Tomo	Tomo-Orinoco	Cumaribo/Vichada	Colombia				5.34917	-67.82597	60
O	LBP 2212	1	37.97	Laguna de Castilleros	Orinoco	Caicara del Orinoco /Bolivar	Venezuela				7.51414	-66.15550	55
O	LBP 2298	1	52	Lagoa marginal do rio Orinoco	Orinoco	Caicara del Orinoco /Bolivar	Venezuela				7.52314	-66.05450	39
O	USNM 100791	1	127.4	Meta Basin	Meta-Orinoco	Villavicencio/Meta	Colombia		1		Unknown	Unknown	
O	USNM 163188	3	70.5–107.2	Few Miles of Puerto Ayacucho	Orinoco	Amazonas	Venezuela		3		Unknown	Unknown	
O	USNM 260135	3	159.7–181.3	Caño Falcon	Apure-Orinoco	Guarico	Venezuela		2		8.23000	-67.58000	57
BS	LBP 24858	3	100.4–109.7	Ribeirão Taxidermista	Teles Pires-Amazonas	Alta Floresta/MT	Brazil				-9.81531	-56.14054	242
BS	LBP 4002	1	143.3	Lago Morto	Araguaia-Amazonas	São Félix do Araguaia/MT	Brazil				-11.66917	-50.85008	194
BS	LBP 2980	2	130.9–158.5	Lagoa da Égua	Araguaia-Amazonas	Cocalinho/MT	Brazil				-13.33475	-50.70450	222
BS	LBP20882	4	83.4–139.9	Afluente rio Lagoa Rosa	Arinos-Tapajós-Amazonas	Diamantino/MT	Brazil				-13.90532	-57.08762	503
BS	LBP 15723	1	125.8	Tributário rio Suiá-Missu	Xingu-Amazonas	Ribeirão Cascalheira/MT	Brazil				-12.88453	-52.03342	331
BS	LBP 20253	1	171.3	Rio Apiacás	Tapajós-Amazonas	Alta Floresta/MT	Brazil				-10.35019	-56.98242	256
BS	LBP 12740	2	111.7–183.7	Rio Araguaia	Tocantins-Amazonas	Cocalinho/MT	Brazil				-13.31036	-50.61322	217

Lin.	Catalog number	N	SL range	Locality	Basin	City, State	Country	Photo	X-ray	C&S	Lat	Long	Altitude
BS	LBP 25107	5	61.4–79.3	Riacho afluente do rio Curuá	Xingu-Amazonas	Altamira/PA	Brazil				-8.82000	-54.96972	454
BS	LBP 15875	2	58.4–65.1	Tributário rio Coluene	Xingu-Amazonas	Canarana/MT	Brazil				-13.42525	-52.27972	346
BS	LBP 9259	1	104.2	Lagoa do Chico	Araguaia-Amazonas	Cocalinho/MT	Brazil				-13.32300	-50.62242	225
BS	LBP 25265	2	74.7–82	Afluente Rio Braço do Norte	Tapajós-Amazonas	Novo Progresso/PA	Brazil				-9.29972	-54.83306	514
BS	LBP28484	1	200.13	Ribeirao Santo Antonio	Arinos-Amazonas	Diamantino/MT	Brazil				-14.16456	-57.17075	524
BS	LBP 28505	1	158.9	Ribeirao Santo Antonio	Arinos-Amazonas	Diamantino/MT	Brazil				-14.16456	-57.17075	524
BS	LBP 21603	3	188–201.1	Rio Apiacás	Tapajós-Amazonas	Alta Floresta/MT	Brazil				-10.34169	-56.98331	248
BS	USNM 199201	13	68.2–142.3	Upper Juruena	Juruena	Mato Grosso	Brazil			6	Unknown	Unknown	
BS	USNM 310474	5	74.1–126.7	Small Tributary of Batovi River	Xingu	Mato Grosso	Brazil			5	-11.93333	-53.60000	318

Table S2. Loadings of variance and eigenvalues of morphometric measurements of *Hoplerythrinus unitaeniatus* used in Principal Component Analysis (PCA). Discriminant characters in bold.

	PC1	PC2	PC3
Eigenvalue	0.01	0.01	0
% of Variance	31.9	25.0	10.3
Body depth	**-0.43000**	0.01596	0.49497
Head length	0.55709	-0.09090	0.40334
Pectoral-fin length	0.29805	0.24815	0.27229
Pelvic-fin length	0.37120	0.33300	0.42063
Anal-fin length	0.34226	**0.80851**	0.13008
Dorsal-fin length	0.39443	0.12010	0.57580
Dorsal-fin base length	-0.03325	0.15214	0.59140
Anal-fin base length	0.12660	**0.97219**	-0.09630
Pre-pectoral length	**0.72211**	-0.08654	0.31083
Pre-pelvic length	0.23082	-0.00225	0.09275
Pre-dorsal length	0.32794	-0.23626	0.39278
Pre-anal length	0.06340	**-0.24785**	-0.01149
Caudal-peduncle depth	-0.42019	-0.04528	0.62709
Caudal-peduncle length	-0.29794	**-0.57910**	-0.00413
Head depth at quadrate	**-0.57276**	0.07304	0.22819
Head depth at eye	-0.38230	0.06602	-0.00927
Snout length	-0.10042	0.10862	-0.62452
Snout width	-0.27326	-0.06639	-0.63637
Pre-nasal distance	-0.05056	-0.05192	-0.43260
Orbital diameter	**0.96112**	-0.18887	-0.06535
Interorbital bony width	**-0.56311**	0.13954	-0.41692
Upper jaw length	-0.27686	-0.02486	0.22989

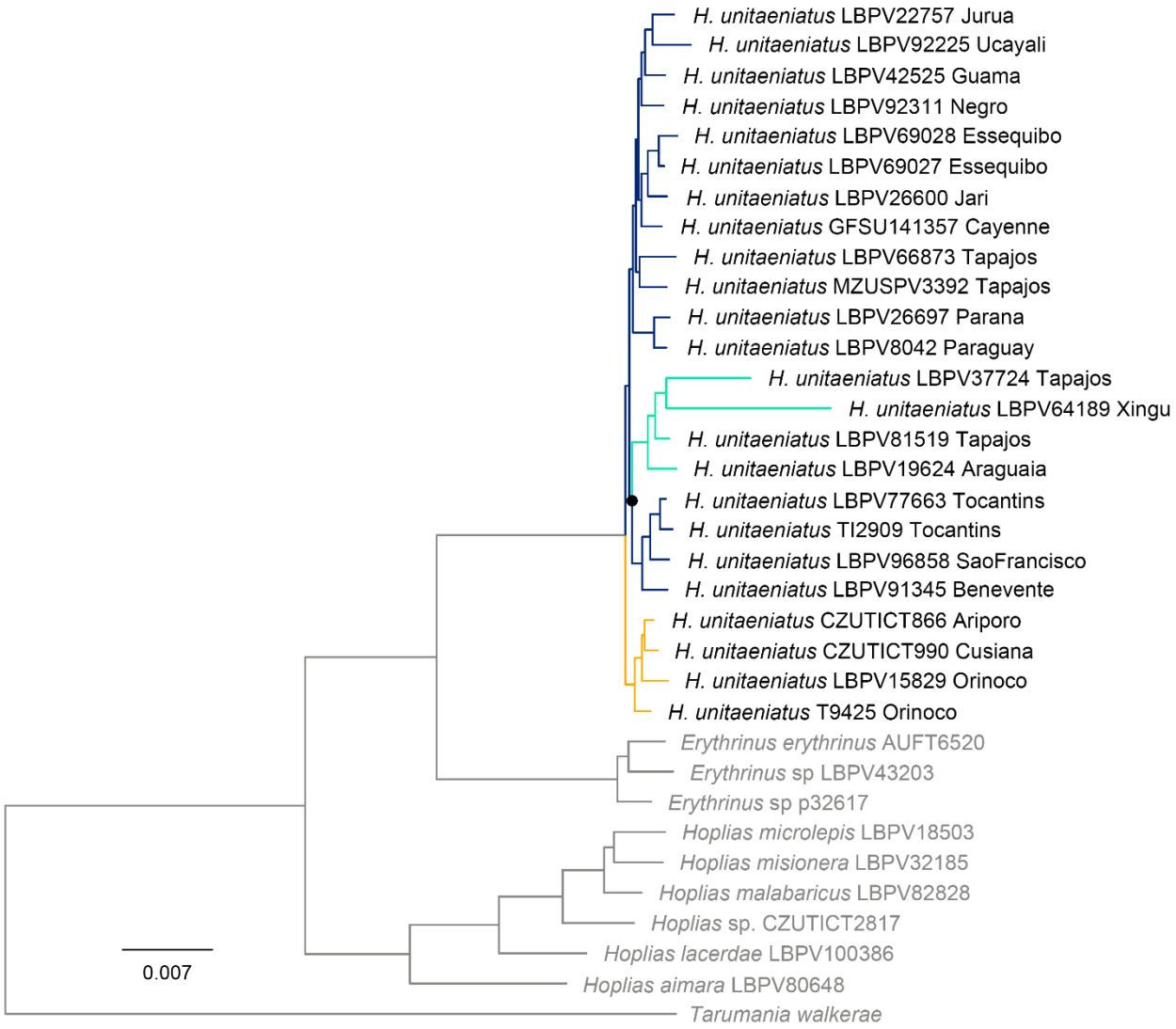

Fig S1. Bayesian inference (BI) using 75% complete matrix (edge-trimmed, unpartitioned). No symbols at nodes indicate Bayesian posterior probabilities of 1, and black circles denoted values between 0.85-0.99.

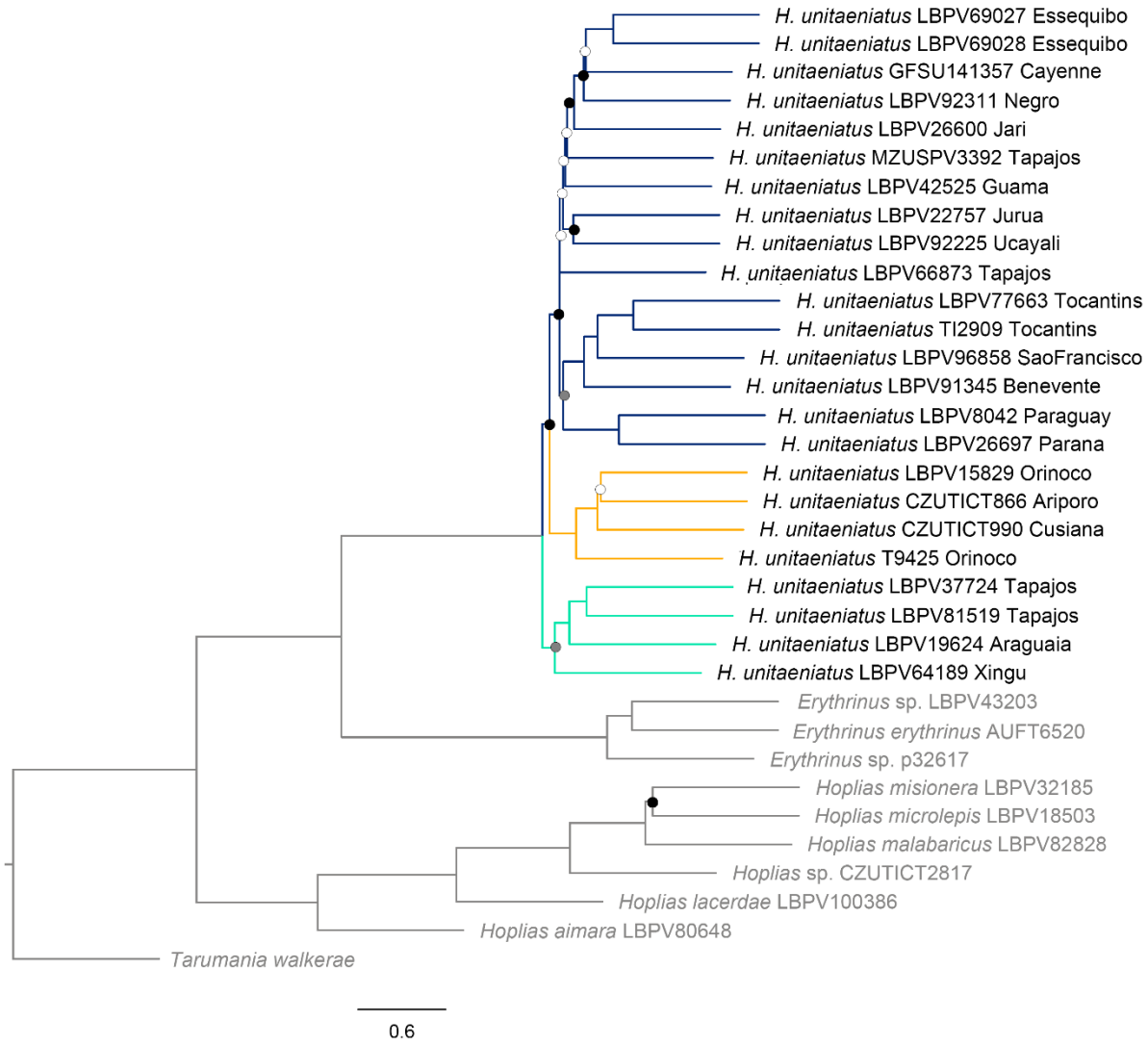

Fig S2. Species tree inference from Astral-III, based on the 75% complete matrix. No symbols at nodes indicate support values between 1, black circles denoted nodal support between 0.99-0.85, gray circles denoted nodal support between 0.85-0.60, and white circles denoted nodal support inferior to 0.60.

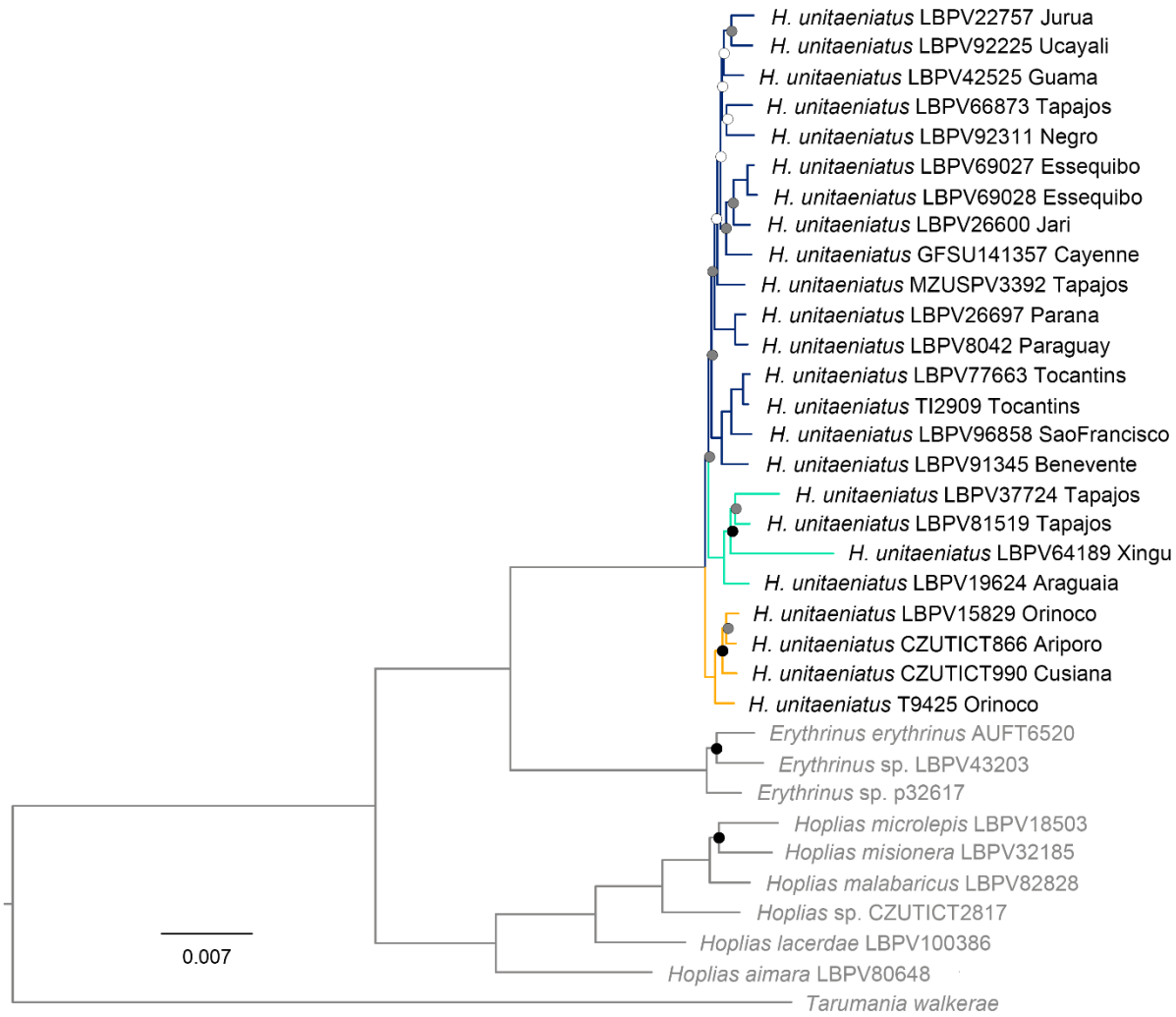

Fig S3. Phylogenetic relationships of *Hoplerythrinus* based on a maximum likelihood analysis of the edge-trimmed and partitioned 90% complete matrix of ultraconserved elements. Data for 110 loci and 57,514 bp. No symbols at nodes indicated bootstrap support values (ML-BP) of 100, black circles denoted values between 85-99, gray circles denoted values between 60-85, and white circles denoted values inferior to 60.

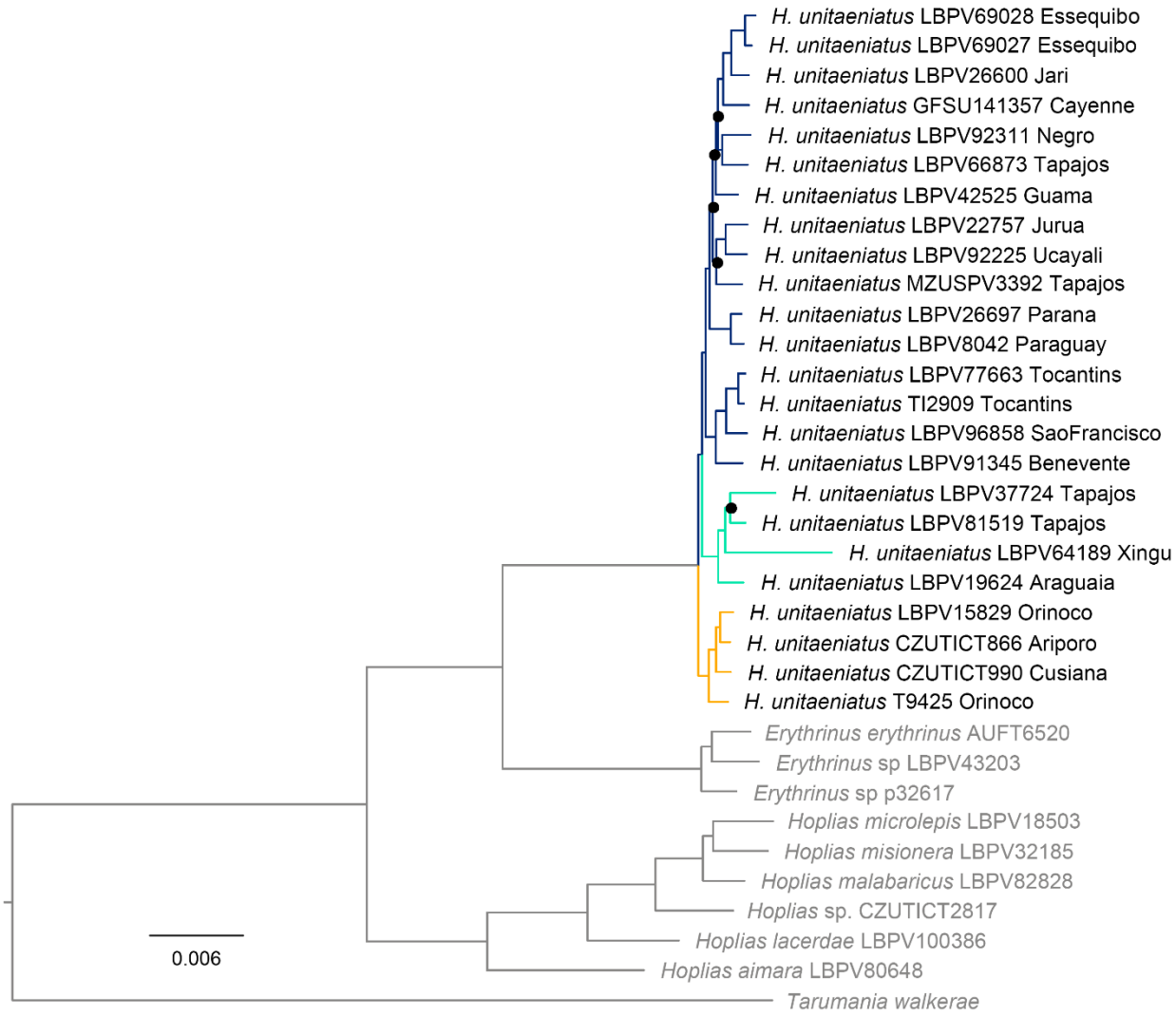

Fig S4. Bayesian inference (BI) using 90% complete matrix (edge-trimmed, unpartitioned). No symbols at nodes indicate Bayesian posterior probabilities of 1, and black circles denoted values between 0.85-0.99.

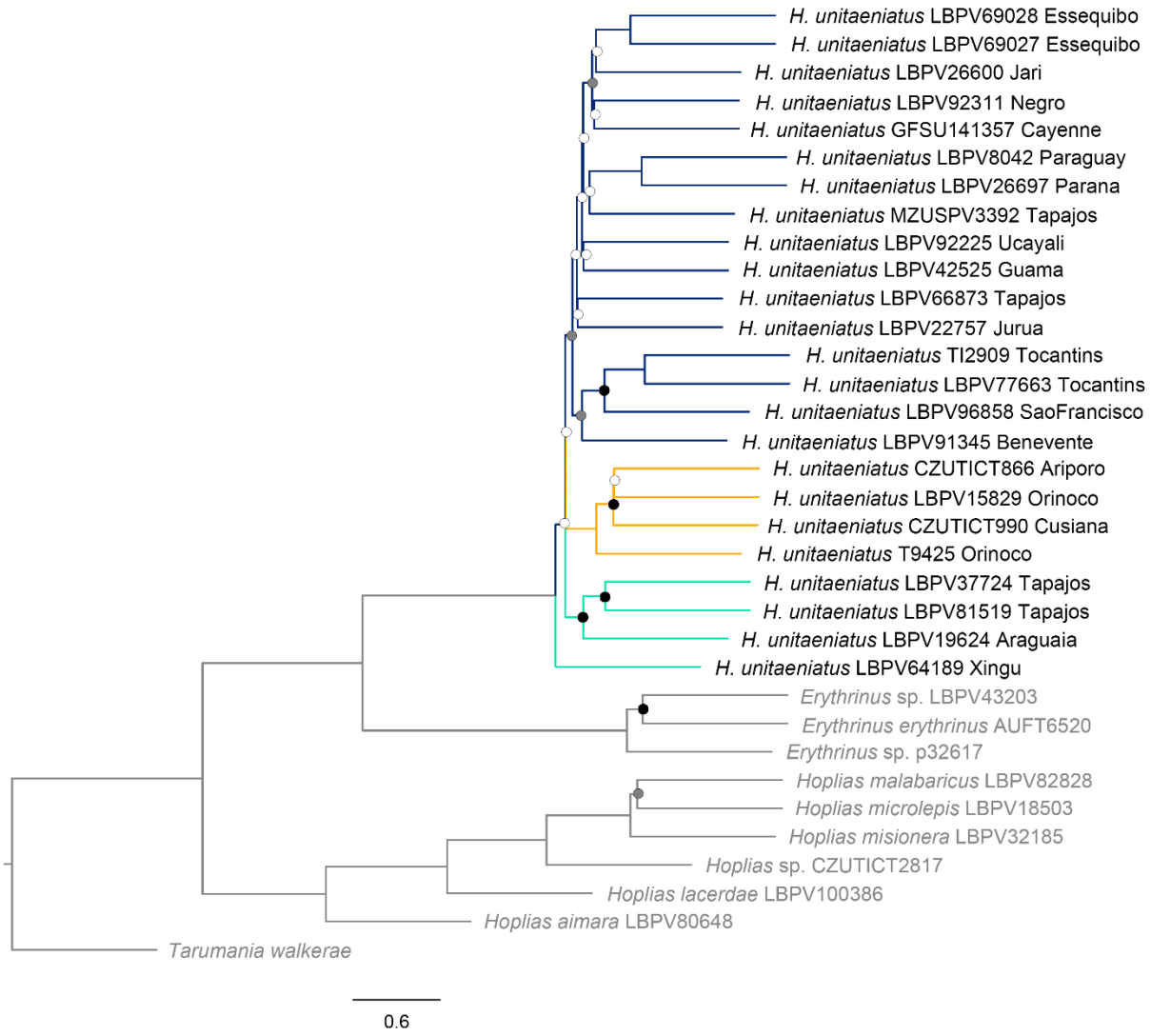

Fig S5. Species tree inference from Astral-III, based on the 90% complete matrix. No symbols at nodes indicate support values between 1, black circles denoted nodal support between 0.99-0.85, gray circles denoted nodal support between 0.85-0.60, and white circles denoted nodal support inferior to 0.60.

Fig S6. Syntypes of *Hoplerythrinus gronovii*, MNHN-IC 0099, A: 103.4 mm SL, B: 109.7 mm SL, C: 116.9 mm SL, Cayenne, French Guiana. Credits: MNHN - Ferrara C. – 2013.

Fig S7. Holotype of *Hoplerythrinus cinereus*, USNM 5882, 187.1 mm SL, Western portion of Trinidad, Trinidad and Tobago. Credits: Raredon, Sandra J - NMNH

Fig S8. Syntype of *Erythrinus vittatus*, MNHN-IC 9758, 123.5 mm SL, Rio de Janeiro, Brazil. Credits: MNHN - Ferrara C. – 2013.

Fig S9. Syntypes of *Erythrinus vittatus*, MNHN-IC 9759, A: 107.7 mm SL, B: 130.2 Rio de Janeiro, Brazil. Credits: MNHN - Ferrara C. – 2013.

Fig S10. Syntypes of *Erythrinus vittatus*, MNHN-IC 9760, A: 110.1 mm SL, B: 120.8, Cayenne, French Guiana. Credits: MNHN - Ferrara C. – 2013.

Fig S11. Syntype of *Erythrinus vittatus*, MNHN-IC 9761, 254.8.5 mm SL, Suriname. Credits: MNHN - Ferrara C. – 2013.

Fig S12. Holotype of *Pseuderythrinus rosapinnis*, ZMA.PISC 100.310, 104.6 mm SL, Near Paramaribo, Suriname. Credits: Esther Dondorp (Naturalis Biodiversity Center).

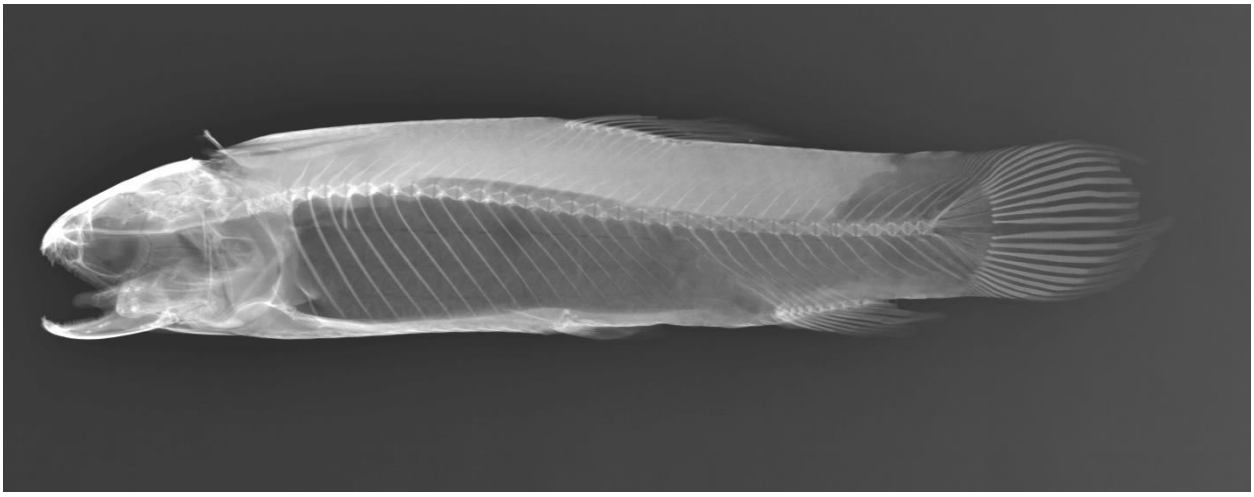

Fig S13. Radiograph of the holotype of *Pseuderythrinus rosapinnis*, ZMA.PISC 100.310, 104.6 mm SL, Near Paramaribo, Suriname. Credits: Esther Dondorp (Naturalis Biodiversity Center).